



UNIVERSITAT DE
BARCELONA

Intermolecular Pauson-Khad reaction: study of the regioselectivity, photochemistry of the adducts and synthetic applications

Hélée Khaizourane

ADVERTIMENT. La consulta d'aquesta tesi queda condicionada a l'acceptació de les següents condicions d'ús: La difusió d'aquesta tesi per mitjà del servei TDX (www.tdx.cat) i a través del Dipòsit Digital de la UB (diposit.ub.edu) ha estat autoritzada pels titulars dels drets de propietat intel·lectual únicament per a usos privats emmarcats en activitats d'investigació i docència. No s'autoritza la seva reproducció amb finalitats de lucre ni la seva difusió i posada a disposició des d'un lloc aliè al servei TDX ni al Dipòsit Digital de la UB. No s'autoritza la presentació del seu contingut en una finestra o marc aliè a TDX o al Dipòsit Digital de la UB (framing). Aquesta reserva de drets afecta tant al resum de presentació de la tesi com als seus continguts. En la utilització o cita de parts de la tesi és obligat indicar el nom de la persona autora.

ADVERTENCIA. La consulta de esta tesis queda condicionada a la aceptación de las siguientes condiciones de uso: La difusión de esta tesis por medio del servicio TDR (www.tdx.cat) y a través del Repositorio Digital de la UB (diposit.ub.edu) ha sido autorizada por los titulares de los derechos de propiedad intelectual únicamente para usos privados enmarcados en actividades de investigación y docencia. No se autoriza su reproducción con finalidades de lucro ni su difusión y puesta a disposición desde un sitio ajeno al servicio TDR o al Repositorio Digital de la UB. No se autoriza la presentación de su contenido en una ventana o marco ajeno a TDR o al Repositorio Digital de la UB (framing). Esta reserva de derechos afecta tanto al resumen de presentación de la tesis como a sus contenidos. En la utilización o cita de partes de la tesis es obligado indicar el nombre de la persona autora.

WARNING. On having consulted this thesis you're accepting the following use conditions: Spreading this thesis by the TDX (www.tdx.cat) service and by the UB Digital Repository (diposit.ub.edu) has been authorized by the titular of the intellectual property rights only for private uses placed in investigation and teaching activities. Reproduction with lucrative aims is not authorized nor its spreading and availability from a site foreign to the TDX service or to the UB Digital Repository. Introducing its content in a window or frame foreign to the TDX service or to the UB Digital Repository is not authorized (framing). Those rights affect to the presentation summary of the thesis as well as to its contents. In the using or citation of parts of the thesis it's obliged to indicate the name of the author.

Intermolecular Pauson-Khand Reaction:
Study of the regioselectivity, photochemistry of the adducts and
synthetic applications



Héléa Khaizourane



UNIVERSITAT DE
BARCELONA

Programa doctorat de Química Orgànica

Intermolecular Pauson-Khand Reaction:
Study of the regioselectivity, photochemistry of the adducts
and synthetic applications

Héléa Khaizourane

Programa doctorat de Química Orgànica
Universitat de Barcelona

Director de tesi: **Antoni Riera Escalé**

Departament de Química Orgànica

IRB Barcelona



UNIVERSITAT DE
BARCELONA

Memoria presentada per Héléa Khaizourane per optar al grau de doctora en química orgànica
per la Universitat de Barcelona.

Héléa Khaizourane

Revisada per

Pr. Antoni Riera escalé

Barcelona, Març 2016

Aquesta treball ha estat realitzat amb el suport econòmic de "la Caixa" mitjançant una beca predoctoral. La tasca s'ha finançat pels projectes de recerca del Ministeri d'Economia i Competitivitat (CTQ2011-23620) i de la Generalitat de Catalunya (2009-SGR-00901).

El treball experimental s'aquesta tesi s'ha dut a terme en el laboratori de la Unitat de Recerca en Síntesi Asimètrica de l'Institut de Recerca Biomèdica (IRB Barcelona) situat en el Parc Científic de Barcelona (PCB).

Acknowledgments

A Voldria agrair als doctors Antoni Riera i Xavier Verdaguer l'oportunitat d'integrar-me en el seu grup de recerca, tota la ajuda i el suport que m'han donat durant aquests anys per poder dur a terme aquesta tesi doctoral. Especialment al Toni per la seva sensibilitat, humanitat i paciència quan jo estava aprenent l'espanyol. Moltes gràcies per la teva ajuda en els moments més difícils de la meva vida personal que eren difícils de superar sola. Gràcies també per "obligar-me" a cantar en el cor de la Universitat de química orgànica, és amb vostè que em vaig aprendre una miqueta de català! Gràcies a tot, a Victor i a tot las sopranos.

També vull agrair als membres del meu TAC (Dr. Jordi Garcia, Dr. Ciril Jimeno i Dr. Jan Spengler) per el seu interès i els seus consells i idees. M'agradaria donar les gràcies a tot el personal dels serveis científico-tècnics del Parc Científic, la UB i l'IRB pel seu ajut, molt especialment, a la Vicky i la M^a Antonia. Mar i Marta pel seu esforç en ionitzar lo inionitzable. Tanmateix, vull agrair a Enantia S.L., molt especialment a Ester, pels anàlisis de HPLC. I would like to thanks Alex for our vegi wednesday lunches sharing your dreams of nature, music and exploration spirit!

I would like to thanks the IRB administration team (Parti, Leyre, Alba, Luca, Sara, Eric) for their helps and making the IRB pleasant and dynamic with all the activities proposed!

Thanks to Helaja's group, Erika, Mikko and Juho for that nice collaboration.

Res hagués estat igual sense els meus companys de grup. Gràcies a tots els que heu passat per aquí (Thierry, Jean-Claude, Ana, Marc, Séan, Pablito, Yi Ning, Aida, Ferran, Agustí, Nuria). Merci Thierry, pour ton amitié et nos nombreuses discussions du café de 8h et mardis au soleil! M'agradaria agrair al meu amic i gran company de laboratori amb Silvia que va créixer i compartim les llàgrimes junts! Vas fet el meva integració súper fàcil i ràpida en el món català (música, les arts, la natura!). El Edgar per compartir el corredor amb el super Dan i fer gran partit de tennis. To Super Dan, thanks for your optimism and joy! Life was easy and always happy with you. To "La fontaine", for the singing moments that we shared in that incredible corridor remixing all song such as the famous "Panky Pang"! To Chris, "fair enough, for organizing the chemistry seminars and helping me with the 2D spectra." To the peptide team, Alvarrooo & Escola", we had nice laughs together and good luck Anna, we are doing with your cells! To Craig "Dantongue", pleasure to meet a nice Scottish like you, always happy and smily. To the new URSA generation, Ernesto, Marta i Albert good luck with your thesis and the PKRs. To the IRB community that made my stay really dynamic, to Samira, Irena, Laura, Alex, Mar, Radeck, IRB volley team: Jasha, Luca, Adri, Marta). I would like to thanks my two young and dynamic students, thiphaine and Eva for their help with the synthesis.

I would like to thanks Steven, for your support, your motivation, your passion for life and for all the moments that we shared and will share.

Finally, to my all family. Merci pour votre soutien. Ça a été quatre années incroyablement dures et intenses en émotions. Nous sommes définitivement plus forts et plus soudés que jamais. Merci à mes parents, ma grand-mère, mes frères et sœurs. J'ai hâte de commencer nos nouveaux projets tous ensemble.

A ma famille.

*« La vie est un mystère qu'il faut vivre,
non un problème à résoudre. »*

Gandhi

Contents

Abbreviations

1. Introduction and objectives	1
II. Study of the regioselectivity of the intermolecular Pauson-Khand reaction	9
III. Applications to the synthesis of natural products	53
IV. Photochemical reaction of Pauson-Khand adducts	85
V. Conclusions	115
VI. Experimental part	117
VII. Selected spectra	152
Appendix I. Publications	170
Appendix II. Summary in Catalan	172
Appendix III. Index of Structures	205

α	alpha	ESI	electrospray ionization
β	beta	Et ₂ O	diethylether
°C	Celsius degree	EWG	electron-withdrawing group
δ	NMR chemical shift	h	hour(s)
λ	wavelength	HMBC	heteronuclear multiple-bond correlation spectroscopy
add.	addition	HMPA	hexamethylphosphoramide
Bn	benzyl	HPLC	high Performance Liquid Chromatography
Boc	<i>tert</i> -butoxycarbonyl	HRMS	high Resolution Mass Spectrometry
cat.	catalytic	HSQC	heteronuclear singular-quantum correlation spectroscopy
COSY	correlation spectroscopy	h ν	ultraviolet radiation
DBU	1,8-diazabicyclo [5.4.0.] undec-7-ene	IR	infrared
DCM	dichloromethane	<i>J</i>	coupling constant
DFT	density Functional Theory	LUMO	lowest Unoccupied Molecular Orbital
DMAP	4-(dimethylamino)pyridine	MA	maleic anhydride
DMF	<i>N,N</i> -dimethylformamide	min	minute(s)
DMSO	dimethylsulfoxide	Mol. sieves	molecular sieves
DMP	Dess-Martin periodinane	MW	microwaves
dr	diastereomeric ratio	NBD	norbornadiene

eq.	equivalent	TBAF	tetrabutylammonium fluoride
ee	enantiomeric excess	THF	tetrahydrofuran
EDG	electron-donating group	THP	tetrahydropyran
NBO	natural bond orbital	TLC	thin layer chromatography
nd	not determined	TMANO	trimethylamine- <i>N</i> -oxide
NMO	<i>N</i> -methylmorpholine- <i>N</i> -oxide	TMS	trimethylsilyl
NOESY	nuclear Overhauser effect spectroscopy	TS	transition state
NMR	nuclear Magnetic Resonance	W	watt(s)
Nu	nucleophile		
<i>o</i>	ortho		
<i>p</i>	para		
<i>Ph</i>	phthalimide		
PDA	phytyldienoic acid		
PKR	Pauson-Khand reaction		
PNSO	<i>N</i> -phosphino sulfinamide		
ppm	parts per million		
rac	racemic		
rt	room temperature		
s	second(s)		
SM	starting material		
t_R	retention time		

CHAPTER I

Introduction & Objectives

The Pauson-Khand reaction (PKR), introduced by Pauson and Khand in 1973, is an efficient method to access the synthesis of five-membered rings in one single step.¹

This reaction is a transition metal-mediated [2+2+1] carbocyclisation between an alkyne, an alkene and carbon monoxide (CO). It forms a cyclopentenone where two new asymmetric centres would be created if the alkene is disubstituted (figure 1.1). This reaction is commonly mediated by a cobalt complex such as $\text{Co}_2(\text{CO})_8$.

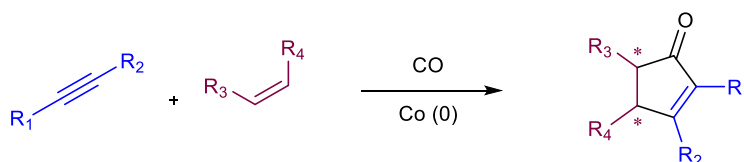


Figure 1.1.

PKR arouses great synthetic interest even five decades after its discovery due to its easy handling procedure and its compatibility with many functional groups. The intramolecular PKR is a widely used method for the construction of the cyclopentane core of numerous polycyclic natural compounds. Recent examples of total syntheses in which the intramolecular PKR has been used are (+)-Fusarisetin² and Ingenol³ represented in figure 1.2.

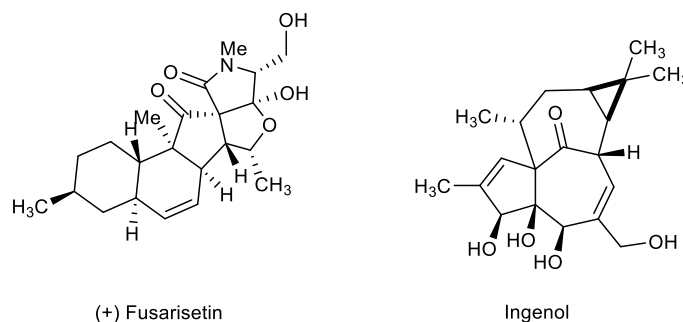


Figure 1.2.

The main drawback of the intramolecular version of the PKR is its strong dependence on the substrate and the difficulty of the enyne synthesis. The intermolecular PKR, on the other hand, has the advantage to be more general and the substrates are much simpler to synthesize. However, some limitations slow down its exploitation. The first limitation of the intermolecular PKR is the small range of alkenes that leads to satisfactory yields. Indeed, strained alkenes such as norbornadiene, norbornene or cyclopropene, give excellent results; ethylene is an exception to the rule since it is an excellent substrate.⁴ Symmetrical bicyclic alkenes induce the formation of two isomers (*endo* and *exo*) where the *exo* adduct is usually the main reaction product (figure 1.3).

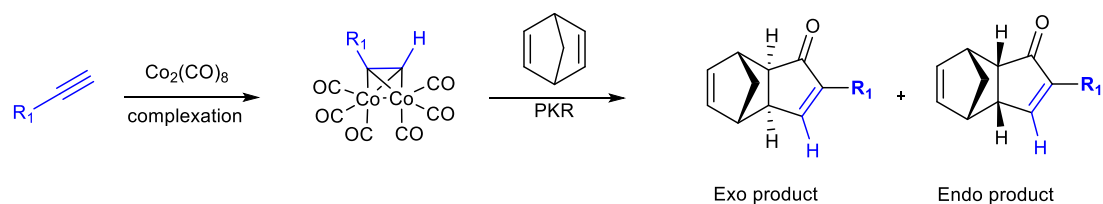


Figure 1.3.

When the synthesis involves terminal alkynes, the reaction is highly regioselective affording a single cyclopentenone with the substituent in α to the carbonyl group. However, unsymmetrical internal alkynes can afford two regioisomers (figure 1.4). The use of unsymmetrical internal alkyne may have the drawback of the difficult prediction of the regiochemical outcome of the PKR.

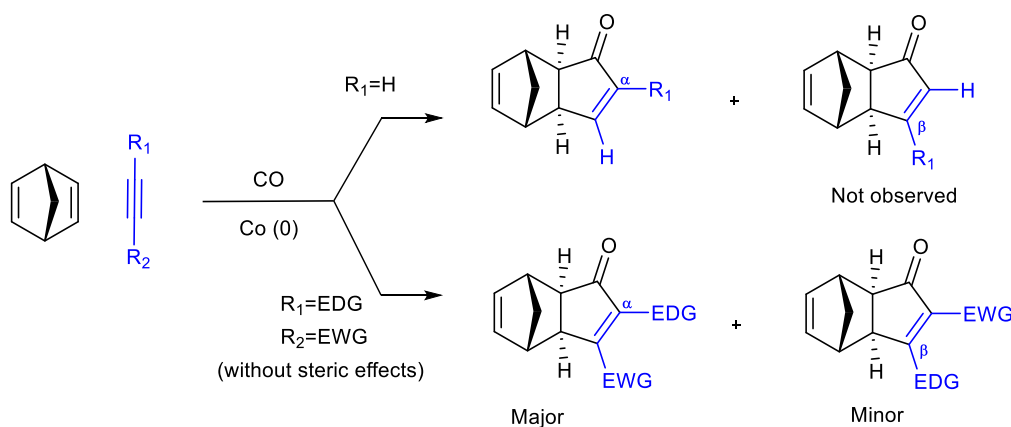


Figure 1.4.

It has been established that the regioselectivity of alkyne is guided by both electronic and steric effects.⁵ Electron-withdrawing groups tend to be positioned in β position of the ketone, whereas a bulky and electro donating groups tend to end up in α position of the ketone. Gimbert and co-workers have shown in several examples that the initial C-C-bond is formed with the more electron rich alkyne carbon according to the Natural Bonding Orbital (NBO) charges.⁶

Nevertheless, some cases reported in our group some years ago, showed high preference for one regioisomer which were not consistent with the predictions. The cases reported in figure 1.5 show a surprisingly high regioselectivity toward one regioisomer. In the first case, the steric and electronic differences between CH_2OTBS and the propyl groups do not show great difference but induce a high regioselectivity to the β isomer. The CF_3 is a highly electron-withdrawing group, however the PKR affords the alpha-isomers with high regioselectivity no matter the electronic and steric nature of the other substituent.^{7,8} This fact showed us that the regioselectivity cannot be always easily predicted suggesting that a theoretical calculation could be helpful.

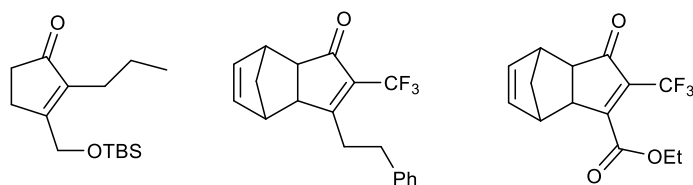


Figure 1.5.

Helaja and co-workers published in 2012, a new vision for understanding the regioselectivity, based on the electronic density of functionalised diarylalkynes. Thus, the α -alkyne NBO charges were investigated rather than direct polarisation of the triple bond previously proposed (figure 1.6).⁹

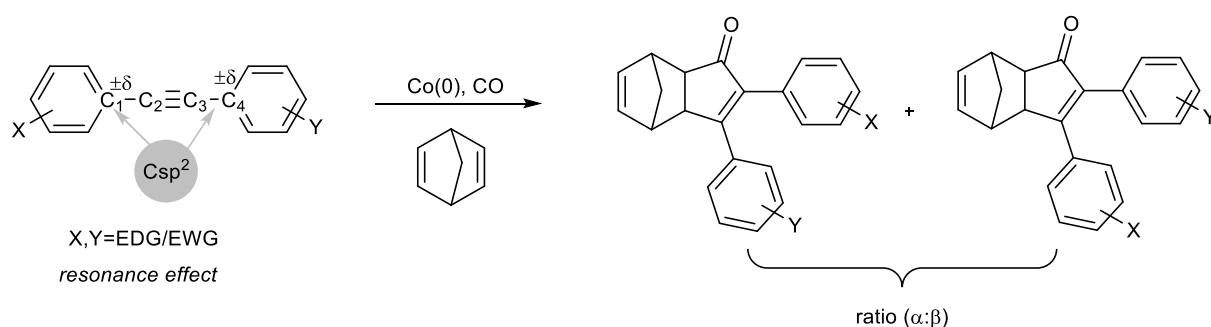


Figure 1.6.

They studied the PKRs of functionalised diarylalkynes showing that the regioselectivity of the PKR correlates with the Hammett-values of the substituent in para position of aromatic ring of the alkyne. Although the regioselectivities observed were poor, about 1:1.3, the slight excesses were in good accordance with the C1-C4 difference of NBO charges calculated at the DFT level (figure 1.7).

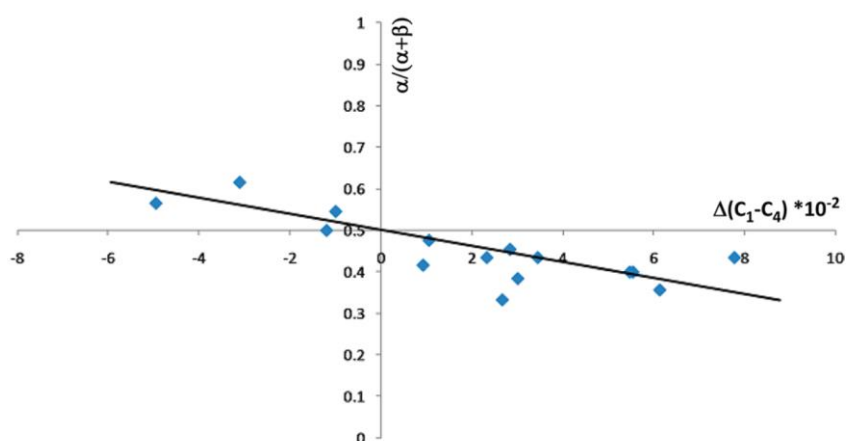


Figure 1.7.

Taking into account Helaja's work, we thought that this approach could lead us to better understanding and/or prediction of our high regiochemical outcomes in the PKR of internal aliphatic alkynes.¹⁰

The first objective of the present doctoral thesis was to study the regiochemistry of the PKRs of aliphatic unsymmetrical substituted alkynes. For that purpose, a collaboration was made with

Helaja's group bringing to the project his computational expertise. Thus, a large range of unsymmetrical internal alkynes was synthesised and the experimental regiochemical outcome of each reaction was collected and computationally analysed. Our results will be discussed in the **chapter 2** (figure 1.8).

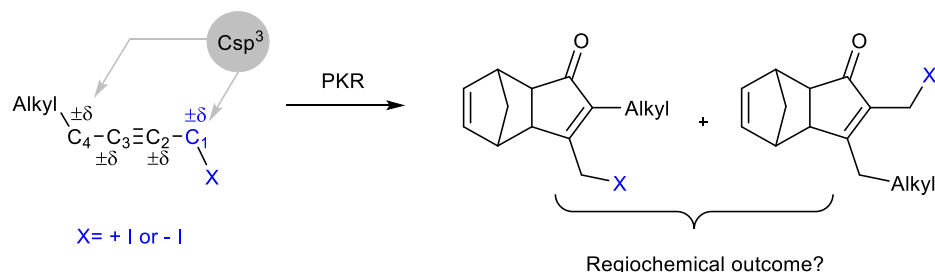


Figure 1.8

The unexploited field of the intermolecular PKR had motivated our group to develop new asymmetric versions of the reaction and to apply it to the synthesis bioactive compounds such as (-)-carbovir¹¹, DPPJ₁-I,¹² PGB₁⁸ or the 13-epi-12-oxo PDA¹³ using our methodologies (figure 1.9).

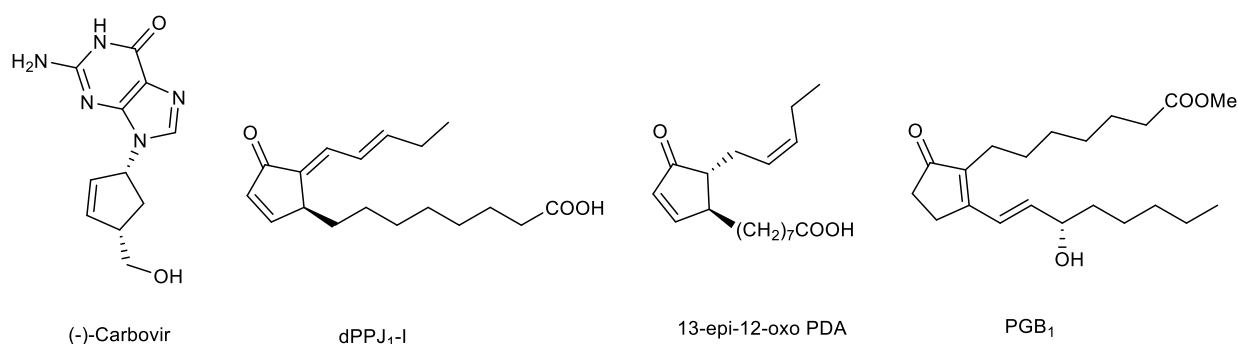


Figure 1.9.

To continue with in this research line, a new approach to the synthesis of sarkomycin and jasmonate was planned using internal regioselective PK reactions. **This was the second objective of the present doctoral thesis.** Our efforts toward these syntheses will be described in the **chapter 3** (figure 1.10).

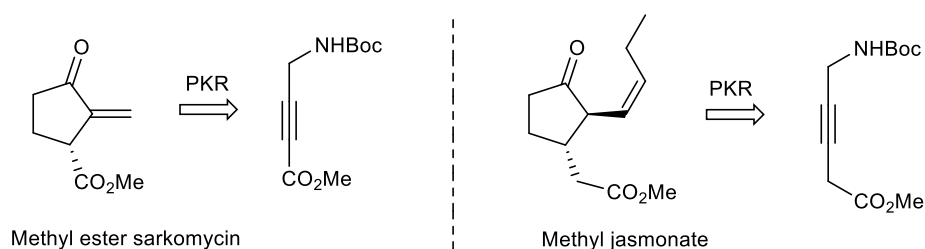


Figure 1.10.

Traditionally, to introduce a β side chain into the cyclopentenone ring, the organometallic conjugate addition was the main pathway. However, photochemical reactions have also showed a great potential.¹⁴⁻¹⁶ Working with the photochemical conjugate addition of hydroxymethyl into PK adducts, in 2005, Agustí Lledó in his thesis discovered two new photochemical reactions of PK adducts. Whereas PKRs of aliphatic alkynes gave a novel transposition product, diaryl alkynes afforded an electrocycloisatation reaction affording phenanthrenes (figure 1.11).¹⁷ Later on, the electrocycloisatation reaction was optimised and studied by Yining Ji in her PhD thesis.¹⁸

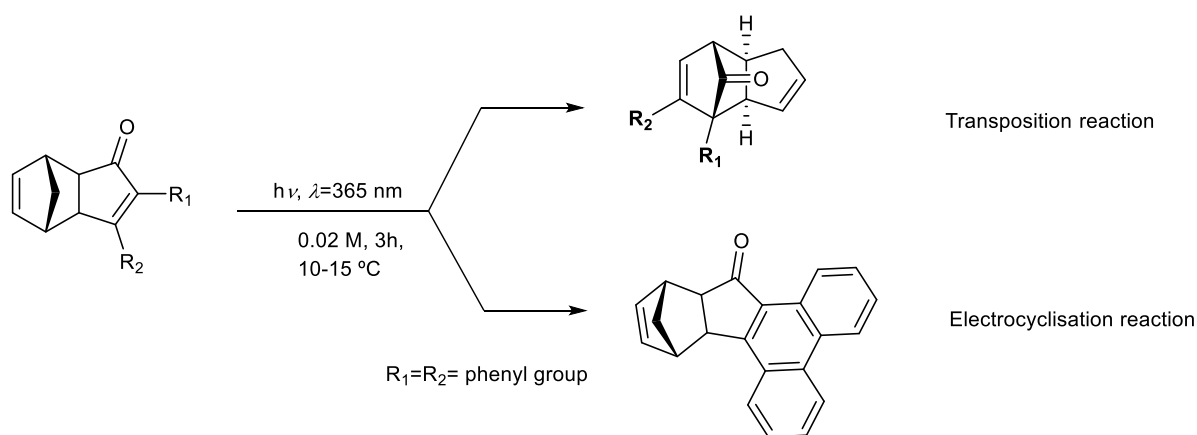


Figure 1.11.

Yining Ji observed that the PKRs of disubstituted aryl alkynes afforded two helicene-like compounds. The steric hindrance of the substituents imposed a structural distortion of the polycyclic molecule affording two twisted atropisomeric phenanthrene structures P and M (figure 1.12).

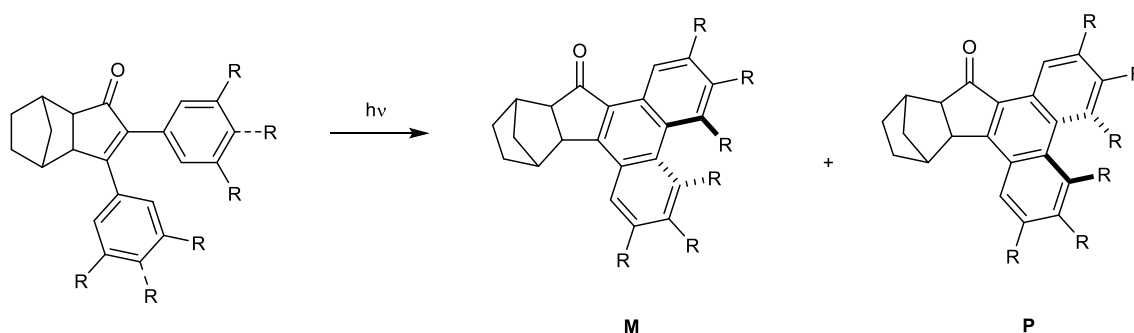


Figure 1.12.

In chapter 4, we completed the study of PKRs of disubstituted aryl alkynes previously initiated. The synthesis of this helicene-like compounds will represent **the first part of the chapter 4**.

Helicenes are a family of polycyclic aromatic molecules that have interesting thermal electronic properties useful in optic and electronic devices (liquid crystals, polymers...) and also in biomedicine.¹⁹

In the second part of the chapter 4, we wanted to extend this methodology to heterocyclic alkynes (figure 1.13). The PKR adducts of pyridyl alkynes would afford after photochemical cyclisation, potential candidates for the synthesis of chiral phenanthroline ligands.

On the other hand, the thiophenyl derivative would be a potential candidate to undergo a reversible photocyclisation leading to family of photoswitchable compounds.

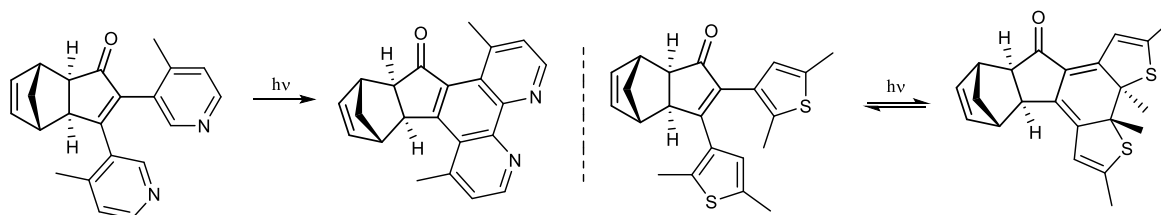


Figure 1.13.

The forth objective of the doctoral thesis was to determine if pyridyl and thiophenyl motive would be compatible with the PKR and also, to study the behaviour of these adducts under photochemical conditions.

To sum up, in the present doctoral thesis, we would focus on the intermolecular Pauson-Khand reaction with these three main objectives:

1. To study the regioselectivity of the intermolecular PKR of internal alkynes (chapter 2).
2. To synthesize new bioactive molecules such as sarkomycin and jasmonate using PKRs of internal alkynes (chapter 3).
3. To complete the study of helicene-like compounds prepared by PKR and to extend it to heterocyclic precursors (chapter 4).

References

- (1) Khand, I. U.; Knox, G. R.; Pauson, P. L.; Watts, W. E.; Foreman, M. I. *J. Chem. Soc. Perkin Trans. 1* **1973**, 977.
- (2) Huang, J.; Fang, L.; Long, R.; Shi, L.-L.; Shen, H.-J.; Li, C.; Yang, Z. *Org. Lett.* **2013**, *15*(15), 4018–4021.
- (3) McKerrall, S. J.; Jørgensen, L.; Kuttruff, C. A.; Ungeheuer, F.; Baran, P. S. *J. Am. Chem. Soc.* **2014**, *136*(15), 5799–5810.
- (4) Rios Torres, R. *Pauson-Khand Reaction: Scope, Variations and Applications*; John Wiley and Sons, 2012.
- (5) Bruin, T. J. M. De; Milet, A.; Gimbert, Y.; Greene, A. E.; Ledss, C. R.; March, R. V. *J. Am. Chem. Soc.* **2001**, No. 10, 7184–7185.
- (6) De Bruin, T. J. M.; Michel, C.; Vekey, K.; Greene, A. E.; Gimbert, Y.; Milet, A. *J. Organomet. Chem.* **2006**, *691*(20), 4281–4288.
- (7) Aiguabella, N.; del Pozo, C.; Verdaguer, X.; Fustero, S.; Riera, A. *Angew. Chem. Int. Ed.* **2013**, *52*(20), 5355–5359.
- (8) Vázquez-Romero, A.; Verdaguer, X.; Riera, A. *Eur. J. Org. Chem.* **2013**, *2013*(9), 1716–1725.
- (9) Fager-Jokela, E.; Muuronen, M.; Patzschke, M.; Helaja, J. *J. Org. Chem.* **2012**, *77*(20), 9134–9147.
- (10) Vázquez-Romero, A.; Cárdenas, L.; Blasi, E.; Verdaguer, X.; Riera, A. *Org. Lett.* **2009**, *11*(14), 3104–3107.
- (11) Vázquez-Romero, A.; Rodríguez, J.; Lledó, A.; Verdaguer, X.; Riera, A. *Org. Lett.* **2008**, *10*(20), 4509–4512.
- (12) Iqbal, M.; Evans, P.; Lledó, A.; Verdaguer, X.; Pericàs, M. A.; Riera, A.; Loeffler, C.; Sinha, A. K.; Mueller, M. J. *Chembiochem* **2005**, *6*(2), 276–280.
- (13) Aiguabella, N.; Pesquer, A.; Verdaguer, X.; Riera, A. *Org. Lett.* **2013**, *15*(11), 2696–2699.
- (14) Turro, N. J.; Schuster, G. *Science* **1975**, *187*(4174), 303–312.
- (15) Bach, T.; Hehn, J. P. *Angew. Chem. Int. Ed.* **2011**, *50*(5), 1000–1045.
- (16) Hoffmann, N. *Chem. Rev.* **2008**, *108*(3), 1052–1103.
- (17) Lledó, A.; Benet-Buchholz, J.; Solé, A.; Olivella, S.; Verdaguer, X.; Riera, A. *Angew. Chem. Int. Ed. Engl.* **2007**, *46*(31), 5943–5946.
- (18) Ji, Y.; Verdaguer, X.; Riera, A. *Chem. Eur. J.* **2011**, *17*(14), 3942–3948.

- (19) Gingras, M. *Chem. Soc. Rev.* 2013, 42(3), 1051–1095.

CHAPTER II

Study of the Regioselectivity of the Intermolecular Pauson-Khand Reaction

Contents

2.1 General introduction to the intermolecular Pauson-Khand reaction	9
2.1.1 Mechanism	9
2.1.2 Scope of the reaction	10
2.1.3 Improvement of the Pauson-Khand reaction	11
2.3.4 Catalytic Pauson-Khand reaction	12
2.1.5 Asymmetric Pauson-Khand reaction	12
2.1.6 Selectivity in the Pauson-Khand reaction	19
2.2 Results and discussion	27
2.2.1 Design of the internal alkynes	28
2.2.2 Synthesis of the internal alkynes	29
2.2.3 Synthesis of the Pauson-Khand adducts	35
2.3 Conclusions	47

2.1 General introduction to the intermolecular Pauson-Khand Reaction

In the present chapter, we will describe the main accomplishments and improvements regarding the reactivity, stereoselectivity of the reaction as well as the different procedures, catalytic and asymmetric versions to perform the intermolecular PKR.

2.1.1 Mechanism

Since its discovery,¹ the mechanism of the PKR has been the subject of several studies. Magnus et al. first proposed the currently accepted mechanism for the stoichiometric reaction in 1985 to rationalize the regio and stereochemical outcome observed in numerous PKR examples (figure 2.1).²

The recent advances in theoretical chemistry permitted Nakamura in 2001³, Pericàs in 2002⁴ and Gimbert in 2004⁵ to support the main features of the proposed mechanism. Nevertheless, there still are some mechanistic steps that need to be deeply studied.⁶

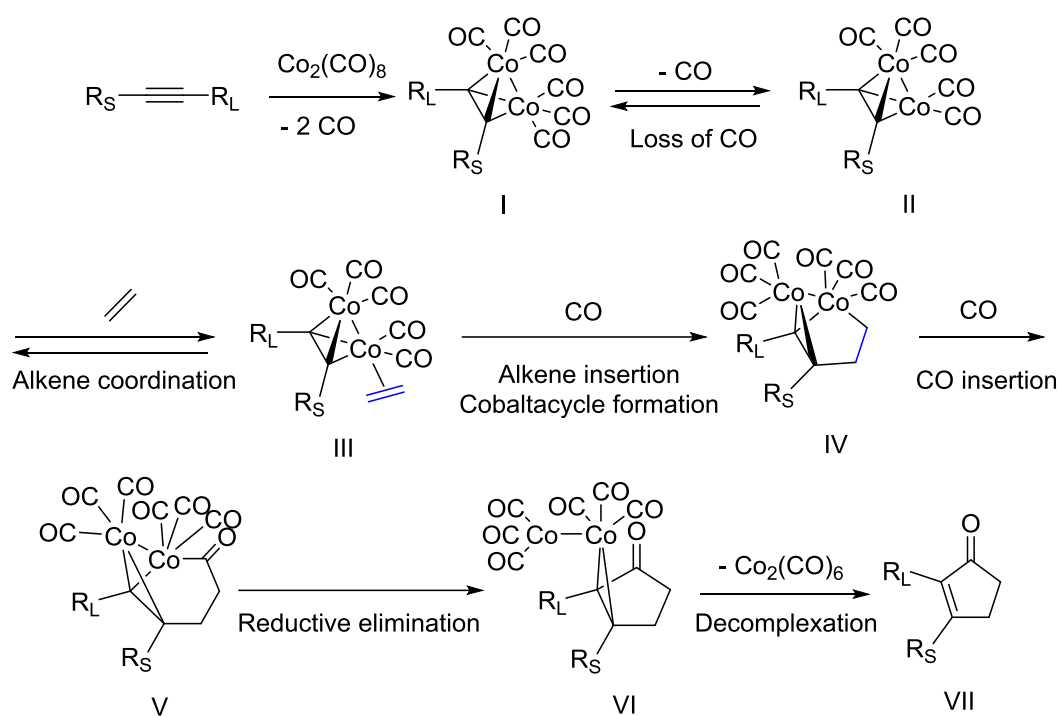


Figure 2.1. Magnus' mechanism for the stoichiometric PKR.

The first step of this mechanism corresponds to the coordination of the alkyne to $Co_2(CO)_8$, with the subsequent loss of two CO molecules to form a generally stable and isolable tetrahedral dicobalt-alkyne complex. The complex I will suffer the loss of another carbonyl ligand that generates a transitory coordination vacant which can then coordinate the alkene, affording complex III. This step, strongly endothermic, is the rate-determining step which consequently can be accelerated by the usage of promoters such as amine N-oxides are commonly used.^{7,8} The alkene insertion takes place into the sterically least hindered Co-C bond, leading irreversibly to cobaltacycle IV. Since both the regio- and the stereochemistry of the final product is established during that stage, this is actually the product determining

step. The regio- and the stereo-chemistry will be reviewed in the present chapter. After the coordination with a CO ligand (complex **IV**) and its insertion, the acyl cobalt complex **V** is formed. The cyclopentenone **VII** is finally released by reductive elimination followed by decomplexation.

In 2014, Gimbert and co-workers have questioned the origin of CO in the final product through computational and mass spectrometry experiments.⁶ They suggested that the insertion of the CO ligand in complex **IV** to acylcobaltacycle **V** is not likely coming from an external CO addition but probably from the intramolecular migration of one CO of the complex. They conclude that still complementary studies are needed to elucidate important steps of the mechanism.

2.1.2 Scope of the reaction

The scope of the reaction depends on steric and electronic effects introduced by both the alkyne and alkene. Sterically hindered substrates tend to be low yielding, and terminal alkynes are known to react easier than internal alkynes. While the PKR tolerated many functionalised alkynes, such as halides, tertiary amines, acetals, esters, amides, ethers, alcohols, carbonyls,⁹ the alkene use is extremely restricted. Although there are exceptions, in general olefins without strain hardly react in the intermolecular PKR whereas good reactivity is observed with strained cyclic alkenes such as cyclopentene, cyclopropene, norbornene, norbornadiene. Exceptionally, ethylene and allene react with good yield. The medium sized trans-cycloalkenes were reported in our group to proceed in good yields in the intermolecular PKR.¹⁰

First proposed by Pericàs and co-workers, this reactivity could be explained in the formation of cobaltacycle **IV**, where the olefin change of hybridization from sp^2 to sp^3 releasing its strain.⁴

In 2010, our group confirmed and further explored those results.¹¹ In all these studies, a clear correlation between the exothermic character of the cobaltacycle formation step and the olefin strain was observed.

The theoretical studies of Greene, Gimbert and co-workers have studied the reactivity of the alkenes from molecular orbital perspective.⁵ According to their study, the reactivity of the alkenes is directly related to the back donation of the electrons from the d orbitals of the cobalt atom to the lowest unoccupied orbital (LUMO), π^* orbitals of the alkene substrate. In general, the lower the LUMO of the alkene is, the greater the back donation of the cobaltacycle would be and therefore, the higher the reactivity of the alkene will be. The study also shows that a correlation exists between the C=C-C angle of the alkene (cyclohexene 125°, cyclopentene 112°, norbornene 107°) and the energy level of its LUMO: the smaller the angle is, the lower the LUMO energy would be. Sterically hindered alkenes are disfavoured which yields in many cases to moderate results. In 2012, it was found in our group that steric bulky norbornene ring such as tetramethylnorbornadiene enforces an extremely high diastereoselectivity toward the *exo*-cyclopentenone in good yield.¹²

2.1.3 Improvement of the PKR

To overcome limitations linked to the use of high temperature, pressure and long reaction time, many modifications have been developed.¹³ They mainly involve improvement of the reaction efficiency by promoters^{7,8,14}, the development of catalytic^{15,16} and asymmetric versions.^{17,18}

2.1.3.1 Use of additives

The first decarboxylation of the complex **I** (figure 2.1) is highly endothermic and so it requires high reaction temperature. Many methods emerged over the decades to facilitate the coordination of the alkene into the cobalt centre, such as the uses of physical means, oxidative, non-oxidative promoters, single electron transfers and other metals.

Focusing on the use of physical promoters to accelerate the rate of the PKR, the first significant achievement was done by Smit and co-workers in 1986 with the dry support adsorption conditions (DSAC) on silica or alumina.¹⁹ Adsorbing the cobalt-ene-yne complex over a solid support and heating it mildly, decreased reaction times of the intramolecular PKR and yields were much better than under standard thermal conditions. Later on, this methodology was expanded to the intermolecular PKR.²⁰ The authors proposed that the donor sites at the surface of the solid support could facilitate the ligand exchange process, therefore increasing the PKR rate.

The use of molecular sieves has also gained ground over the past few years.²¹ These zeolites are supposed to work as micro-reactors, bringing together the alkene and the alkyne-cobalt complex, therefore facilitating the PKR.

The other physical promoters later developed in the PKR were ultrasounds by Pauson in 1988²² and microwaves by Evans in 2002.²³

Independently developed by Jeong²⁴ and Schreiber⁷, the use of amine N-oxides became the most popular way to afford high yields within a shorter reaction time.

N-oxides act by oxidizing one CO ligand to CO₂ creating the desired vacant coordination site in the cobalt complex for the alkene coordination.²⁵ The most popular amine N-oxides are N-methylmorpholine N-oxide (NMO) and trimethylamine N-oxide (TMANO) (figure 2.2).²⁶

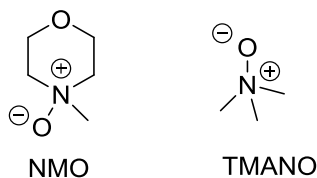


Figure 2.2. Most used N-oxides promoters in the PKR.

Other additives such as sulfides¹⁴ thioureas²⁷, phosphane sulfides²⁸ are also reported to accelerate the PKR.

2.1.4 Catalytic PKR

Since the original protocol for the PKR required over stoichiometric amount of a metal complex, Pauson himself in 1973, performed the first example of catalytic PKR using catalyst loading >10 mol%.¹ Nonetheless, the PKR afforded 14% yield and was restricted to norbornene or norbornadiene and acetylene (figure 2.3).

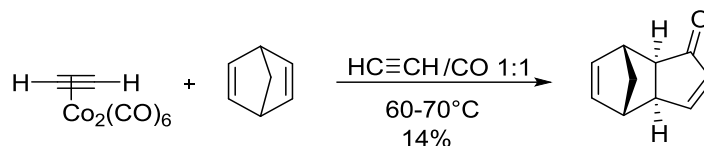


Figure 2.3. Early example of catalytic intermolecular PKR by Pauson.

Later on, great improvements have reduced significantly the catalyst loading but still using harsh reaction condition of CO pressure and temperature. For example, in 1990, Rautenstrauch *et al.* reported the first satisfactory result of the catalytic PKR to reach 47% yield of the PK adduct with 0.0022 equivalent of catalyst with 100 barg CO pressure at 150°C (figure 2.4).²⁹

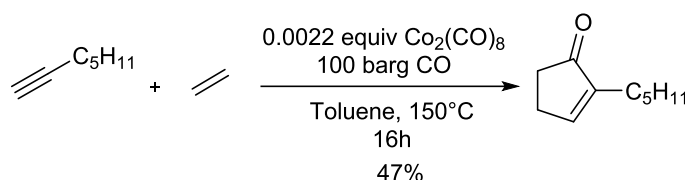


Figure 2.4. Rautenstrauch's example of catalytic PKR.

To allow alkene coordination, the loss of CO ligand is necessary. In that particular case, employing such high pressure was disfavoured the PKR, reason why high temperature was needed and moderate yield observed. Riera and Verdaguer examined the kinetic study of the catalytic intermolecular PKR with $\text{Co}_2(\text{CO})_8$. They demonstrated that low pressure (2 up to 4 barg) was important to perform catalytic PKR in good yields.³⁰

2.1.5 Asymmetric PKR

Extensive efforts have been devoted to prepare optically pure PK adducts. Depending on the substitution group present in the alkene, its alkene insertion leads to two new stereogenic centres.

In general, the asymmetric control is done either by the chiral substrates, or by the reagents that transfer their chiral information to the cyclopentenone. These categories use chiral auxiliaries, chiral promoters or chiral ligands that are going to be explained in the present section. Although most of examples correspond to intramolecular PKRs, we will focus the discussion on the intermolecular PKR.³¹

2.1.5.1 Chiral promoters

The use of chiral promoters as source of chirality in the PKR permits a straight control of the enantioselectivity. This approach was the first to enable the synthesis of enantiomerically enriched products from the intermolecular PKR. The promoter performs a selective decarbonylation of one CO ligand in the metal cluster, generating an optically enriched cyclopentenone after the cyclization. Even though the early examples were not practical and far to be general, it was found that chiral N-oxides such as brucine N-oxide, a bulky amine, afforded good enantioselectivities in some cases (figure 2.5).^{32,33}

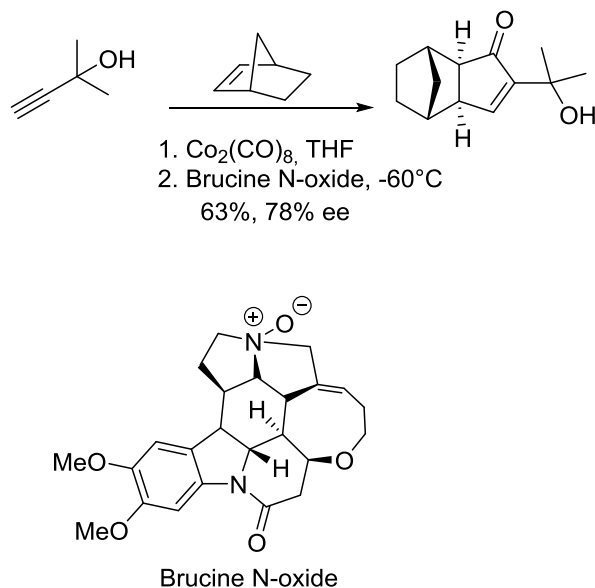


Figure 2.5 Example of the use N-oxide chiral promoter for the asymmetric intermolecular PKR.

2.1.5.2 Use of chiral auxiliaries

The action mechanism of chiral auxiliary favours one of the possible diastereomeric transition states, leading to an enantio enriched product after cleavage of the chiral source. The works of Moyano, Riera, Pericàs and co-workers in the PKR described for the first time the use of chiral auxiliaries bonded to the alkyne. They developed numerous chiral auxiliaries such as sulfoxides,³⁴ sultames,³⁵ oxazolidinones³⁶ and alkoxyacetylene camphor derivatives³⁷ (figure 2.6).

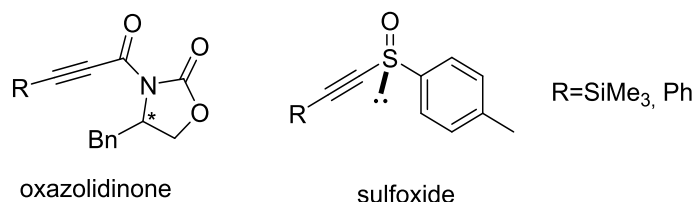


Figure 2.6. Examples of chiral auxiliaries such as oxazolidinone and sulfoxide.

Their important contribution to the field was further followed by the design of an improved auxiliary equipped with suitable chelating atoms such as the sulfur and nitrogen atoms to increase the selectivity.

They act by transferring their chirality to the cobalt cluster by coordinating to one the cobalt atoms and promoting the diastereoselective coordination of the alkene. Theoretical and experimental studies have been undertaken to understand how the camphor derived sulfur auxiliary worked in the asymmetric discrimination (figure 2.7).²⁶

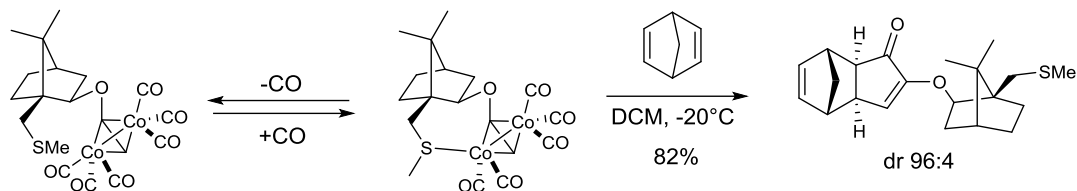


Figure 2.7. Example of camphor sulphur auxiliary for the asymmetric intermolecular PKR.

These studies revealed that norbornadiene coordinated to the cobalt atom bound to the sulphur and further theoretical studies established that the coordination occurred by the loss of the sulfur ligand generating a vacant orbital. The chiral auxiliary is considered hemilabile since it can coordinate or de-coordinate directing the alkene to one precise cobalt atom.

On the other hand, combining the reactivity of the amide with camphor sultame framework, the level of selectivity and the yield for the PKR reached a maximum efficiency with the family of N-(2-alkynoyl)sultams represented in figure 2.8.³⁵ The PK adduct was 93% of yield and a diastereomeric ratio of 800:1 detected by HPLC.

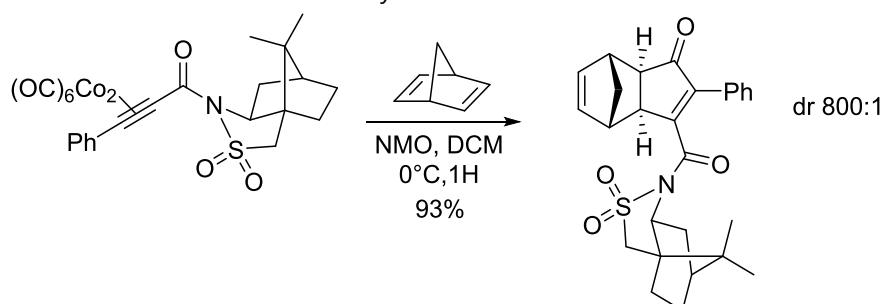


Figure 2.8. Example of high diastereoselectivity obtained in PKR with N-(2-alkynoyl)sultams and NBD.

Less popular, the use of chiral auxiliaries bonded to the alkene have also been studied in the asymmetric intermolecular PKR. Carretero and co-workers, introduced the use of chiral sulfoxides for the PKR of non-strained alkenes.³⁸ They could achieve moderate yield and high diastereoselectivity which can be explained by the proximity of the chiral sulfur atom to olefin (figure 2.9). After conjugated addition over the cyclopentenone, the sulfoxide auxiliary can be easily removed heating up to toluene reflux.

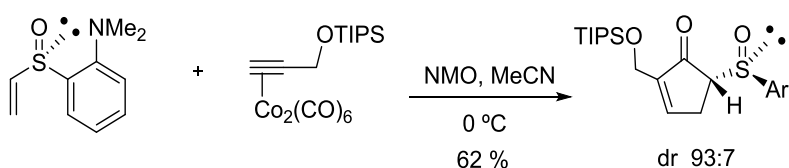


Figure 2.9. Example of Carretero's chiral sulfoxides.

2.1.5.3 Use of chiral ligands

Taking into account the mechanism of the PKR, the modification of the environment of the metal by a chiral ligand will permit an easy differentiation of the two cobalt atoms of its complex leading to the preferential formation of one enantiomer rather than the other. To clearly explain how the chiral ligand would act in the intermolecular PKR, some mechanistic details will be presented.

Based on the mechanism proposed by Magnus², when a terminal alkyne and norbornadiene coordinate to the cobalt cluster, the four possible pathways can be involved to yield to the final cyclopentenone. Each cobalt complex **II** lead to the formation of two cobaltacycles **III**: anti and syn when the coordination takes place through the less hindered face of the olefin leading to *exo* diastereomers. The *endo* diastereomers would come from the insertion to the opposite (more hindered) face of the olefin. Solely taking into account the formation of the *exo* diastereomers, these pathways can be found in figure 2.10.

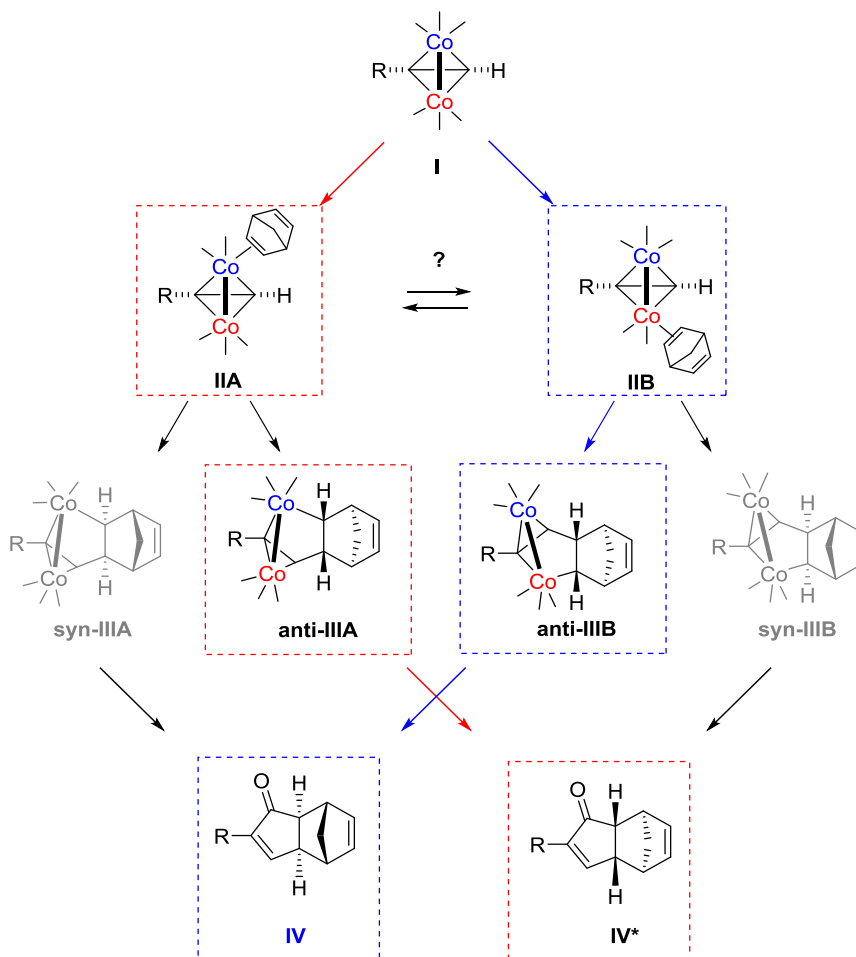


Figure 2.10. Mechanistical pathways leading to cyclopentenone enantiomers **IV**. For simplification, CO ligands have not been represented.

Once the cobalt complex **I** loses a CO ligand, a coordination vacant is generated and norbornadiene coordinates to the cobalt atom. The alkene can then coordinate indistinctly to any of the two cobalt atoms, yielding **IIA** or **IIB**. Preferentially, the alkene insertion then takes place in the less hindered Co-C bond. However, when inserting the norbornadiene into Co-C bond, it has now two different ways which can form two different complexes: the **syn** or the **anti** (**syn-IIIa**, **anti-IIIa**, **syn-IIIb** and **anti-IIIb**). Then, the latter 4 forms isomers give the enantiomers **IV** and **IV***. Indeed, both **anti-IIIa** and **syn-IIIa** lead to the different enantiomers **IV***. In 1999³⁹ and 2010⁴⁰ mechanistic studies have demonstrated that **anti** cobaltacycles are more stable and therefore they are preferentially formed than the **syn** ones. Therefore, selective coordination to one of the cobalts usually leads to good enantioselectivity.

It is back in 80's that the use chiral ligands in the PKR were imagined by Brunner and Pauson introducing the glycerol derived monophosphine, GLYPHOS as desymmetrizing element.⁴¹ The complexation reaction yielded a diastomeric mixture of the two alkyne cobalt complexes in a 6:4 ratio. Each diastereomer was then separated by chromatography and subjected to the PKR with norbornene. It gave the opposite enantiomer of the desired cyclopentenone with excellent enantiomeric excess of 90% ee at 45°C (figure 2.11).

In this procedure, high temperatures induced the racemization of the complex. In addition, simply mixing the hexacarbonyl complex with optically pure GLYPHOS to perform the PKR led to racemate final product.

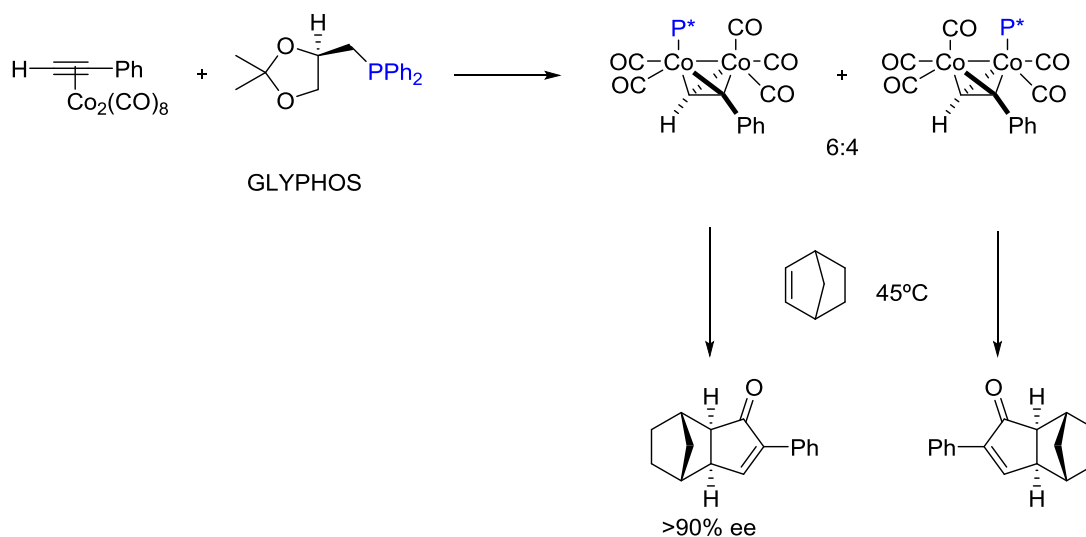


Figure 2.11. Asymmetric PKR with GLYPHOS.

Later on, Kerr *et al.* used this approach with an N-oxide activation which permitted to obtain good enantiomeric excess and increase the yield of reaction.⁴² However, the differentiation of the two cobalt atoms by the ligands was not possible to achieve, until the development of the bidentate ligands which made finally accessible the diastereoselective synthesis of the cobalt complexes.

Numerous monodentate ligands were first studied, taking into account the positive impact of the chelation to the metal complex. BINOL-derived monodentate phosphoramidites developed by Gimbert, have the chiral carbon backbone which can be modified and used in the intermolecular PKR (figure 2.12).⁴³

Even though the yields were good, the enantioselective excesses reported were low in all cases below 40% ee.

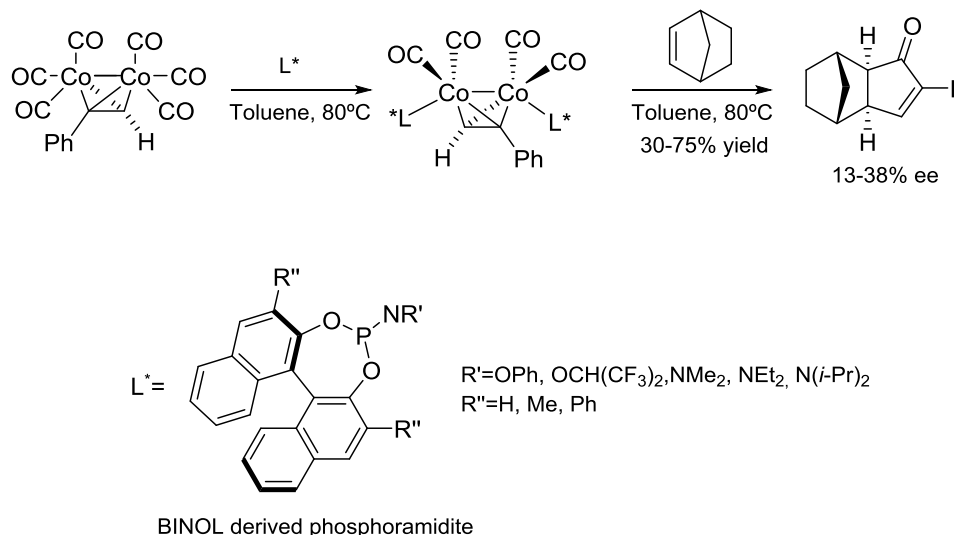


Figure 2.12. BINOL-derived monodentate phosphoramidites used in asymmetric PKR.

In 2000, Riera and Verdaguer prepared a series of bidentate P,S ligands with chiral backbone such as PuPHOS, derived from (+)-pulegone and various CamPHOS derivatives from the camphor (Figure 2.13).^{44,45,46,47} Through the phosphorus and the sulfur atoms, these complexes coordinate a bridged mode between the two cobalt atoms.

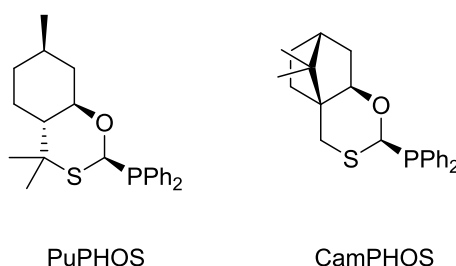


Figure 2.13. Hemilabile P,S ligands.

The complexation of a series of hexacarbonyl alkynes with PuPHOS yielded bridged cobalt complexes in a range of 4.5:1 ratio that could be separated by crystallisation. The major diastereomers reacted with NBD and NMO as promoter giving excellent yields and high enantioselective ratios depending on the ligands and reaction conditions used.

Subsequently, in our research group, new ligands for the asymmetric PKR bearing a chiral sulfinamide bridging the phosphorus and sulfur were introduced.^{48,49} PNSO ligands stand for N-phosphino sulfamide since phosphorous, nitrogen, sulfur and oxygen atoms are placed in a row. The phosphorous atom would provide strong binding to the cobalt center while the sulfur contains the chiral information. The nitrogen atom would act as a liaison element, transmitting the chiral information through the ligand (figure 2.14).

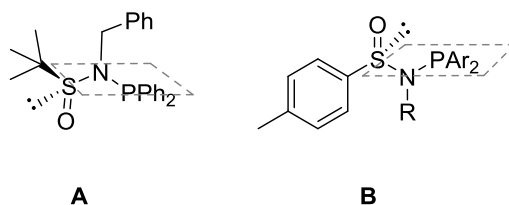


Figure 2.14. Two different families of PNSO ligands.

This improved generation of P,S ligands could be readily available as both enantiomers and usually provide high diastereoselectivity (up to 20:1). These hemilabile family is easier to synthesise, versatile and highly tunable (figure 2.15).

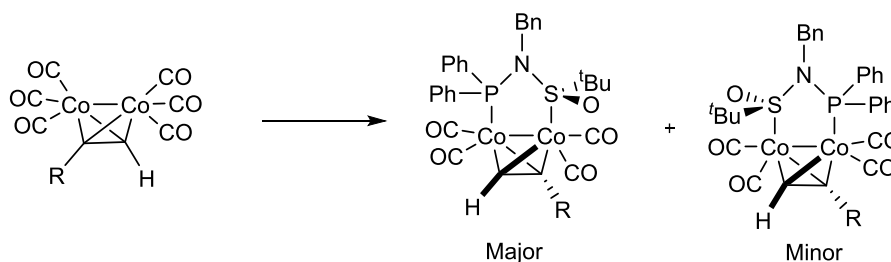


Figure 2.15. Scheme of the synthesis of the diastereomeric P,S cobalt ligands.

Although, these ligands provide excellent selectivity in the stoichiometric intermolecular PK, the selectivity drops dramatically in a catalytic system. Recently, our group developed a new family of chiral bis-phosphanes named ThaxPHOS containing oxazaphospholidine unit (figure 2.16).³¹

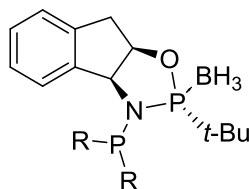


Figure 2.16. ThaxPHOS ligand.

They were successfully applied in the first asymmetric intermolecular and catalytic PK reaction described so far. However, the reaction is very limited in scope being useful only in the reaction of norbornadiene and trimethylsilylacetylene (figure 2.17).

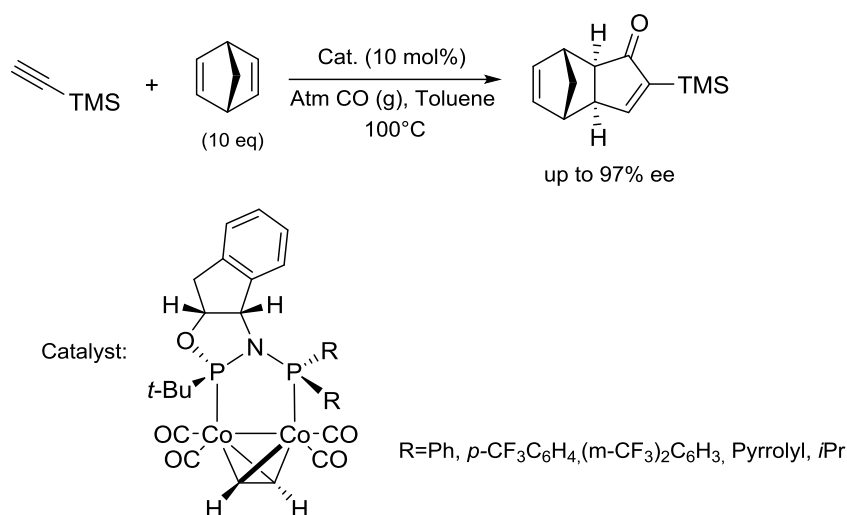


Figure 2.17. Example of asymmetric PKR using ThaxPHOS ligand.

2.1.6 Selectivity in the Pauson-Khand reaction

2.1.6.1 Stereoselectivity: *endo/exo*

For bicyclic symmetrical alkenes, two products can be obtained, the *endo* and the *exo* PK adducts. The formation of one or the other isomer depends on the insertion face of the alkene into the Co-C bond from complex II to III (figure 2.18).

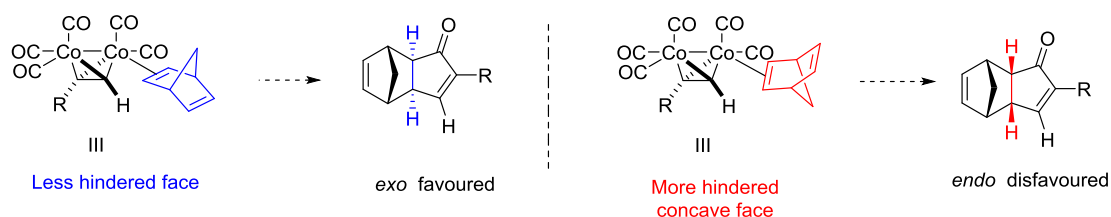


Figure 2.18. Faces of insertion of the alkene.

In general, the insertion step takes place by the less hindered face of the alkene, yielding to the *exo* PK adduct in a high stereoselective ratio. The example of trimethylsilyl ethyne which reacting with norbornadiene afforded almost exclusively the *exo* adduct in a 99:1 ratio (figure 2.19).

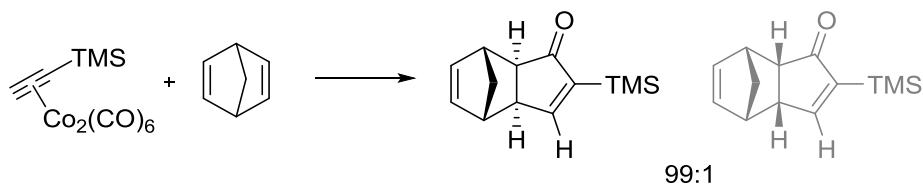


Figure 2.19. Example of high stereoselectivity in PKRs of trimethylsilyl ethyne with norbornadiene.

It was noticed that during the catalytic PKR, substantial amounts of *endo* adduct can be detected while stoichiometric PKR gave usually higher stereoselective outcome.²²

2.1.6.2 Regioselectivity of the alkyne

The regioselectivity of the intermolecular PKR of non symmetrical internal alkyne is one of the most complicated issue. Indeed, depending how the alkene inserts into the cobalt cluster, regiochemical outcomes change. Generally, symmetrical alkynes are used in the intermolecular PKR.

Once the complex **III** is formed, the alkene must insert into one of the two Co-C bonds to form complex **IV**. It has been established that the regiochemistry of the reaction is as well controlled by steric and electronic factors induced by the alkyne. Regarding to the steric effects, preferentially the alkene insertion takes place into the Co-C bond bearing the smaller substituent (R_S in figure 2.20) placing consequently, the largest substituent (R_L in figure 2.30) in α of the ketone in the final cyclopentenone **VII**.

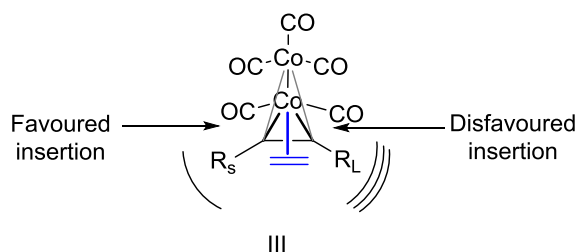


Figure 2.20. Possible insertion sites for the alkene.

In general, the largest the difference in size of the substituents is, the larger the selectivity will be. In practice, when terminal alkyne is used, the regioselectivity outcome affords a single cyclopentenone with the substituent in α to the carbonyl group^{29,50,51,52} whereas unsymmetrical alkyne leads a mixture of two regioisomers called α - and β -Pauson-Khand adducts (figure 2.21).⁵³

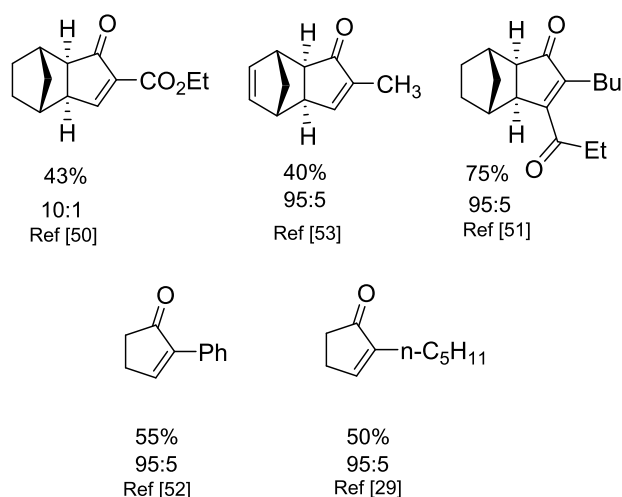


Figure 2.21. Example of high regioselectivity in the intermolecular PKR.

The use of unsymmetrical alkyne makes more difficult to predict the regiochemical outcome of the PKR that can generate a mixture of constitutional isomers in variable proportions.

Considering the electronic effects, electron donating alkyne groups (EDG) tend to end up in α -position of the cyclopentenone, while electron withdrawing alkyne groups (EWG) have a preference for the β -position (figure 2.22).

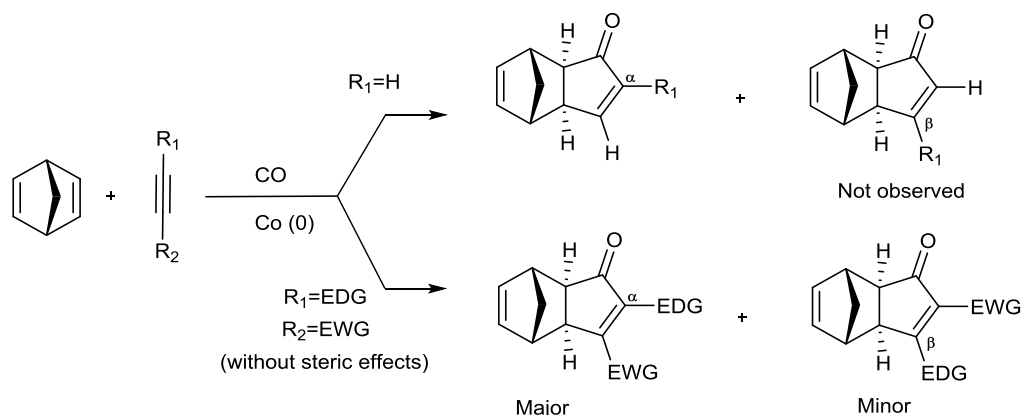


Figure 2.22. Regiochemical outcomes of the intermolecular PKR using norbornadiene and varying the nature of the alkyne.

In 2001, to rationalize the regio guidance phenomena involving the substituents of the alkyne in the reaction, Gimbert, Greene and co-workers undertook the first computational calculation.^{54,55} The theoretical study supported the fact that electron-donating groups would prefer the α -position of the ketone and electron withdrawing groups would be more favourable to the β -position. However, their main example shown in figure 2.23 was proved (years later by Helaja and our group) to be wrong yielding a mixture of isomers in 1,3:1 and 2.5:1.⁵⁶

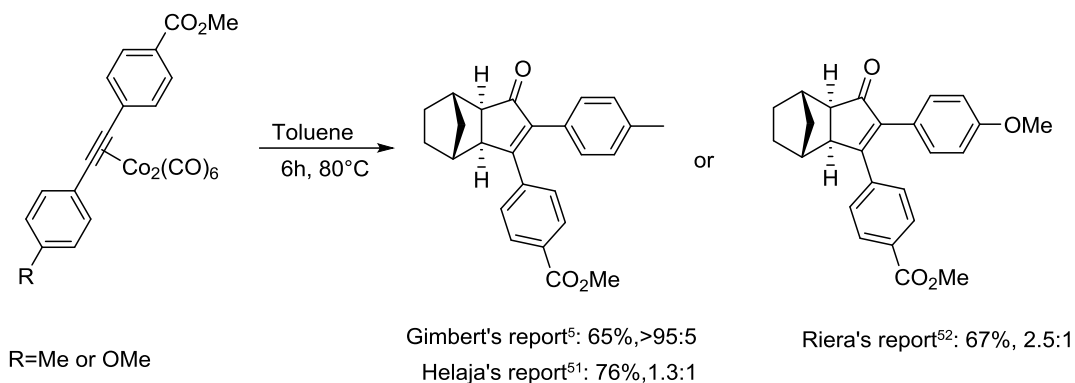


Figure 2.23. Regioselectivity of diarylalkynes with NBN: Gimbert, Riera and Helaja's results.

Their calculations showed that the initial C-C-bond is formed with the more electron rich carbon of the cobalt cluster according to the NBO charges (Natural Bonding Orbital) due to its carbon bond polarization (figure 2.24).⁵⁵

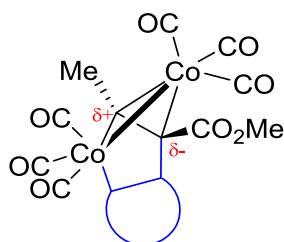


Figure 2.24. Polarisation of the complex of the alkyne.

Somewhat surprisingly, the electron-withdrawing group induces a greater electronic density to the attached carbon which will form the new C-C bond. In other examples, it is shown that the electronic influence of the substituents is not strong enough to overcome steric effect, thus, the substituents provoke only a weak polarisation of the alkyne and mixture of isomers was observed (figure 2.25).⁵⁰

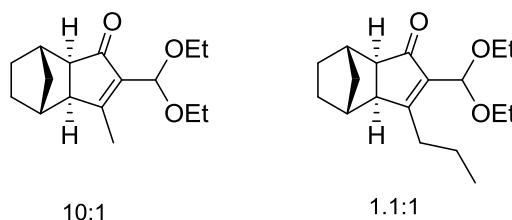


Figure 2.25. Examples of duality between steric and electronic effects with disubstituted alkynes with acetal and alkyl chain.

In our group, a total regioselectivity was found using the trifluoromethyl group and NBD. Surprisingly, the strong electron-withdrawing effect is widely overlapped by steric hindrance, leading to the formation of a single α -regioisomer (figure 2.45).⁵⁷

Interestingly, when Konno and co-workers worked on similar trifluoromethyl substrates but using NBN instead of NBD, regioselectivities were high but not total like shown in the figure 2.26.

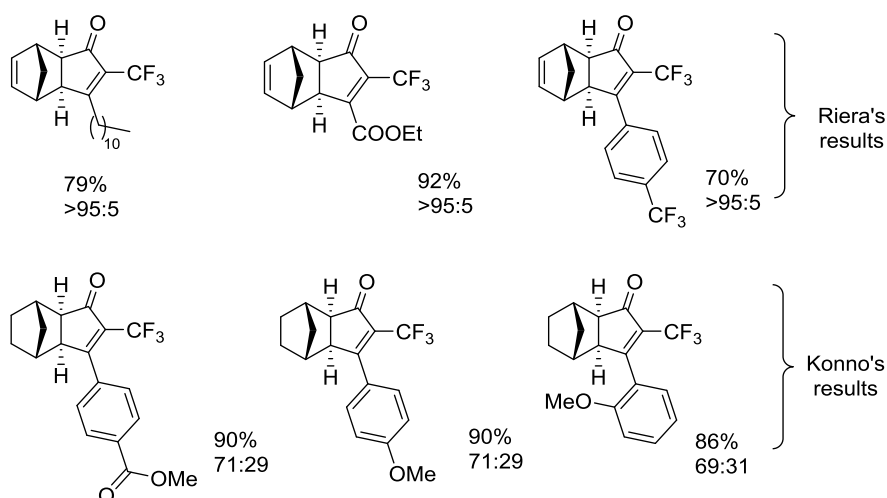


Figure 2.26. Examples of PKRs of trifluoromethyl-substituted alkyne with NBD⁵⁷ and NBN⁵⁸.

These cases reveal the complexity to predict the regiochemical outcome and show that the reactivity of the NBD slightly higher than the NBN, influences as well the regio guidance of the intermolecular PKR.⁵⁸

Fairlamb *et al.* in 2011 undertook a study of the regioselectivity of heteroaromatic internal alkynes, sterically similar but electronically different.⁵⁹ They could identify a series of alkynes that were favouring either α or β -isomers (figure 2.27).

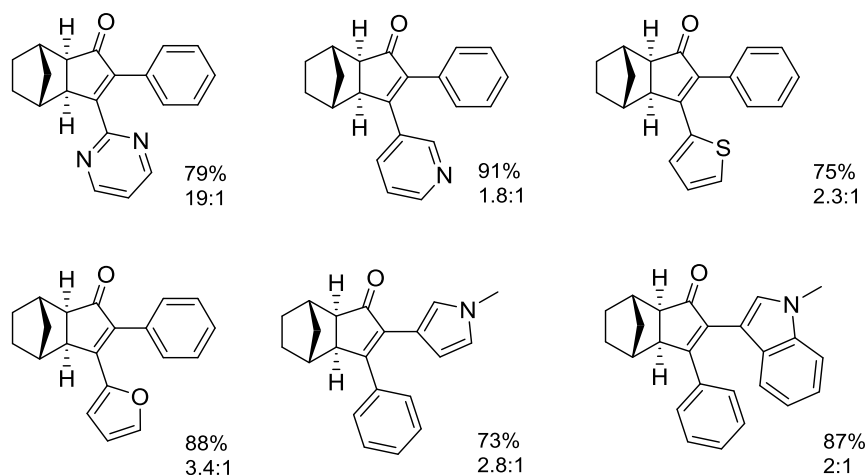


Figure 2.27. Examples of regioselectivity of heteroaromatic diarylalkynes.

Their study showed the difficulty to understand the electronic role of the substituents in the PKR. Even though their regiochemical outcomes could be in part explained by the Gimbert's prediction, they identified that the nature of the heteroaromatic group influenced the selectivity. The heteroatom itself and its position in the alkyne also played a role in the regiochemical outcome, stabilizing the cobalt cluster.

Taking into account the Fairlamb's experiments of sterically similar groups but electronically different, Helaja and co-workers focused their attention on the electronic effect of sterically equivalent diaryl alkynes. Rather than direct polarisation of the cobalt cluster previously proposed by Gimbert's calculations (really difficult to obtain),⁵⁴ Helaja and co-workers proposed to investigate the direct polarisation of the alkyne carbons (C2-C3) and the α -carbons (C1-C4) (figure 2.28).

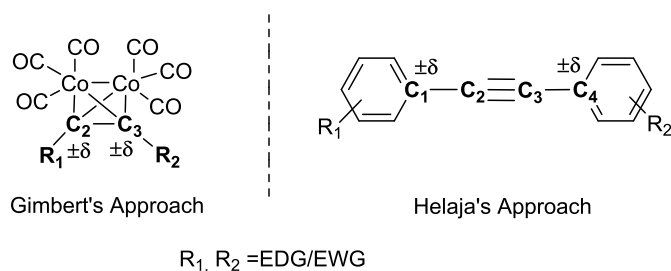


Figure 2.28. Atoms used to predict the regioselectivity of the intermolecular PKR.

They found that the regioselectivity correlates well with the direct polarisation of the alkyne carbons (C2-C3) and also with the cobalt cluster Gimbert's prediction. Moreover, better correlation was observed with the polarisation of the α -carbon C1-C4 of the alkyne.

Indeed, the C-C bond is formed with the more electron rich alkyne carbon C2 or C3 according to the Natural Bonding Orbital charges (NBO). Thus, with an EDG/EWG groups, the electrons are pulled by resonance effect along the system inducing an electronic difference within C2-C3 carbons respectively the opposite than around the C1-C4 carbons (figure 2.29).

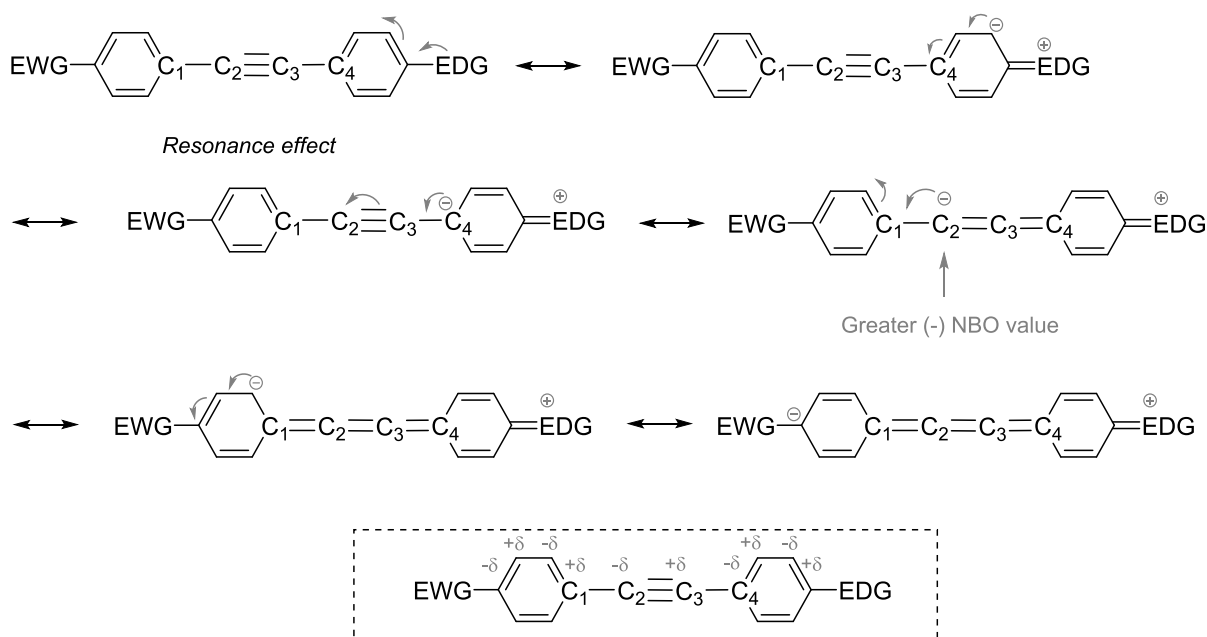


Figure 2.29. Relative alkyne polarisation induced by resonance effect.

By DFT calculations, the measurement of NBO relative values around C2-C3 indicates that if the difference $\Delta(C2-C3)$ NBO values is negative, it means that the richer atom would be C2, the one involved in the C-C bond formation which will place the C2 group in β of the final cyclopentenone and the C3 group in α -position.

Then, considering the $\Delta(C1-C4)$ NBO values, it would afford opposite result than $\Delta(C2-C3)$. For example, if the difference $\Delta(C1-C4)$ NBO values is negative, it means that C1 is richer in electron than C4, which in turn makes the C2 carbon weaker in electron and C3 richer affording the C3 group in β of the final cyclopentenone.

Thus, Helaja's group measured the NBO values in the C2-C3 and C1-C4 carbons of the alkynes and experimentally reacted para and meta-functionalized functionalized diarylalkynes with norbornadiene to afford a mixture of α/β -PK adducts (figure 2.30).

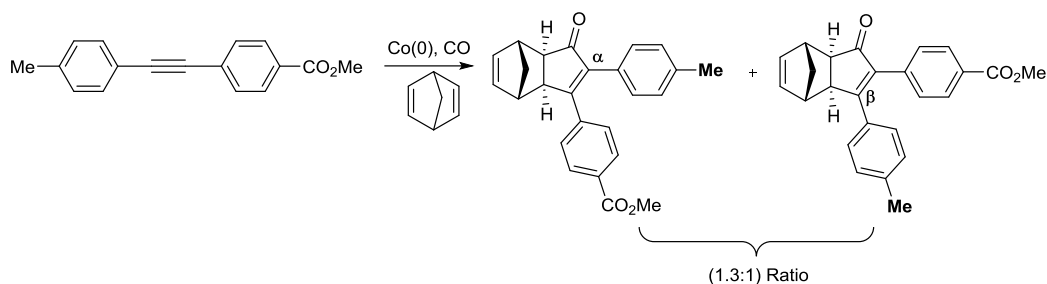


Figure 2.30. Example of the regioselectivity of the PKR of functionalized diarylalkynes.

To explain the study, several examples of the para functionalized diarylalkynes were selected and are shown in figure 2.31 and table 2.1.

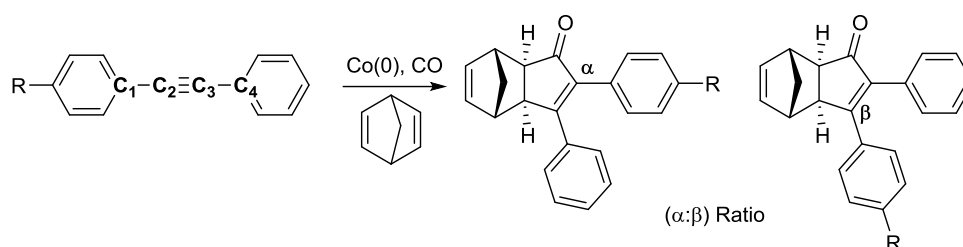


Figure 2.31. Helaja's model for the understanding of the regioselectivity of the PKR of functionalized diarylalkynes.

The correlation between the regiochemical outcomes and the NBO values was analysed and compared in the tables below. Experimentally, the introduction of EDG substituent in para of the alkyne slightly favoured the α isomer (table 2.1, entry 1).

The DFT calculation of $\Delta(C2-C3)$ NBO charges was positive which meant that the C3 carbon had a richer electronic density than C2 carbon, favouring the C-C bond formation in the C3 position which in turn would place in α of the cyclopentenone the EDG group. When the $\Delta(C1-C4)$ NBO charges was calculated, it gave a negative value, indicating that the electronic density was higher in C1 in good agreement with the fact that C2 carbon had lower electronic density than C3 carbon.

Entry		(α : β) Ratio	C1	C2	C3	C4	$\Delta(C1-C4).10^{-2}$	$\Delta(C2-C3).10^{-2}$
1		1.6:1	-0.152	0.01302	-0.00287	-0.12099	-3.1	1.59
2		1:1.25	-0.10042	0.00115	0.02759	-0.12885	2.84	-2.64
3		1:1.3	-0.10588	-0.00224	0.02903	-0.12922	2.33	-3.13
4		1:2	-0.10645	-0.01172	0.04369	-0.1331	2.67	-5.5

Table 2.1. Table of the experimental and computational results of Helaja's approach.⁵⁶

The introduction of EWG substituents in para or meta slightly favoured the β isomer (table 2.1, entries 2-4). Indeed, the $\Delta(\text{C2-C3})$ NBO charges was that time negative, indicating that the C2 carbon had a higher electronic density than the C3 carbon favouring the EWG group in β of the cyclopentenone. In the case of the $\Delta(\text{C1-C4})$ NBO charges, it gave a positive value, indicating that the electronic density was higher in C4 carbon in good agreement with the fact that C3 carbon had lower electronic density that C2 carbon. We can notice that the $\Delta(\text{C1-C4})$ gave more accurate results regarding regiochemical outcomes than $\Delta(\text{C2-C3})$ NBO values. Indeed, the $\Delta(\text{C1-C4})$ compared to $\Delta(\text{C2-C3})$ NBO values reflected better the α/β ratios. The $\Delta(\text{C1-C4})$ values around 2.33 to 2.84 were more accurate than $\Delta(\text{C2-C3})$ which oscillated between -3 to -5.

Even though the α/β -regioisomer ratios observed were lower than expected (up to 1:2) the slight excesses were in good accordance with the hypothesis that α -alkyne polarization dictated the α/β -regioselectivity of the final cyclopentenones except for some cases. Although some values were overestimated, the $\Delta(\text{C1-C4})$ and $\Delta(\text{C2-C3})$ NBO values qualitatively predicted the experimental results. It was noticed that $\Delta(\text{C1-C4})$ NBO charges correlated to regiochemical outcome more accurately than $\Delta(\text{C2-C3})$ (figure 2.32).

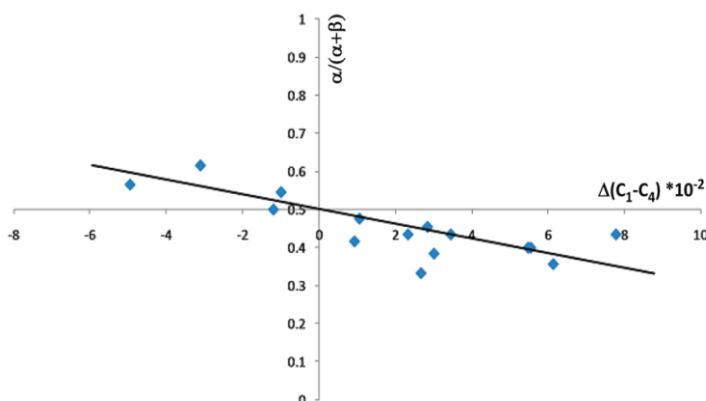


Figure 2.32. Correlation between the $\Delta(\text{C1-C4})$ NBO values and the regioselectivity.

Moreover, comparing the Hammett values of each substituent with the α/β -regioisomer ratios were qualitatively correlated expected for the aryl group bearing OMe and Me groups (figure 2.33). The Hammett value being a parameter that indicates the relative electronic character of substituents.

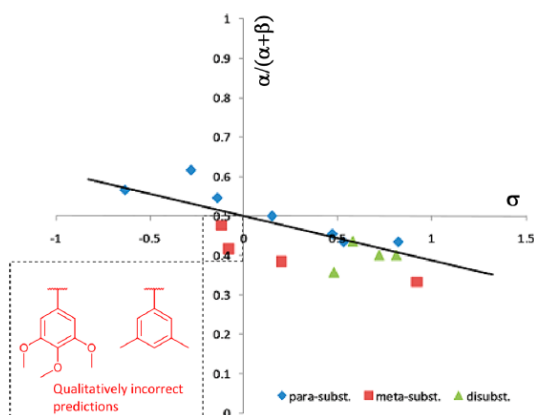


Figure 2.33. Correlation between the Hammett value with the regioselectivity.

Their hypothesis was based on the fact that the polarisation of an alkyne can take place by the resonance and inductive effects. In the case of resonance effect described in the figure 2.34, the pushing of electrons from the substituted aryl induced the delocalisation of the electron of the triple bond toward the C3.

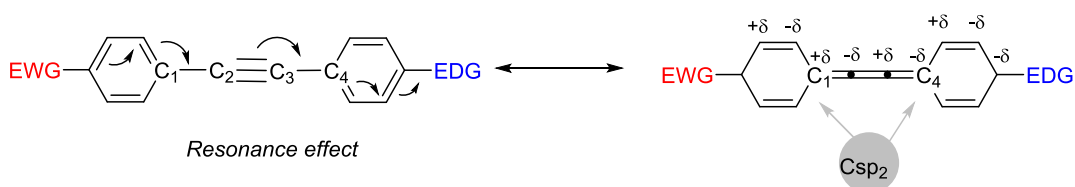


Figure 2.34. Resonance effect inducing the regioselectivity in diarylalkyne.

They have concluded that in the intermolecular PKR, the alkyne polarization was mainly the result of the sp_2 -hybridized propargylic carbon induced by resonance effect of the EDG/EWG substituents.

We planned to perform a similar study of the regioselectivity of disubstituted aliphatic unsymmetrical alkynes in the intermolecular PKR, still not well understood.

2.2 Results and discussion

For the intermolecular PKR, it was found in our group that in the cases of aliphatic internal alkynes with NBD or ethylene, the regioselectivity was surprisingly high or almost total in the case of trifluoromethyl⁵⁷ and silyloxymethylacetylenes (figure 2.35).⁶⁰

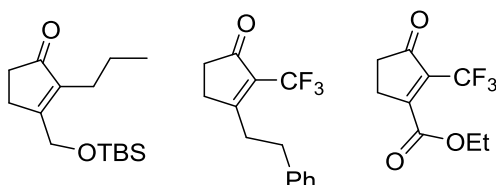


Figure 2.35. Examples of completely regioselective intermolecular PKRs of internal alkynes.

With the OTBS group in comparison to the propyl tail, the steric hindrances were comparable, however, the regioselectivity largely favours the β isomer. In the case of the CF_3

group, such great electrowithdrawing group always induced the total regioselectivity toward the α -isomer no matter the size of the other substituent.

Encouraged by these examples, we undertook a systematic study of the regioselectivity of internal aliphatic alkynes of intermolecular PKR from a computational and experimental approach. The aim was to find out the rules that could allow us to predict such regiochemistry.

For that purpose, we supported our work developing a collaboration with Helaja's group from the Helsinki University for his strong expertise in the calculation shown in the study of the PKR of diarylalkynes.⁵⁶

The experimental and computational results obtained regarding regioselectivity of the intermolecular PKR will be discussed in this chapter.

2.2.1 Design of the internal alkynes

The work consisted into study the relation between the electronic changes of unsymmetrical alkynes and regiochemical outcomes of the PKR. Thus, the substituents of the alkynes were modified in such a way that the regioselectivity observed would only be caused by inductive effects without any resonance effects and steric influences.

To this end, the electronic group of the alkyne was deliberately spaced from the triple bond by one methylene. One side of the alkyne would bear a propyl chain and the other side different functional groups (figure 2.36).

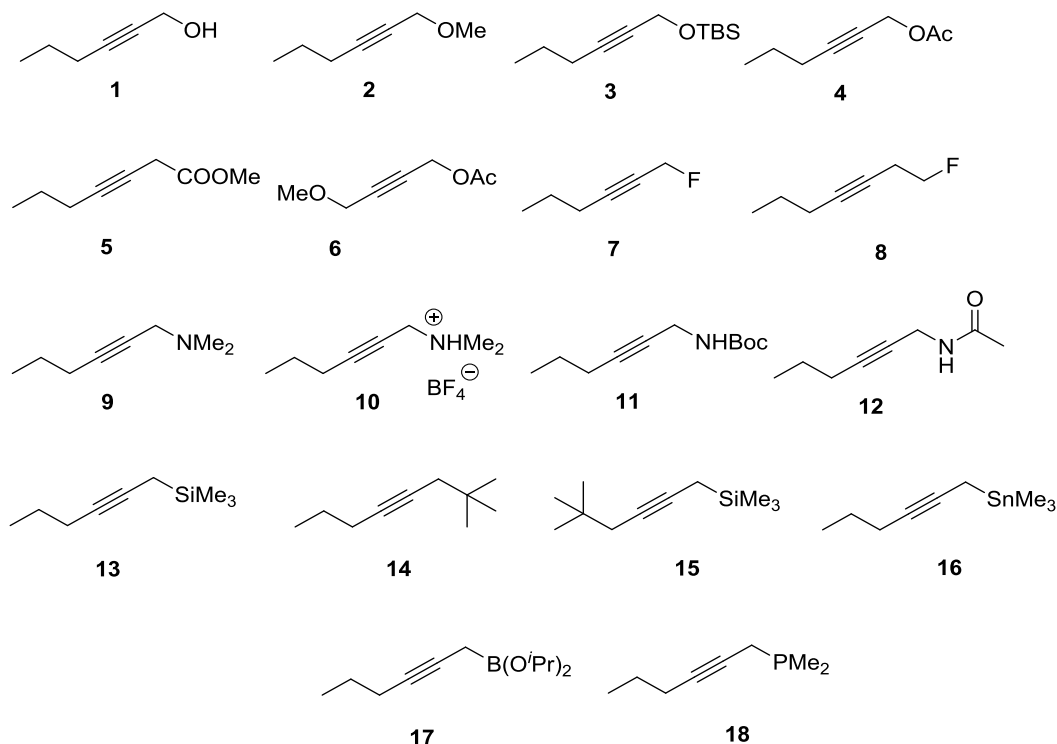
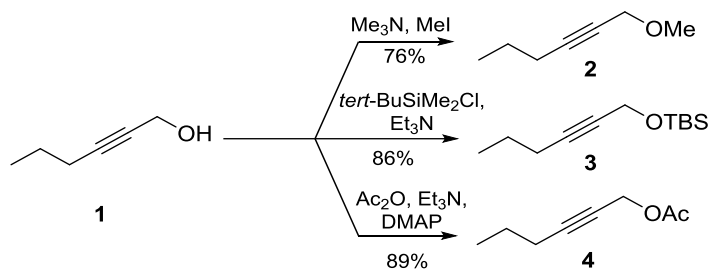


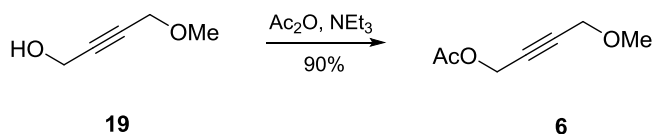
Figure 2.36. Alkynes envisaged for this study.

2.2.2 Synthesis of the internal alkynes

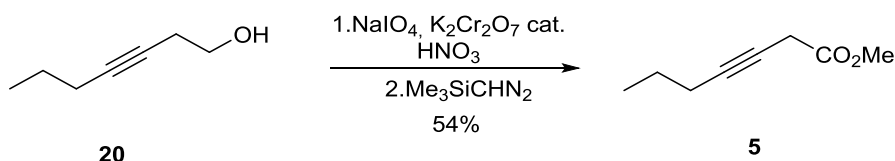
The study started with the synthesis of the oxygenated derivatives **2** to **4**. The alkynes were prepared from 2-hexyn-1-ol (**1**) by standard procedures (figure 2.37). Treatment of **1** with iodomethane and trimethylamine yielded **2** in 76%. The treatment with chloro *tert*-butyl dimethylsilane and triethylamine yielded **3** in 86% and finally using acetic anhydride, triethylamine with a catalytic amount of DMAP afforded **4** in 89%.

Figure 2.37. Synthesis of the alkynes **2-4**.

Synthesis of the 4-methoxybut-2-yn-1-yl acetate **6** was performed in Helsinki by Erika Fager-Jokela, from 4-methoxybut-2-yn-1-ol by treatment using acetic anhydride, triethylamine afforded **6** in 90% yield (figure 2.38).

Figure 2.38. Synthesis of the alkyne **6**.

Synthesis of the alkynes **5** with a second carbon atom bearing an electron-withdrawing methyl ester was prepared from hept-3-yn-1-ol by oxidation using sodium periodate, with a catalytic amount of potassium dichromate and nitric acid followed by its methylation using trimethylsilyl diazomethane in 54% over two steps (figure 2.39).

Figure 2.39. Synthesis of the Alkyne **5**.

The fluorinated alkynes **7-8** were attempted from hex-2-yn-1-ol **1** and hept-3-yn-1-ol using as nucleophilic fluorinating agent, diethylaminosulfur trifluoride (DAST) (figure 2.40). Hex-3-yn-1-ol and its homologue, the hept-3-yn-1-ol were treated at -20°C with 3 equivalents of DAST. The compound **7** was never observed whereas compound **8** was obtained as a mixture fluorinated compounds and by-products. Due to its high volatility and stability, the compound **8** was not isolated and directly engaged in next step, complexation into **44** which will be presented in the next paragraph.

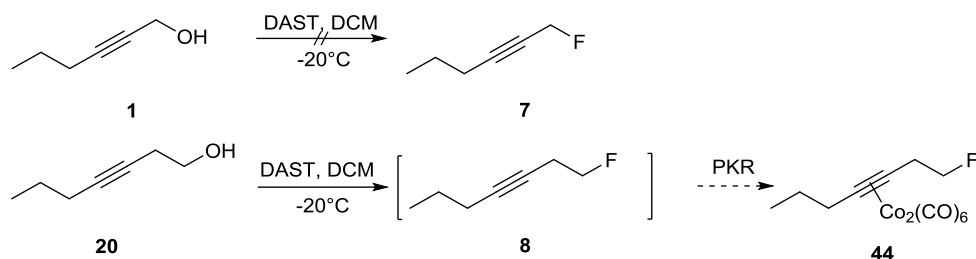


Figure 2.40. Synthesis of the fluoroalkynes 7 and 8.

Alkynes 9 to 12 with a nitrogenated function at the propargylic position were synthesized in Helsinki by Erika Fager-Jokela. Alkynes were prepared from 1 by mesylation to give compound 21 in 95% following the general scheme of the figure 2.41.

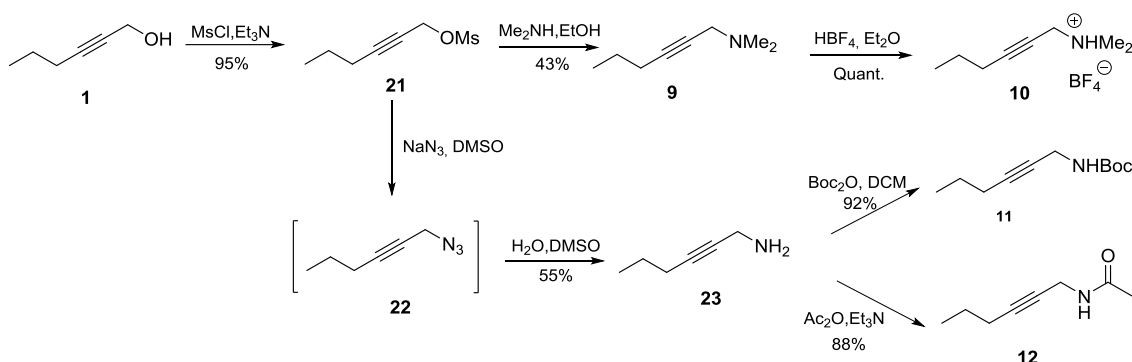


Figure 2.41. Synthesis of the alkyne 9 to 12.

As we will discuss later, in all these cases, the main regioisomer found was β . Therefore, the major electronegativity of the atom attached to C1 seemed to play an essential role. Thus, heteroatom with lower electronegativity than the carbon at the propargylic position of the alkyne was imagined to reverse the regiochemical outcome of the PKR (figure 2.42).

H																	He
Li	Be											B	C	N	O	F	Ne
Na	Mg											Al	Si	P	S	Cl	Ar
K	Ca	Sc	Ti	V	Cr	Mn	Fe	Co	Ni	Cu	Zn	Ga	Ge	As	Se	Br	Kr
Rb	Sr	Y	Zr	Nb	Mo	Tc	Ru	Rh	Pd	Ag	Cd	In	Sn	Sb	Te	I	Xe
Cs	Ba	Ln	Hf	Ta	W	Re	Os	Ir	Pt	Au	Hg	Tl	Pb	Bi	Po	At	Rn
Fr	Ra	Ac	Th	Pa	U	No-Lr											

Figure 2.42. Pauling table of the periodic classification.

Indeed, the electronegativity described by Pauling referred to "the power of an atom in a molecule to attract electrons to itself".⁶¹ Electronegativity of such a system was identified with the negative of its electrochemical potential.⁶²

Regarding to the Pauling table, elements with lower electronegativity than the carbon are the boron, phosphorus, silicon, and tin atoms. Thus, the alkynes bearing those groups, **13** to **18** would be potential good candidates for the study (figure 2.43).

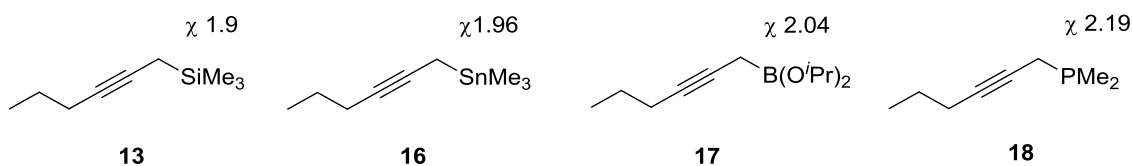


Figure 2.43. Negative electronegative difference between the atom X at the propargylic positions and carbon.

Although Brown and Soundararajan published in 1997 the synthesis of acyclic and some cyclic 2-alkynylboronates, these intermediates were highly instable and could only be manipulated in situ like shown in the figure 2.44.⁶³ Therefore, the synthesis of the alkyne **17**, both isolation and characterization of alkynylboronate was considered to be very difficult.

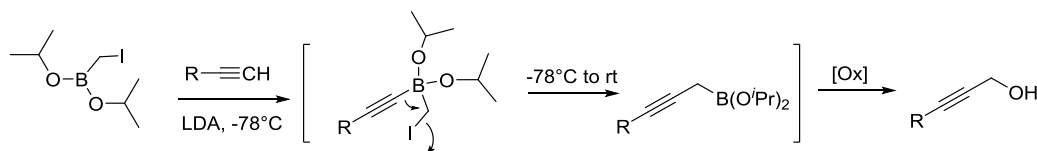


Figure 2.44. 2-alkynylboronate's synthesis used as intermediate of reaction.

Substituted alkynyl phosphine, such as **18** was as well envisaged but trivalent aliphatic phosphine is known to be air sensitive.⁶⁴ The resulted oxidized phosphine would not be of any interest in our study since we would like to focus on the positive inductif effect provoked by its substituents. Consequently, the two feasible substrates that could be synthesized were the silyl and stannyl alkynes, **13** and **16**.

Regarding the synthesis of the silyl alkyne **13**, two retrosynthetic pathways have been investigated and involved alkylation of trimethylsilyl 2-propyne to (**route A**) or alkylation of the 1-pentyne to (**route B**) (figure 2.45).

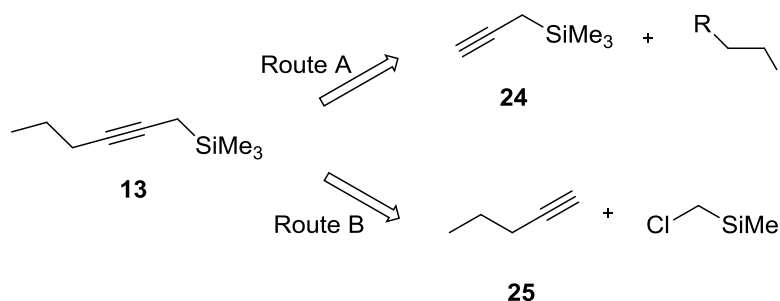


Figure 2.45. Retrosynthetic approaches for the design of the silyl alkyne **13**.

The route **A** was first undertaken. The propargyl trimethylsilane, **24**, was treated with LiNH_2 prepared from condensed ammonia and lithium with catalytic amount of ferric

nitrate at -33°C (figure 2.46). To the acetylide solution was then added bromopropane and after aqueous work-up, the dried organic layer was straight away reacted in a thermal stoichiometric PKR at 70°C . The expected PK adduct was not observed, but instead the desilylated product **26** was detected in 57% yield, with the propyl chain in α to the ketone.

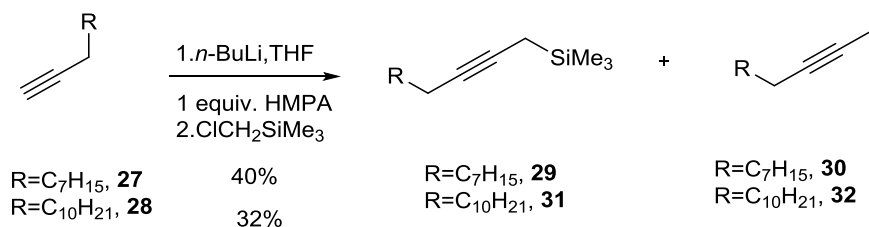


Figure 2.46. Route A.

With the purification problems due to the volatility of **13**, we could not identify if the cleavage of the silyl moiety occurred before the formation of **13** or during the PKR. In addition, optimisations of the **route A** indicated that results could not be reproducible probably caused by the instability of the propargyl trimethylsilane.

In response those issues, the **route B** was then undertaken changing the reaction procedure. The original bromopropane was replaced by (chloromethyl) trimethylsilane and propargyl trimethylsilane **24** replaced by decyne **27** or tridecyne **28**.

We generated the alkynyl anion **27** or **28** with 1 equivalent of the *n*-BuLi in presence of hexamethylphosphoramide (HMPA) at -78°C where the (chloromethyl) trimethylsilane was then added. After stirred for 3-4 hours, it afforded 40% and 32 % yield respectively of the undecyltrimethylsilane **29** and **31** and the desilylation products **30** and **32** (figure 2.47).

Figure 2.47. Synthesis of alkyne **29** and **31**.

Like highly polar aprotic solvents such as HMPA are reported to accelerate organolithium reactions and alkyl condensations by coordination to the lithium, its quantity was investigated. Changing the *n*-BuLi for LDA and increasing the concentration of HMPA to 6 equivalents (or 15 vol%) permitted to form predominantly the product **31** with traces of by-products (such as **31A** to **31C**) in a ratio **31**:**31A** of (8:1) (figure 2.48). After distillation, it afforded 93% yield of the silyl product **31** in an almost pure form by ^1H NMR, (12:1 ratio).

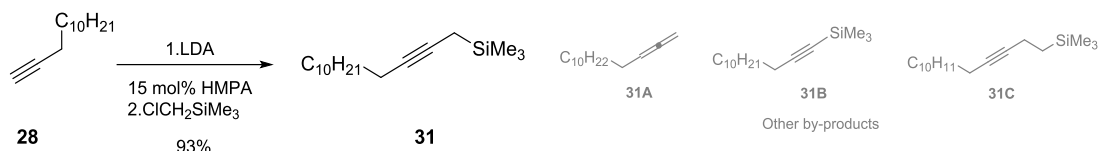


Figure 2.48. Formation of alkyne **31**.

Since the silyl derivative cannot be smaller, the carbon analogue version of the trimethyl silyl alkyne was also envisaged to check the steric influence of the substituent over the PKR. To avoid volatility problems, the propyl tail was also replaced by undecyl and the 1,1-dimethylhexadec-4-yne, compound **29** was envisaged (figure 2.49).

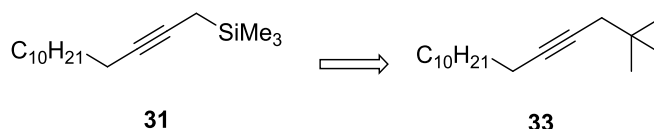


Figure 2.49. Carbon analogue of trimethylsilyl alkyne (**33**).

n-BuLi with 10 vol % of HMPA and 1-iodo-2,2-dimethylpropane were reacted at -40°C for 7h. Like the reaction rate was extremely slow, we decided to increase the temperature from 45 to 78°C which afforded after three days, a 35% conversion rate. Some optimizations permitted to identified that best conditions were obtained with 1.2 equivalent of *n*-BuLi at -78°C and then 70°C with 50 vol % of HMPA to afford 70 % yield of the compound **33** over 3 days. Some remained terminal alkyne was detected in a 7:1 ratio (figure 2.50).

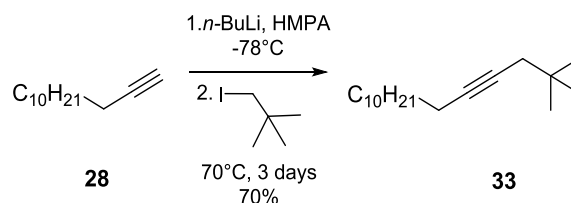


Figure 2.50. Synthesis of the compound **33**.

Relative to compounds **31** and **33**, we also tried to synthesize compound **15**, a combination of both substituents, having to one side the silyl and to the other the neopentyl groups. We reacted the propargyl trimethylsilane with *n*-BuLi, 10 vol % of HMPA and 1-iodo-2,2-dimethylpropane at -78°C and 70°C (figure 2.51). The crude resulted very difficult to work up due to the high volatility of reactants and product. The desired product **15** could not be obtained.

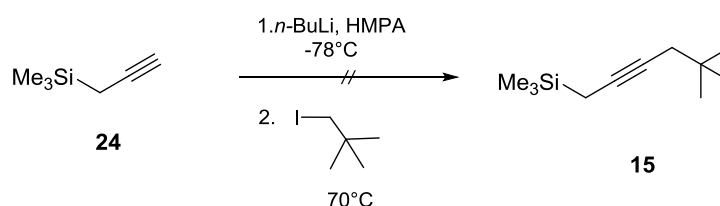


Figure 2.51. Attempt to the synthesis of the compound **15**.

The synthesis of the stannyl alkyne (**36**) bearing a pentyl tail instead of a propyl (**16**) was envisaged through a palladium-catalyzed addition of hexamethylditin to triple bond described by Szabó et al.⁶⁵

The reaction consisted to react 1-chloro-oct-2-yne **34**, with hexamethylditin and 10 mol % of a freshly formed catalyst, NCN-pincer palladium complex, compound **35** (figure 2.52).

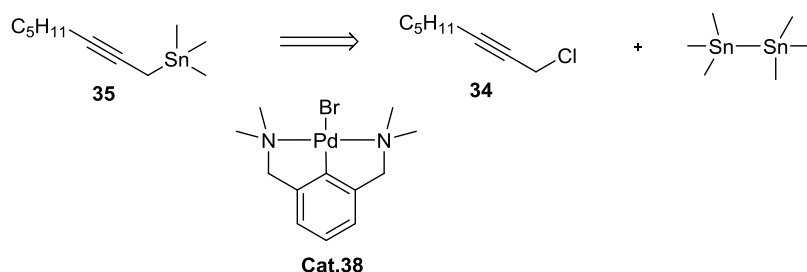


Figure 2.52. Retrosynthesis of the stannyl alkyne **35**.

The preparation of the catalyst was carried out in two steps synthesis by reacting the 1-bromo-1,3-bis-bromomethyl-benzene **36**, with an excess of dimethylamine in DCM, to get the 1,1-(2-bromo-1,3-phenylene)bis(N,N-dimethylmethanamine) compound **37** in 53 % yield (figure 2.53). Then, the pincer palladium complex **38**, was made by ligand exchange with Pd(dba)₃/CHCl₃ in toluene at 60°C affording a white solid in 72% yield.

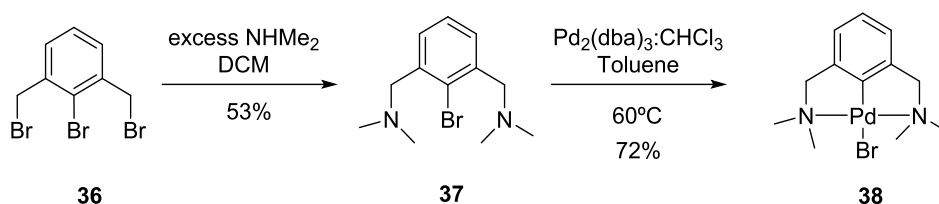


Figure 2.53. Synthesis of the NCN-pincer palladium complex, **38**.

Then, the desired stannyl alkyne **35** was synthesized by reacting commercial chloro-oct-2-yne **34** with 1 equivalent of hexamethylditin and 10 mol % of the catalyst freshly formed (figure 2.54). It afforded mainly the desired product in 57% yield. A careful purification had to be done to remove small amount of allenylstannane **35A**.

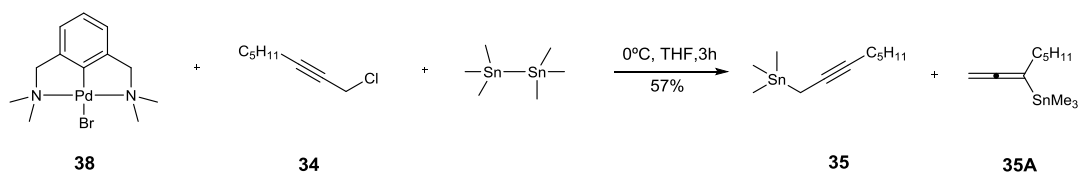


Figure 2.54. Synthesis of stannyl alkyne, **35**.

2.2.3 Synthesis of the PK adducts

With the alkynes **1** to **16** and **35** in hand, we undertook the PKRs. We proceeded in two steps reaction where first the cobalt complex was isolated and then left to react with NBD. The crudes of reaction were chromatographed and the ratio of the four possible regioisomers was measured by ^1H NMR (figure 2.55).

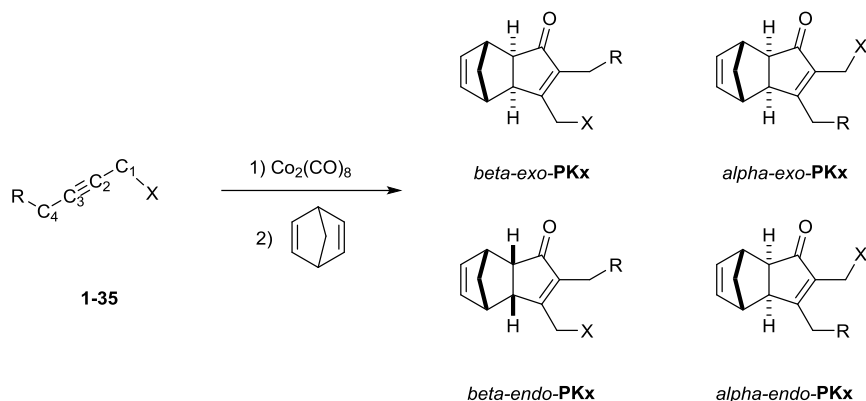


Figure 2.55. PKR's of selected alkynes with norbornadiene.

On the other hand, DFT calculations of all the alkynes were carried out by Mikko Muuronen from the Helaja's group. They were performed at DFT level in gas phase with TPSS-D3 meta-GGA functional together with high quality triple ζ basis set def2-TZVPP. The alkyl tail was treated as propyl in all computations. The calculated NBO charge differences of the alkynyl carbons (C2-C3) and the α -carbons (C1-C4) were measured to study the influence of the electronic factors over the regioselectivity.

Like mentioned in the introduction, the electronic influence of the substituent over the polarisation of the carbons (C2-C3) and the α -carbons (C1-C4) of the alkyne is crucial to guide the regioselectivity.

Search of the best condition to perform the PKR

The different ways to perform the PKR were tested to identify which were the most appropriated reaction conditions. Thus, thermal, stoichiometric, catalytic, promoted PKRs were investigated with the substrates **2-4**. The results are summarized in the table 2.3.

The determination of the ratio of the different PK adducts present were obtained by chromatography of crudes where each fraction enriched in PK adducts was weighted and analysed by NMR. By the integrations of easy identified proton signals of enriched PK adducts, the exo/endo and α/β ratios could be measured like shown in figure 2.56.

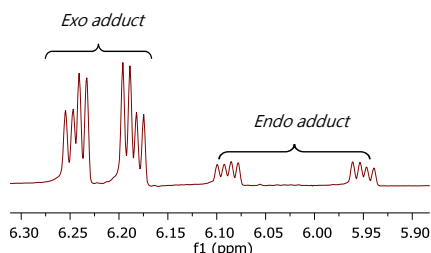


Figure 2.56 Example of the alkene region of the ^1H NMR of one isolated fraction enriched with the diastereomer β -endo.

Depending on the PKR conditions used, yields of the PKRs of oxygenated alkynes **1-6** with norbornadiene varied but affording always a remarkably high regioselectivities and high ratio exo/endo. Mainly the PKR gave the β exo isomer and small amount of the β endo isomer.

With the alkynes **1** and **2**, only one isomer could be detected by NMR in good yield, the β exo isomer with a high exo/endo ratio, using stoichiometric or N-oxide promoted PKR. (table 2.3, entries 1,3).

With alkynes **3** and **4**, we studied the thermal stoichiometric, catalytic and the use of N-oxide promoter in the PKR. In all the cases, stoichiometric version gave better yields for **3** and **4**, 60-66% against 42-60% for the catalytic version (table 2.3, entries, 4-9). When the PKR was promoted by NMO, it gave for **3** 41% yield (table 2.3, entry 6) and induced the decomposition of the complex of **4** (table 2.3, entry 9). Similar observation was found with the alkyne **2** where yield dropped down from 82% in stoichiometric version to 41% using NMO (table 2.3, entries 2,3).

With the alkyne **5**, the influence of the amount of NBD was studied. Changing the number of equivalents from 5 to 3, a great decrease in the yield of the reaction was observed from 80 to 23 % (table 2.3, entries 10-11).

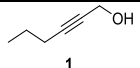
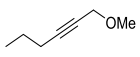
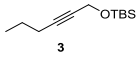
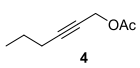
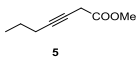
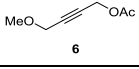
Entry	Alkyne used	Conditions of PKR	Yield (%)	Ratio $\alpha:\beta$	Ratio endo:exo
1		Thermal, 5 eq. NBD, Toluene, 70°C	72	0:1*	1:10
2		Thermal, 5 eq. NBD, Toluene, 70°C	82	0:1*	1:11
3		N-oxide, 6 eq. NBD, rt	60	0:1*	1:20
4		Thermal 5 eq. NBD, Toluene, 70°C	66	~1:27	1:11
5		Catalytic, 3 eq. NBD, 70°C	60	1:11	1:15
6		N-oxide, 6 eq. NBD, rt	41	1:27	1:39
7		Thermal, 5 eq. NBD, Toluene, 70°C	60	~1:30	1:30
8		Catalytic, 3 eq. NBD, 70°C	42	1:27	1:4
9		N-oxide, 10 eq. NBD, rt	-	-	-
10		Thermal, 5 eq. NBD, Toluene, 70°C	80	~1:22	1:10
11		Thermal, 3 eq. NBD, Toluene, 70°C	23	1:21	1:15
12		Thermal, 5 eq. NBD, Toluene, 70°C	34	1:1.1	-

 Table 2.3. Regiochemical outcomes of the PKR of alkyne 1-6. * α -adduct not observed.

So far, the best yields of reaction were afforded by thermal, stoichiometric conditions, in toluene at 70°C with five equivalents of NBD.

Then, we investigated the possible role of the reaction conditions over the regiochemical outcome of the thermal and stoichiometric PKR with the substrate 2 (figure 2.57).

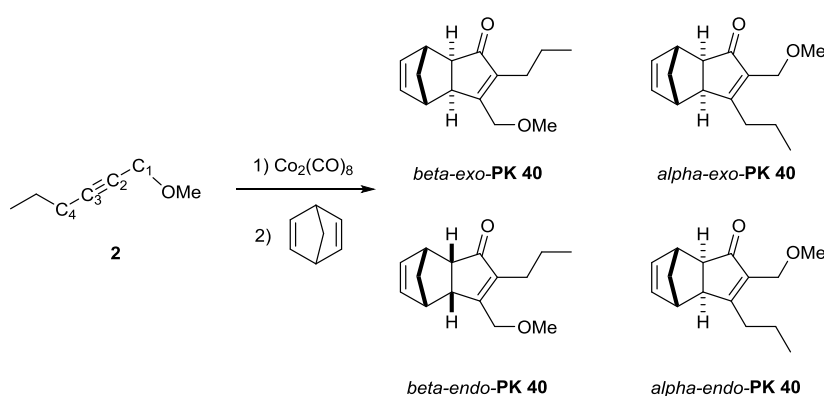


Figure 2.57. PKR's of selected alkynes with norbornadiene.

The parameters of the stoichiometric PKR were modified and ratios determined by changing the quantity of alkene, nature and volume of the solvent, temperatures and heat source (table 2.4). In general, it seems that the reaction conditions do not have a major influence on the isomer ratio, even though the yield and exo/endo ratio changed. The amount of alkene

(table 2.4, entry 1-5), the dilution (table 2.4, entry 6,7) the reaction temperature (table 2.4, entry 8,9) and the use of microwaves (table 2.4, entry 10) do not remarkably change the ratio of the isomer.

The use of the norbornene (NBN) instead of the NBD lowered the amount of endo product, only the exo adducts were detected (table 2.4, entry 11).

The solvent was the only parameter that has a dramatic effect on the stereo- and regioselectivity. DCE or THF (table 2.4, entry 12-13) did not make any notable effect. Instead, when the reaction was performed in acetonitrile, the endo-isomer was the only adduct detected (table 2.4, entry 14). Weakness of this reaction was the low yield compare to those in toluene. We tried to optimise the conditions in a mixture acetonitrile/toluene; in a 1/1 mixture, the yield increased to 50%, while the endo adduct was still dominating the endo/exo ratio in a 27/21 mixture (table 2.4, entry 15). A change up to 9:1 mixture toluene/acetonitrile, produced high yield (82%) and high stereoselectivity toward the exo adduct (table 2.4, entry 16).

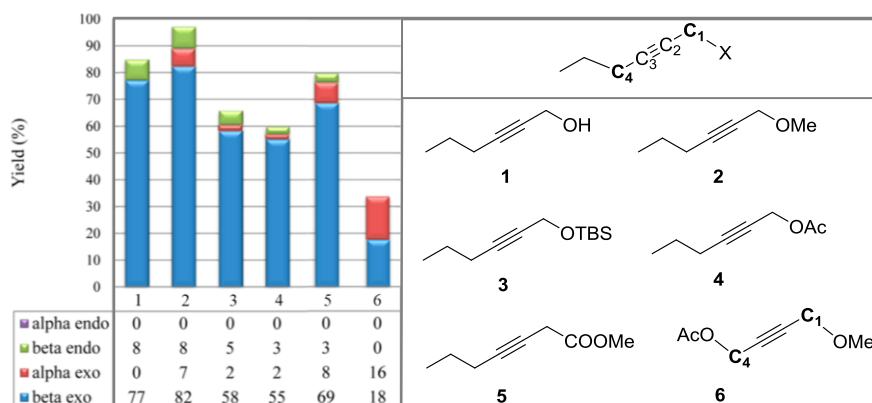
Entry	Conditions of the PKR	Yield (%)	Ratio $\alpha:\beta$	Ratio endo/exo
1	1 equiv NBD, 70°C, toluene	24	1:23	2/22
2	3 equiv NBD, 70°C, toluene	56	7:49	8/48
3	5 equiv NBD, 70°C, toluene	97	7/90	8/89
5	10 equiv NBD, 70°C, toluene	84	6/87	7/86
6	5 equiv NBD, 70°C, toluene	85	6/79	6/79
7	5 equiv NBD, 70°C, toluene	71	5/66	5/66
8	5 equiv NBD, 50°C, toluene	77	7/74	7/74
9	5 equiv NBD, 90°C, toluene	81	4/73	5/72
10	5 equiv NBD, MW 70°C, toluene	82	7/75	7/75
11	5 equiv NBN, 70°C, toluene	61	11/50	0/1
12	5 equiv NBD, 70°C, DCE	70	5/65	5/65
13	5 equiv NBD, 70°C, THF	71	5/66	4/67
14	5 equiv NBD, 70°C ACN	27	1/26	22/5
15	5 equiv NBD, 70°C, 1/1 toluene/MeCN	50	0/1	27/21
16	5 equiv NBD, 70°C, 9/1 toluene/MeCN	82	7/75	9/73

Table 2.4. Influence of the parameters over the regioselectivity and stereoselectivity.

In conclusion, the best reaction conditions to perform the PKR were: thermal, with toluene at 70°C with 5 equivalents of NBD which permitted to study the regioselectivity of the reaction.

Regiochemical outcome of the intermolecular PKR

Regarding oxygenated alkynes **1** to **5**, high regioselectivity toward the β -exo isomer was observed with the formation of a small amount of the β endo isomer. The only exception was with the alkyne **6** bearing very similar groups OAc and OMe (figure 2.58 and table 2.5).



2.58. Regioselectivity and diastereoselectivity observed with alkyne **1** to **6**.

From hex-2-yn-1-ol **1** and OMe derivative **2**, PK adducts were obtained 72 % and 82% yield in a complete regioselective way, although sometimes aldehydes were obtained as side products due to oxidation of the alcohol.

The OTBS derivative **3** and acetylated **4** both gave almost complete regioselectivity. Surprisingly, the steric hindrance of the OTBS group did not affect the regioselectivity when comparing to the series of the other oxygenated derivatives.

Entry	Alkyne used	Ratio α : β	C1	C2	C3	C4	Δ (C1-C4).100	Δ (C2-C3).100
1		0:1	-0.12	-0.08	0.01	-0.45	32.77	-9.02
2		0:1	-0.13	-0.05	0.02	-0.45	32.03	-6.9
3		~1:27	-0.11	0.05	0.02	-0.45	33.77	-6.36
4		~1:30	-0.13	-0.07	0.05	-0.45	31.86	-11.38
5		~1:22	-0.54	-0.03	0.02	-0.45	-9.48	-4.89
6		1:1.1	-0.14	-0.03	0.02	-0.14	-0.37	-4.47

Table 2.5. NBO charge differences of the alkynyl carbons Δ (C2-C3) and (C1-C4).

From a computational point of view, for substrates **1** to **4**, both Δ (C1-C4) and Δ (C2-C3) NBO charges predicted the expected β regioisomer (table 2.5, entry, 1-4) as it was found experimentally. The Δ (C2-C3) NBO charges gave negative values in good agreement with the hypothesis that the C-C bond formation takes place in the C2 (figure 2.59).

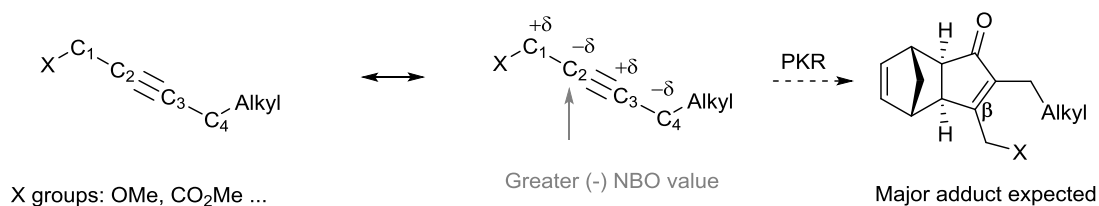


Figure 2.59. Relative alkyne polarisation induced by the difference of electronegativity between substituents and α -carbons of the alkyne.

The $\Delta(\text{C1-C4})$ NBO charges of the alkyne 1 to 4 were more quantitative than $\Delta(\text{C2-C3})$ values. Indeed, the $\Delta(\text{C1-C4})$ NBO magnitudes were almost identical around 31 to 32, while $\Delta(\text{C2-C3})$ NBO values oscillated from -6 to -11 (table 2.5, entry, 1-4).

The alkyne 5 gave as well high regioselectivity even its alkyne polarization [$\Delta(\text{C2-C3})$ -4.89], predicted a smaller regioselectivity than alkyne 4, [-11.38] (table 2.5, entries 4,5). Notably, the α -position was inversely polarized, while the heteroatom was located one carbon further from the alkyne, at γ -position. Therefore, the $\Delta(\text{C2-C3})$ fits better than $\Delta(\text{C1-C4})$ NBO charges.

The disubstituted alkyne 6 bearing the OMe and OAc groups afforded a mixture of regioisomers in 1:1.1 ratio and 34% yield (table 2.5, entry 6). Indeed, the two substituents had similar electronegative effect over the polarisation of the alkyne predicting unselective PKR. Thus, when the range of the $\Delta[(\text{C1-C4})-0.37]$ was compared to [$\Delta(\text{C2-C3})$ -4.47], the unselective outcome of the reaction showed better concordance with the polarization of the $\Delta(\text{C1-C4})$.

Yet, both the computed NBO charge differences of the alkynyl carbons $\Delta(\text{C2-C3})$ and the α -carbons $\Delta(\text{C1-C4})$ correlated quite well with the experiments. Those results were in good agreement with the fact that the C-C bond is formed with the more electron rich alkynyl carbon where indeed, higher electronic charges were observed in the C2 carbon (figure 2.60). Like the C2 carbon will be involved in the C-C formation with the alkene, the substituent of the C2 position will end up in the β -position of the cyclopentenone. In those cases, the $\Delta(\text{C1-C4})$ calculations qualitatively well predicted the regiochemical outcome.

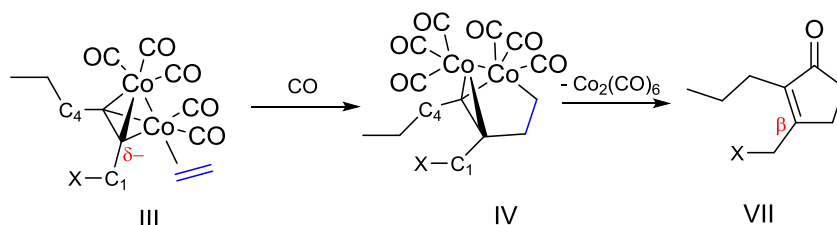


Figure 2.60. Magnus' mechanism to explain the regioguidance of the intermolecular PKR.

PKR's of the nitrogenated alkyne series **9** to **12** performed in Helsinki gave also good selectivity towards the β exo isomer with lower yields than with oxygenated series. High selectivities was observed expect in the case of **11** and **12** alkynes which gave some α -isomer (figure 2.61 and table 2.6).

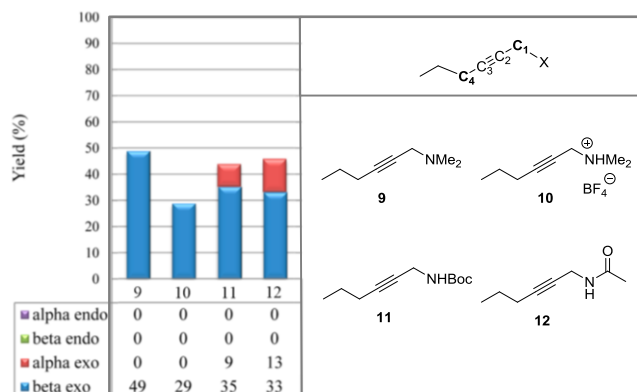


Figure 2.61. Regioselectivity and diastereoselectivity observed with alkynes **9** to **12**.

N,N-dimethylhex-2-yn-1-amine **9** and its tetrafluoroborate salt **10** afforded exclusively the β -exo isomer in 49% and 29% yield (table 2.6, entries 1, 2).

From computational point of view, interestingly, the protonation of the dimethyl amine group (**9** \rightarrow **10**) did not inverse the alkyne polarization but intensified it.

The N-Boc and N-acetyl derivatives **11** and **12** both gave 35 and 33% yield of β -exo isomer accompanied with noticeable amounts of α -exo adducts in a 1:3 and 1:1.5 ratio (table 2.6 entries 3, 4).

The $\Delta(C1-C4)$ and $\Delta(C2-C3)$ NBO charges did not well predicted the lower regioselectivity observed in **11** and **12** even the difference of electronegativity between nitrogen (3.0) and oxygen (3.5) was also visible on the α -positions. Therefore, the $\Delta(C1-C4)$ NBO charges gave weaker alkyne polarization for nitrogenated series ~ 17 to 22 against ~ 32 for the oxygenated series.

With the nitrogenated series, the major isomer formed was only qualitative predicted by the calculations of the NBO charges.

Entry	Alkyne used	Yield (%)	Ratio $\alpha:\beta$	C1	C2	C3	C4	$\Delta(C1-C4).100$	$\Delta(C2-C3).100$
1		49	0:1	-0.27	-0.06	-0.01	-0.45	17.23	-4.39
2		29	0:1	-0.25	-0.17	0.16	-0.47	22.37	-32.52
3		35	1:3	-0.27	-0.05	0.01	-0.45	17.59	-6.26
4		33	1:1.5	-0.28	-0.05	0.01	-0.45	16.91	-6.24

Table 2.6. PKR's results of the nitrogenated alkynes and NBO charges.

In the case of the fluoro-hex-3-yne, **8**, from the crude of reaction, it was performed the complexation with dicobalt complex but several products were formed. After purification, an isolated cobalt complex **40**, in mixture with an undetermined complex were submitted to stoichiometric PKR with five equivalents NBD at 70°C (figure 2.62).

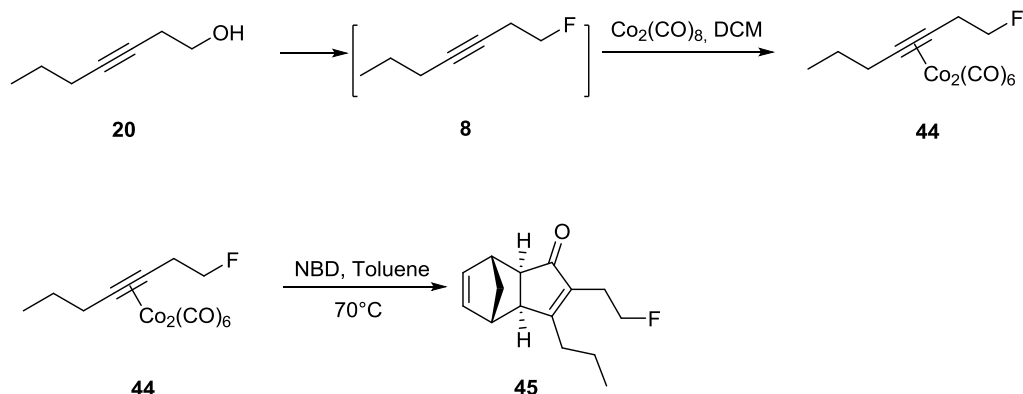


Figure 2.62. Attempt to synthesis the fluoro PKR **44**.

The analysis of the crude of reaction clearly showed the predominated formation of one regioisomer. The formation of the fluoro-PK adducts was confirmed by HR-MS and the 19F NMR but the assignation of which regioisomer was mainly formed resulted difficult to determine. Optimization of the reaction was tried but only few mgs of the final products can be formed probably due to the instability to the fluoroalkyne.

Alkynes bearing less electronegative atom than the carbon at the propargylic position were then subjected to the PKR.

PKR of stannyl alkyne was tried for the first time. After complexation of the alkyne **35** with dicobalt octacarbonyl complex for 2h, a quick filtration over SiO₂ permitted to isolate complex **46** which was engaged with five equivalents of NBD. From the crude of reaction, one single adduct of PKR was observed, compound **49** where the stannyl group was cleaved (figure 2.63). The pentyl group was placed in α-position while methyl in β-position of the cyclopentenone. The purification afforded 90 % yield of one single PK adduct **49**.

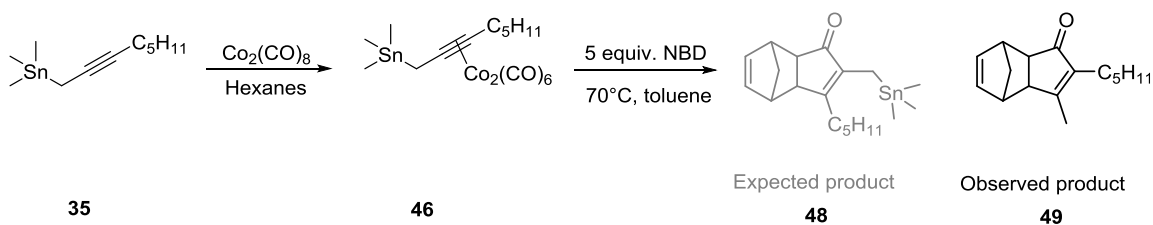


Figure 2.63. Attempt to the synthesis of the stannyl PK adduct, **48**.

The loose of trimethyltin moiety was investigated by monitoring of the PKR using TLC plates and 1H NMR. Two hypotheses could be formulated either the substituent was unstable in presence of the dicobalt complex or it was sensitive to the PKR conditions (figure 2.64).

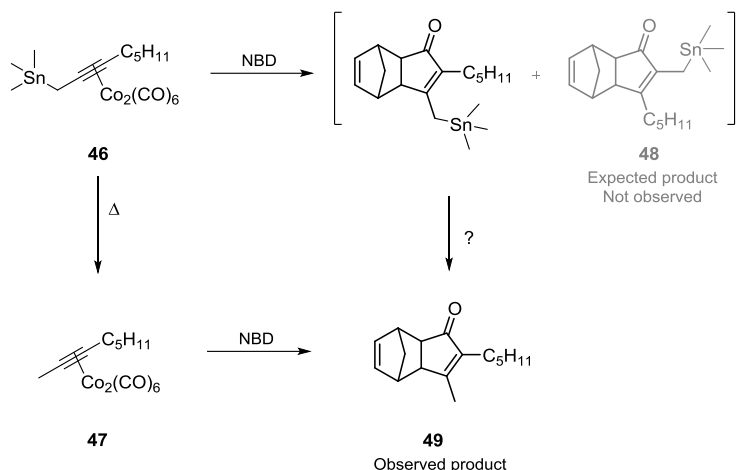


Figure 2.63. Hypotheses formulated of loose of trimethyltin moiety of the compound **46**.

The complexation of stannyl alkyne under different temperatures was studied by NMR where it was identified that stannyl complex **46** was partially stable at 0°C and afforded **47** at room temperature.

PKR at low temperature using NMO as promoter was consequently performed in DCM with 10 equivalents of NBD during 3 hours. The PK adduct observed was unfortunately again **49** without the stannyl group.

As last attempts, the alkyne was dissolved in toluene was kept at 0°C or heated up at 70°C. Slowly, via a syringe pump, the dicobalt hexacarbonyl complex dissolved in toluene was added over the alkyne solution which afforded in both cases the cleaved PK adduct **49**.

Therefore, the unstable stannyl dicobalt cobalt complex led to the cleavage of the stannyl moiety affording excellent yield towards one α -regioisomer where the alkyl tail was placed in α and methyl in β -position. Even though some stannyl dicobalt cobalt complex remained during the PKR, the α - and β -regioisomer stannyled adduct was never observed in the crude of reaction.

With the alkyne **31** in hand, the complexation with dicobalt octacarbonyl complex was performed. As happened with the stannyl alkyne, the silyl group of the alkyne cobalt complex **50** had the tendency to be cleaved and afforded the PK adduct **52** in 40% yield (figure 2.64).

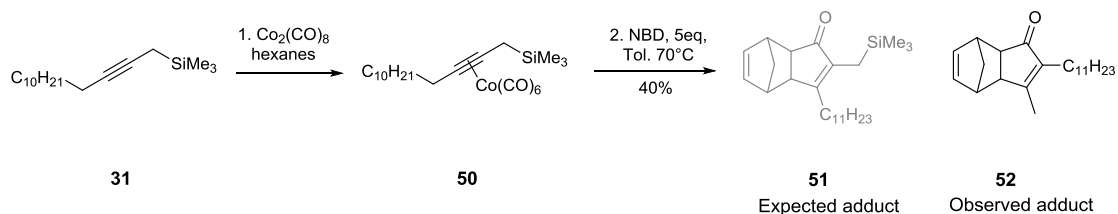


Figure 2.64. Attempt to synthesis the silyl PKR **51**.

The stoichiometric PKR with the isolated complex **50** was carried out with five equivalents of NBD at 70°C. The reaction being not complete, it was heated up at 100°C during 8 hours but

only 22% of PK adducts were detected as a mixture of desilylated **52** and expected adduct **51** in a (7:1) ratio. The formation of the desilylated PK adduct afforded the undecyl group in α -position and the regiochemistry of few mgs of silylated PK adduct could not be determined. At that point, we could clarify if the cleavage of the silyl moiety occur during the PKR or because of the unstability of the final PK adduct. Therefore, to verify the influence of the steric effect, an aliphatic alkyne bearing alkyl tail and methyl group **27** was carried out which gave a complete regioselectivity to the α -isomer **54** in 86% yield, the methyl in β position (figure 2.65).

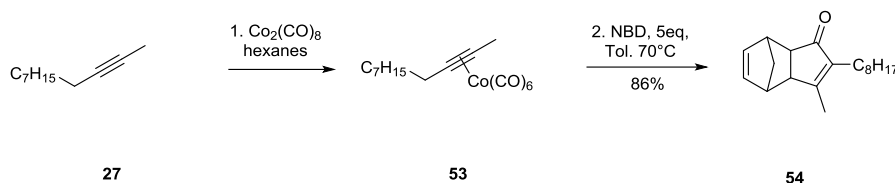


Figure 2.65. Synthesis of the PK adduct **54**.

Optimization of the reaction suggested that the silyl group was temperature sensitive. Indeed, to a solution of 10 equivalents of NBD in toluene (0.04 M referred to alkyne) was slowly added with a syringe pump the preformed dicobalt hexacarbonyl alkyne in toluene over 3-5 hours at 100°C. Spectacularly, we increased the yield of the PK adduct of silyl alkyne, **51** up to 80% (figure 2.66). As it could be anticipated, the alkyne with the more electropositive trimethylsilyl group gave the opposite regioisomer, α -*exo* isomer as a single product and high *exo/endo* ratio (24:1).

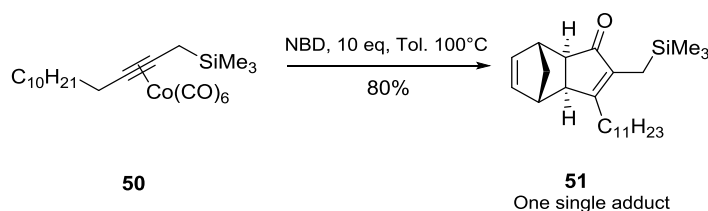


Figure 2.66. PKR of the silylated alkyne, **51**.

The alkyne **33**, the analogue version of the silyl alkyne was subjected to thermal and stoichiometric PKR using five equivalents of NBD at 70°C overnight. One single regioisomer **56** could be observed in 49% yield with the neopentyl group in α -position of the cyclopentenone and a high ratio *endo/exo* ratio of (1:32). (figure 2.67). Yield was improved by using 10 equivalents of NBD at 100°C affording 79% yield of a single α -regioisomer **52**.

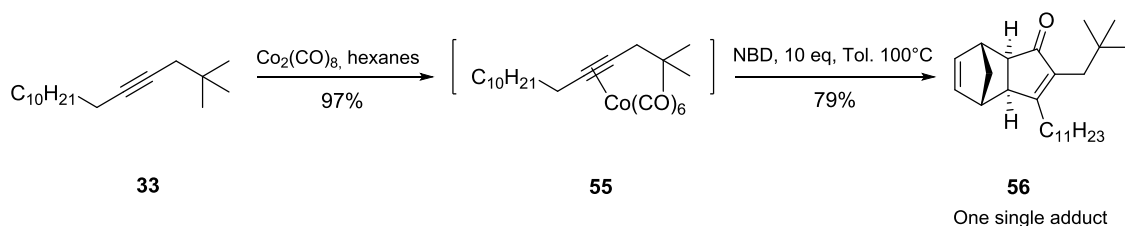


Figure 2.67. PKR of the neopentyl alkyne, **56**.

The substrate **31** and **33** favoured in good yield the α -exo PK adducts.

From computational calculations, both $\Delta(C1-C4)$ and $\Delta(C2-C3)$ predicted the PK adduct experimentally formed (table 2.7).

The total regioselectivity of the alkyne **31** well correlated with the greater $\Delta(C1-C4)$ value calculated than $\Delta(C2-C3)$. Although, we cannot forget that the steric effect will favour the same regioisomer.

Positive inductive effect bearing an atom of lower electronegative value than the carbon induced a greater electronic density over C1 carbon than C2. Thus, the difference of electronic density around $\Delta(C2-C3)$ would be positive favouring the α -regioisomer (figure 2.68).

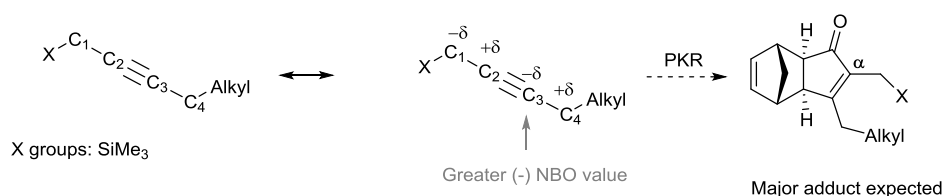


Figure 2.68. Relative alkyne polarization induced by the difference of electronegativity between substituents and α -carbons of the alkyne.

In the case of the alkyne **33**, the high regioselectivity observed did not correlate with the small polarization effect compared to the previous alkynes studied. However, this small polarization effect observed on the $\Delta(C1-C4)$ and $\Delta(C2-C3)$ NBO charges shown the C–C bond to be formed on the more electron rich carbon.

Like the steric and electronic effects guided the regioselectivity toward the same α -regioisomer, the impact of either steric and electronic effects cannot be estimated, even the steric factors are decisive for the regioselectivity of the intermolecular PKR.

Entry	Alkyne used	Yield (%)	Ratio $\alpha:\beta$	C1	C2	C3	C4	$\Delta(C1-C4).100$	$\Delta(C2-C3).100$
1		80	1:0	-0.88	-0.02	-0.04	-0.44	-43.77	1.42
2		79	1:0	-0.45	-0.02	-0.02	-0.44	-0.87	0.21

Table 2.7. Results of the PKRs of the alkynes **31** and **33** and NBO charges.

Overall, the observed regioselectivity in the intermolecular PKR of alkynes 1–14 with NBD clearly indicates that, in the absence of steric effects, the electronegativity of the atom bonded to the propargylic sp_3 -hybridized carbon plays a fundamental role. We can therefore assume that the propargylic substituents can polarize the carbon–carbon triple bond via inductive effects providing highly regioselective reactions.

From NBO charges, it is clear that the initial C–C bond formation, that dictates the regiochemistry takes place with the more electron rich carbon, even though quantitatively the data obtained does not allow curve fitting (Figure 2.69). In similar fashion, inspection of the carbons at the propargylic position (C1–C4) predicts the regiochemistry surprisingly well, although the prediction fails to give correct outcome for substrates 5 and 6.

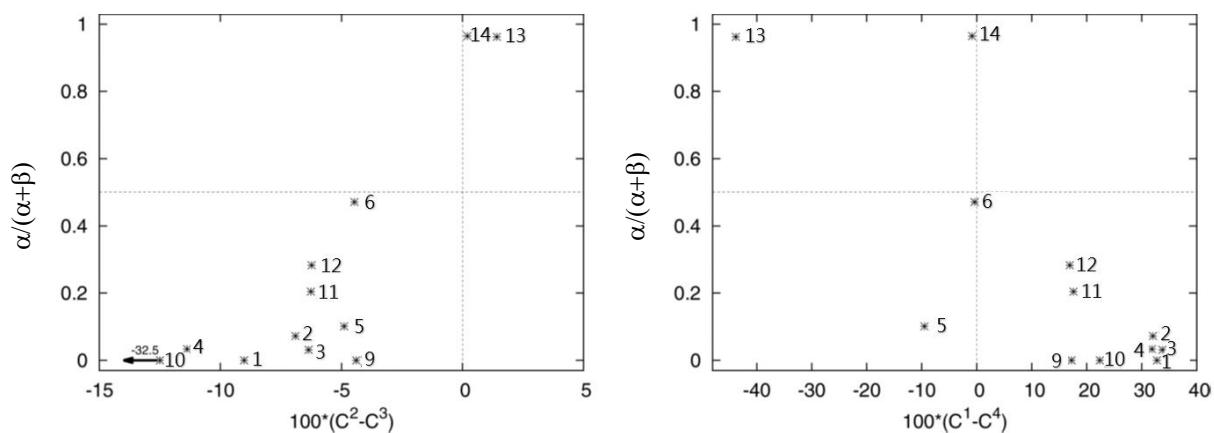


Figure 2.69. Plot of the NBO charge differences (C2-C3/C1-C4) of alkynyl carbons (TPSS-D3/def2-TZVPP) versus the regiochemical outcome of the PKR.

2.3 Conclusion

The regioselectivity of the intermolecular Pauson-Khand reaction has been successfully studied using a full set of aliphatic alkynes bearing sterically similar but electronically different substituents.

We have shown that:

1. Electronic polarization of the substituents in α -position of the alkynes can alone result significant in the regiochemical outcome of the PKR. When substituents bearing more electronegative atom than the carbon were placed in β -position of the alkyne (-I groups), it yielded β -*exo* regioisomer with a remarkably high regioselectivity in the case of oxygenated series. The nitrogenated series gave lower selectivities and yield toward the β -*exo* isomer. We showed that less electronegative atom than the carbon placed in β -position of the alkyne inverted the regioselectivity of the PKR toward the formation of the α -*exo* isomer the major stereoisomer in excellent yield.
2. For the first time, PKRs of stannyl aliphatic alkynes have been attempted. In the case of the stannyl, it revealed that alkyne easily afforded the elimination of the substituent before the cyclisation reaction occurred.
3. The computational NBO charges, indicated clearly that the polarization of alkyne was inductively mediated from the heteroatom. The initial C-C bond formation, that dictates the regiochemistry was confirmed to take place with the more electron rich carbon. In similar fashion, inspection of the carbons polarization at the propargylic position $\Delta(C1-C4)$ predicted the regiochemistry surprisingly well, although the prediction failed for substrates **3** and **6**. The alkyne polarization alone gave only qualitative prediction of regioselectivity since other interactions competed with it. Remarkably, small steric factors can easily override the electronic factors in the regiochemical outcomes. Nevertheless, the regioselectivity in intermolecular PKR of aliphatic alkynes has been explained by theoretical calculations of the alkyne alone.

Our study permits to clarify and rationalize the regiochemical outcome of the intermolecular PKR proposing to scientific community a tool to predict its regioguidance which have been published in *Journal of Organic Chemistry*, **2014**, *22*, 10999–11010.

References

- (1) Khand, I. U.; Knox, G. R.; Pauson, P. L.; Watts, W. E.; Foreman, M. I. *J. Chem. Soc. Perkin Trans. 1* **1973**, 977.
- (2) Magnus, P.; Principe, L. M. *Tetrahedron Lett.* **1985**, 26(40), 4851–4854.
- (3) Yamanaka, M.; Nakamura, E. *J. Am. Chem. Soc.* **2001**, 123(8), 1703–1708.
- (4) Pericàs, M. A.; Balsells, J.; Castro, J.; Marchueta, I.; Moyano, A.; Riera, A.; Vázquez, J.; Verdaguer, X. *Pure Appl. Chem.* **2002**, 74(1), 167–174.
- (5) De Bruin, T. J. M.; Milet, A.; Greene, A. E.; Gimbert, Y. *J. Org. Chem.* **2004**, 69(4), 1075–1080.
- (6) Lesage, D.; Milet, A.; Memboeuf, A.; Blu, J.; Greene, A. E.; Tabet, J.-C.; Gimbert, Y. *Angew. Chem. Int. Ed. Engl.* **2014**, 53(7), 1939–1942.
- (7) Shambayani, S.; Crowe, W. E.; Schreiber, S. L. *Tetrahedron Lett.* **1990**, 31(37), 5289–5292.
- (8) Brown, D. S.; Campbell, E.; Kerr, W. J.; Lindsay, D. M.; Morrison, A. J.; Pike, K. G.; Watson, S. P. *Synlett* **2000**, 2000(11), 1573–1576.
- (9) Pauson, P. L., Khand, I. U., Ann, N. Y. *Acad. Sci.* **1977**, 295, 2–24.
- (10) Lledó, A.; Fuster, A.; Revés, M.; Verdaguer, X.; Riera, A. *Chem. Commun. (Camb)*. **2013**, 49(29), 3055–3057.
- (11) Ferrer, C.; Benet-Buchholz, J.; Riera, A.; Verdaguer, X. *Chem. Eur. J.* **2010**, 16(28), 8340–8346.
- (12) Revés, M.; Lledó, A.; Ji, Y.; Blasi, E.; Riera, A.; Verdaguer, X. *Org. Lett.* **2012**, 14(13), 3534–3537.
- (13) Rios Torres, R. *Pauson-Khand Reaction: Scope, Variations and Applications*, John Wiley and Sons, 2012.
- (14) Sugihara, T.; Yamada, M.; Yamaguchi, M.; Nishizawa, M. *Synlett* **1999**, 1999(6), 771–773.
- (15) Jeong, N.; Hwang, S. H.; Lee, Y.; Chung, Y. K. *J. Am. Chem. Soc.* **1994**, 116(7), 3159–3160.

- (16) Gunawan, M. A.; Hierso, J.-C.; Poinso, D.; Fokin, A. A.; Fokina, N. A.; Tkachenko, B. A.; Schreiner, P. R. *New J. Chem.* **2014**, *38*(1), 28–41.
- (17) Gimbert, Y.; Robert, F.; Durif, A.; Averbuch, M.-T.; Kann, N.; Greene, A. E. *J. Org. Chem.* **1999**, *64*(10), 3492–3497.
- (18) Sturla, S. J.; Buchwald, S. L. *J. Org. Chem.* **2002**, *67*(10), 3398–3403.
- (19) Smit, W. A.; Gybin, A. S.; Shashkov, A. S.; Strychkov, Y. T.; Kyz'mina, L. G.; Mikaelian, G. S.; Caple, R.; Swanson, E. D. *Tetrahedron Lett.* **1986**, *27*(11), 1241–1244.
- (20) Smit, V. A., Tarasov, V. A., Daeva, E. D., Ibragimov, I. I. *Izv.Akad.NaukSSSR, Ser.Khim.* **1987**, 2870–2871.
- (21) Pérez-Serrano, L.; Casarrubios, L.; Domínguez, G.; Pérez-Castells, J. *Org. Lett.* **1999**, *1*(8), 1187–1188.
- (22) Billington, D. C., Helps, I., Pauson, P. L., Thomson, W., Willison, D. *J. Organomet. Chem.* **1988**, *354*, 233–242.
- (23) Iqbal, M.; Vyse, N.; Dauvergne, J.; Evans, P. *Tetrahedron Lett.* **2002**, *43*(44), 7859–7862.
- (24) Jeong, N.; Chung, Y. K.; Lee, B. Y.; Lee, S. H.; Yoo, S.-E. *Synlett* **1991**, *1991*(03), 204–206.
- (25) Shen, J.; Gao, Y.; Shi, Q.; Basolo, F. *Organometallics* **1989**, *8*(9), 2144–2147.
- (26) Verdaguer, X.; Vázquez, J.; Fuster, G.; Bernardes-Génisson, V.; Greene, A. E.; Moyano, A.; Pericàs, M. A.; Riera, A. *J. Org. Chem.* **1998**, *63*(20), 7037–7052.
- (27) Y. Tang, L. Deng, Y. Zhang, G. Dong, J. Chen, Z. Y. *Org. Lett.* **2005**, *7*, 1657–1659.
- (28) Hayashi, M.; Hashimoto, Y.; Yamamoto, Y.; Usuki, J.; Saigo, K. *Angew. Chem. Int. Ed. Engl.* **2000**, *39*(3), 631–633.
- (29) Rautenstrauch, V.; Mégard, P.; Conesa, J.; Küster, W. *Angew. Chemie Int. Ed. English* **1990**, *29*(12), 1413–1416.
- (30) Cabot, R.; Lledó, A.; Revés, M.; Riera, A.; Verdaguer, X. *Organometallics* **2007**, *26*(5), 1134–1142.
- (31) Orgué, S.; León, T.; Riera, A.; Verdaguer, X. *Org. Lett.* **2015**, *17*(2), 250–253.
- (32) Kerr, W. J.; Kirk, G. G.; Middlemiss, D. *Synlett* **1995**, *1995*(10), 1085–1086.

- (33) Derdau, V.; Laschat, S. *J. Organomet. Chem.* **2002**, *642*(1-2), 131–136.
- (34) Montenegro, E.; Moyano, A.; Pericàs, M. A.; Riera, A.; Alvarez-Larena, A.; Piniella, J.-F. *Tetrahedron: Asymmetry* **1999**, *10*(3), 457–471.
- (35) Fonquerna, S.; Moyano, A.; Pericàs, M. A.; Riera, A. *J. Am. Chem. Soc.* **1997**, *119*(42), 10225–10226.
- (36) Fonquerna, S.; Rios, R.; Moyano, A.; Pericàs, M. A.; Riera, A. *European J. Org. Chem.* **1999**, *1999*(12), 3459–3478.
- (37) Bernardes, V.; Verdaguer, X.; Kardos, N.; Riera, A.; Moyano, A.; Pericàs, M. A.; Greene, A. E. *Tetrahedron Lett.* **1994**, *35*(4), 575–578.
- (38) Rodríguez Rivero, M.; De La Rosa, J. C.; Carretero, J. C. *J. Am. Chem. Soc.* **2003**, *125*(49), 14992–14993.
- (39) Vázquez, J. Theoretical Study on the Mechanism of the Pauson-Khand Reaction, Universitat de Barcelona (Spain), 1999.
- (40) Fjermestad, T. Computational Studies on the Mechanism of the Pauson-Khand Reaction, Universitat Rovira i Virgili (Spain), 2010.
- (41) Bladon, P.; Pauson, P. L.; Brunner, H.; Eder, R. *J. Organomet. Chem.* **1988**, *355*(1-3), 449–454.
- (42) Hay, A. M.; Kerr, W. J.; Kirk, G. G.; Middlemiss, D. *Organometallics* **1995**, *14*(11), 4986–4988.
- (43) Konya, D.; Robert, F.; Gimbert, Y.; Greene, A. E. *Tetrahedron Lett.* **2004**, *45*(37), 6975–6978.
- (44) Verdaguer, X.; Moyano, A.; Pericàs, M. A.; Riera, A.; Maestro, M. A.; Mahía, J. *J. Am. Chem. Soc.* **2000**, *122*(41), 10242–10243.
- (45) Verdaguer, X.; Pericàs, M. A.; Riera, A.; Maestro, M. A.; Mahía, J. *Organometallics* **2003**, *22*(9), 1868–1877.
- (46) Verdaguer, X.; Lledó, A.; López-Mosquera, C.; Maestro, M. A.; Pericàs, M. A.; Riera, A. *J. Org. Chem.* **2004**, *69*(23), 8053–8061.
- (47) Solà, J.; Riera, A.; Verdaguer, X.; Maestro, M. A. *J. Am. Chem. Soc.* **2005**, *127*(39), 13629–13633.

- (48) Revés, M.; Achard, T.; Solà, J.; Riera, A.; Verdaguer, X. *J. Org. Chem.* **2008**, *73*(18), 7080–7087.
- (49) Solà, J.; Revés, M.; Riera, A.; Verdaguer, X. *Angew. Chem. Int. Ed. Engl.* **2007**, *46*(26), 5020–5023.
- (50) Krafft, M. E.; Romero, R. H.; Scott, I. L. *Synlett* **1995**, 577–578.
- (51) Gordon, A. R.; Johnstone, C.; Kerr, W. J. *Synlett* **1995**, *1995*(10), 1083–1084.
- (52) MacWhorter, S. E.; Schore, N. E. *J. Org. Chem.* **1991**, *56*(1), 338–346.
- (53) Krafft, M. E.; Romero, R. H.; Scott, I. L. *J. Org. Chem.* **1992**, *57*(20), 5277–5278.
- (54) Bruin, T. J. M. De; Milet, A.; Gimbert, Y.; Greene, A. E.; Ledss, C. R.; March, R. V. *J. Am. Chem. Soc.* **2001**, No. 10, 7184–7185.
- (55) De Bruin, T. J. M.; Michel, C.; Vekey, K.; Greene, A. E.; Gimbert, Y.; Milet, A. *J. Organomet. Chem.* **2006**, *691*(20), 4281–4288.
- (56) Fager-Jokela, E.; Muuronen, M.; Patzschke, M.; Helaja, J. *J. Org. Chem.* **2012**, *77*(20), 9134–9147.
- (57) Aiguabella, N.; del Pozo, C.; Verdaguer, X.; Fustero, S.; Riera, A. *Angew. Chem. Int. Ed.* **2013**, *52*(20), 5355–5359.
- (58) Konno, T.; Kida, T.; Ishihara, T. *J. Fluor. Chem.* **2012**, *144*, 147–156.
- (59) Moulton, B. E.; Whitwood, A. C.; Duhme-Klair, A. K.; Lynam, J. M.; Fairlamb, I. J. S. *J. Org. Chem.* **2011**, *76*(13), 5320–5334.
- (60) Vázquez-Romero, A.; Rodríguez, J.; Lledó, A.; Verdaguer, X.; Riera, A. *Org. Lett.* **2008**, *10*(20), 4509–4512.
- (61) Linus Pauling. *The Nature of the Chemical Bond, An Introduction to Modern Structural Chemistry*, Cornell Un.; Press, C. U., Ed.; 1960.
- (62) Gyftopoulos, E. P.; Hatsopoulos, G. N. *Proc. Natl. Acad. Sci. U. S. A.* **1968**, *60*(3), 786–793.
- (63) Brown, H. C.; Roy, C. D.; Soundararajan, R. *Tetrahedron Lett.* **1997**, *38*(5), 765–768.
- (64) Barder, T. E.; Buchwald, S. L. *J. Am. Chem. Soc.* **2007**, *129*(16), 5096–5101.

- (65) Kjellgren, J.; Sundén, H.; Szabó, K. J. *J. Am. Chem. Soc.* **2004**, *126* (2), 474–475.

CHAPTER III

Synthetic applications of the intermolecular PKR

Contents

3.1 Synthetic proposal	53
3.2 Sarkomycin synthesis	55
3.2.1 Introduction	55
3.2.2 Synthetic background	55
3.2.3 Results and discussion	60
3.3 Jasmonate synthesis	72
3.4 General conclusions	82

3.1 Synthetic proposal

Over the diversity of synthesis developed for sarkomycin and jasmonic acid (JA) (figure 3.1), only few were obtained in an enantioselective manner and none of them used the Pauson-Khand reaction for the formation of five-membered ring.

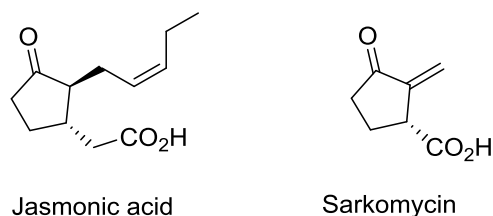


Figure 3.1. Structure of the JA and Sarkomycin.

With the objectives to search for synthetic development and applications of the PKR, our group acquired a strong expertise in the field of the Pauson-Khand reaction. Among the synthesis of natural products, our group recently developed the synthesis of the 13-epi-12-oxo PDA from the PK adduct of the NBD and the N-Boc propargyl amine (figure 3.2).¹ In the case of the 13-epi-12-oxo PDA, the final cyclopentenone came from a retro Diels-Alder reaction. The α -chain resulted from conjugate addition over the exocyclic enone which was the product of the elimination reaction of Boc-protected amine. The β -chain was attached to the PK adduct of norbornadiene and N-boc-propargylamine by conjugate addition and chemical transformations.

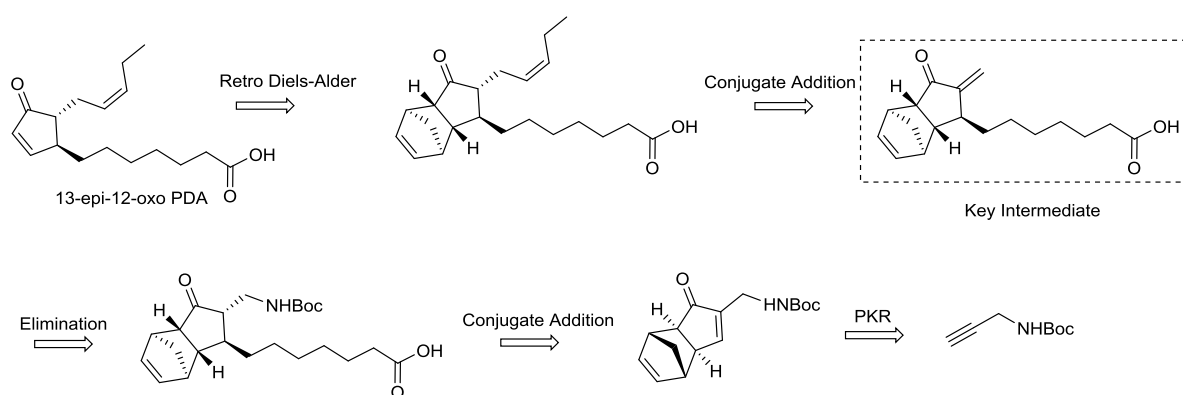


Figure 3.2. Riera's synthesis of the 13-epi-12-oxo PDA.

Inspired by this synthetic pathway, the formation of the exocyclic enone would be the key step in the design of the sarkomycin. Two routes were envisaged which involve one enantioselective synthesis starting from the Pauson-Khand reaction between N-Boc-propargylamine and norbornadiene or one racemic using PKR of internal alkynes (figure 3.3). With the enantioselective version, the insertion of the β -chain with the right stereochemistry would be obtained by photochemical addition of methanol over the PK adduct which after oxidation and methylation reactions would afford the methyl ester function. The cyclopentenone of the sarkomycin would be liberated via retro Diels-Alder reaction and converted into cyclopentanone after hydrogenation. As final step, β -elimination would afford the methyl ester sarkomycin.

With the racemic synthesis, the installation of the two substituents and the cyclopentenone would be obtained in a single step with a PKR.

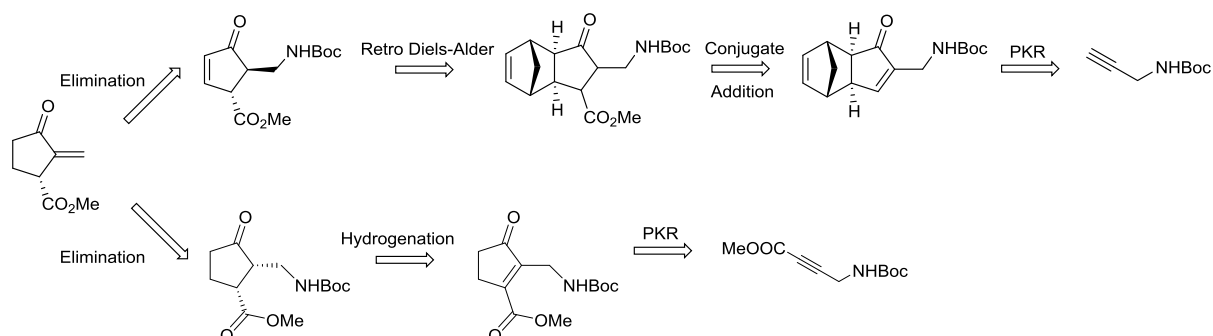


Figure 3.3. Two retrosynthesis envisaged for the methyl ester sarkomycin.

In the case of the methyl jasmonate, two approaches were envisaged. The first route would install in a single step the cyclopentenone with the α - and β -chains by regioselective PKR of disubstituted alkyne. The α -chain would afterward be introduced by conjugate addition over the exocyclic enone (figure 3.4). The retro Diels-Alder reaction followed by selective hydrogenation would afford the MeJA.²

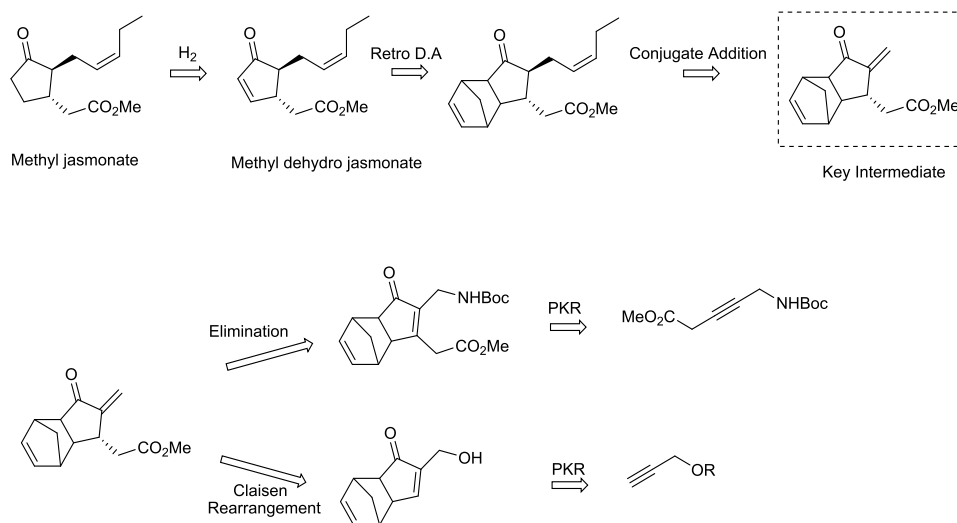


Figure 3.4. Retrosynthesis envisaged for the MeJA.

The second route started from PKR of a propargylic alcohol with NDB. The resulted adduct would be engaged into a Claisen-Johnson rearrangement to introduce in a single step the β -chain. Due to the steric environment of the PK adduct, we expected that the rearrangement might be stereoselective. As in the first approach, the conjugate addition over the enone would introduce the α side chain. Then, a retro-Diels-Alder reaction would afford the methyl jasmonate after selective reduction.

3.2 Sarkomycin synthesis

3.2.1 Introduction

Progress to struggle diseases such as infections caused by bacteria have been spectacular. Nevertheless, a global resistance phenomena is dramatically growing³, forcing health authorities to undertake major political actions to overcome this problem. Planned by the Japanese government in 60' s, large screening campaigns over microorganisms to search for new anti-bacterial and anti-cancer substances permitted to discover among others the sarkomycin.⁴ Isolated from *Streptomyces erythrochromogenes* by Umezawa *et al.*⁵ in 1955, sarkomycin exhibited low toxicity⁶ and efficiency on Ehrlich ascites carcinoma, acting as a selective inhibitor of the DNA synthesis.⁵ Hopper *et al.* revealed and structurally elucidated the active principle of the Sarkomycin, the 2-methylene-3-oxocyclopentanecarboxylic acid.⁷ In 1956, began phase III clinical trials in Japan, USA and England for its antitumor property.⁸ Due to its synthetic difficulties, it finally launched the market decades later by the Takeda Japanese pharmaceutical Company.

Sarkomycin is a cyclopentanone bearing an exocyclic methylene with a carboxylic acid side chain. Its absolute configuration initially attributed S was unambiguously refuted, by Hill in 1967 to be R.⁹

Before the great development of syntheses of sarkomycin, its early beginning was quite tedious due to its high volatility and the highly reactivity of the exocyclic enone.⁷ Even though it is simple structure, specific issues were faced to reach its synthesis such as its decomposition under cold storage, evaporation steps, the use of high temperatures and strong acid or basic treatments which led to isomerization, polymerization and decomposition.¹⁰ To overcome those issues and facilitate the handling, protected forms of sarkomycin have been developed such as ester or lactone (cyclosarkomycin) (figure 3.5).

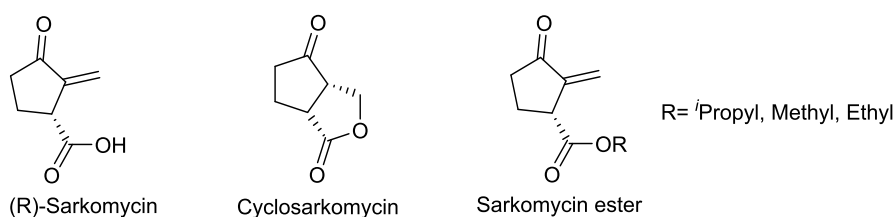


Figure 3.5. Structure of the sarkomycin and its protected forms.

3.2.2 Synthetic background

More than thirty syntheses have been published to reach either the racemate or the pure enantiomer of sarkomycin or its esters. Nowadays, sarkomycin is still of interest since it is used as a benchmark for synthetic methodology.¹¹

Reviewing the literature available related to Sarkomycin ester, identification of common pathways has been tagged. General overview of the different methodologies as well as some

examples of enantioselective synthesis will be briefly detailed placing in its context their work in the field.

Basically, two routes are used for the construction of sarkomycin protected forms, either functionalised olefins are engaged in cyclisation or commercially available cyclic derivatives are transformed. Independently from the initial substrate used, the synthesis of different protected forms of the sarkomycin can be obtained from common intermediates like depicted in the figure 3.6.

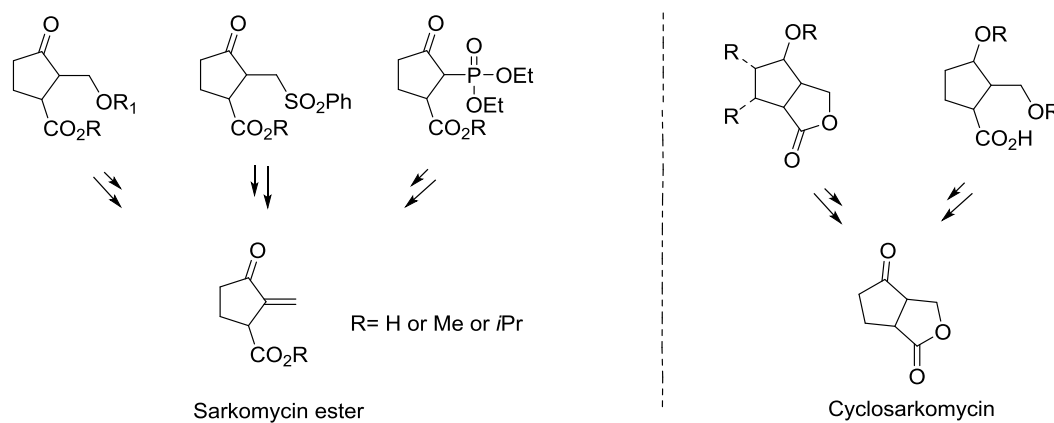


Figure 3.6. Common intermediates used in synthesis of the protected sarkomycin.

Synthetic challenges involved the methylene formation and the introduction of the carboxylic acid function (enantioselective or not).

For the synthesis of the ester sarkomycin, the commercially available cyclopentenone was widely used. The exocyclic enone was formed by β -elimination after acidic treatment from protected alcohol or sulfone (figure 3.7). The carboxylic acid was inserted by a previous conjugate addition over the Michael acceptor cyclopentenone. Nucleophiles could be cyanide, nitro, vinyl or sulphur derivatives which were oxidised into the corresponding acid. The enantioselective induction usually employed catalysts that will be described later.

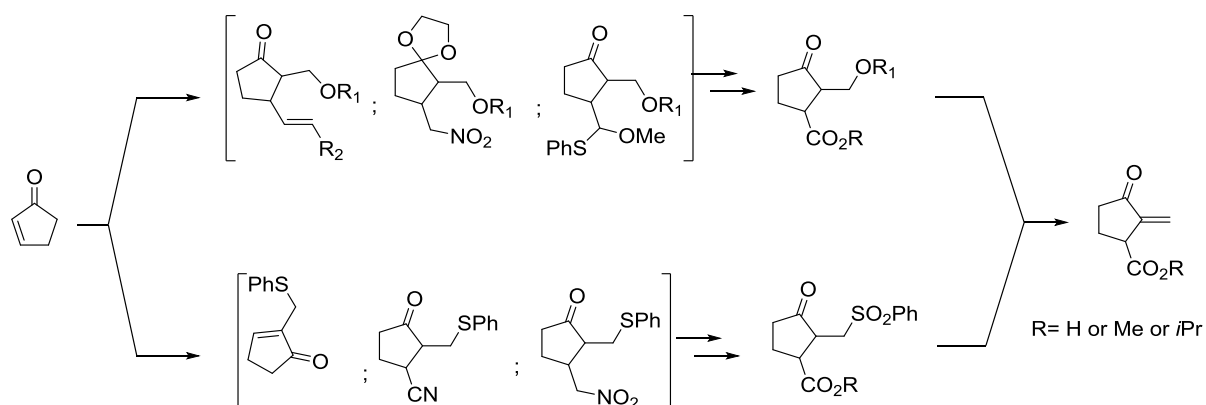


Figure 3.7. Synthesis of the sarkomycin esters from cyclopentenone.

The first synthesis of *rac*-sarkomycin ester available was described by Toki *et al* (1957) in four steps.¹² Unfortunately, the first step, a claimed regiospecific Mannich condensation was reported twenty years later by Hill¹³ to be a mixture of isomers, (1:2) ratio of the C3 and C5 products, obviously not detectable by instrumentations at that time (figure 3.8).

The strategy began with a Mannich condensation of a non-commercially available ethyl cyclopentanone-3-carboxylate. The resulting tertiary amine obtained in low yield was then basified and heated up to allow the elimination, and formation of the *rac*-Sarkomycin ester. Hard hydrolysis of ethyl ester to the free acid was accompanied by decomposition of the product.

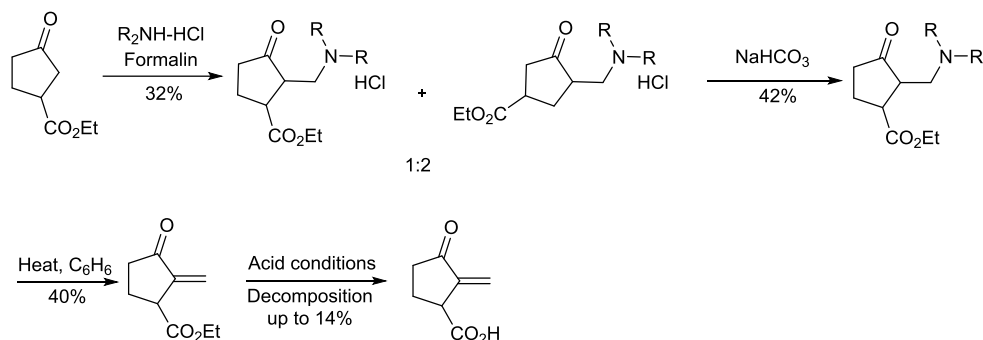


Figure 3.8. First synthesis of the *rac*-Sarkomycin ester.

The first regioselective synthesis proposed by Minaskanian⁷ involved a reactive 2-carbomethoxy-cyclopent-2-enone as starting material (figure 3.9). The *rac*-Sarkomycin was obtained in 8 steps, with 7% overall yield. The 2-carbomethoxycyclopentanone reacted with benzeneselenyl chloride to give after oxidation the 2-carbomethoxy-cyclopent-2-enone. With an excess of diethylaluminium cyanide it afforded a 10:1 mixture of the trans/cis isomers in 38% yield over three steps. The ketone group was protected as ketal and the reduction of the ester in alcohol by using mixture lithium borohydride/sodium hydroxide was obtained in 80% yield. Then, mild basic hydrolysis of the cyano group into its acid induced the epimerization of C3 which cyclised into the protected keto lactone depending on the neighboring group participation. Hydrolysis of the keto lactone liberated the cyclosarkomycin in good yields. The final deprotection was reported to be done in mild acidic treatment to give the β -elimination into *rac*-Sarkomycin in 43% yield.

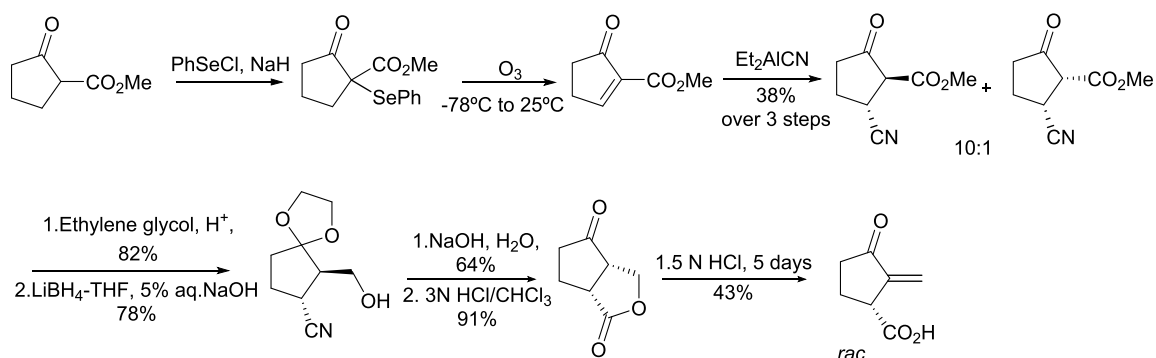


Figure 3.9. Minaskanian's regioselective synthesis of *rac*-Sarkomycin.

Mikolajczyk *et al.* (1996) used as key intermediate the diethyl 1-diazo-2-oxohept-6-ene-phosphonate (figure 3.10).¹⁴ In the first step, the starting material was alkylated with homoallyl bromide to give the β -oxo-phosphonate in 78% yield which under typical diazo-transfer reaction conditions gave the α -diazophosphonate in 82% yield. This intermediate was engaged into promoted cyclisation with rhodium (II) acetate affording *trans*-3-carboxy-2-diethoxyphosphorylcyclopentanone in 58% yield. The transformation of the 3-vinyl moiety into the carboxylic acid was allowed by ozonolysis to give the corresponding acid which underwent oxidation by Jones reagent in racemic and almost quantitative form. The resolution of the racemate was performed by kinetic enzymatic reaction with α -chymotrypsin. In that case, enzymatic hydrolysis gave the corresponding acid in 77% ee and 50% conversion. As last step, the Wittig-Horner reaction afforded the exocyclic methylenic moiety of the sarkomycin in 61% yield.

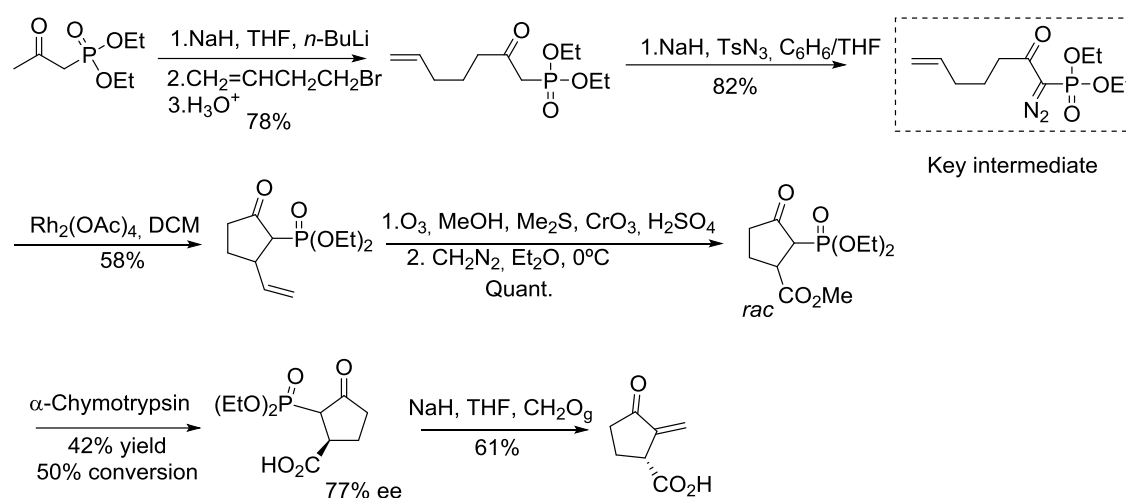


Figure 3.10. Mikolajczyk's synthesis.

The great difficulty to construct regio- and enantioselective synthesis of such kind of simple compound is demonstrated by the few enantioselective synthesis available in the literature.

Boeckman *et al.* (1980) reported the first enantioselective synthesis of Sarkomycin where the right chirality at the β -position of the sarkomycin was induced by the chiral auxiliary, (-)-8-phenyl menthyl acrylate (figure 3.11).¹⁵ The synthesis of the starting material was obtained by a enantioselective Diels-Alder reaction given a cyclohexene core in 83% yield, which was then transformed into the free alcohol in 70% yield and 98% ee.

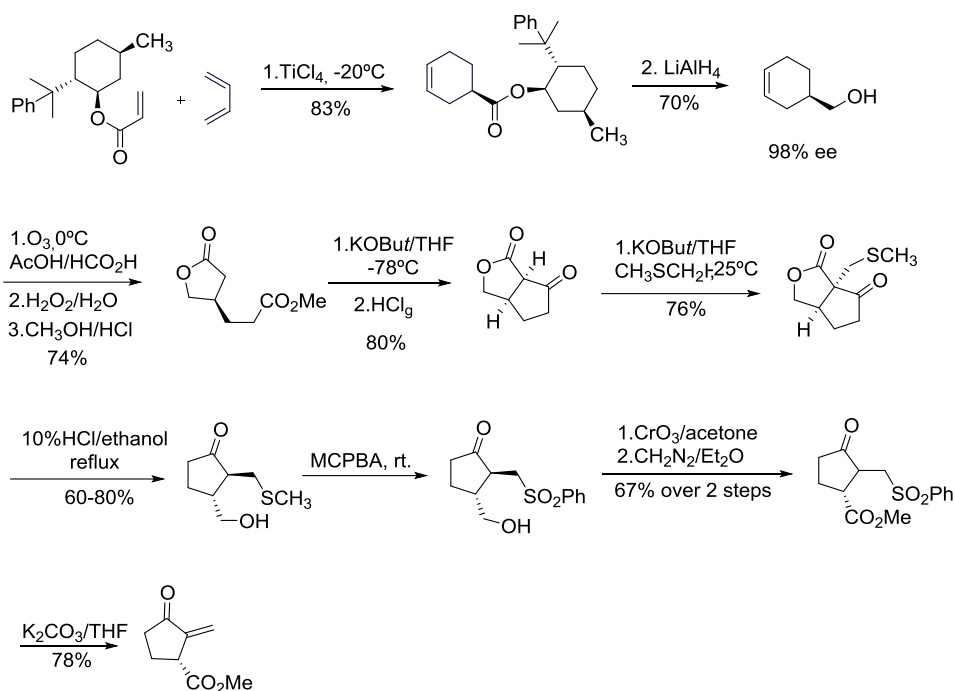


Figure 3.11. Boeckman' synthesis.

After ozonolysis in HOAc/HCOOH, oxidative workup and esterification it afforded the lactone ester in 74% yield. Dieckmann cyclisation under KO t Bu in THF followed by acidic treatment with HCl afforded the bicyclic keto lactone in 80%. Introduction of the required methylene was accomplished by the alkylation with (iodomethyl)methyl sulfane generated in situ providing the bicyclic lactone in 76% yield. It was then performed the lactone hydrolysis and decarboxylation by 10% aqueous HCl releasing the free alcohol. Oxidation to sulfone followed by Jones oxidation to the acid and methylation permitted to obtain the final intermediate of synthesis in 67% yield over two steps. Elimination of the sulfone to the methyl ester R-sarkomycin was allowed by basic treatment in 78% yield.

In 2013, Zeszschwitz *et al.* developed the first synthesis using asymmetric catalysis to introduce the stereogenic centre.¹¹ Sarkomycin was prepared in 5-step total synthesis with 19% overall yield from cyclopent-2-en-1-one (figure 3.12). The first step consisted in a rhodium-catalysed asymmetric conjugate alkenyl addition with subsequent silyl tapping in 95% yield and 96% ee. Mukaiyama aldol reaction with aqueous formaldehyde, followed by the conversion of the free alcohol into tetrahydropyranyl (THP) acetal was performed in 37% yield over two steps. The double bond was cleaved and oxidised with ruthenium chloride (III)/sodium periodate in 62%. Sarkomycin was finally liberated under acid condition via microwave-assistance.

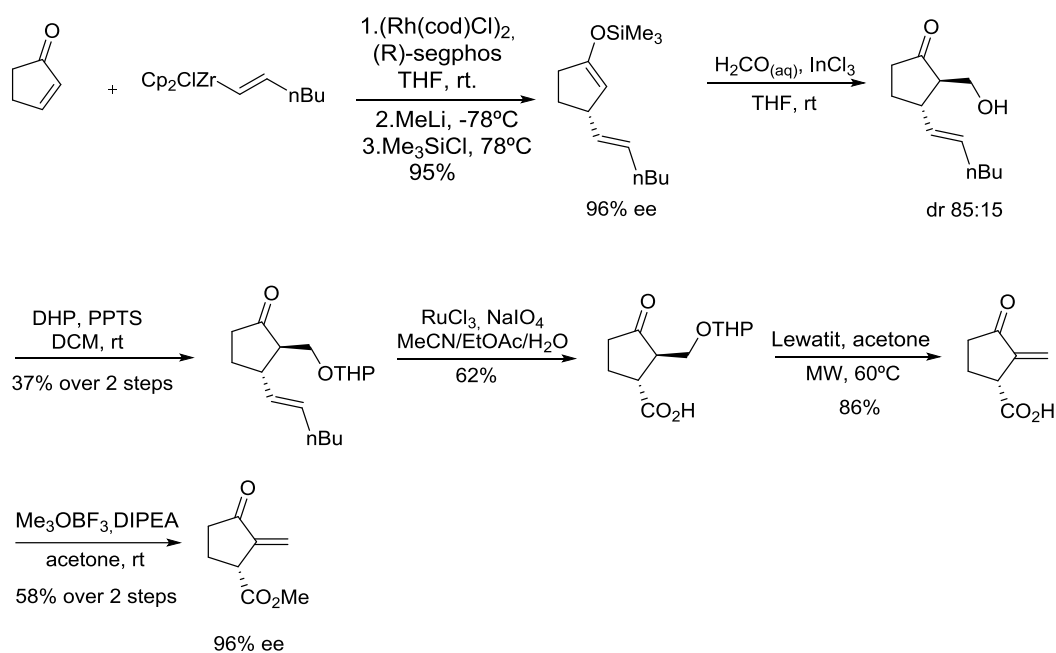


Figure 3.12. Zezschwitz's synthesis.

3.2.3 Results and discussion

Our approach to the methyl ester sarkomycin in its enantioselective and racemic versions follow a general pathway which involved for the construction of the cyclopentenone unit using the Pauson-Khand reaction. The β -elimination of the amine would afford the exocyclic double bond. Different PK adducts were synthesised to identify which would be the best candidate to perform the synthesis of the sarkomycin ester.

Inspired by the previous work developed in our group, the enantioselective synthesis would involve as key step the stereoselective introduction of the β -chain into the PK adduct of different protected propargylamines and norbornadiene (figure 3.13).

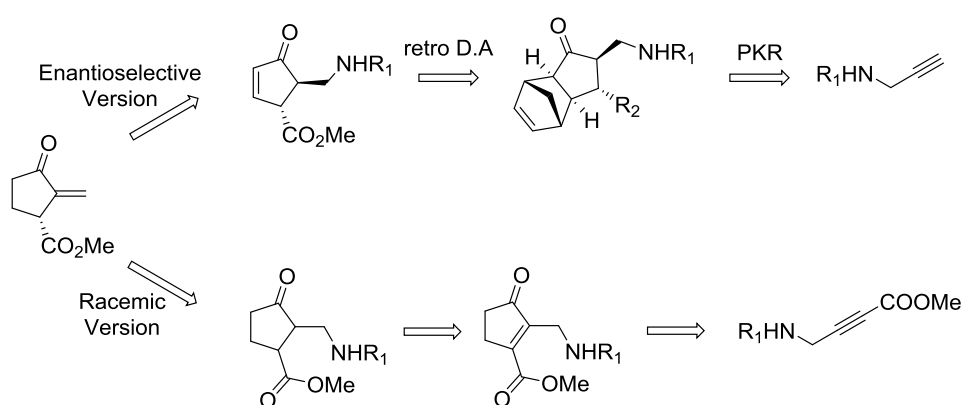


Figure 3.13. Enantioselective and racemic synthesis envisaged.

For its racemic version, the PKR of ethylene and a disubstituted propargylic amine alkyne methyl ester was envisaged to introduce the two chains in one single step.

The final step would involve a simple reduction of the double bond followed by the β -elimination affording the methyl ester of the ester sarkomycin.

3.2.3.1 PKR study

PK adducts of several protected propargylamines such as Boc, Cbz or phthalic groups were envisaged for the study of the synthesis of the sarkomycin methyl ester. The synthesis started with the preparation of the different alkynes, **58-60**. Treating the propargyl amine with Boc_2O afforded the N-Boc-protected amine **58** in 82% yield. **59** was obtained in 66% yield by treating the propargyl amine with CbzCl (figure 3.14). The phthalimide propargyl amine **60** was synthesised by the direct treatment with phthalic anhydride in 62% yield.

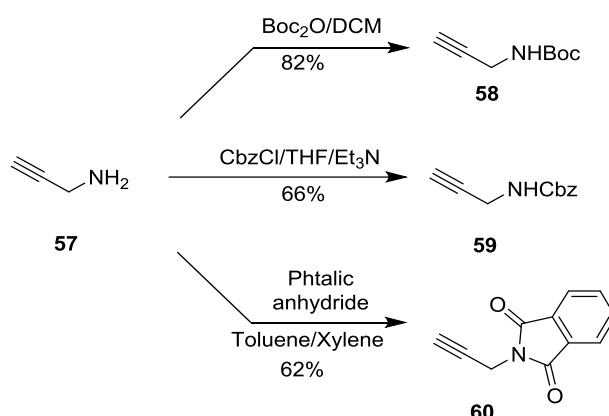


Figure 3.14. Synthesis of the starting material **58-60**.

Then, the intermolecular PKR was tried between the protected amine and the NBD. N-Boc propargyl amine and norbornadiene afforded 49% yield of the PK adduct **61** with a high *exo/endo* diastereomer ratio 94:6 (figure 3.15). Improvement was performed under catalytic condition with 10% of triphenylphosphine dicobalt heptacarbonyl, under 2 barg pressure of carbon monoxide. 60-79% yields were obtained and only traces of *endo* product could be detected by NMR. The asymmetric version of this reaction was successfully optimised using a chiral ligand in Nuria Aiguabella's thesis.

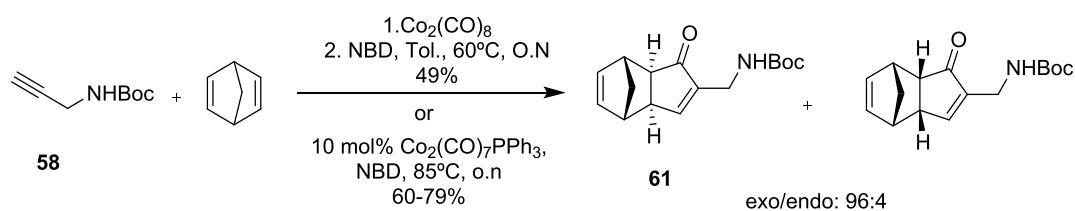


Figure 3.15. Synthesis of the PK adduct, **61**.

The PK adduct of the alkynes **59** and **60** with norbornadiene heating up overnight at 70°C afforded about 50% of the compound **62** and 40% yield of the compound **63** (figure 3.16). Substantial improvement was observed by changing temperature of reaction and equivalents of NBD.

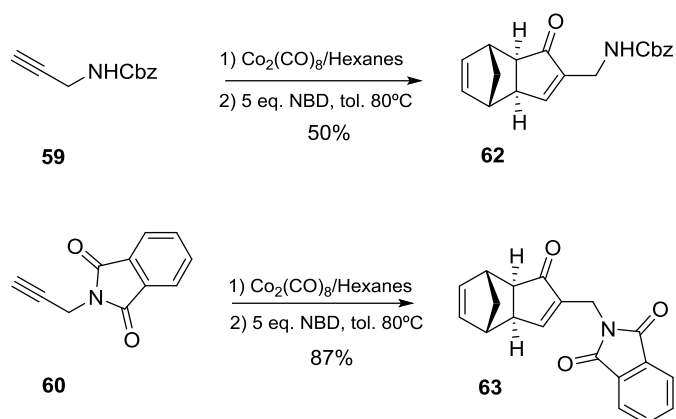


Figure 3.16. Synthesis of the different PK adducts **62-63**.

Optimisation of the reaction afforded 87% yield of the PK adduct **63** with high endo/exo ratio 37:1, at 80°C and 5 equivalents of NBD. With the PK adducts **62-63** in hand, we undertook the study of the introduction of the β -chain of the cyclopentenone.

3.2.3.2 Study of the β -chain introduction

To identify which methodology was the most suited one to stereoselectively introduce the carboxylic acid in β -position of the cyclopentenones **53-55**, different methodologies were envisaged (figure 3.17). The introduction of methanol, nitromethane, dioxolane and cyanide were tried as protected form of the methyl ester function.

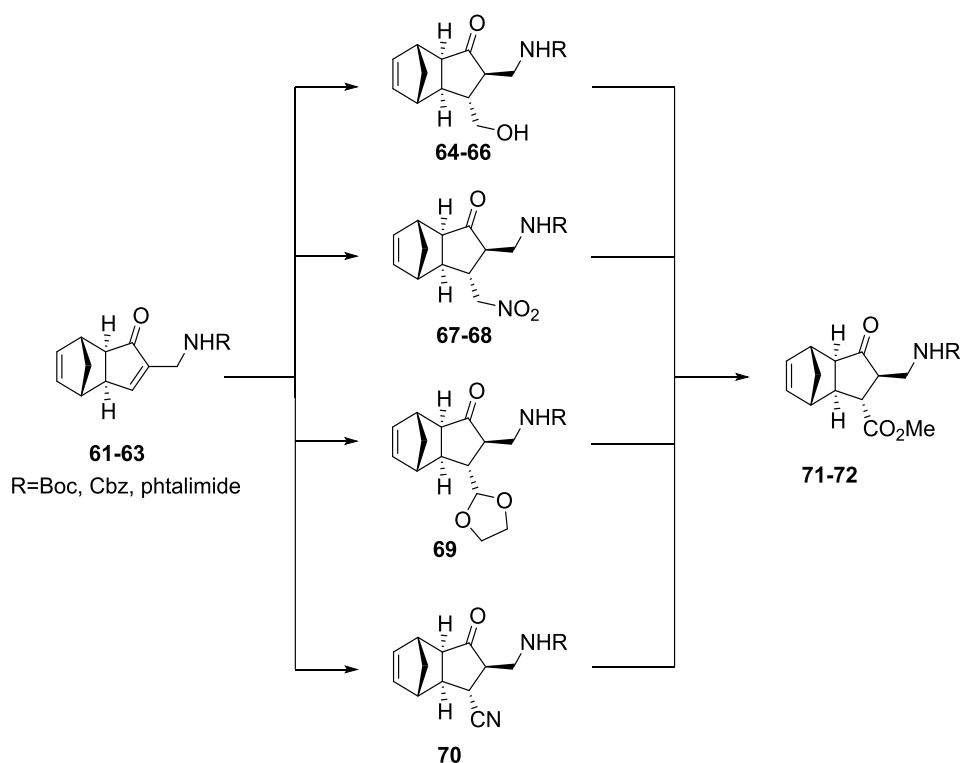


Figure 3.17. Different pathways envisaged to reach the methyl ester precursor of the sarkomycin.

Thus, the nitromethyl group would afford the corresponding carboxylic acid after a Nef reaction and the dioxolyl group, protected form of the aldehyde would be cleaved by an acidic treatment. The alcohol moiety and the cyanide group would afford after direct hydrolysis the corresponding acid function.

In our group, it was identified that the introduction of the methanol or dioxolane over PK adducts could be done by photochemistry. Good yields were obtained with the PK adducts of trimethylsilyl alkyne **73**¹⁶ or propargylic protected amine¹ using a photosensitizer, benzophenone in degassed methanol at 350 nm (figure 2.18). Even though this reaction was an efficient and selective method for the introduction of hydroxymethyl group, it was observed with the trimethylsilyl alkyne and without benzophenone a competition reaction of transposition shown in the figure 3.18.

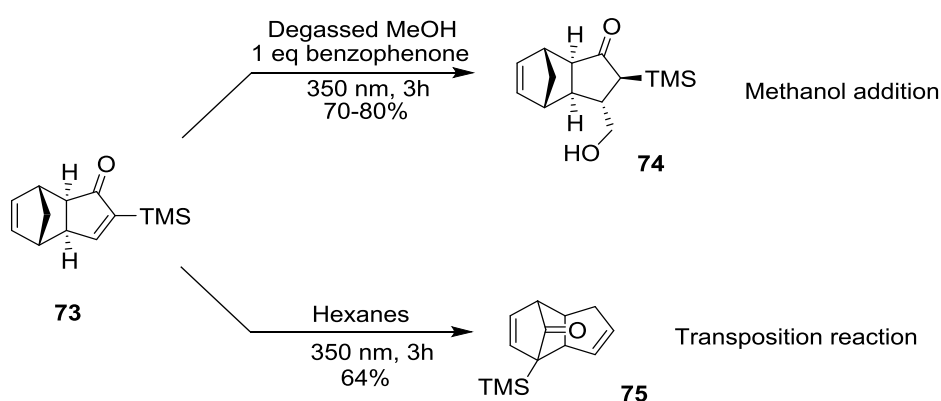


Figure 3.18. Photo-induced reaction over compound **73**.

Depending on solvent and concentration in triplet photosensitizer used, the methanol addition or the transposed isomer were obtained.

As first alternative, the hydroxymethyl photochemical addition over Pauson-Khand adducts was tried. The methanol radical was generated with degassed methanol, 1 equivalent of benzophenone at 350nm with a Rayonet® apparatus (16 lamps). The steric environment of the PK adduct imposed a nucleophilic attack on the less hindered side of the molecule leading to the formation of one single diastereoisomer.

Under light, PK adducts **61** and **62** led to the formation of a complex mixture of products where the desired product was obtained in only 30-40% yield (figure 3.19).

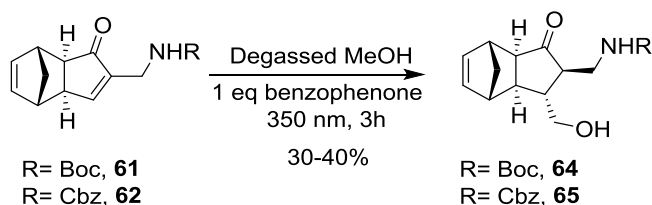


Figure 3.19. Photo-induced methanol addition over **61-62**.

From these results, optimisation of the reaction conditions was tried with the PK adduct **61**, changing parameters that could influence the photochemical reactions.

Thus, wavelength, type of glassware, concentration in substrate were modified and presented in the table 3.1 below.

The reaction turned out to be unreliable and yields to get **64** oscillated from 10 to a maximum of 54%. We observed that the scale up of this reaction was impossible where yields dropped dramatically passing from 54% at 150 mg to 13% at 800 mg scale (table 3.1, entry 1). Regarding the type of glassware, for same reaction condition, the use of typical borosilicate glass vs. quartz flask, did not show any improvement. The quantity of benzophenone was investigated from 0.06 to 5 equivalents benzophenone without any success (table 3.1 entry 2) and yields dropped to 9% with 0.06 equivalents of photosensitizer.

Entry	Eq. Benzophenone	Quantity	Wavelength	Nature of glassware	Yield
1	1	296-800 mg	350 nm	Quartz	10-54%
2	0.06-5	100-150 mg	350 nm	Quartz	9-28%
3	1	300 mg	350 nm	Borosilicate at 10°C	12%
4	1	468 mg	254 nm	Borosilicate	---

Table 3.1. Optimisation of the photochemical reaction of compound **56**.

The Pauson-Khand adduct of trimethylsilyl alkyne **73** was described in our group to give the methanol addition and dioxolane in good yield (about 80%) at 13°C (figure 3.20). Since 16 lamps generated a temperature of 35°C and a yield of 40%, the reaction was ran at 10°C but it afforded **64** in 10% yield (table 3.1, entry 3).

To the light of results, control reactions were performed. The photochemical reaction of **73** was carried out at 35°C where it gave a quantitative addition of the methanol, compound **74** and 80% of the dioxolane addition, compound **76**. The reaction crudes were perfectly clean even the standard condition was reported to be done at low temperature.

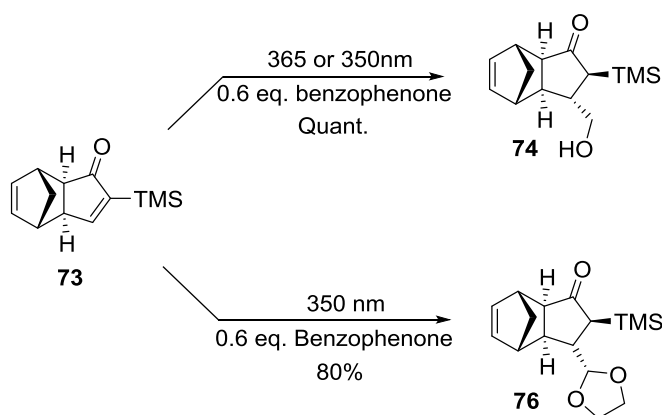


Figure 3.20. Photochemical controls with Pauson-Khand adduct **73**.

This controls indicated that the inner physical properties of the N-protected PK adducts were engaged in the photochemical decomposition phenomena.

350nm wavelength lamp was replaced by 254 nm lamp but entire decomposition of the starting material occurred (table 3.1, entries 4).

The adduct **63** afforded a mixture of the expected adduct **66** in about 15% yield and somehow surprisingly the transposed product compound **77** in about 30% yield (figure 3.21).

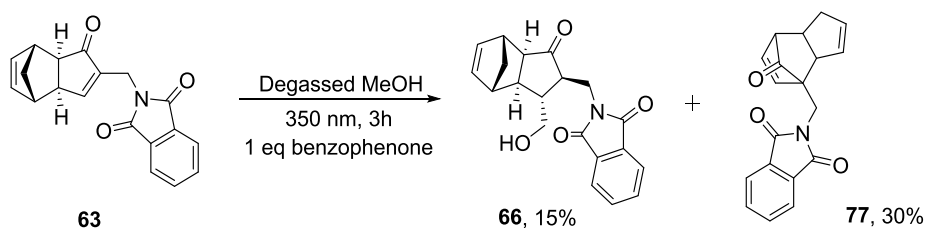


Figure 3.21. Transposition reaction occurring with the PKR, **63**.

In the case of the compound **63**, it was envisaged to optimise the photochemical reaction, reducing the proportion of transposed adduct. The type, concentration of the photosensitizer and the nature of wavelength were investigated. Replacement of the benzophenone by 4,4'-dihydroxybenzophenone was subsequently tried without significant improvement. Indeed, for an optimal photochemical transformation to occur, the energy captured by the photosensitizer need to be efficiently transmitted to the substrate. It was observed that under catalytic concentration of the sensitizer and no matter its nature, the reaction was not complete and formed only the transposed adduct in a ratio (1:1.4) in the case of 4,4'-dihydroxybenzophenone and 1:2.9 with benzophenone (table 3.2, entries 1, 2). At 2 equivalents and 350 nm, the reaction turned out to be complete and 12% of **66** and 25% of **77** were isolated (table 3.2, entry 3). Increase in the quantity of equivalents of benzophenone up to 5 as well as greater dilution of the substrate did not show significant changes (table 3.2, entry 3-4). For last attempts, shorted wavelength was used but again induced the decomposition of the compound **63** (table 3.2, entry 5).

Entry	Wavelength	Sensitizer	Eq.	63	66	77	[63]mol.L ⁻¹
1	350nm	Ph ₂ CO	0.7	1	-	2.9	0.08*
2	350nm	Ph ₂ (OH) ₂ CO	0.6	1	-	1.4	0.08**
3	350nm	Ph ₂ CO	2	-	12-31%	25-37%	0.02*
4	350nm	Ph ₂ CO	2-5	-	8-15%	18-33%	0.05*
5	254nm	Ph ₂ CO	2	-	-	-	0.05*

Table 3.2. Attempt to optimise the transformation of **63** to **77**.

To conclude, our best results afforded 31% of methanol addition **66** with 37% of the transposed product **77** working at 2 equivalents of benzophenone, 350 nm and about 0.02M concentration.

As alternatives for the hydroxymethyl addition, the conjugated addition of the nitromethane, 1,3-dioxolane and the nitrile were envisaged over different PK adducts (figure 3.22).

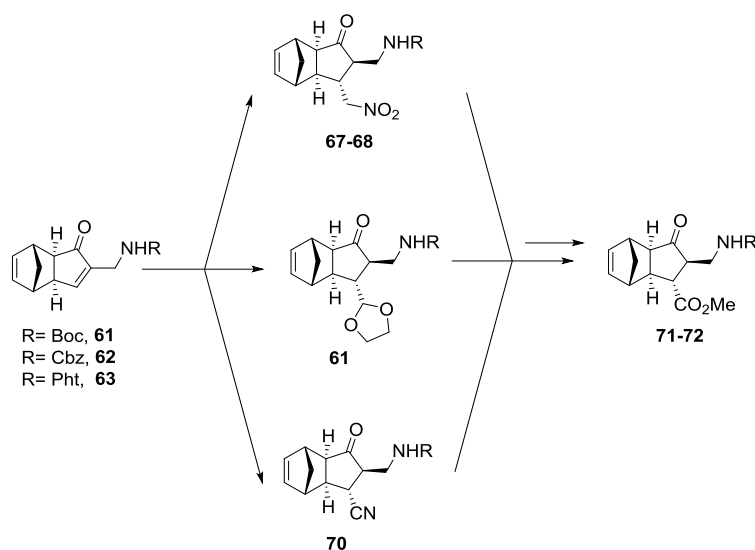


Figure 3.22. Alternatives to photochemical addition of methanol.

The addition of the nitromethyl group on **61-62** was obtained under microwave conditions at 50 Watt, 70°C in 40 and 60% yield respectively. The Nef reaction to form the acid was tried with sodium nitrite in acetic acid or nitronate salt under acidic condition without showing any traces of the final acid in the crude of reaction.

To validate the Nef reaction procedure, controls were performed using PKR of the trimethylsilane alkyne **73** which turned out positive yielding to **79** in 83% yield (figure 3.23).

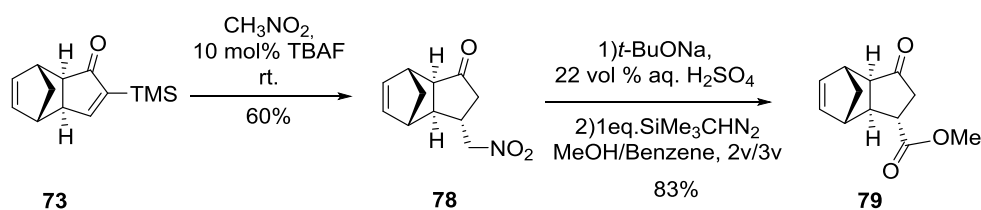


Figure 3.23. Control reaction with the PKR of the trimethylsilane alkyne **73**.

The photochemical addition of 1,3-dioxolane over **61** afforded 37% yield of compound **69** but its deprotection of under hydrochloric acid condition resulted difficult to achieve (figure 3.24).

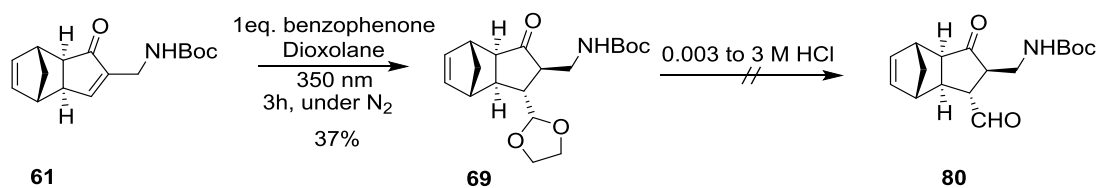


Figure 3.24. 1,3-dioxolane photochemical addition reaction over compound **61**.

The introduction of the nitrile group into PK adducts **61** and **63** were tried with NaCN, in basic condition and led to the cleavage of the protecting group to release the methyl chain in 53% yield, compound **81** (figure 3.25).

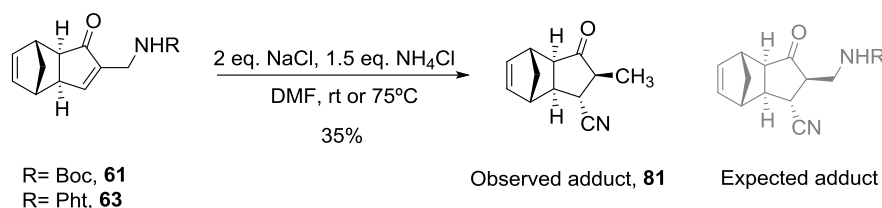


Figure 3.25. Nucleophilic addition of nitrile over compound **61** and **63**.

Over the diverse methodologies investigated, the only way to introduce the carboxylic acid over PK adduct **61** was obtained with the photochemical addition of methanol. Even the yield of reaction was moderate and the reaction unreliable, we decided to continue the synthesis in order to see if our synthetic route to afford the sarkomycin methyl ester was viable.

3.2.3.3 Retro Diels-Alder study

With the mgs collected of the adduct **64**, the primary alcohol was transformed into methyl ester compound **71**, using catalytic amount of potassium dichromate (0.02 eq.) in nitric acid (20%mol) to afford in 69% yield after esterification with trimethylsilyl diazomethane (figure 3.26).

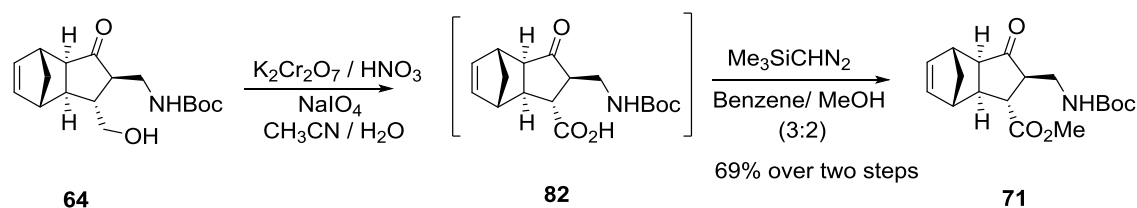


Figure 3.26. Oxidation reaction of the PK adduct **64**.

As mentioned in the synthetic approach, previous doctoral work of Nuria Aiguabella performed the release 12-oxo-13 PDA from PK adduct by a microwave-assisted retro-Diels-Alder (DA) reaction.¹ Procedure afforded 54% yield of the desired product at 20 mg scale (figure 3.27). In our case, the study of the cleavage of the NBD unit by the retro Diels-Alder reaction was considered with several PK adducts (figure 3.27). With the small amount of compound **71** available, the reaction was carried out with 10mg scale and analysed by LC/MS. The reaction was performed at 250 Watt, 70°C during 60 sec, in presence of 1 equivalent of methylaluminum dichloride and 15 equivalents of maleic anhydride.

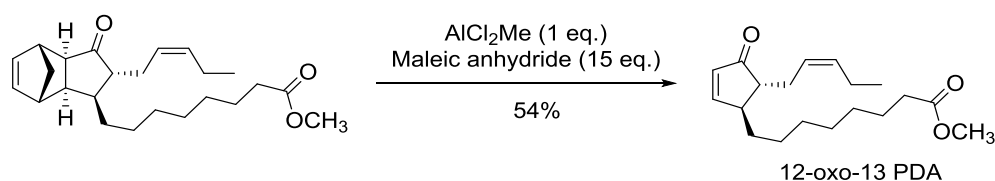


Figure 3.27. Microwave-assisted retro Diels-Alder reaction of PK adducts.

In the case of the PK adduct of the N-Boc protected amine **71**, retro Diels-Alder reaction led to the formation of a complex mixture. By LC-MS analysis, we could detect the presence of a small amount of the expected product where its free amine reacted with maleic anhydride (**83**) (figure 3.28). The main product observed was the result of the reaction between the deprotected PK adduct which reacted with maleic anhydride, compound **84**.

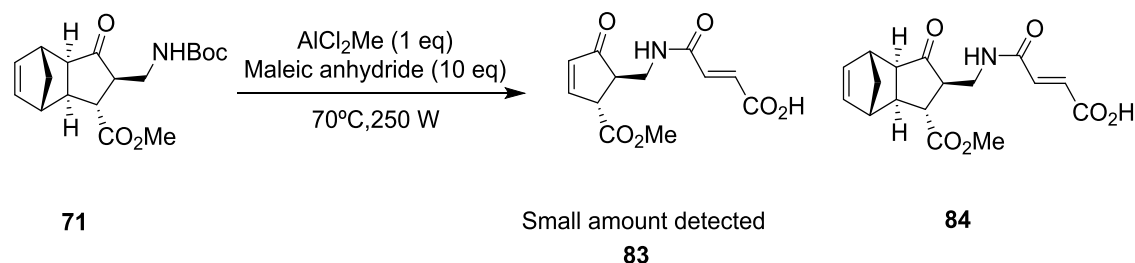


Figure 3.28. Side reactions occurring during the retro Diels-Alder reaction of compound **71**.

The behaviour of PK adducts **63** and **73** under the retro-Diels Alder reaction were undertaken as control reaction without any difficulties (figure 3.29). The PK adduct **79** without the presence of α -chain was used as control in the retro Diels-Alder reaction. N-Boc protecting group was replaced by greater acid resistant group such as phthalimide group substrate **86** that shown compatibility with the condition used to perform the retro Diels-Alder reaction.

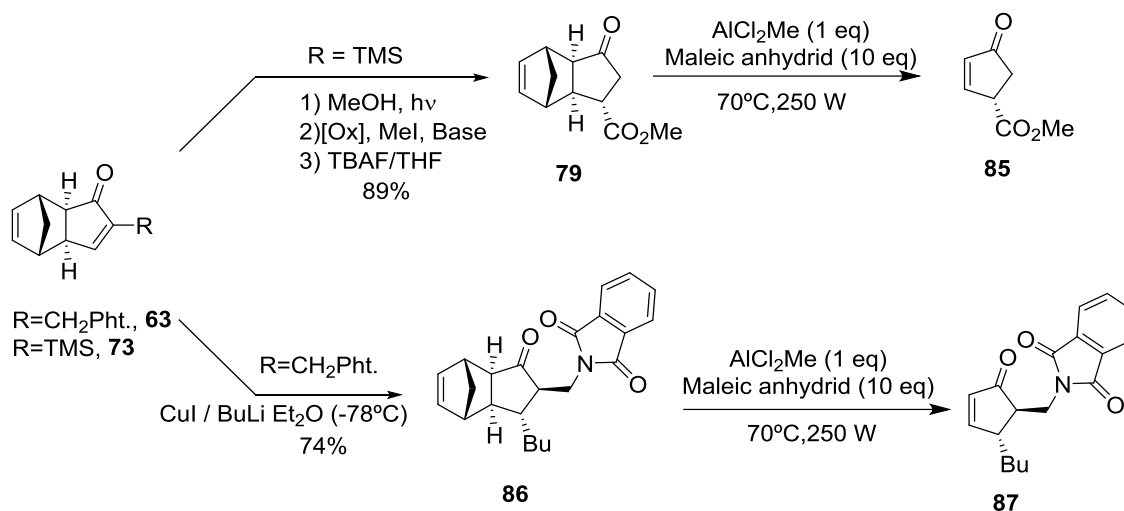


Figure 3.29. Study of the retro Diels-Alder reaction of PK adducts **63** and **73**.

With the attempt to synthesis of the enantioselectively (R)-Sarkomycin methyl ester, we identified synthetic issues and studied a variety of alternatives. The synthetic design imagined faced two challenges: (1) Introduction of the carboxylic acid through photochemical reaction (2) The release of the cyclopentane core through the retro Diels-Alder reaction.

To overcome those issues, we have performed the screen of several PK adducts of protected amine alkyne and observed that the inner properties of the PK adduct selected for the study were not the best candidates for the synthesis envisaged. Indeed, the photochemical addition of

methanol over PK adduct of N-Boc alkyne resulted in low yield and unreliable (15 up to 50% yield).

Optimisation of the photochemical reaction was performed with the screening of different PK adducts. We have identified that during the photochemical reaction, with the PK adduct bearing phthalimide protecting group, the transposition reaction was favoured. Alternatives were undertaken to lead to the formation of the carboxylic acid function in β -position of the cyclopentenone not suitable to continue with the synthesis of the sarkomycin.

Regarding the retro Diels-Alder reaction, we have identified that the NHBoc PK adducts led to the formation of different side products where in all cases the N-protected amine was deprotected to react with the reagent.

In consequence, we decided to change the strategy avoiding then the two issues encountered in this synthesis.

3.2.3.5 Synthesis of the *rac*-sarkomycin

New route to synthesis the *rac*-sarkomycin was envisaged relying on a regioselective PKR between disubstituted alkyne and alkene already equipped with two precursors, the methylene and the carboxylic function. After hydrogenation and β -elimination, *rac*-Sarkomycin ester would be formed (figure 3.30).

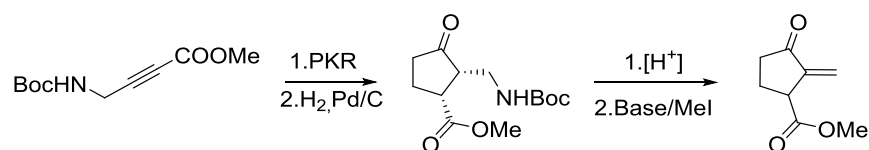
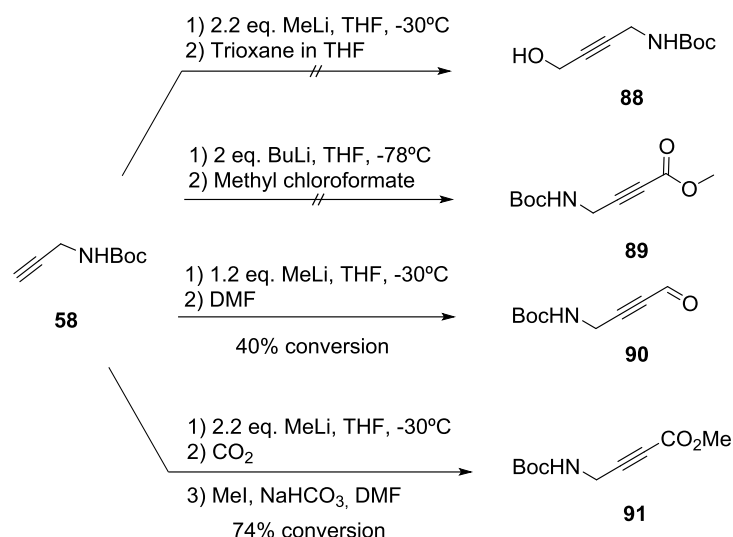
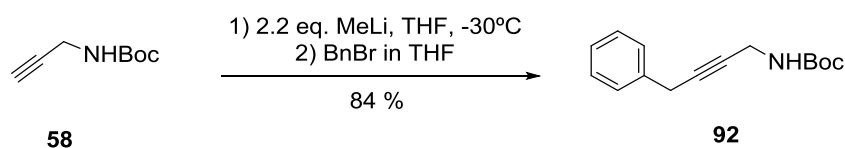


Figure 3.30. Alternative synthesis for the sarkomycin ester.

Our strategy commenced with the preparation of alkynes bearing an ester group on one side and N-Boc amine at the other side. For the introduction of the ester group, several routes were envisaged which consisted to react amidure of the N-Boc-protected propargyl amine with methylchloroformate, trioxane or DMF (figure 3.31). First attempts using methylchloroformate (**89**), trioxane, (**88**) failed while, using DMF as electrophile afforded 40% of conversion of **90**.

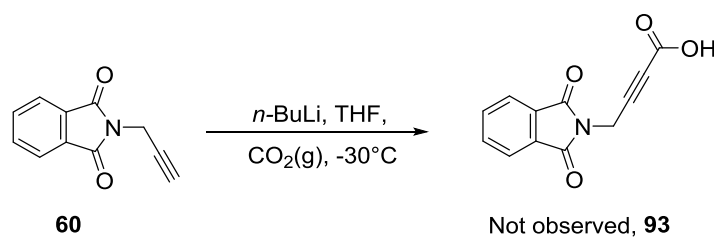
Figure 3.31. Reactions tried to synthesize the alkyne **91**.

To the view of those results, the methodology and procedure were controlled. In same reaction conditions, the benzyl chloride was used and the compound **82** was obtained in good yield, 84% (figure 3.32).

Figure 3.32. Reaction control, synthesis of the alkyne **92**.

As last attempt, we decided to bubble carbon dioxide from commercial pressure bottle containing less than 3ppm of water connected through a highly concentrated sulphuric acid bubbler as a drying agent. The free acid was satisfactorily obtained which converted into the ester using methyl iodide and Na_2CO_3 in DMF. It afforded **92** in 74% yield over 2 steps.

Several other alkynes bearing more resistant protecting groups such as phthalimide group, compound **60** were also investigated. It turned out that the insertion of the carboxylic acid using the previously described procedure was quite capricious (figure 3.33). The base seemed to behave as nucleophile since the addition of the butyl chain over the compound **60** was detected by LC/MS. Other sterically hindered bases were used without success (such as LDA).

Figure 3.33. Attempt to synthesis of the alkyne, **93**.

With the alkyne **91** in hand, the PKR with dicobalt octacarbonyl and ethylene was then undertaken. As first experiment, we have tried the PKR in thermal conditions, 8 barg pressure of ethylene at 85°C in toluene (figure 3.34).

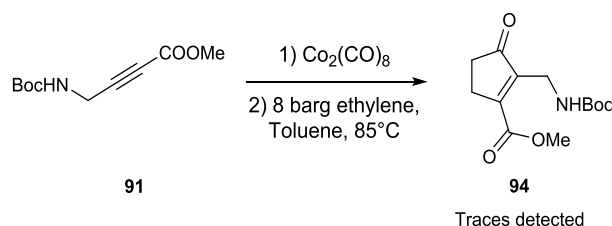


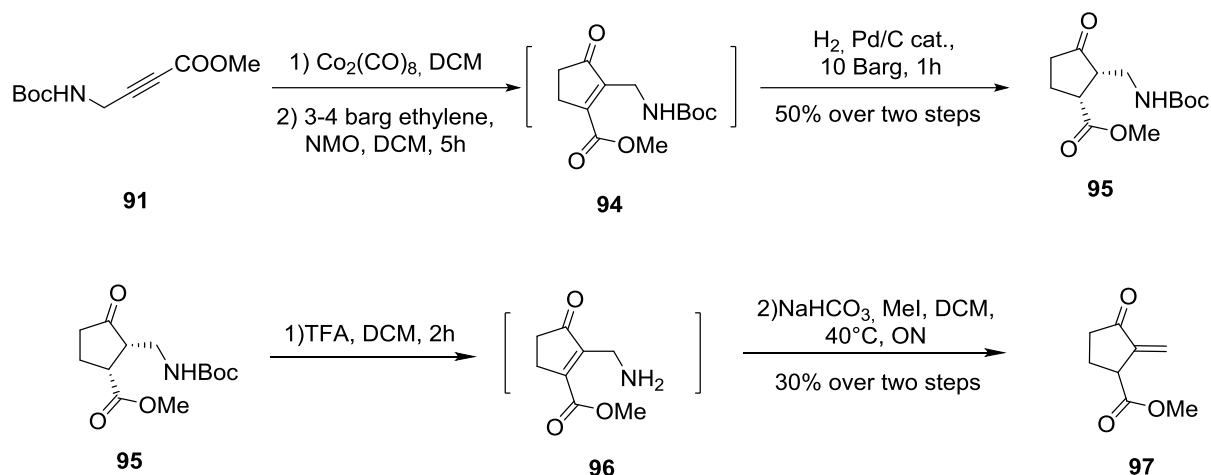
Figure 3.34. Thermal PKR performed with ethylene.

In crude of reaction, lots of by-products were formed and traces of the final product **94** were detected by LC/MS. Different parameters have been included for optimization. The beneficial effect of zeolites is well-known to increase the availability of ethylene in the solvent by acting as a micro-reactor. In our group, molecular sieves were sometime used to increase yield of reaction over intermolecular PKR with ethylene. Unfortunately, it was not the case with that substrate **86**.

N-oxide promoter was considered to perform the PKR at room temperature favouring then the ethylene solubility.

At room temperature, the PKR was carried out with 10 equivalents of NMO and 3 or 4 barg of ethylene which yielded to the exclusive formation of the cyclopentenone **94** (figure 3.35). After filtration over celite only 39% of crude weight was obtained, and the following purification over silica afforded a 6 to 20% yield. In addition to the volatility of the product, we suspected the compound to decompose during filtration and to cyclise into the corresponding lactone (detected by LC/MS). Confronted to those limitations, we decided to avoid the purification.

Thus, we performed the hydrogenation reaction directly in the crude of reaction, in the same reactor used to perform the PKR. The hydrogenation reaction was carried out with Pd/C 20-30 mol% at 10 barg of H₂, for 2 hours. We were pleased to detect and isolate without any difficulties the pure racemic compound **95** as a white solid in 50% overall yield (2 steps). The reaction could be easily performed at 1g scale. Over that amount, a flash filtration of the crude over celite was required to remove the cobalt complexes poisoning the catalyst. With the racemate **95**, we performed the deprotection of the amine with 1.25 M HCl/MeOH or TFA/DCM followed by a straight basification in situ with Na₂CO₃ and addition of methyl iodide. The mixture was heated up at 40°C over two days to afford the *rac*-sarkomycin methyl ester of **95** in about 30% yield (figure 3.36). We believe that the low yield is due to the volatility of the product.

Figure 3.35. Synthesis of the *rac*-Sarkomycin ester, **97**.

In summary, the present work of the *rac*-Sarkomycin methyl ester was accomplished in only 2-pots procedure in 15% overall yield. This is the shortest route to sarkomycin from acyclic precursor ever described proving that intermolecular PKR of internal alkynes can be a valuable synthetic tool.

3.3 Jasmonate synthesis

3.3.1 Introduction

Jasmonates are lipid mediators widely distributed in the plant kingdom. The methyl jasmonate (MeJA) was first isolated from *Jasmonium Grandiflorum* and identified as a cyclopentenone-based component of the essential oil of several plants while jasmonic acid (JA) was obtained from fungal culture.¹⁷ Four stereoisomers of the methyl jasmonate exist but only the (+)-1*R*,2*S*-methyl *epi*-jasmonate possesses the strongest odour which is nowadays used in the perfume industry. The 1*R*,2*R* (-)-methyl jasmonate has a weak odour while the two remaining isomers are odourless (figure 3.36).¹⁸

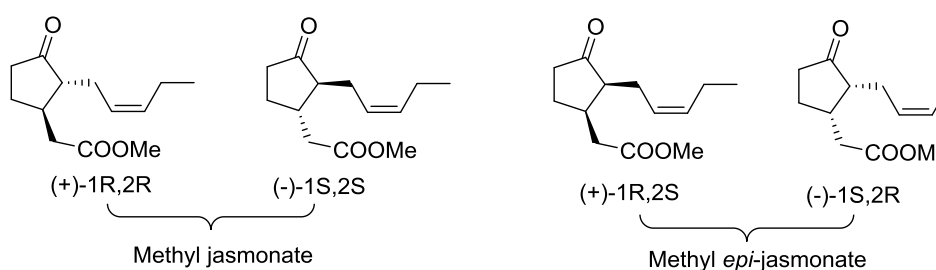


Figure 3.36. Four stereoisomers of the methyl jasmonate.

Jasmonic acid (JA) and its methyl jasmonate (MeJA) are phytohormones which control defence gene expression in response to wounding and other environmental stresses. Jasmonates can modulate aspects of fruit ripening, production of viable pollen, root growth, cell-to-cell transport and plant resistance to insects and pathogens.²⁰ In the agronomical field, the methyl jasmonate is responsible of the damage of vegetables that comes just after it has been cut from its plants²¹ and the preservation of the quality of the fresh-cut fruits and vegetables represents a worldwide

market of several billion euros. This phytohormone is also involved in the plant-growth regulation used as pesticide.

The enzymatic cascade leading to jasmonic acid's biosynthesis starts from the α -linolenic acid oxidized by lipoxygenase (LOX) into 13-hydroperoxylinolenic acid which in turn is converted into 12,13-EDT via an allene oxide synthase (AOS) (figure 3.37).¹⁹ The allene oxide cyclase (AOC) allows the transformation of 12,13-EDT into 12-oxo-phytyldienoic acid (12-oxo PDA) through several steps. The latter is reduced and oxidized three times to afford *epi*-JA which is then converted in its ester form.

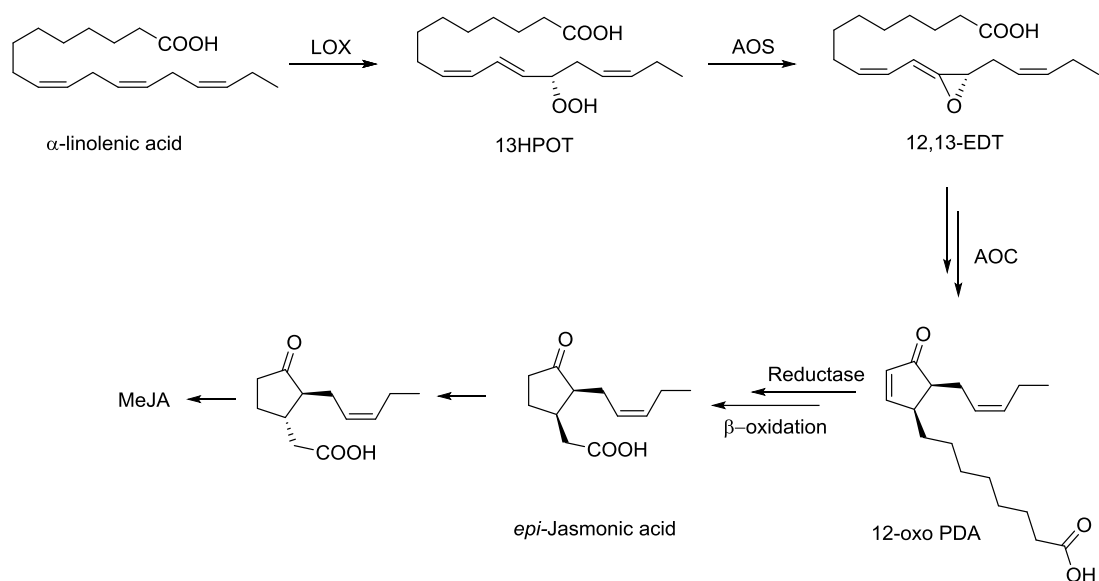


Figure 3.37. Biosynthetic pathway of the JA and MeJA.

With the difficulty to isolate phytohormones from natural sources²² and the strong industrial demand, scientific community get interested to find efficient methods to access to Jasmonates. The four isomers are valuable compounds that can be used in diverse fields. The enantioselective synthesis of (-)-MeJA is of major economic interest for fragrance application.

From a biotechnological point of view, the methyl jasmonate was smartly utilised as building blocks by Bonfill *et al.* who induced the production in cell culture of the Baccatin III, precursor of the important anti-cancer drug, Paclitaxel (taxol) isolated from the Pacific yew tree, *Taxus brevifolia*.²³

3.3.2 Synthesis methyl jasmonates

Plants metabolize linolenic acid to classes of cyclopentanones and α -enones such as the well-known prostaglandins or jasmonates. Different from the prostaglandins, the side chains of the *epi*-jasmonate are positioned to the same direction (*cis* configuration) which renders the metabolites susceptible to isomerisation at the α -carbon to produce the thermodynamically more stable *trans* isomer. Stereocontrolled synthesis and conformational instability represent great synthetic challenge. Most of the synthesis of the MeJA and *epi*-MeJA are racemic and few are enantioselective due to the fact that the enantiopure starting material is not commercially available.²⁴

Buchi *et al.* proposed the synthesis of the MeJA from 1,3-cyclohexadione which underwent alkylation using 1-bromo-2-pentyne in 83% yield (figure 3.38).²⁵ The chlorination with *tert*-butyl hypochlorite in α of the ketone was obtained in 76 % yield. The cyclopentenone core was released in 74 % yield after decarbonylation with sodium carbonate. Malonate conjugate addition in β of the ketone and its subsequent decarboxylation in basic condition afforded the methyl ester in 87 % yield after esterification. Acetylene functionality was finally reduced utilizing Lindlar's catalyst to produce *rac*-methyl jasmonate in 94 % yield.

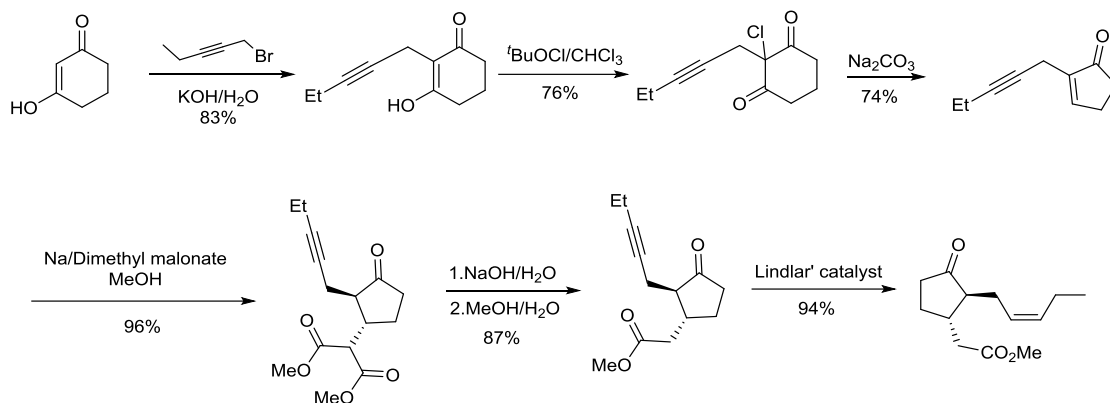


Figure 3.38. Buchi's synthesis.

Nakada *et al.* (2006) proposed an asymmetric synthesis of the (-)-MeJA starting from the enantiopure chiral compound prepared from intramolecular cyclopropanation reaction (IMCP) of the α -diazo- β -keto 1-naphthyl sulfone (figure 3.39).²⁴ The asymmetric IMPC produced a cyclopropane in 97% yield and 81% ee which reacted with sodium cyanide to give the cyanomethyl group in β position of the cyclopentanone in 95% yield. After alkylation with the 1-bromo-2-pentyne, in 59% (6:1 ratio) and crystallisation of the good diastereomer, the conversion into JA engaged the following steps: desulfonylation with SmI_2 in quantitative yield, hydrogenation by Lindlar's catalyst (90% yield) and the hydrolysis of the cyanide by KOH with epimerization to the *trans* isomer to produce the desired and single product. The MeJA was finally esterified with methyl iodide in 88% yield over two steps.

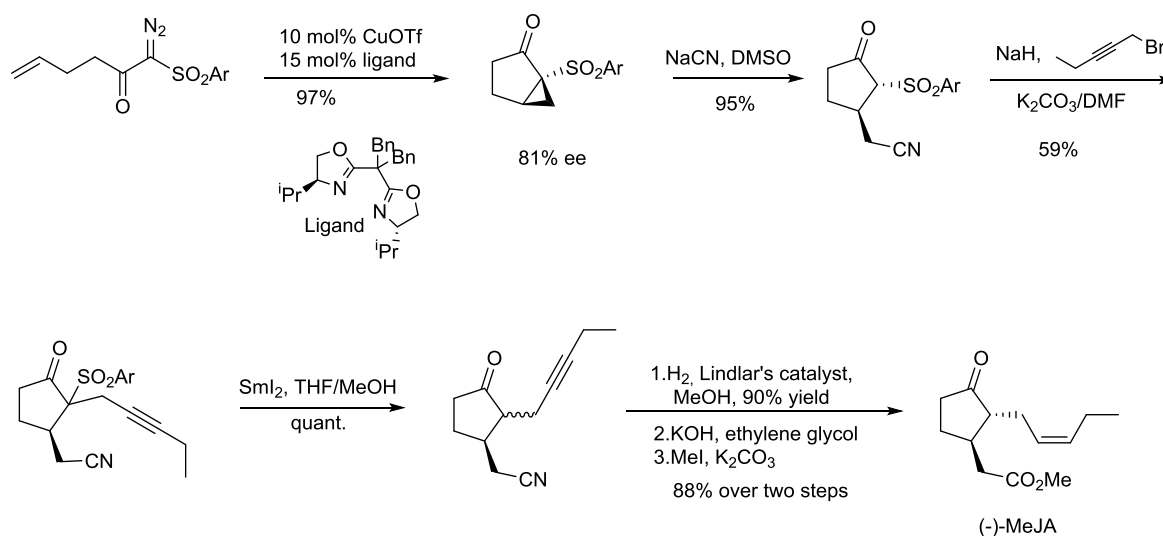


Figure 3.39. Nakada's synthesis.

Kobayashi *et al.* (2010) synthesised the *epi*-JA by Wittig reaction with a key aldehyde, prepared stereoselectively from enzymatic hydrolysis with pig pancreatic lipase of the corresponding diacetate into the (1R)-acetate (figure 3.40).²⁶ Allylic substitution of the (1R)-acetate with Grignard reagent (CH₂CHMgBr) was performed in the presence of CuCN and LiCl to afford in 93% yield of the complete stereoselectivity.

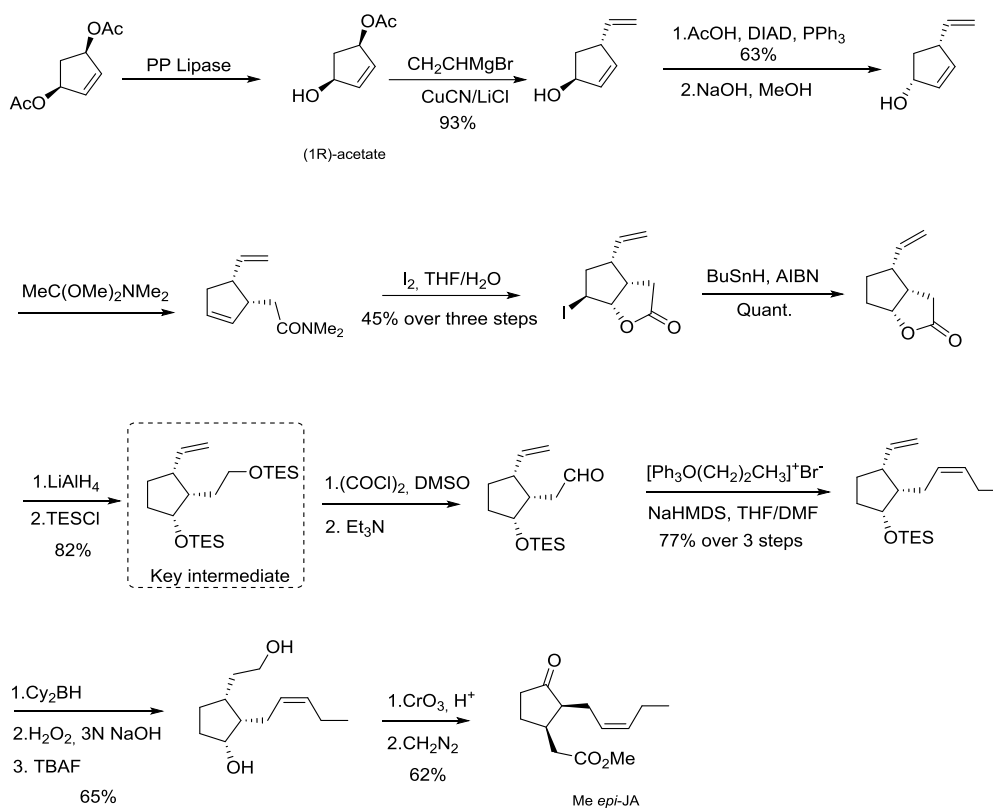


Figure 3.40. Kobayashi's synthesis of the MeJA.

The stereochemistry of the alcohol was inverted by a Mitsunobu reaction in 63% yield followed by hydrolysis of the acetate. The corresponding free alcohol underwent an Eschenmoser reaction with MeC(OMe)₂NMe₂ afforded the amide which was then subjected to iodolactonization with iodine to afford iodolactone in 45% yield over 3 steps. The iodine was removed with Bu₃SnH and AIBN and the reduction of the lactone with LiAlH₄ followed by silylation afforded 82% of the bis-TES ether, key intermediate of the synthesis. The Swern oxidation of the primary protected alcohol TESOCH₂ group proceeded regioselectively to get aldehyde as a unique product. Then, transformation into *epi*-JA was performed with an ylide derived from [Ph₃P(CH₂)₂Me]⁺Br⁻ and NaHMDS to form the exclusive *cis* olefin in 77% yield. Regioselective hydroboration with Cy₂BH (Cy: *c*-C₆H₁₁) produced the alcohol in 65% yield after oxidative workup. Finally, desilylation of the TES group and Jones oxidation of the resulting diol furnished *epi*-JA in 62% yield which was methylated into MeJA.

3.3.3 Results and discussion

Two pathways were investigated the synthesis of methyl jasmonate (figure 3.41). First pathway would start with the installation of the cyclopentenone by regioselective Pauson-Khand reaction between NDB and disubstituted alkyne. The experimental result would be correlated to the predictive model developed in the **chapter II** regarding the regioguidance of substituted alkynes. The exocyclic enone would be obtained by β -elimination of the free amine which would be subjected to a conjugate addition. As last steps, the retro Diels-Alder would allow the access to racemic dehydro MeJA which in turn could be selectively reduced into MeJA.

The second pathway would start with the PKR of protected propargylic alcohol where the PK adduct of free propargylic alcohol would be engaged in a Claisen-Johnson rearrangement to form the desired exocyclic enone, key intermediate. Taking into account the PK adduct, we supposed that the Claisen rearrangement would be diastereoselective. Then, the resulting exocyclic enone adduct would follow the same pathway described in the first approach.

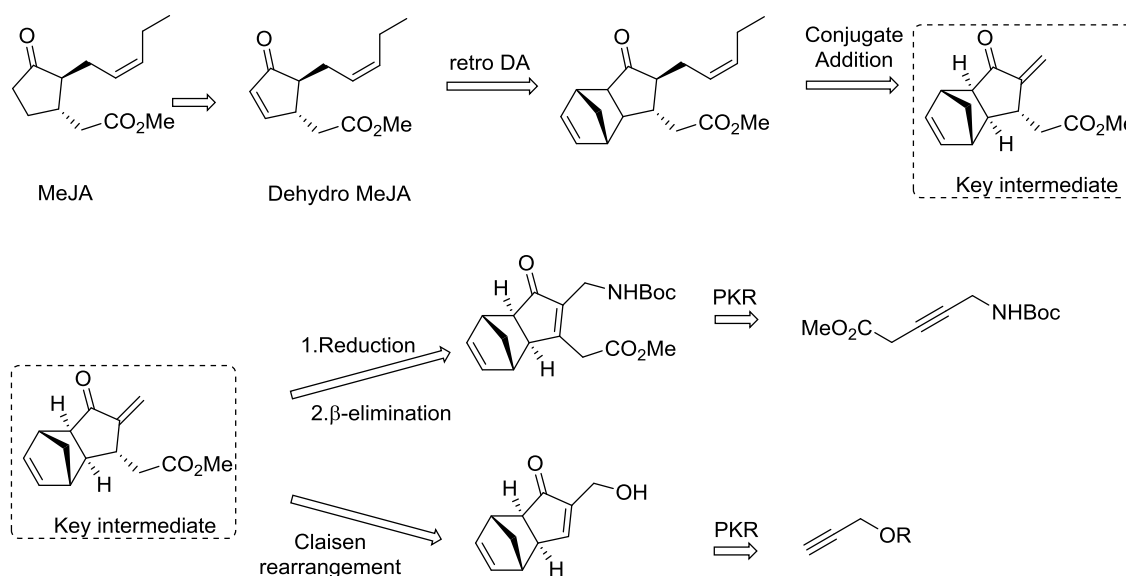
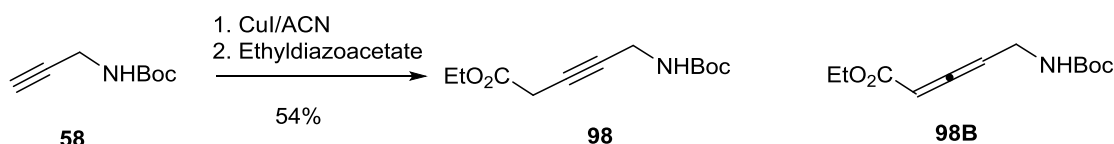


Figure 3.41. Retrosynthesis of the MeJA.

3.3.3.1 First approach

The internal alkyne **98** was obtained by reacting the N-Boc propargylamine **58** with ethyl diazoacetate to give the desired compound as main product of reaction in 54% yield and 18% of its corresponding allene, **98B** (figure 3.42).

Figure 3.42. Synthesis of the alkyne **98**.

The alkyne was subjected to the stoichiometric PKR with dicobalt octacarbonyl and NBD to afford PK adduct **99** in 86% yield with a complete regio- and diastereoselectivity (*endo/exo* ratio, 1:32) (figure 3.43). The PK adduct was analysed by HMQC, HMBC experiments where we could determine that the ester function ended up in α -position while the N-Boc methylene group was placed in β -position.

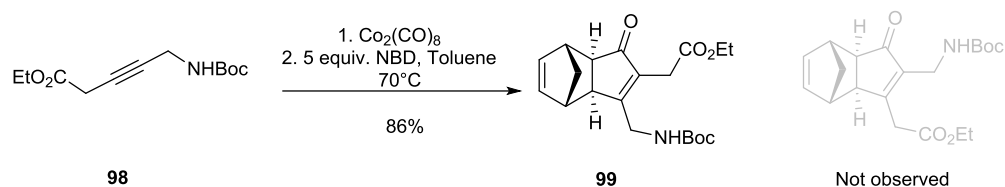


Figure 3.43. Highly regioselective PKR of alkyne **99**.

Therefore, comparing the regiochemical outcome with the previous results observed in chapter II, we obtained a surprisingly high regioselectivity (figure 3.44). Indeed, a high regioselectivity of CO_2Me (**43**) and low regioselectivity of NHBoc (**100**) was observed even the $\Delta(\text{C}2\text{-C}3)$ NBO charges of the compound **100** were higher than expected. In the present case, combining the two substituents in the same alkyne **98** let us imagine that the alkyne would afford a low regioselectivity toward the NHBoc in β position favouring thus the CO_2Me in β -position. Therefore, it favoured one PK regioisomer with the CO_2Me in α -position.

The impact of different groups over the polarisation of the triple bond α -carbons was measured by computational calculation. We were pleased to observe that computational result qualitatively predicted the regiochemical outcome of the reaction favouring the methyl ester in α -position and the NHBoc in β -position.

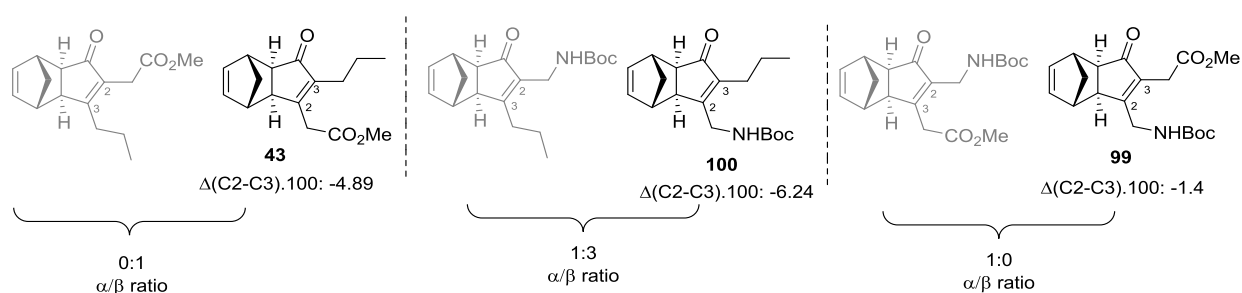


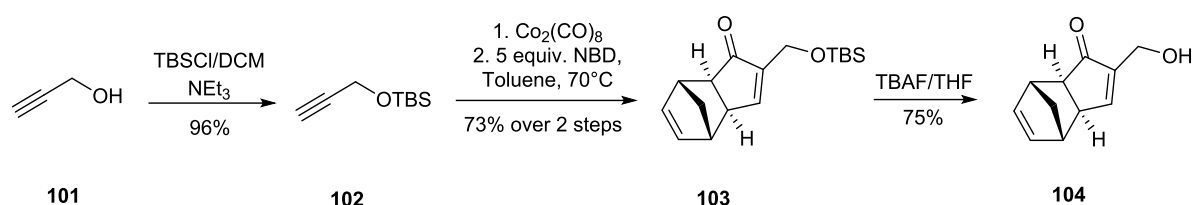
Figure 3.44. Regioselectivity observed with adducts **43**, **99** and **100**.

The $\Delta(\text{C}2\text{-C}3)$ NBO charges was of -1.4, which was in good agreement with the regioisomer formed even the regioselectivity calculated was lower than experimental outcome.

For our synthetic purpose, this adduct would not be used since the Boc-protected amine was needed in α -position. Our attention was then focused on the second approach.

3.3.3.2 Second approach

The second approach consisted in the introduction of the β -carboxymethyl side chain via Claisen-Johnson rearrangement. Like the thermal PKR of the propargylic alcohol **101** with NBD afforded the PK adduct **104** in low yield, the PKR of propargylic alcohol protected by *tert*-butyl dimethyl silyl group was envisaged (figure 3.45). The alkyne **102** was easily prepared from propargylic alcohol with TBSCl in 96% yield. The dicobalthexacarbonyl complex was isolated and then subjected to a thermal PKR with NBD to afford 73% yield of isolated PK adduct **103** in high *exo/endo* ratio 25:1. The compound **103** was deprotected with TBAF in 75% yield to afford the starting material for the Claisen-Johnson rearrangement **104**.

Figure 3.45. Synthesis of the PKR of the propargylic alcohol, **104**.

Standard Claisen-Johnson rearrangement was performed reacting compound **104** with trimethyl orthoacetate and catalytic amount of acetic acid heated up at 120°C like the procedure described by Amos Smith III (figure 3.46).²⁷ The reaction was monitored by TLC.

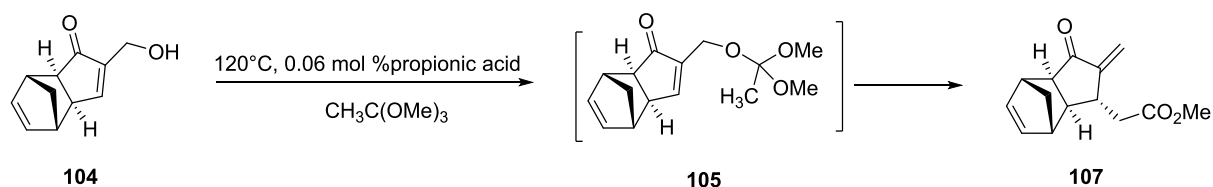


Figure 3.46. Claisen rearrangement envisaged for the MeJA' synthesis.

After 2 hours, starting material was observed so the mixture was then heated up at 150°C for 3 hours more hours. The crude was analysed by NMR showing a mixture of Claisen adduct **107** with a significant amount of other products of reaction (figure 3.47). Indeed, signals the exocyclic enone of the Claisen adduct were observed around 5.3 and 6.3 as doublets and unknown signals were present around 6.05 as two triplets of same and great intensities.

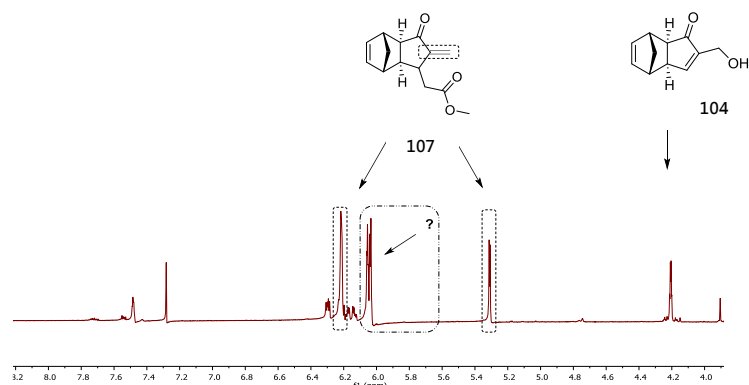


Figure 3.47. ^1H NMR of the different species present in the crude of the Claisen rearrangement after 7h reaction.

To complete the reaction, the crude was heated overnight to 150°C and the NMR showed that almost all the Claisen product **107** was transformed into other products like shown in the figure 3.48, spectrum T25h. While signals of the exo cyclic enone of the Claisen adduct disappeared at 6.2, the two triplets already observed in figure 3.47 remained in the crude of reaction even the ratio had changed. NMR at 36 hours permitted to reveal that one of the triplet disappeared in time (figure 3.48, spectrum T36h).

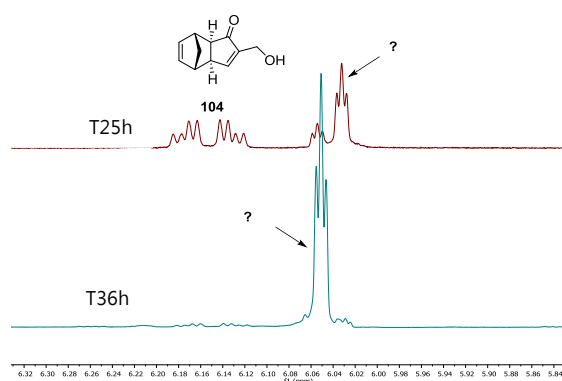
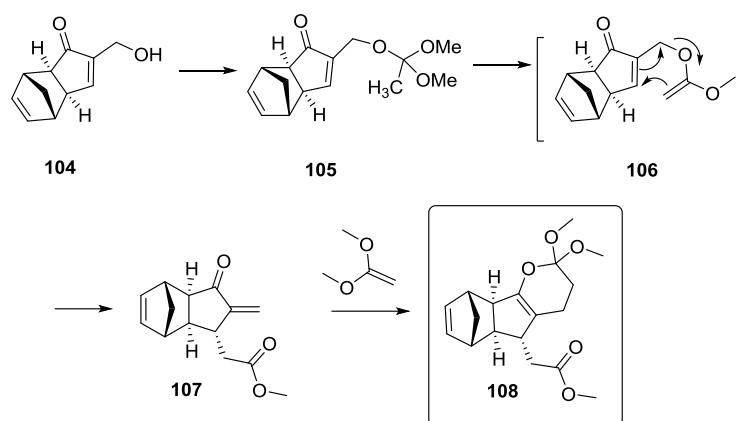


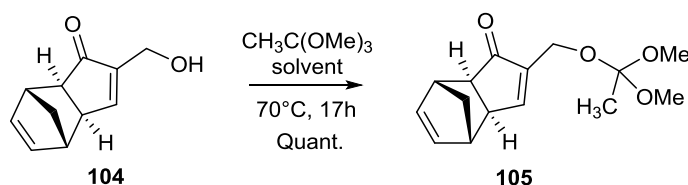
Figure 3.48. NMR of the different un-known species observed at 25h and 36h during the Claisen-Johnson rearrangement.

After purification, we could recover a small amount of the starting material and isolate one of the unknown adduct. The identification by COSY, HMQC and HMBC NMR experiments permitted to establish that the unknown molecule (**108**) was the result of the Diels-Alder reaction between the Claisen rearranged adduct and 1,1-dimethoxyethene formed for ethyl orthoacetate (figure 3.49).

Figure 3.49. Formation of the compound **108**.

For better understanding of the reactivity and control of the reaction, the rearrangement was done step by step. Like the reaction was not complete, we first attempted to fully transform the starting material into the intermediate of the Claisen reaction **105**. We modified the quantity of the orthoacetate and acid, the nature of the acid and the temperature of reaction.

In summary, we identified that in presence of acid, the reaction was never complete. Our best results favoured the compound **105** in a 5:1 ratio with an excess of orthoacetate, 2.2 equiv. of propionic acid at room temperature, overnight. We finally found that the complete conversion of **104** into **105** was achieved without presence of acid, heating up at 70°C during 17h with an excess of trimethyl orthoacetate (figure 3.50).

Figure 3.50. Formation of the compound **105**.

The rearrangement conditions previously used was employing the trimethyl orthoacetate as solvent which was reacting with the final product of the Claisen rearrangement in a hetero Diels-Alder reaction. To avoid this side reaction, in the following experiments, the rearrangement was undertaken from isolated intermediate **105**, at different temperatures (40°C, 90°C and 106°C) using deuterated solvents (benzene and CDCl₃), for 2 hours (figure 3.51).

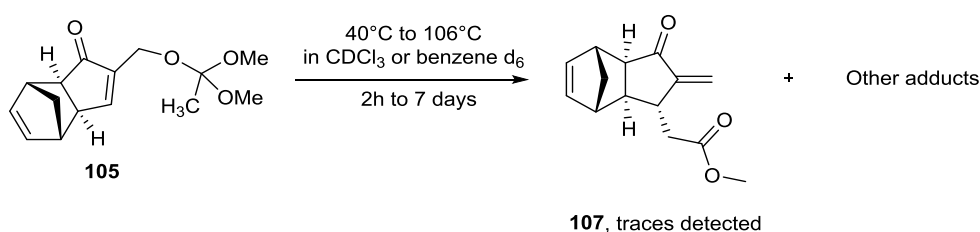


Figure 3.51. Claisen rearrangement attempts without acid and orthoacetate using deuterated solvents.

At 40°C to 90°C, almost no Claisen adduct was detected by NMR but instead it was detected the formation of several unknown products which could not be identified. At 106°C, NMR revealed the formation of lots of by-products and small amount of Claisen adduct. The identification of those molecules of high weight resulted unknown even many hypothetic products of Diel-Alder, retro Diels-Alder, polymerisation reactions were envisaged.

Although first attempts were promising and permitted to characterize a derivative of the Claisen-Johnson adduct, more investigation would be carried out in order to control and optimise the rearrangement. We have been able to identify the general trend and reactivity of PK adduct in different reaction conditions with ethyl orthoacetate, proving that the Claisen-Johnson rearrangement in the PK adducts might be a useful reaction.

3.4 General conclusions

In this chapter, synthetic applications of intermolecular PKR adducts directed to the synthesis of natural products have been investigated. The complex use and reactivity of functionalised PK adducts challenged us to constantly redesign the synthetic route envisaged.

We attempted to apply the regioselective PKR to the synthesis of natural products, sarkomycin and methyl jasmonate. With the attempt to synthesis of the enantioselectively (R)-sarkomycin methyl ester, we performed the screen of a variety of PK adducts of protected amine alkyne and identified that:

1. The photochemical introduction of the carboxylic acid fragment was substrate dependent since the α -substituted PK adducts had different photochemical behaviours. We demonstrated that the inner properties of the PK adducts were competing with other chemical pathways. The photochemical addition of methanol to PK adduct of N-Boc propargylamine was achieved in 15-50% too unreliable for further investigation. We have also identified that the photochemical reaction of PK adduct of N-phthalimide propargylamine favoured a transposition reaction. Multitude of alternatives were undertaken to lead to the formation of the carboxylic acid function in β -position of the cyclopentenone which were not suitable to continue the synthesis.
2. The release of the cyclopentane core of the PK adducts through the retro Diels-Alder reaction led to the formation of different side products where the N-Boc amine was deprotected to react with the reagent. We have identified that phthalimide protecting group was the best candidate to perform the retro Diels-Alder reaction since its cleavage was not observed. However, we could not introduce the β chain.
3. PKR with internal alkynes proved to be the best method to synthesize the *rac*-sarkomycin methyl ester. Thus we were able to propose the fastest total synthesis of the *rac*-sarkomycin methyl ester in 2-pot reaction and 15 % overall yield.
4. With the synthesis of the methyl jasmonate, we have successfully applied our predictive model regarding regiochemical outcome of the PKR. For the first time, Claisen-Johnson rearrangement was tried with PK adduct of the propargylic alcohol. Our preliminary results on the way to the synthesis of the methyl jasmonate allowed us to identify that the Claisen-Johnson rearrangement could be applied in the synthesis of the methyl jasmonate where we observed the formation of one single Claisen-Johnson adduct in low yield.
5. The study of the PK adduct under Claisen-Johnson rearrangement toward the synthesis of the MeJA permitted to afford a general overview of the reactivity. We have identified the general trend and reactivity of PK adduct in different reaction conditions with ethyl orthoacetate, proving that the Claisen-Johnson rearrangement in the PK adducts might be a useful reaction for further investigation.

References

- (1) Aiguabella, N.; Pesquer, A.; Verdaguer, X.; Riera, A. *Org. Lett.* **2013**, *15*(11), 2696–2699.
- (2) Nokami, J.; Fujii, K.; Mizutani, Y.; Omatsu, R.; Watanabe, K.; Yasuda, H.; Inokuchi, T. *Nat. Prod. Commun.* **2013**, *8*(7), 919–923.
- (3) Longley, D. B.; Johnston, P. G. *J. Pathol.* **2005**, *205*(2), 275–292.
- (4) Honors, M. A.; Kinzig, K. P. *Support. Care Cancer* **2013**, *21*(10), 2687–2694.
- (5) Sung, S. -c. *Antibiotics* **1967**, 156.
- (6) Blokhin, N.; Larionov, L.; Perevodchikova, N.; Chebotareva, L.; Merkulova, N. *Ann. N. Y. Acad. Sci.* **1958**, *68*(3), 1128–1132.
- (7) Minaskania, G. Synthesis of an anti-cancer compound, sarkomycin, and some Analogs, University of Texas, 1979.
- (8) Ishiyama, S. *J. Antibiot., Ser. A.* **1954**, *7*, 82.
- (9) Hill, R. K.; Foley, P. J.; Gardella, L. A. *J. Org. Chem.* **1967**, *32*(7), 2330–2335.
- (10) Kondo, S., Nakamura, H., Ikeda, Y., Maeda, K., Takeuchi, T. *J. Antibiot.* **1997**, *50*, 363.
- (11) Westmeier, J.; Kress, S.; Pfaff, C.; von Zezschwitz, P. *J. Org. Chem.* **2013**, *78*(21), 10718–10723.
- (12) Toki, K. *Bull. Chem. Soc. Japan* **1957**, *30*, 450–452.
- (13) Hill, R. H., Foley, P. J., Gardella, C. A. *J. Org. Chem.* **1967**, *32*, 2330–2333.
- (14) Mikołajczyk, M.; Żurawiński, R.; Kietbasiński, P.; Wieczorek, M. W.; Błaszczuk, J.; Majzner, W. R. *Synthesis (Stuttg)*. **1997**, *1997*(03), 356–365.
- (15) Boeckman, R. K.; Naegely, P. C.; Arthur, S. D. *J. Org. Chem.* **1980**, *45*(4), 752–754.
- (16) Lledó, A.; Benet-Buchholz, J.; Solé, A.; Olivella, S.; Verdaguer, X.; Riera, A. *Angew. Chem. Int. Ed. Engl.* **2007**, *46*(31), 5943–5946.
- (17) Demole, E. Lederer, E. Mercier, D. *Helv. Chim. Acta* **1962**, *45*, 675–685.
- (18) Acree, T. E. Nishida, R. Fukami, H. *J. Agric. Food. Chem.* **1985**, *33*, 425–427.
- (19) Vick, B. A.; Zimmerman, D. C. *PLANT Physiol.* **1984**, *75*(2), 458–461.

- (20) *Climate Change and Plant Abiotic Stress Tolerance*; Tuteja, N., Gill, S. S., Eds.; Wiley-VCH Verlag GmbH & Co. KGaA: Weinheim, Germany, 2013.
- (21) Creelman, R. A.; Mullet, J. E. *Annu. Rev. Plant Physiol. Plant Mol. Biol.* **1997**, *48*, 355–381.
- (22) Zhang, F. J.; Jin, Y. J.; Xu, X. Y.; Lu, R. C.; Chen, H. J. *Phytochem. Anal.* **19**(6), 560–567.
- (23) Bonfill, M.; Bentebibel, S.; Moyano, E.; Palazón, J.; Cusidó, R. M.; Eibl, R.; Piñol, M. T. *Biol. Plant.* **2007**, *51* (4), 647–652.
- (24) Takeda, H.; Watanabe, H.; Nakada, M. *Tetrahedron* **2006**, *62* (34), 8054–8063.
- (25) Buchi, G.; Egger, B. *J. Org. Chem.* **1971**, *36* (14), 2021–2023.
- (26) Nonaka, H.; Ogawa, N.; Maeda, N.; Wang, Y.-G.; Kobayashi, Y. *Org. Biomol. Chem.* **2010**, *8* (22), 5212–5223.
- (27) Wexler, B. A.; Toder, B. H.; Minaskanian, G.; Smith, A. B. *J. Org. Chem.* **1982**, *47* (17), 3333–3335.

CHAPTER 4

Photochemistry of Pauson-Khand adducts

Contents

4.1 General introduction and objectives	85
4.2 Synthesis of helicene-like compounds	88
4.2.1 Introduction to photochemical reactions	88
2.2.2 Results and discussion	93
4.3 Attempt to the synthesis of phenanthrolic compound	98
4.3.1 Introduction	98
4.3.2 Results and discussion	99
4.4 Toward photoswitchable diarylethenes	102
4.4.1 Introduction and objectives	102
4.4.2 Results and discussion	105
4.5 General conclusions	109

4.1 General introduction and objectives

During the past decade, our group opened new horizons applying photochemistry to PKR adducts. Continuing that challenging research line program, the present doctoral thesis had the objectives to widen the scope of photochemical transformations of PK adducts, investigating the reactivity of substituted aromatic and heterocyclic alkynes. From the previous doctoral thesis developed by Ji Ning Yi, it was demonstrated that PKRs of diphenylacetylene underwent an electrocycloisatation reaction to form helicene-like polycyclic structures (figure 4.1). Thus, the first objective consisted to optimise the photochemical reaction (time and scope of reaction) previously uncovered.

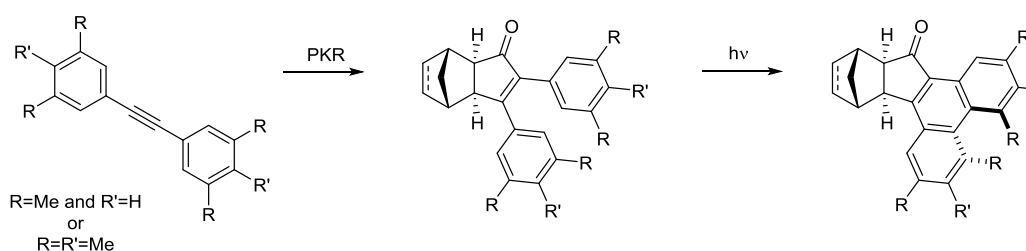


Figure 4.1. PK adducts envisaged for the formation of helicene-like compounds.

As second objective, the study of heteroaromatic alkynes regarding the PKR and their behaviour under light-induced transformation was undertaken (figure 4.2). Such families could lead to formation of metal complexes (1,10-phenanthrolic)^{1,2,3} and photoswitchable compounds^{4,5}.

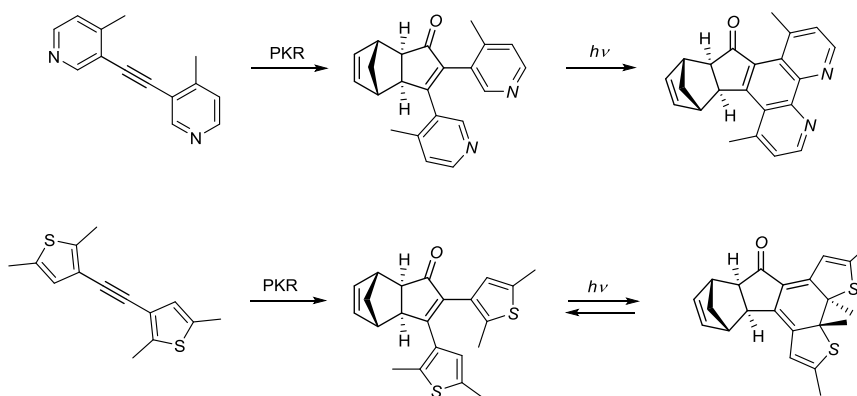


Figure 4.2. 1,10-phenanthrolic and thiophenyl groups envisaged.

1,10-Phenanthroline and derivatives coordinate as ligands to transition metals and disturb the functioning of a wide variety of biological systems with for examples antifungal,⁶ antibacterial⁷ or anti-cancer activities.^{8,9,10}

Combining photochemical reaction of PK adduct with 1,10-phenanthrolic structure, we were interested to provide suitable access of parented structures, never been reported in the literature (figure 4.3).

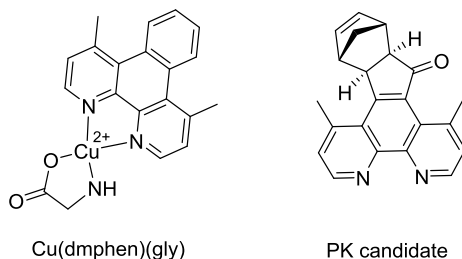


Figure 4.3. Example of copper complex of 1,10-Phenanthroline derivative and PK candidate.

Photoswitchable molecules emerged in response to uncontrolled drug activity and selectivity inducing toxicity and side effects.¹¹ Photochromic unit such as dithienyl has been introduced in pharmacological structure to create a new category of drugs (figure 4.4).¹²

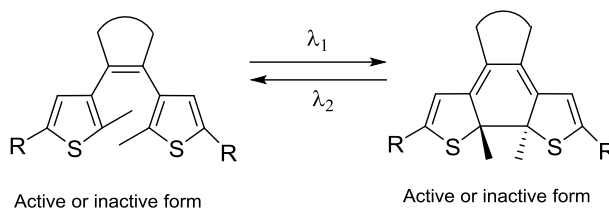


Figure 4.4. Example of photoswitch unit used in photopharmacology, dithienyl compound.

The control of the biological response will be triggered by the use of the light.¹³ Combining photochemical reaction of PK adduct with photoswitch unit, we were interested to provide a new synthetic tool to access to parented structures (figure 4.5).

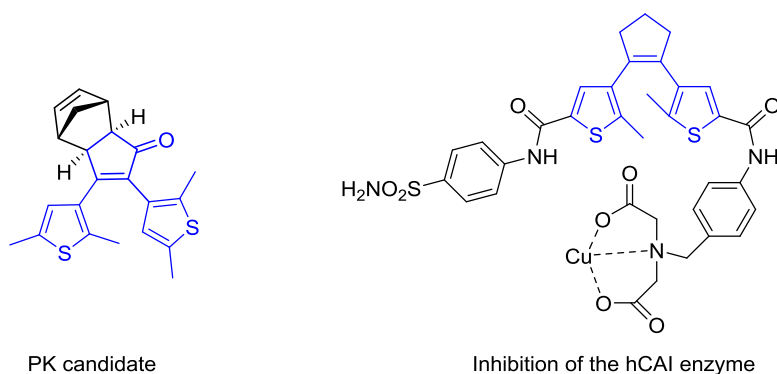


Figure 4.5. Example of photocontrolled inhibition of the hCAI enzyme using 1,2-dithienylethenyl unit and PK candidate.

Photochemistry contributes nowadays in a significant way to carbon-carbon bond forming reactions involved in the synthesis of polymers, optical devices and biologically active compounds.¹⁴ The absorption of light by a molecule permits to facilitate reaction pathways that could not be obtained by conventional methods. The substrate activation

leads to an electronically excited state which can be carried out the by visible or UV light often without additional reagents, which may reduce by-product formations.

Frequently, small changes in the structure of the starting material involve different physical and chemical properties which lead to a complete different photochemical reactivity and outcome. This is the result of the different electronic distribution in the molecule on its induced excited states (M^*) compared to the ground state (M).¹⁵ Depending of the structure, light-induced reactions can afford multitude of photochemical transformations such as reversible and irreversible cyclisations¹⁶, [2+2] cycloaddition of olefins,^{17,18} Paternò-Büchi reaction,¹⁹ Norrish-Yang cyclisation²⁰ or rearrangements (figure 4.6).²¹⁻²³ The 6- π photocyclisation reaction and the reversible photocyclisation will be further detailed and employed in this doctoral thesis.

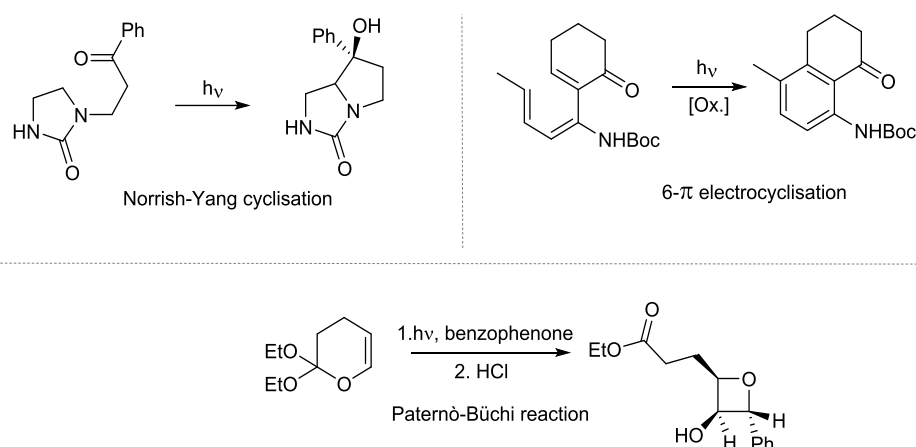


Figure 4.6. Examples of photochemical transformations.^{19,20}

Thus, complex polycyclic and highly functionalised structures can be obtained using photochemistry which can significantly shorten its total synthesis. We can mention among others the important implications of photochemistry in synthesis of natural products (silphiperfol),^{22,23} exotic molecules (helicenes²⁴, ladderanes²³, cage hydrocarbons²⁵ and fullerenes²⁶) and in organic photochromism²⁷ (figure 4.7).

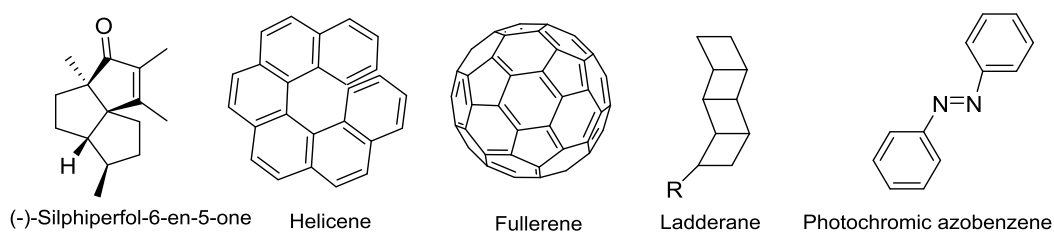


Figure 4.7. Examples of molecules obtained under light-induced reaction.

The field of the photochemistry and its applications are growing exponentially in consequence of the great development of nanotechnologies,²⁸ electronic devices and demands in green chemistry.²⁹ Their implications as key steps in organic synthesis and in natural product synthesis have been broadly reviewed by Hoffmann²³, Bach²² and in several books.^{30,31}

Among the diversity of the substrates that can be photoactivated, cyclopentenones are one of most widely used. This family can undergo photochemical [2+2] cycloadditions with alkenes and alkynes,³² photoactivated conjugated additions³³ and photoactivated rearrangements³⁴ (figure 4.8).

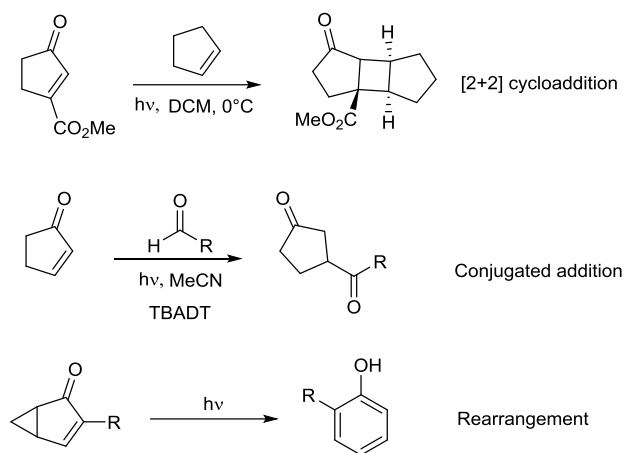


Figure 4.8. Examples of photochemical transformations of cyclopentenones.

For the first part of this chapter IV, we investigated the use of PK adducts to afford helicene like compounds.

4.2 Synthesis of helicene-like compounds

4.2.1 Introduction to : *helicenes*, [6- π] photocyclisation, Pauson-Khand reaction and *photochemistry*

Known a century ago, helicenes constitute a family of distorted polycyclic or heterocycle *ortho*-linked aromatic perfectly π -conjugated (figure 4.9). When the number of rings is higher than four, those three-dimensional aromatic systems cannot be planar and adopt helical structures to relieve the tension. This non-planarity leads to two atropoisomers that can be named as P helicenic conformation for plus, right handed or M conformation for minus, left handed. The enantiomeric stability depends on the steric interaction which usually increases with the number of rings.³⁵

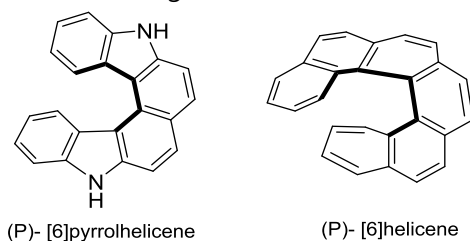


Figure 4.9. Examples of carbo and hetero-helicenes.

Such molecules are inherently chiral and exhibit extraordinary thermal and electronic properties extensively used in supramolecular chemistry, in nanotechnology (liquid crystals, optical fibres ...), in polymers and materials' science but still poorly studied in biomedicine.²⁴

Many efforts have been devoted to the synthesis of carbohelicenes and heterohelicenic molecules and allowed a large-scale racemic or enantioselective synthesis.^{36,37} The construction of helicenic structures can involve photochemical reactions, Diels-Alder reactions, Friedel-Craft type reactions, metal-catalysed cyclisations, radical cyclisations, [6 π] photocyclisation or other type of cyclisation reactions.^{22,23}

In 1967, Martin and co-workers reported the first photo-induced synthesis of hexahelicene generated from the oxidative photocyclodehydrogenation reaction (figure 4.10).³⁸ The starting material was easily prepared by Wittig olefination. The resulting *trans* starting material was isomerized to *cis* isomer by irradiation and thereafter oxidative ring closure took place with I₂ as oxidant and an Hg lamp as an irradiation source. Since then, it has remained the best method to produce helicenes analogues for [5] to [14]helicene.

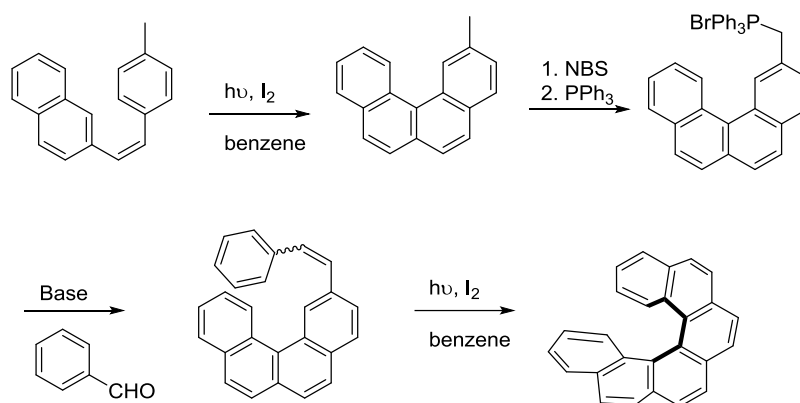
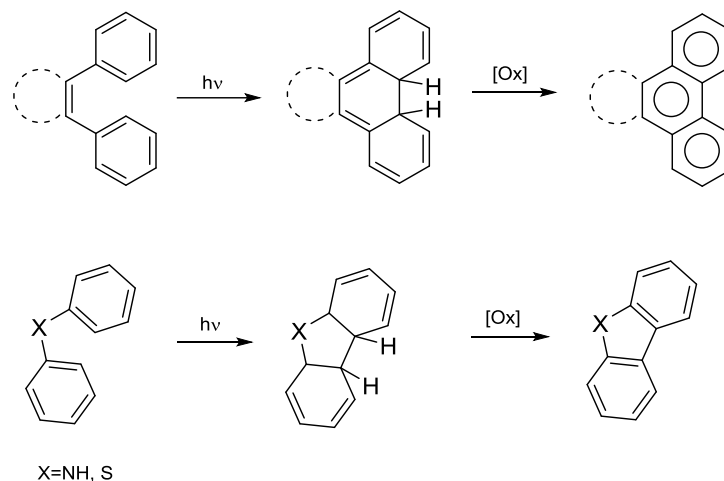


Figure 4.10. Martin's synthesis.

Photocyclisation refers to light-induced pericyclic ring closing reactions where the most important reactions of this type involve conrotatory [6- π] cyclisation and disrotatory [4- π] cyclisation. These photochemical reactions occur mostly on the singlet hypersurface and deliver the respective photoproducts stereospecifically. The potential-energy hypersurface topology is employed to describe the energy of excited state and the ground state.^{39,40}

[6- π] cyclisation reaction can be classified depending on the type of substrate employed, thus, the majority of these reactions involve 1,3,5-trienes and enamides to generate respectively carbocyclic or heterocyclic products (figure 4.11).

Figure 4.11. Examples of substrates used in the [6- π] electrocycisation.

The electrocycisation mechanism is done in 2 steps, where first the absorption of light lead to excited state of the compound permitting the cyclisation to occur. It formed the intermediate *trans* dihydrophenanthrene which undergoes final aromatization possible through oxidative trapping with O₂ or iodine (figure 4.12).

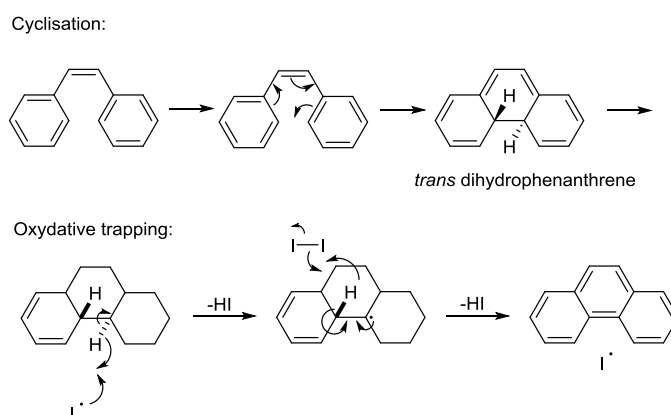


Figure 4.12. Photocyclisation mechanism of stilbene-like molecule.

[6- π] photocyclisation and photorearrangement of Pauson-Khand adducts have been successfully developed for first time in our research group with the work of Agustí Lledó and Yining Ji's doctoral thesis.^{41,42} Light induced reaction over various Pauson-Khand adducts led to the discovery of three different photo-chemical transformations depending on the conditions used and the nature of the substrate (figure 4.13).⁴¹ Working on the photo-induced hydroxymethyl conjugate addition of over PKR of the trimethylsilyl alkyne, a side reaction called transposition reaction was taking place yielding in addition to the expected product compound **II**, the compound **I**. In the case of PKRs of diphenylacetylene, the photochemical reaction afforded compound **III** in 55% yield as a result of an [6 π] electrocyclic ring-closure followed by final aromatisation.

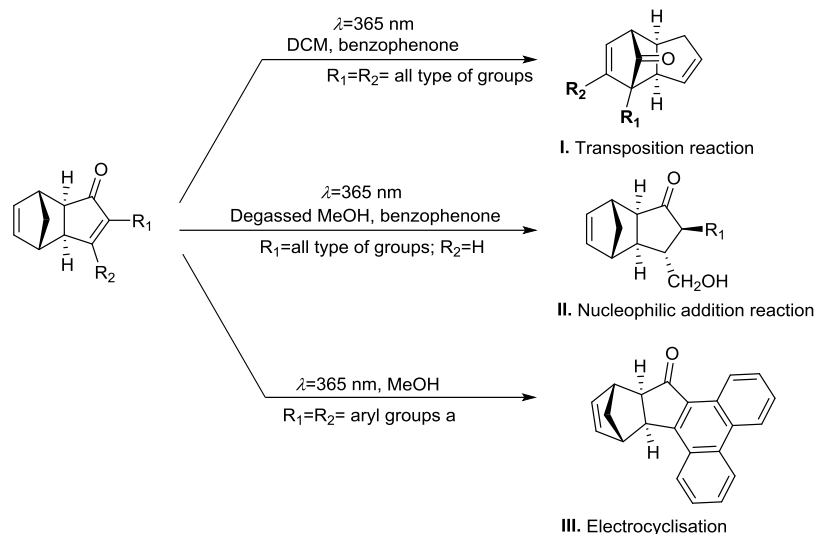


Figure 4.13. Three different photochemical transformations involving PK adducts.

Depending on the electronic properties of the bis-aryl alkyne substituents and reaction conditions, the photochemical outcome of the PK adduct led to compound **I** or **III** (figure 4.14). Thus, degassed DCM at 365 nm and an electro-withdrawing groups favour the formation of the photorearranged products **I** whereas non-degassed MeOH at short wavelength (300nm) and an electro-donating group are the ideal reaction conditions for the preparation of the phenanthrenes **III**.⁴²

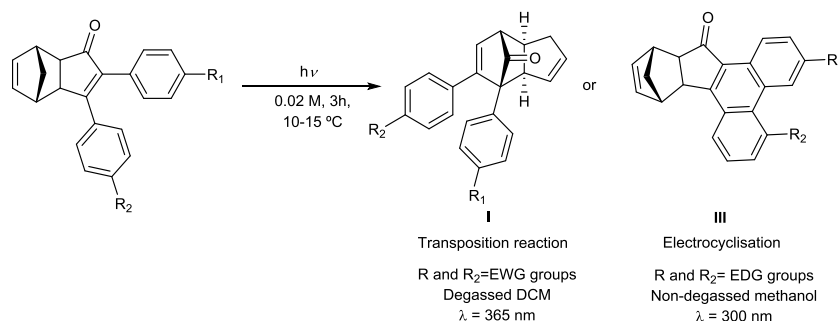


Figure 4.14. Optimised conditions to form the electrocyclic or transposed compounds from PK adducts.

In complement, it was identified that working with Pauson-Khand adducts of norbornene with the bis-aryl acetylenes substituted in 3- and 5-positions or 3-, 4-, and 5-positions, 112 and 121 at the aryl groups resulted to form a mixture of two isomers, named atropisomer **M** and **P** (figure 4.15). Indeed, a relatively bulky alkyl group (R) leads to helical twist of the aromatic plane of the PK adduct in response of the steric hindrance caused by van der Waal's repulsion between the two closely arranged substituents in 3- and 5-positions.

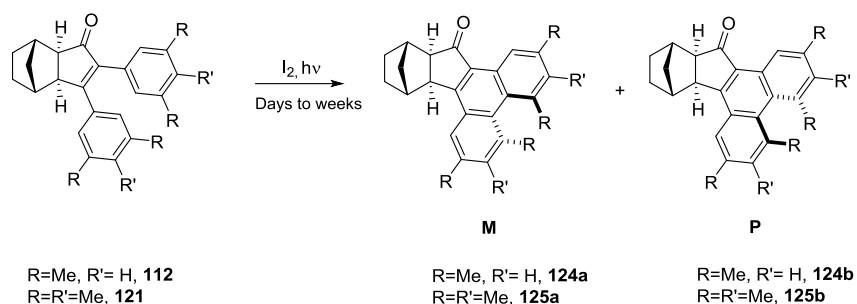


Figure 4.15. Conformationally restricted phenanthrenes obtained from PKR of the bis-aryl acetylenes by PhD Yi Ning Ji.

The undertaken study identified that the chirality of the bicyclic backbone of the PK adduct **112** and **121** can be translated to the helical fragment and thereby, produced an asymmetric induction and a new access to helicene-like molecules.⁴³ The steric congestion was relieved by the formation of two conformationally restricted chiral helicene-like diastereoisomers, which was observed with the cyclopentenones **124a/b** and **125a/b**.

Crystal structures of the major isomers in both cases revealed non-planar helical phenanthrene structures where the substituents in 3-, 4- and 5-positions were displaced out of the mean plane of the aromatic system to escape from sterical hindrance (figure 4.16).⁴³ The difference in the helical twist imposed by the methyl groups at the 4- and 5-positions resulted in a higher conformational stability in **112** since both atropisomers **124a/b** were isolated.

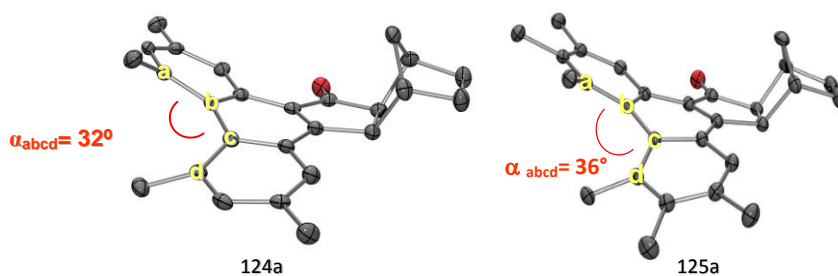


Figure 4.16. X-ray crystallography of **124a** and **125a**.

For the synthesis of helicene-like compounds, preliminary results obtained over the pericyclic reaction of PKRs of diphenylacetylene, **112** and **121** revealed that main drawback was the irradiation time far too long (more than a week). The steric hindrance of the aromatic substituents of the PK adduct **121** reduced considerably the conversion rate of the pericyclic reaction. With the target to **improve the irradiation time and scope of reaction, comparative study** of PKR of the substituted 3- and 5-positions or 3-, 4-, and 5-positions bis-aryl acetylenes of norbornadiene and norbornene will be presented in the present chapter.

4.2.2 Results and discussion

To perform the electrocycloaddition reaction, the synthesis of the PKRs was undertaken. The methyl and isopropyl groups were selected for their steric and electro-donating properties which favoured the electrocycloaddition reaction like represented in figure 4.17.

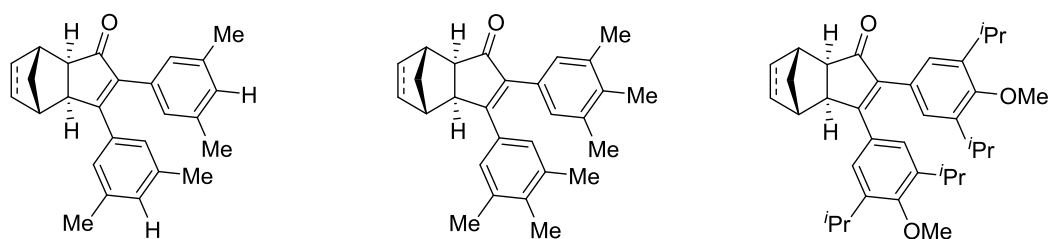


Figure 4.17. PK adducts selected.

4.3.4.1 Synthesis of the PK adducts

The synthesis of the starting materials, bis(3,5-dimethylphenyl)acetylene **110** and bis(3,4,5-trimethylphenyl)acetylene **115** was carried out by using a modified Sonogashira coupling reaction⁴⁴ from the corresponding aryl iodide or aryl triflate.

The commercially available 3,5-dimethyliodobenzene **109** afforded the diaryl alkyne **110** in 75% yield. The PK reaction with NBD yielded to **111** in 92% whereas the PKR with NBN afforded the cycloadduct **112** in 43% yield (figure 4.18).

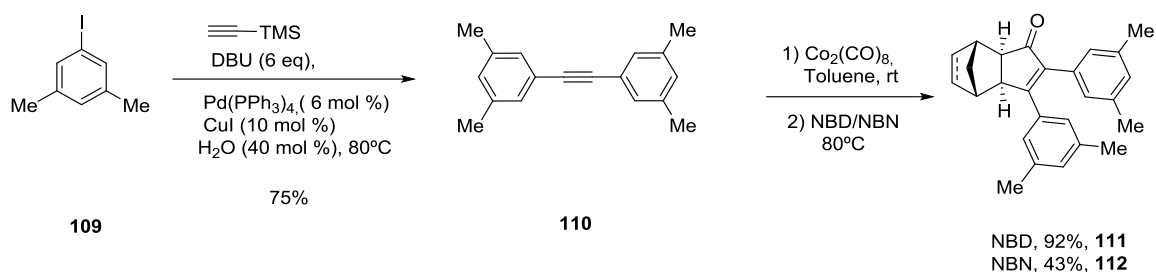


Figure 4.18. Synthesis of the PK adduct 111-112.

The bis(3,4,5-trimethylphenyl)acetylene **115** was obtained by direct treatment of the 3,4,5-trimethylphenol **113** in trifluoromethanesulfonic anhydride and trimethylamine to afford the corresponding aryl triflate **114** in 82% yield (figure 3.19). Sonogashira coupling reaction of **114** permitted to obtain 42% yield of the alkyne **115** and the PK reaction was performed with NBD yielded to the cycloadduct **116** in 89% yield.

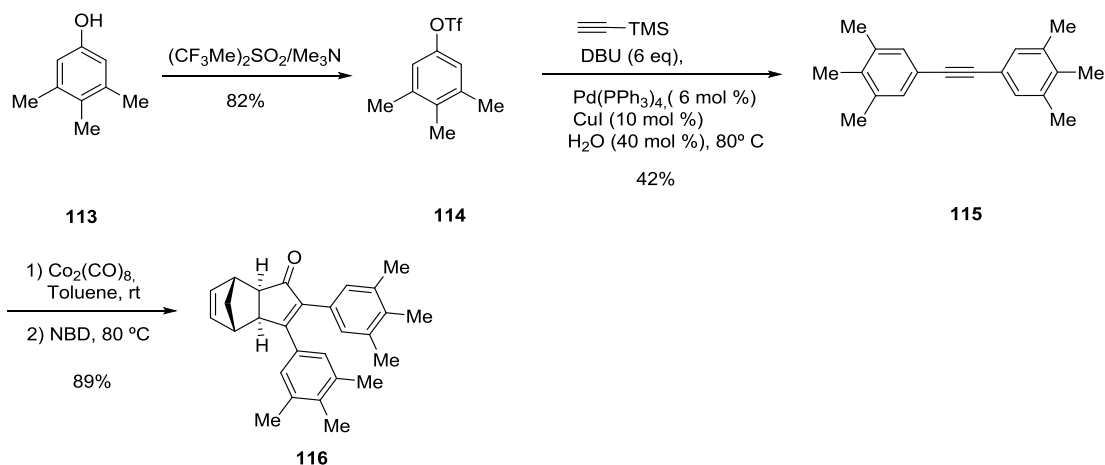


Figure 4.19. Synthesis of PK adduct, 116.

The bis(3,5-di-*iso*-propylphenyl)acetylene 119 was obtained by treatment of 2,6-di-*iso*-propylphenol 117 with cesium carbonate and iodomethane to afford the corresponding methyl ether which was then directly transformed into the compound 118 using glacial acetic acid and iodine monochloride in 80% yield. The Sonogashira reaction afforded the alkyne 119 in 60% yield and the PKR with NBD afforded the cycloadduct 120 in 93% yield (figure 4.20).

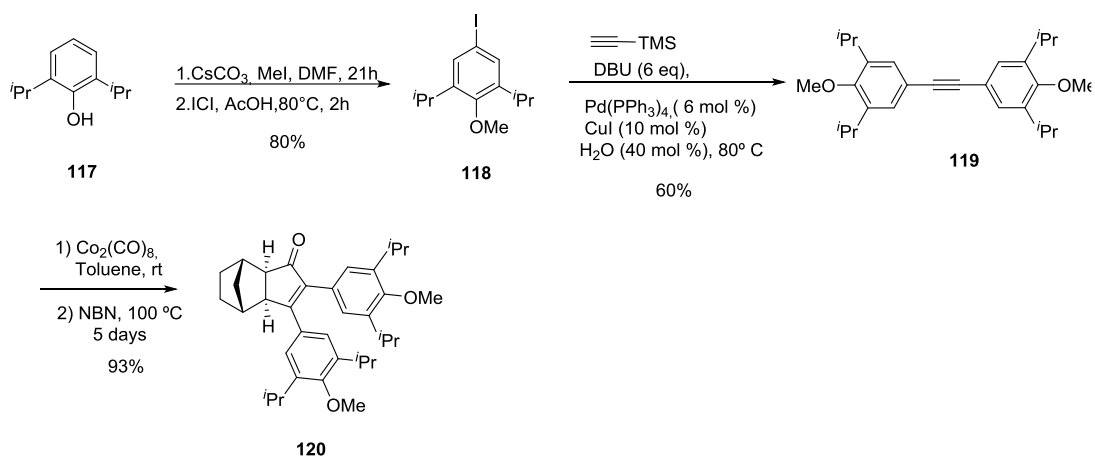


Figure 4.20. Synthesis PKR of the 120.

As iodine is reported to accelerate the final aromatization in the electrocyclic reaction, the double bond present in the NBD skeleton of the PK adduct was removed via hydrogenation with palladium catalysis affording 112 and 121 in 85% and 87% yield respectively (figure 4.21).

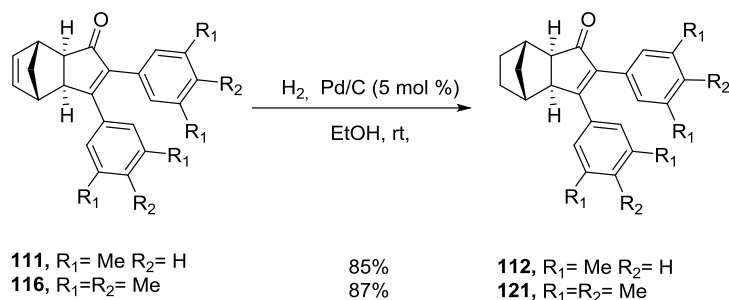


Figure 4.21. Hydrogenation of the PKR of NBD 112 and 121.

4.3.4.2 Electrocyclisation study

With cyclopentenones in hand, the photochemical reactions were performed (figure 4.22).

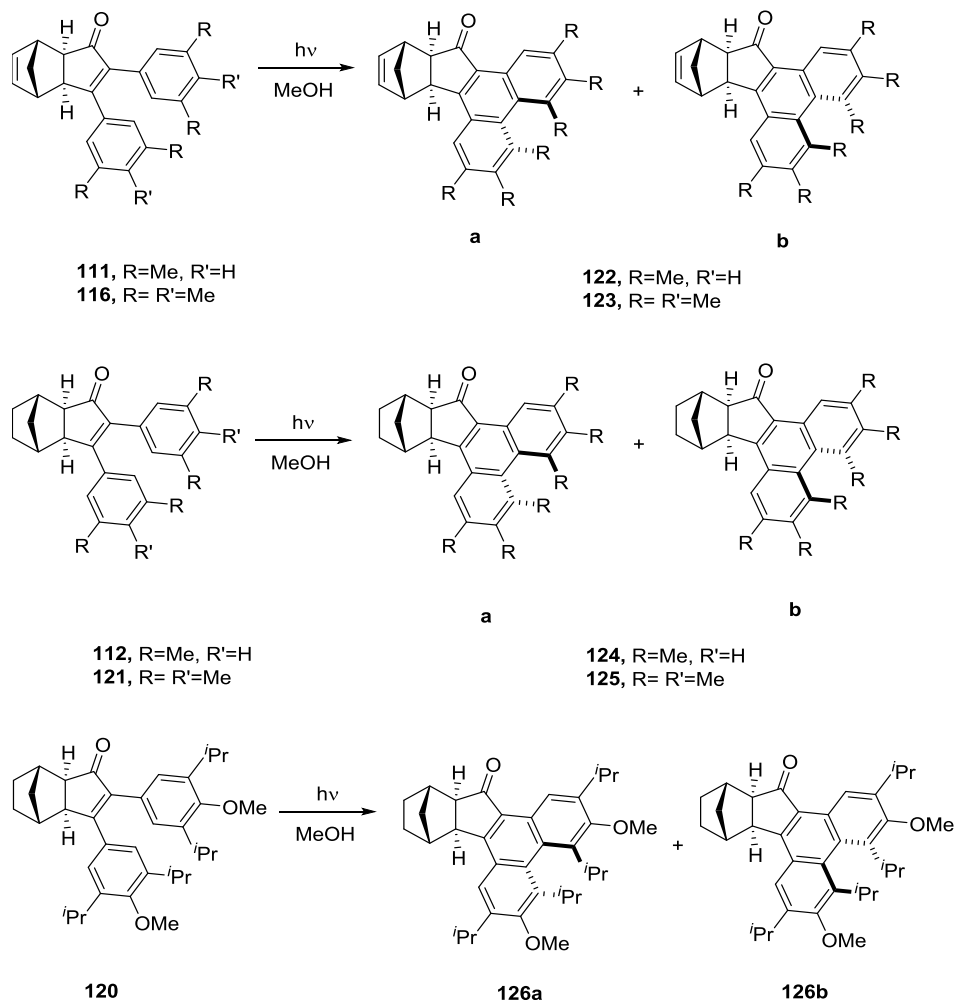


Figure 4.22. Photochemical reaction of substrates 112/112/116/120/120.

We identified that slight changes in photochemical reaction conditions allow us to obtain complete conversion rate working with 16 lamps at 300 nm with an oxidizing agent and the Rayonnet apparatus presented in the figure 4.23.



Figure 4.23. Rayonet apparatus used in the present study.

Thus, the results revealed that the reaction time was spectacularly speeded up from one week to 36 hours in the case of **112** and from 10 days to 53 hours in the case of **121**, (table 4.1, entries 1-4).

In addition, we were pleased to reach a total conversion for the substrates **112/121** which was around 60% of conversion over 10 days for the compound **121** (table 4.1, entries 2, 4 and 3). The photochemical adducts revealed a mixture of atropoisomers for compound **124** in a 3: 1 ratio and for compound **125** in 6:1 ratio.

The compounds **111/116** were tried without iodine. Irradiation of **111** in methanol solution at 300 nm gave phenanthrene compound **122** in only 33% yield over 10 days (Table 4.1, entry 5). The presence of the additional methyl groups in compound **116** further hampered the reaction, giving less than 13% yield of **123** after 6 days of irradiation where only one atropoisomer was observed by ¹H NMR (Table 4.1, entry 6). Even though, reactions were slow, new compounds were possible to be formed in long time reaction.

The substrate **120** was attempted but the pericyclic reaction did not occur, probably due to the large steric hindrance induced by the *iso*-propyl groups (table 4.1, entry 7).

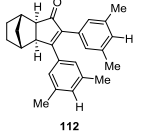
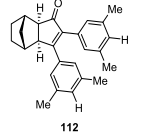
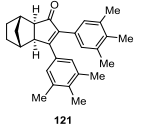
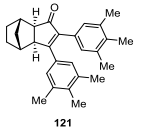
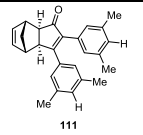
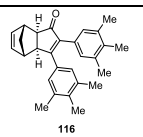
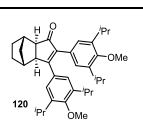
Entry	Substrate	λ (nm)	Number of lamps	Oxidant	Yield	M/P ratio	Time of reaction
1	 112	365	8 ^a	I ₂	96%	3:1	7 days
2	 112	300	16	I ₂	96%	3:1	36 hours
3	 121	365	8 ^a	I ₂	60%	6:1	10 days
4	 121	300	16	I ₂	94%	6:1	53 hours
5	 111	300	16	O ₂	33%	n.d	10 days
6	 116	300	16	O ₂	13%	n.d	6 days
7	 120	300	16	I ₂	0%	n.d	7 days

Table 4.1. Comparative photochemical reactions of the Pauson-Khand adducts 111/112/116/120/121. *n.d.*: non-determined ratio; ^a results obtained by the PhD YiNing Ji.

Improvement in the electrocyclisation reaction condition had been successfully achieved. We have performed the electrocyclisation of Pauson-Khand adducts of bis(3,5-dimethylphenyl)acetylene 111/112 and bis(3,4,5-trimethylphenyl)acetylene 116/121.

The placement of extra methyl groups in 4-positions of the aryl substituents enhanced the steric crowding by "buttressing" the methyl groups located at 3- and 5-positions, which resulted in a more strained and helical distorted phenanthrenes, a higher reaction time and moderate conversion rate.

We have shown that those limitations could be overcome with the substrates 112 and 121 where time was reduced to 36h against weeks of reaction in 100% conversion with Rayonet apparatus at 300nm, 16 lamps and 1 equivalent of iodine.

We have identified that electrocyclisation of PKRs **111/116** without oxidant afforded low conversion rates of 13–33% over a week of reaction.

The repulsion between the two methyl groups in the 3- and 5-positions of the phenanthrenic systems provoked a helical distortion of the planar aromatic system yielding to the formation of one major product in the mixture of the two atropoisomers formed.

We identified that the large sterically hindered group such as isopropyl group, too bulky is not suitable for the design of new phenanthrenes from PKR adducts.

Results of the previous doctoral and the present study of helicene-like compounds from Pauson-Khand adducts were combined for publication in *European Journal of Organic chemistry*, 2012, volume 2012, Issue 30, pages 6058–6063.

4.3 Attempt to synthesis of phenanthrolic compound

4.3.1 Introduction

1,10-phenanthroline, 2,2'-bipyridine (2,2'-bipy) and their derivatives, both in the metal-free state or as ligands coordinate to transition metal and disturb the functioning of a wide variety of biological systems with antifungal⁶, antibacterial^{3,7} and anti-cancer activities (figure 4.24).^{8,9,10} The copper-based 1,10-phenanthroline's series such as casiopeine were reported to be selectively cytotoxic against leukaemia cell lines and human ovarian carcinoma.^{45,46}

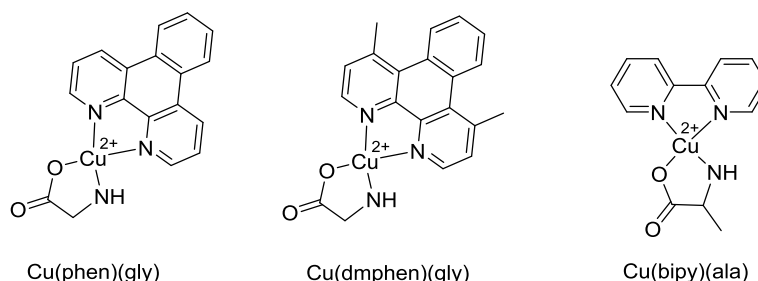


Figure 4.24. Examples of copper complexes of 1,10-Phenanthroline, 2,2'-bipyridine (2,2'-bipy).

Phenanthrolines are also motifs found in sensitive and selective methods of analysis of a wide range of analytes called electrochemo-luminescence (ECL) which involves among others immunoassays, enzymatic activity assays, binding assays or nucleic acid detection assays.^{47,48}

In the second part of this chapter, the aim was to widen the scope of photochemical transformation of PK adducts, studying the reactivity of heteroaromatic alkynes.

4.3.2 Results and discussion

Interested in extending the library of Pauson-Khand adducts that could undergo electrocyclic reaction, the 1,10-phenanthroline derivative, **132** was imagined. To do so, the first objective was to study the PKR of bis pyridyl alkynes and the electrocyclisation reaction of the adducts (figure 4.25).

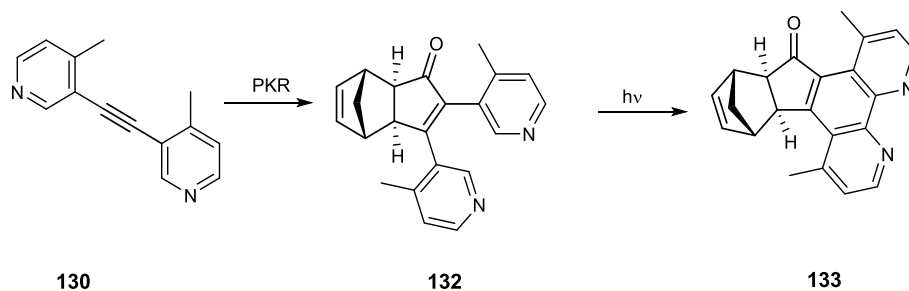


Figure 4.25. Envisaged synthesis for the photochemical reaction of the PK adduct, **132**.

The design of the PK adduct was imagined with methyl groups in both 2-position of the pyridyl group in order to lock the free rotation allowing a good coordination to a potential metal complex (figure 4.26).

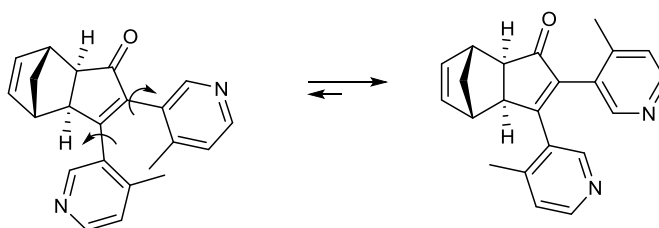
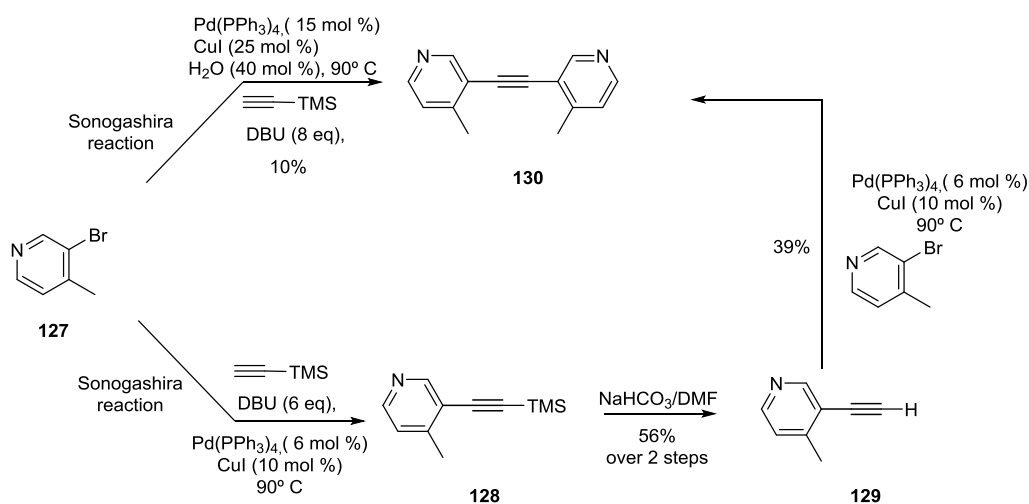
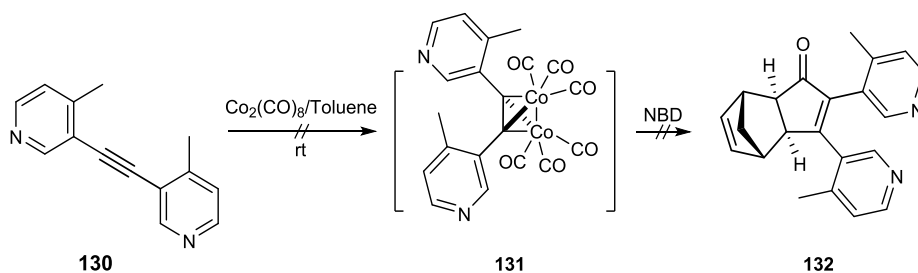


Figure 4.26. Design of the phenanthrolic PK adduct **132**.

The synthesis of the starting material of the PKR used the previous conditions the Sonogashira reaction with 3-bromo-4-methyl pyridine was tried but it turned out that reaction mainly stopped to the formation of the Sonogashira intermediate **128** (figure 4.27). After optimising conditions, 10% yield of the compound **130** was observed. We decided to perform the Sonogashira reaction in two steps with first the full conversion of 3-bromo-4-methylpyridine into trimethylsilyl **129** from the ethynyltrimethylsilane. After deprotecting of the trimethylsilyl moiety with NaHCO_3 into **129**, another equivalent of 3-bromo-4-methyl pyridine was added to afford a moderate 39% yield of the final product **130**.

Figure 4.27. Synthesis of the bis-pyridyl alkyne, **130**.

With the bis-pyridyl alkyne **130** in hand, the complexation was then tried in toluene with 1.05 equivalents of octacarbonyl dicobalt complex blocked from the incidence of the light (figure 4.28). Unfortunately, we observed the straight decomposition of the octacarbonyl dicobalt complex, from purple solution to black solid deposit.

Figure 4.28. Attempt to synthesise PKR of bis-pyridyl alkyne **132**.

Perhaps caused by lone pairs of the pyridyl motif, the synthesis of N-heteroaryl alkyne borane complex **134** was imagined to mask its lone pairs. It consisted in the treatment of bis-pyridyl alkyne **130** in dry toluene with 2 equivalents of a solution at 1M of borane in THF at 0°C to afford **134** as a white solid in 62 % yield (figure 4.29).⁴⁹ The borane complex was then subjected to complexation. Even though, the starting material was not soluble in toluene, DCM, hexane or AcOEt, the compound **134** was reacted with octacarbonyl dicobalt complex at room temperature and 50°C but the complexation into complex **135** did not occur.

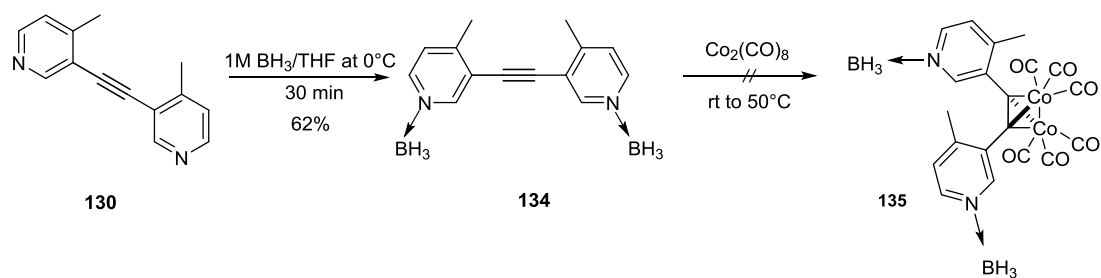


Figure 4.29. Attempt to synthesis of the borane hexamethyl dicobalt complex, **135**.

For further investigation, the impact of the pyridyl motif over the complexation with octacarbonyl dicobalt complex was investigated with the monosubstituted pyridyl alkyne **129** in its free and borane version. Monosubstituted pyridyl alkyne **129** was synthesised via Sonogashira reaction followed by a basic deprotection and the aryl borane **137** was obtained in 76% yield by direct treatment with borane (figure 4.30). The complexation of the alkynes **129** and **137** was tried in different solvent (AcOEt, DCM, toluene) where it did not lead to any traces of the hexacarbonyl cobalt complexes.

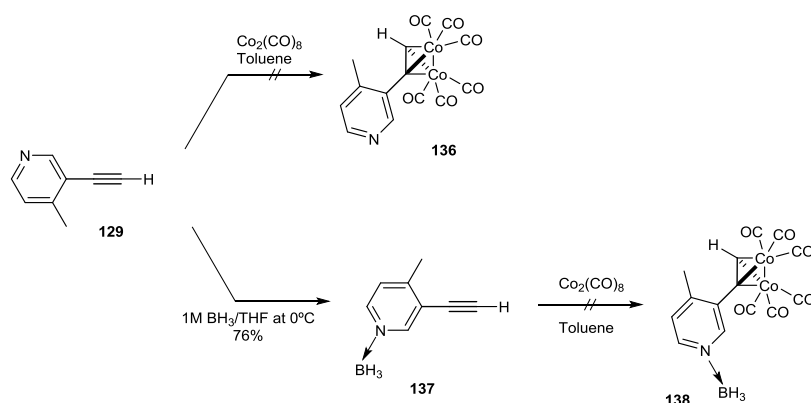


Figure 4.30. Attempt to form the hexacarbonyl cobalt complex from terminal pyridyl alkyne **136** and borane version **137**.

In the view of those results, the substrate-metal interaction led always to the coordination failure of the alkyne and the decomposition of the dicobalt complex which was assumed to be provoked by the pyridyl motif.

In the last part of this chapter, another heteroaromatic alkyne such as thiophenyl motif was envisaged to widen the scope of photochemical transformation of PK adducts which will be presented in the following section.

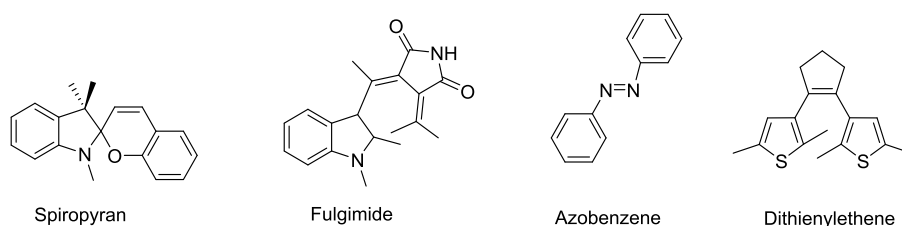
4.4 Toward photoswitchable diarylethenes

4.4.1 Introduction and objectives

Nowadays, compounds that change colour under the light influence, named photochromic molecules, are omnipresent devices of our daily life to medical use.⁵⁰ It was back in 1867 that Fritzsche discovered the curious phenomena of photochromism observing the bleaching of an orange coloured solution in daylight that re-colored at night.⁵¹ In general, photochromism is defined by reversible light-induced transformation of a compound into two stable forms which differ in their geometrical and electrical structures. The phenomena is easily appreciable by a reversible coloration changes upon exposure to light. Those differences lead to changes in the physical properties of the molecules, such as their absorption and fluorescence spectra, refractive index and electrical conductivity.^{52,53}

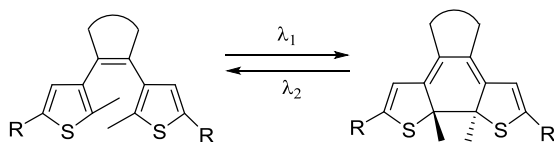
Photoswitching (often a type of photochromism) refers to the reversible light-induced switching of fluorescence (colour or intensity) from one configuration to another, for example, ring-closure vs. ring-opening. A good candidate for photoswitchable molecule requires two indispensable electronic properties: thermal irreversibility and fatigue resistant where the coloration/decoulation or isomerisation cycles could be repeated more than 10^4 times keeping its photochromic performance.⁵⁴ Since the transformation between the isomers is induced by light, optical switching can be realised by the use of photochromic building blocks.

Over the decades, families of photochromic entities have been identified such as the most popular classes azobenzenes, spiroyrans, fulgimides and diarylethenes (figure 4.31).⁶⁰ Photoswitches offer the fabrication of variety of molecules involved in "smart" polymers,⁵⁵ optical devices,^{27,56,50} data or energy storage^{54,57,58} and photopharmacology.^{4,59}



Figures 4.31. Families of photochromic building blocks.

For the present study, the dithienylethene (DTE) was chosen. Containing five-membered heterocyclic rings, they have a high sensitivity and fatigue resistance properties. The photochromic changes in diarylethene take place between two isomers, the ring-opened form, called the hexatriene usually colorless and cyclohexatriene, the ring-closed form that can develop depending on the substituents a yellow, red or blue coloration (figure 4.32).



Figures 4.32. Example of photoswitch unit, dithienylethene in its two isomeric forms.

In photopharmacology, a photoswitchable unit can be introduced into the molecular structure of the bioactive compound itself.¹³ Indeed, the electronic changes are triggered by a determined wavelength which permitted to pass from ring-opened to ring-closed form and from an active to inactive pharmacological response. Photopharmacology can be a valuable method when the disease is localised on the skin, eyes and on deeper tissues by the specific use of red light for solid tumours and infections.

If the photoswitch is introduced in an appropriate manner inside the pharmacophore, which means that biological activity is retained in at least one of the isomeric form, the drug can reversibly pass from a low to high affinity state.⁵⁹ In the family of photochromic molecules mentioned above, two of them have attracted the attention for biological purposes, azobenzenes (the most developed) and diarylethenes (used for that study).¹²

The pionners in this field were the group of and Nachmansohn who studied in the 1960's the inhibitions of the acetylcholinesterase by using an azobenzene unit.^{61,62} In the 2000's photoswitchable bioactive molecules were applied to inhibit proteases,⁶³ kinases,⁶⁴ mitochondrial complex,⁶⁵ and ion-channel receptors.^{66,67}

Introducing azobenzenic structure into anaesthetics, such as propofol⁶⁶ or lidocaine⁶⁸, the Tauner's group in 2012 could evaluate *in vivo* the anaesthetic effect of both photoisomers (figure 4.33). With the propofol, a variety of frog (*Xenopus leavis*) was used for the loss of the righting reflex (LORR). When they were placed into the aqueous media, the *trans*-molecule has the same activity has the anaesthetics themselves whereas after irradiation at 360-370 nm all animals spontaneously righted themselves.⁶⁹ Regarding the lidocaine, rats were selected to appreciate the blocking pain sensation via K^+ -channel. Good anaesthetic effect was observed with the *trans* photoswitchable anaesthetic while after irradiation at 360-370 nm the sensation was recovered.

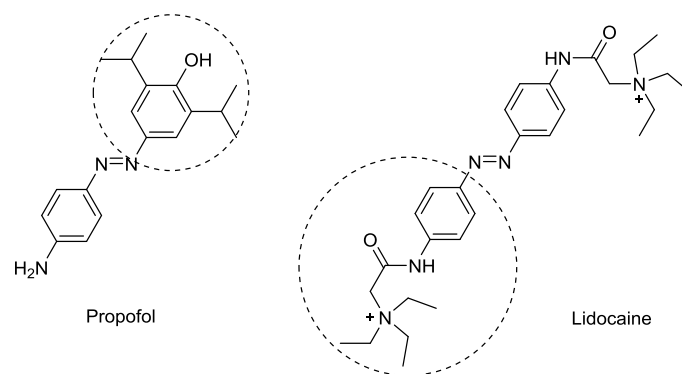


Figure 4.33. Examples of photoactivable prodrugs derived from azobenzene in its active form.

Photoswitch diarylethene units possess a great thermal stability making them the best choice for applications in photomemories and switches,⁵³ however, very few examples are reported in the literature concerning their biomedical applications.

The first report appeared in 2008 where the Branda and König's group described a photoswitchable inhibitor of human carbonic anhydrase I (hCAI), central enzyme to both cellular transport and metabolic processes.⁷⁰ Although a recent azobenzene-based biolabel was reported to control the enzyme activity, the thermal reversibility constrained their use in practical applications.⁷¹ The introduction of 1,2-dithienylethene (DTE) scaffold presents a significant improvement undergoing thermally irreversible photochemical ring-closing and ring-opening reactions (figure 4.34). The design of that photodrug was enhanced by the covalent bond of sulphanylamide to a copper complex. Inhibitory activity was given by the sulphanylamide acting in the active site of the enzyme while copper was believed to coordinate the histidine side chain presents at the surface of hCAI. Like the distance between the active side and the amino acid of the surface is fixed, installing the diarylethene bridge between sulphanylamide and copper complex allows a photocontrol of the enzymatic activity. Irradiation at 312 nm resulted in a total cyclisation to its closed form with a high hCAI inhibitory activity $IC_{50} = 8$ nM when compared to its parent sulphanilamide alone $IC_{50} = 450$ nM. The full reversible process was observed after irradiation with visible light.

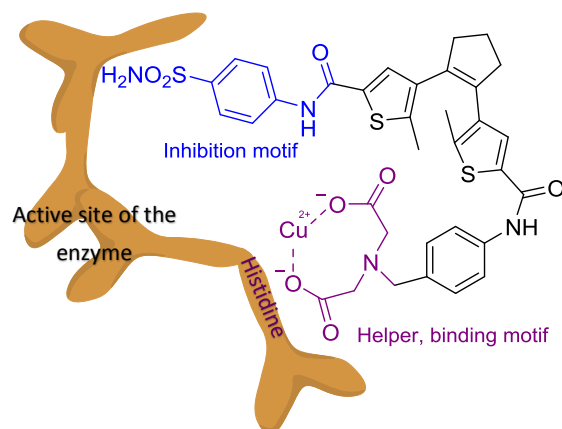


Figure 4.34. 1,2-dithienylethynyl unit, inactive form represented to photocontrolled inhibition of the enzyme hCAI.

Later, diarylethene family was applied to the photocontrolled of partial transcription of the DNA,^{72,73} inhibitions of enzymes^{74,75}, ion-channel involved in anaesthetic effect⁷⁶ and successfully introduced into peptidic⁷⁷ and nucleosidic sequences.⁷³ With the development and applications of DET, preliminary results shown how promising could become the photopharmacology to future biomedical applications.

The applications of DET motifs are also developed in the field of the liquid crystals where chiral DET can induce into an achiral liquid crystal host its chirality to form a self-organised optically tunable helical superstructure.⁷⁸ However, diarylethene motifs being less studied than the azobenzenes,⁷⁹ to date only few examples of chiral diarylethene dopants have been reported.⁸⁰

With the aim to extend the library of heterocyclic PK adducts, the incorporation of a DTE unit into the cyclopentenone would be a plausible candidate for further investigation in the field of photoswitchable compounds proposing a new synthetic methodology. The objective was to obtain a general overview of the reactivity of bis-thiophenyl alkynes under Pauson-Khand reaction and photochemical cyclisation.

4.4.2 Results and Discussion

The synthesis of the PK adduct began with the synthesis of the starting material, 1,2-bis (2,5-dimethylthiophen-3-yl) ethyne, **141** obtained by Sonogashira reaction. The 3-iodo-2,5-dimethylthiophene **140**, starting material for the Sonogashira reaction was prepared in 76% yield from 2,5-dimethylthiophene (**139**) in a solution of chloroform/acetic acid, with iodic acid and iodine (figure 4.35). The 1,2-bis (2,5-dimethylthiophen-3-yl) ethyne, **141** was obtained in 55% yield after several optimisations.

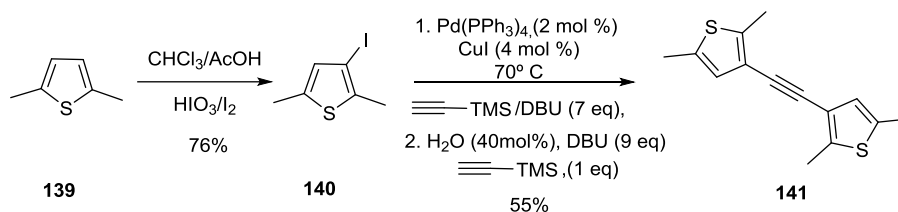


Figure 4.35. Synthesis of the 1,2-bis (2,5-dimethylthiophen-3-yl) ethyne 141.

With the alkyne 1,2-bis (2,5-dimethylthiophen-3-yl) ethyne 141 in hand, we undertook its complexation with $\text{Co}_2(\text{CO})_8$ study of the PKR with in different reaction conditions. The formation of hexacarbonyl cobalt complex of the alkyne was performed in toluene with 1.05 equivalent of octacobonyl dicobalt complex in the dark (figure 4.36). After two hours of reaction, it was appreciated by TLC the successful formation of an unusual green cobalt complex (142) in a clean crude of reaction. In case of instability of the complex, five equivalents of the NBN were added in situ and the mixture was heated up at 70°C .

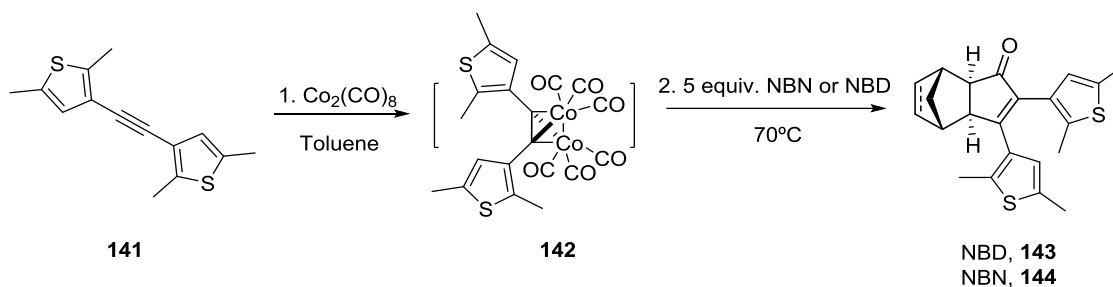


Figure 4.36. Synthesis of the PK adducts 143/144.

This first attempt did not afford any final product 144 (table 4.2, entry 1). The second experiment consisted to change the nature of the alkene from norbornene to five equivalents of norbornadiene and slightly increase in the temperature of reaction from 70 to 80°C . After preparation of the hexacarbonyl cobalt complex, the PKR was done in situ where the presence of the final product was detected in the complex crude of reaction. A preparative chromatography provided 6% yield of the PK adduct 143 (table 4.2. Entry 2).

For the next experiments, the PKRs were performed from isolated green cobalt complex to identify if the impurities present in the crude of hexacarbonyl cobalt complex were somehow plaguing the PKR. The number of equivalents in NBD range from 5 to 7 and temperature range from room temperature to 100°C was investigated (table 4.2. Entries 3,4) but yields dropped down to 0%. N-oxide promoted PKR at 0°C in DCM ended up with the decomposition of the hexacarbonyl cobalt complex (table 4.2, entry 5).

The stoichiometric PKR was then tried in dimethoxyethane (DME) with large excess of NBD (up to 10 equiv.) at 80°C . Therefore, only traces of the final products could be detected (table 4.2, entries 6,7). Its catalytic version was investigated with 5 and 10 equivalents of NBD but unfortunately it did not afford the final product (table 4.2. Entry 8).

As last attempt, through automatic syringe pump system over 3 hours, the green complex dissolved in toluene was added over the alkene solution (NBD) heated up to 80°C, affording the final PK adduct in 5% yield.

In this case, compatibility of that dithiophenyl motif with the metal was ensured by the satisfactory complexation of the alkyne in good yield (85-90%). Therefore, alkene insertion into the cobalt complex led to its failure affording small amount of PK adduct **143**.

Entry	Condition	Alkene	Solvent	T°C	Time	Yield
1	Complex formed in situ	5eq. NBN	Toluene	70°C	18h	0 %
2	Complex formed in situ	5eq. NBD	Toluene	80°C	18h	6%
3	From the complex	7eq. NBD	Toluene	rt to 45°C	4 days	Traces
4	From the complex	7eq. NBD	Toluene	100°C	16h	0%
5	From the complex	10 eq. NBD	DCM, NMO	0°C to rt	1h	0%
6	From the complex	5eq. NBD	DME	80°C	20h	Traces
7	From the complex	10eq. NBD	DME	80°C	2 days	0%
8	Catalytic version	5-10eq. NBD	DME	100°C	19h	0%

Table 4.2. PKR conditions tried with 1,2-bis (2,5-dimethylthiophen-3-yl) ethyne.

The PK adduct **143** in hand was then subjected to electrocyclic reaction study. The PK adduct of the diarylethene alkyne **143** dissolved in DCM (15 mg/mL) afforded a yellowish solution. UV-irradiation of the adduct at 350 nm during 1 minute at 296 K was carried out in the rayonnet® apparatus equipped with 16 lamps. The solution resulted in a coloration change due to the formation of the cyclic isomer into a fresh purple solution like shown in figure 4.37. The cycloreversion reaction of hexatriene system **143** into **145** was allowed at visible light ($\lambda > 400$ nm) in about an hour.

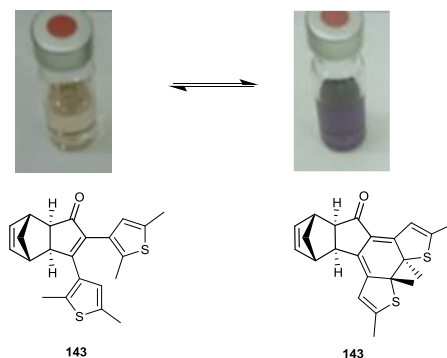


Figure 4.37. UV and visible reversible irradiation of the PKR of the dithiophenyl alkyne, **143/145**

The absorbance spectrums of both ring-closed (**143**) and ring-opened forms (**145**) were measured (figure 4.38). The maxima absorption of the ring-opened form was observed at 247 nm ($\epsilon = 6.25 \cdot 10^3 \text{ L} \cdot \text{mol}^{-1} \cdot \text{cm}^{-1}$) and a slight curve measured around 343 nm ($\epsilon = 2.16 \cdot 10^3 \text{ L} \cdot \text{mol}^{-1} \cdot \text{cm}^{-1}$).

The ring-closed form had absorption pics at 328 nm ($\epsilon = 6.25 \cdot 10^2 \text{ L} \cdot \text{mol}^{-1} \cdot \text{cm}^{-1}$) and 547 nm ($\epsilon = 6.25 \cdot 10^2 \text{ L} \cdot \text{mol}^{-1} \cdot \text{cm}^{-1}$). Stability of the ring-closed form was appreciated where after UV-irradiation, the isomer was left for more than a week into darkness. The ring-closed form absorption spectrum was strictly identical as the freshly form isomer.

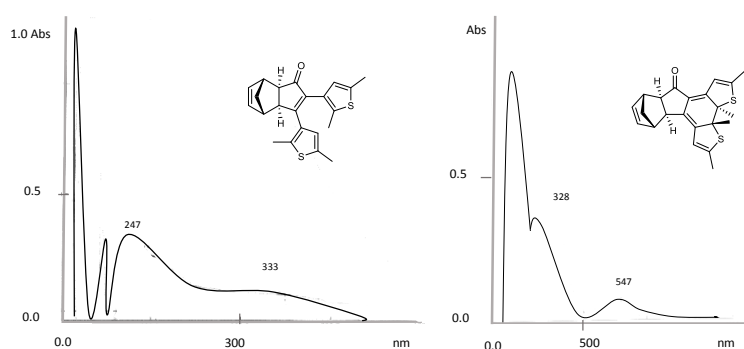


Figure 4.38. Absorbance's of both ring-closed and ring-opened forms ($C = 4 \cdot 10^{-5} \text{ mol} \cdot \text{L}^{-1}$ in DCM at 296 K)

We were pleased to validate our proof of concept where for the first time, a photoswitchable PK adducts was synthesised. Attempts to improve chemical yield of the PKR revealed that adverse reactions were taking place and only 6% yield of the final cyclopentenone could be obtained.

We identified that the hexacarbonyl dicobalt complex was formed and perfectly stable whereas the PKR of thiopentenylyl alkyne did not occur efficiently.

4.5 General conclusions

The photochemical reactivity of the PKR's of heterocyclic mono or di-substituted alkynes was presented in this chapter.

We have improved and completed the study of helicene-like compounds leading to the electrocyclic products from Pauson-Khand adducts.

We have prepared PKR of bis(3,5-dimethylphenyl)acetylene and bis(3,4,5-trimethylphenyl)acetylene of NBD and NBN which led to the electrocyclisation in 100% conversion in the case of NBN and low to moderate conversion rates in the case of the PKR's with NBD.

We have identified that the isopropyl substituent was too bulky, limiting the design of the PKRs that could be used for the formation of new phenanthrenes.

Results of the study of helicene-like compounds from Pauson-Khand adducts were published in *European Journal of Organic chemistry*, 2012, 30, 6058–6063.

We have studied the reactivity of the PKR's of heterocyclic alkynes such as pyridyl and thiophenyl motifs.

We have shown that coordination of the alkyne bearing pyridyl motifs with octacarbonyl dicobalt complex was not possible leading to the decomposition of the dicobalt complex.

We were able to successfully coordinate the dicobalt complex to thiophenyl alkyne in good yield.

Therefore, attempts to improve chemical yield of PKR revealed that adverse reactions are taking place and consequently only 6% yield could be obtained and isolated.

We were pleased to apply and characterise for the first time photoswitchable PK adduct of the thiophenyl alkyne permitting to validate our concept.

References

- (1) Guo, Z.; Sadler, P. J. *Adv. Inorg. Chem.* **1999**, *49*, 183–306.
- (2) Saha, S.; Dhanasekaran, D.; Chandraleka, S.; Panneerselvam, A. *Facta Univ. - Ser. Physics, Chem. Technol.* **2009**, *7*(1), 73–80.
- (3) Chandraleka, S.; Ramya, K.; Chandramohan, G.; Dhanasekaran, D.; Priyadharshini, A.; Panneerselvam, A. *J. Saudi Chem. Soc.* **2014**, *18*(6), 953–962.
- (4) Brieke, C.; Rohrbach, F.; Gottschalk, A.; Mayer, G.; Heckel, A. *Angew. Chem. Int. Ed. Engl.* **2012**, *51*(34), 8446–8476.
- (5) Longley, D. B.; Johnston, P. G. *J. Pathol.* **2005**, *205*(2), 275–292.
- (6) Eshwika, A.; Coyle, B.; Devereux, M.; McCann, M.; Kavanagh, K. *BioMetals* **2004**, *17*(4), 415–422.
- (7) Creaven, B. S.; Egan, D. A.; Kavanagh, K.; McCann, M.; Noble, A.; Thati, B.; Walsh, M. *Inorganica Chim. Acta* **2006**, *359*(12), 3976–3984.
- (8) Mandal, S. M.; Roy, A.; Ghosh, A. K.; Hazra, T. K.; Basak, A.; Franco, O. L. *Front. Pharmacol.* **2014**, *5*, 105.
- (9) Moreno-Sánchez, R.; Hernández-Esquível, L.; Rivero-Segura, N. A.; Marín-Hernández, A.; Neuzil, J.; Ralph, S. J.; Rodríguez-Enríquez, S. *FEBS J.* **2013**, *280*(3), 927–938.
- (10) Vértiz, G.; García-Ortuño, L. E.; Bernal, J. P.; Bravo-Gómez, M. E.; Lounejeva, E.; Huerta, A.; Ruiz-Azuara, L. *Fundam. Clin. Pharmacol.* **2014**, *28*(1), 78–87.
- (11) Edwards, I. R.; Aronson, J. K. *Lancet (London, England)* **2000**, *356*(9237), 1255–1259.
- (12) Broichhagen, J.; Frank, J. A.; Trauner, D. *Acc. Chem. Res.* **2015**.
- (13) Szymański, W.; Beierle, J. M.; Kistemaker, H. A. V.; Velema, W. A.; Feringa, B. L. *Chem. Rev.* **2013**, *113*(8), 6114–6178.
- (14) Roth, H. D. *Angew. Chem. Int. Ed. Engl.* **1989**, *28*, 1193–1196.
- (15) *Handbook of Synthetic Photochemistry*; Albin Angeloi; Fagnoni Maurizio, Ed.; 2009.

- (16) Maurizio, A. A. F. *Photochemically-Generated Intermediates in Synthesis*, Wiley, Ed.; 2014.
- (17) Wang, Z. *Comprehensive Organic Name Reactions and Reagents*, John Wiley & Sons, Inc.: Hoboken, NJ, USA, 2010.
- (18) Brière, J.-F.; Blaauw, R. H.; Benningshof, J. C. J.; van Ginkel, A. E.; van Maarseveen, J. H.; Hiemstra, H. *European J. Org. Chem.* **2001**, *2001* (12), 2371–2377.
- (19) Vogt, F.; Jödicke, K.; Schröder, J.; Bach, T. *Synthesis (Stuttg)*. **2009**, (24), 4268–4273.
- (20) Bach, T.; Aechtner, T.; Neumüller, B. *Chemistry* **2002**, *8* (11), 2464–2475.
- (21) Turro, N. J.; Schuster, G. *Science* **1975**, *187* (4174), 303–312.
- (22) Bach, T.; Hehn, J. P. *Angew. Chem. Int. Ed.* **2011**, *50* (5), 1000–1045.
- (23) Hoffmann, N. *Chem. Rev.* **2008**, *108* (3), 1052–1103.
- (24) Shen, Y.; Chen, C.-F. *Chem. Rev.* **2012**, *112* (3), 1463–1535.
- (25) Gunawan, M. A.; Hierso, J.-C.; Poinso, D.; Fokin, A. A.; Fokina, N. A.; Tkachenko, B. A.; Schreiner, P. R. *New J. Chem.* **2014**, *38* (1), 28–41.
- (26) Li, Z.; Liu, Z.; Sun, H.; Gao, C. *Chem. Rev.* **2015**.
- (27) Gust, D.; Andréasson, J.; Pischel, U.; Moore, T. A.; Moore, A. L. *Chem. Commun. (Camb)*. **2012**, *48* (14), 1947–1957.
- (28) Allen, N. S. *Photochemistry and Photophysics of Polymeric Materials*, Wiley-VCH Verlag GmbH, 2010.
- (29) Amara, Z.; Bellamy, J. F. B.; Horvath, R.; Miller, S. J.; Beeby, A.; Burgard, A.; Rossen, K.; Poliakoff, M.; George, M. W. *Nat. Chem.* **2015**, *7* (6), 489–495.
- (30) Wardle, B. *Principles and applications of photochemistry*, 2009.
- (31) Turro, N. J., Ramamurthy, V., Scaiano, J. C. *Modern molecular photochemistry of organic molecules*, 2010.
- (32) Lange, G. L.; Corelli, N. *Tetrahedron Lett.* **2007**, *48* (11), 1963–1965.
- (33) Esposti, S.; Dondi, D.; Fagnoni, M.; Albini, A. *Angew. Chem. Int. Ed. Engl.* **2007**, *46* (14), 2531–2534.

- (34) Marchueta, I.; Olivella, S.; Solà, L.; Moyano, A.; Pericàs, M. A.; Riera, A. *Org. Lett.* **2001**, *3*(20), 3197–3200.
- (35) Urbano, A. *Angew. Chem. Int. Ed. Engl.* **2003**, *42*(34), 3986–3989.
- (36) Gingras, M. *Chem. Soc. Rev.* **2013**, *42*, 968–1006.
- (37) Gingras, M.; Félix, G.; Peresutti, R. *Chem. Soc. Rev.* **2013**, *42*(3), 1007–1050.
- (38) Flammang-Barbieux, M.; Nasielski, J.; Martin, R. H. *Tetrahedron Lett.* **1967**, *8*(8), 743–744.
- (39) Turro, N. J. *Angew. Chem. Int. Ed. Engl.* **1986**, *25*, 882.
- (40) Mezey, P. G. *Theor. Chim. Acta* **1982**, *62*(2), 133–161.
- (41) Lledó, A.; Benet-Buchholz, J.; Solé, A.; Olivella, S.; Verdaguer, X.; Riera, A. *Angew. Chem. Int. Ed. Engl.* **2007**, *46*(31), 5943–5946.
- (42) Ji, Y.; Verdaguer, X.; Riera, A. *Chem. Eur. J.* **2011**, *17*(14), 3942–3948.
- (43) Ji, Y. New substrates for the intermolecular Pauson-Khand reaction. Photochemistry of the adducts and synthetic applications, Universitat de Barcelona, Spain, 2008.
- (44) Mio, M. J.; Kopel, L. C.; Braun, J. B.; Gadzikwa, T. L.; Hull, K. L.; Brisbois, R. G.; Markworth, C. J.; Grieco, P. A. *Org. Lett.* **2002**, *4*(19), 3199–3202.
- (45) Ruiz-Ramirez, L.; Gracia-Mora, I.; de la Rosa, M. E.; Sumano, H.; Gomez, C.; Arenas, F.; Gomez, E.; Pimentel, E.; Cruces, M. *J. Inorg. Biochem.* **1993**, *51*(1-2), 406.
- (46) De Vizcaya-Ruiz, A.; Rivero-Muller, A.; Ruiz-Ramirez, L.; Kass, G. E. N.; Kelland, L. R.; Orr, R. M.; Dobrota, M. *Toxicol. Vit.* **2000**, *14*(1), 1–5.
- (47) Bernhard, S.; Belser, P. *Synthesis (Stuttg.)* **1996**, 192.
- (48) Yin, X. B.; Dong, S.; Wang, E. *TrAC - Trends Anal. Chem.* **2004**, *23*(6), 432–441.
- (49) Lalevée, J.; Blanchard, N.; Tehfe, M.-A.; Chany, A.-C.; Fouassier, J.-P. *Chemistry* **2010**, *16*(43), 12920–12927.
- (50) Russew, M. M.; Hecht, S. *Adv. Mater.* **2010**, *22*(31), 3348–3360.
- (51) Bouas-Laurent, H.; Dürr, H. *Pure Appl. Chem.* **2001**, *73*(4), 639–665.

- (52) Ud-Dean, S. M. M. *Interdiscip. Sci.* **2011**, *3* (2), 79–90.
- (53) Irie, M. *Chem. Rev.* **2000**, *100* (5), 1685–1716.
- (54) Sauer, M. *Proc. Natl. Acad. Sci. U. S. A.* **2005**, *102* (27), 9433–9434.
- (55) Wang, G.; Yuan, D.; Yuan, T.; Dong, J.; Feng, N.; Han, G. *J. Polym. Sci. Part A Polym. Chem.* **2015**, n/a – n/a.
- (56) Díaz, S. a.; Gillanders, F.; Jares-Erijman, E. a.; Jovin, T. M. *Nat. Commun.* **2015**, *6*, 6036.
- (57) Kucharski, T. J.; Ferralis, N.; Kolpak, A. M.; Zheng, J. O.; Nocera, D. G.; Grossman, J. C. *Nat. Chem.* **2014**, *6* (5), 441–447.
- (58) Adam, V.; Mizuno, H.; Grichine, A.; Hotta, J.; Yamagata, Y.; Moeyaert, B.; Nienhaus, G. U.; Miyawaki, A.; Bourgeois, D.; Hofkens, J. *J. Biotechnol.* **2010**, *149* (4), 289–298.
- (59) Velema, W. A.; Szymanski, W.; Feringa, B. L. *J. Am. Chem. Soc.* **2014**, *136* (6), 2178–2191.
- (60) Fihey, A.; Perrier, A.; Browne, W. R.; Jacquemin, D. *Chem. Soc. Rev.* **2015**.
- (61) Bieth, J.; Wassermann, N.; Vratsanos, S. M.; Erlanger, B. F. *Proc. Natl. Acad. Sci. U. S. A.* **1970**, *66* (3), 850–854.
- (62) Bartels, E.; Wassermann, N. H.; Erlanger, B. F. *Proc. Natl. Acad. Sci. U. S. A.* **1971**, *68* (8), 1820–1823.
- (63) Pearson, D.; Alexander, N.; Abell, A. D. *Chemistry* **2008**, *14* (24), 7358–7365.
- (64) Ferreira, R.; Nilsson, J. R.; Solano, C.; Andréasson, J.; Grøtli, M. *Sci. Rep.* **2015**, *5*, 9769.
- (65) Fujita, D.; Murai, M.; Nishioka, T.; Miyoshi, H. *Biochemistry* **2006**, *45* (21), 6581–6586.
- (66) Stein, M.; Middendorp, S. J.; Carta, V.; Pejo, E.; Raines, D. E.; Forman, S. A.; Sigel, E.; Trauner, D. *Angew. Chem. Int. Ed. Engl.* **2012**, *51* (42), 10500–10504.
- (67) Banghart, M. R.; Mourot, A.; Fortin, D. L.; Yao, J. Z.; Kramer, R. H.; Trauner, D. *Angew. Chem. Int. Ed. Engl.* **2009**, *48* (48), 9097–9101.
- (68) Mourot, A.; Fehrentz, T.; Le Feuvre, Y.; Smith, C. M.; Herold, C.; Dalkara, D.; Nagy, F.; Trauner, D.; Kramer, R. H. *Nat. Methods* **2012**, *9* (4), 396–402.

- (69) Stewart, D. S.; Savechenkov, P. Y.; Dostalova, Z.; Chiara, D. C.; Ge, R.; Raines, D. E.; Cohen, J. B.; Forman, S. A.; Bruzik, K. S.; Miller, K. W. *J. Med. Chem.* **2011**, *54*(23), 8124–8135.
- (70) Vomasta, D.; Högner, C.; Branda, N. R.; König, B. *Angew. Chem. Int. Ed. Engl.* **2008**, *47*(40), 7644–7647.
- (71) Harvey, J. H.; Trauner, D. *ChemBioChem* **2008**, *9*(2), 191–193.
- (72) Cahová, H.; Jäschke, A. *Angew. Chemie - Int. Ed.* **2013**, *52*(11), 3186–3190.
- (73) Singer, M.; Jäschke, A. *J. Am. Chem. Soc.* **2010**, *132*(24), 8372–8377.
- (74) Chen, X.; Wehle, S.; Kuzmanovic, N.; Merget, B.; Holzgrabe, U.; König, B.; Sotriffer, C. A.; Decker, M. *ACS Chem. Neurosci.* **2014**, *5*(5), 377–389.
- (75) Reisinger, B.; Kuzmanovic, N.; Löffler, P.; Merkl, R.; König, B.; Sterner, R. *Angew. Chem. Int. Ed. Engl.* **2014**, *53*(2), 595–598.
- (76) Al-Atar, U.; Fernandes, R.; Johnsen, B.; Baillie, D.; Branda, N. R. *J. Am. Chem. Soc.* **2009**, *131*(44), 15966–15967.
- (77) Fujimoto, K.; Kajino, M.; Sakaguchi, I.; Inouye, M. *Chem. - A Eur. J.* **2012**, *18*(32), 9834–9840.
- (78) Yu, H. *Prog. Polym. Sci.* **2014**, *39*(4), 781–815.
- (79) Irie, M. *Proc. Jpn. Acad. Ser. B. Phys. Biol. Sci.* **2010**, *86*(5), 472–483.
- (80) Li, Y.; Urbas, A.; Li, Q. *J. Am. Chem. Soc.* **2012**, *134*(23), 9573–9576.

CHAPTER V

Conclusions

Conclusions

The doctoral thesis was devoted to the intermolecular Pauson-Khand reaction with the two main axes: the study of its regioselectivity and its synthetic applications.

In the second chapter, the understanding and prediction of the regiochemical outcome of the intermolecular PKR of unsymmetrical alkynes was successfully achieved from experimental and computational point of view. The electronic influence of the alkyne substituents over the regioselectivity was studied with a full set of aliphatic alkynes bearing sterically similar but electronically different substituents. The computational NBO charges of the alkynes permitted to evaluate and predict the influence of the substituents over the polarization of alkyne.

We have shown that:

- The computational NBO charges correlated well the experimental outcome clearly indicating that the polarization of alkyne was inductively mediated from the heteroatom.
- Electronic polarization of the substituents in α -position of the alkynes can alone qualitatively predict the regiochemical outcome of the PKR.
- Experimentally, when substituents bearing an atom more electronegative than carbon (-I groups), the PKR yielded β -exo regioisomer with a remarkably high regioselectivity. Conversely, less electronegative atom than the carbon inverted the regioselectivity toward the formation of the α -exo isomer in excellent yield, although in this case the steric effects could not be ruled out.
- Our study permitted to clarify and rationalize the regiochemical outcome proposing to scientific community a tool to predict its regiodirection which have been published in *Journal of Organic Chemistry*, 2014, 10999–11010.

In the third chapter, synthetic applications of intermolecular PKR adducts directed to the synthesis of natural products were investigated.

We have shown that:

- The PKR of internal alkyne was proved to be the best method to synthesize the *rac*-sarkomycin methyl ester (anti-cancer drug) in 2-pot reaction and 15 % overall yield.
- New pathways were undertaken to obtain methyl jasmonate (frangance) from intermolecular PKR of unsymmetrical alkynes or terminal alkyne.
- The first pathway used the PKR of unsymmetrical alkyne where our model to predict the regioselectivity was employed. It revealed that even the formed adduct gave the opposite isomer that we would expect, the computational NBO charges correlated well the experimental outcome.
- The second pathway was carried out with the PKR of propargyl alcohol. Our preliminary results allowed us to identify that the Claisen-Johnson rearrangement could be applied in the synthesis of the methyl jasmonate.

In the fourth chapter, synthetic applications of intermolecular PKR of symmetrical alkynes toward photochemical transformations were undertaken from diaryl and heterocyclic alkynes.

We have shown that:

- The electrocyclisation reaction of the PKRs of disubstituted aryl alkynes could be optimised affording a new access to phenanthrene derivatives. This photochemical reaction induced the formation of two possible atropoisomers which by the steric hindrance of the PK adducts imposed by its substituents afforded a mixture of twisted isomers assimilated to helicene-like family. The PKR of bis(dimethyl phenyl) and bis(trimethyl phenyl) alkynes and norbornene were optimised affording excellent yields and times of reaction.
- Bulkier substituents on the phenyl alkyne such as *i*-propyl prevented the electrocyclisation reaction.

The results were published in *European Journal of Organic Chemistry*, 2012, 30, 6058–6063.

- The reactivity of heterocyclic alkynes such as pyridyl and thiophenyl motifs regarding the PKR and photochemical reactions were studied. While the pyridyl motif did not afford the PK adduct, for the first time, PK adduct of the bis (dimethyl thiophenyl) acetylene successfully gave the reversible photoswitch reaction.

CHAPTER VI

Experimental part

General considerations

Instrumentations

Chromatography

Chromatographic columns were performed using:

- Silica gel 35-70 μm with compressed air
- $\text{SiO}_2/\text{NEt}_3$ (2.5%): for each 100 mL of silica gel was adding 2.5 mL of Et_3N and shake to obtain an homogeneous power.
- Neutral Al_2O_3 .
- an automated chromatography system (Combiflash®, Teledyne Isco) with hexanes/ethyl acetate gradients as eluent unless noted otherwise.

TLC plates. All reactions were monitored by analytical TLC analysis using Merck 60 F254 silica gel plates on aluminum sheets visualized by UV ($\nu=254$ nm), if possible.

Phosphomolybdic acid and potassium permanganate stainings were used using the following dilutions:

- Phosphomolybdic acid: 23 g of phosphomolybdic acid in 400 mL of ethanol (95%).
- Potassium permanganate: 3 g de potassium permanganate, 20 g de potassium carbonate, 300 mL of water and 5 mL of an aqueous solution at 5% of sodium hydroxide was mixed and protected from the light after good stirring, filtration of the solution afforded the staining.

HPLC-MS. Instrumentation used was Agilent 1100.

Nuclear magnetic resonance (NMR). ^1H NMR and ^{13}C NMR spectra were recorded in CDCl_3 or benzene d_6 at ambient temperature unless otherwise stated with Varian Mercury 400 or a Bruker 300. ^1H spectra were referenced to tetramethylsilane (TMS, 0 ppm) or δ 7.16 ppm for the benzene d_6 . ^{13}C spectra were referenced to solvent carbon CDCl_3 δ 77.16 ppm, C_6D_6 δ 128.06 ppm at 100 MHz. Proton and carbon assignments were made based on COSY, HSQC (Heteronuclear Single Quantum Correlation), HMQC, HMBC spectra. The isomer ratio was determined by NMR by integration of ^1H spectrum. ^{19}F -NMR spectra were referenced by the spectrometer without any external pattern. The following abbreviations were used to define the multiplicities: s, singlet; d, doublet; t, triplet; q, quadruplet; m, multiplet; br s, broad signal; Cq, quaternary carbon; CO, carbonyl; CH, CH_2 , CH_3 . The chemical shifts (δ) are expressed in ppm and the coupling constants (J) in hertz (Hz).

Infra-red spectrometry (IR). IR spectra were recorded in a Thermo Nicolet Nexus FT-IR apparatus by depositing a film of the product on a NaCl window. Absorptions are given in wavenumbers (cm^{-1}).

Melting points (Pf). Melting points were recorded in a Büchi B-540 apparatus.

High and low mass spectrometry analysis. Mass spectrometry analysis was performed as high resolution ESI analysis at the "Mass Spectrometry Core Facility" from the IRB Barcelona. Low and high resolution chemical ionisation was performed at the "Unitat d'Espectrometria de Masses de Caracterització Molecular, CCIUB," from University of Barcelona.

Absorption. Absorption spectra was performed with UV-250-1PC, UV-VIS recording spectrophotometer Shimadzu.

Materials and techniques

Solvents. The use of non-anhydrous solvents were from reagent or HPLC grade quality. Tetrahydrofuran, ether and dichloromethane were obtained using a Solvent Purification System (SPS). Anhydrous N,N-dimethylformamide and toluene were purchased directly from Aldrich and used directly unless otherwise stated. Other solvents, such as nitromethane, were used directly as purchased, with no further purification. Tetrahydrofuran, toluene, ether and dichloromethane were obtained using a Solvent Purification System (SPS) or were distilled according the standard method under inert atmosphere of nitrogen and extemporaneous used over Na/benzophenone or dried over 4Å molecular sieves.

Commercial reagents. All commercial reagents were used without further purification unless noted otherwise.

Cul cristallisation procedure. 4 g de CuI was dissolved in 33 mL of a saturated solution of NaI (180 g NaI/ 100 mL) and heated up to boiling point during 30 minutes. Then, the mixture was filtered still hot and let to cool down. After adding water to the filtrate, it was left CuI recrystallised. The suspension was filtered and dried under high vacuum line and left in the dessicator. HMPA was distilled over CaH₂ and kept over molecular sieves 4 in the dessicator. Lithium derivatives such as BuLi 1.6 or 2.5 M in hexane or MeI was titrated previous to their use with diphenylacetic acid.

Anhydrous conditions. In general, reactions were carried out under a nitrogen atmosphere and the glassware dried overnight at 50°C. For the extremely water sensitive reaction, the glassware was previously flamed under high vacuum line.

Reaction under pressure. For reactions under CO or ethylene pressure, pressure tubes were used. They were attached to a steel cylinder through a steel pipe system bearing a three way valves that allowed the system to be purged through a Teflon Kontes-HI-VAC. For big scale reactions, a 200 to 250 mL Büchi AG miniclave reactor was used with manometer. Reaction could be connected to a 50 L bottle of Co, 5 L-10 L bottle of ethylene using a three-exit to purge and charge safely the reactor. Reactions under microwaves were done in a CEM Discover Microwave Reactor at the Unitat de Química Combinatòria of the PCB.

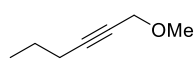
Photochemical reaction conditions. It was used the Rayonnet apparatus with it 16 lamps at 300, 350 or 365 nm, 8 watt. The glassware used was quartz flask and duran glassware.

Cold bath. 0°C was reached working with ice and water. -15°C: ice /NaCl. -20°C: CCl₄/ dry ice. 20- to -80°C acetone/ dry ice.

Calculation. All the experiments have been performed by Helaja's group in Helsinki by Mikko Muuroren. All structure optimisations and single point energy calculations were performed using the Turbomole 6.4 program package. Computations were done in gas-phase as experimental results indicated low impact of the solvent towards the regioselectivity. The TPSS-D3 functional was employed with triple ζ quality basis set, def2-TZVP or def2-TZVPP, as described in the text. The MARI-J approximation was used in all computations with suitable auxiliary basis set. Default settings of the Turbomole program were used throughout expect finer grid option *m4* (cobalt complexes) or *m5* (alkynes) was chosen. Analytical frequency calculations were performed to all optimized structures to confirm the nature of the potential energy surface (minima/maxima) and to obtain the chemical potential (chem. pot.) for Gibbs free energies. The Gibbs free energies were then calculated as $G = E(0) + \text{chem.pot.}$ To inspect transition state energy differences more closely, single-point energy calculations were also performed with PW6B95-D3^{Erreur ! Signet non défini.}, TPSSh-D3 and PBE0-D3 functionals, to ensure the nature of the result. NCI-plots were generated using NCIplot-program using TPSS-D3/def2-TZVP wavefunction from Turbomole. Pictures were generated using Cylview¹ and VMD. The ¹H NMR shieldings were calculated with Orca 3.0 program package (IGLO/TPSSh-D3/def2-TZVPP). Additional settings "TightSCF" and "Grid4" were used.

Chapter II

2-Hexynyl methyl ether, 2.



To a solution of KOH powder (0.5 g, 9.1 mmol, 2 equiv.) in DMSO (4 mL), was added the hex-2-yn-1-ol (0.5 mL, 4.55 mmol, 1 equiv.) and stirred for an hour. Then, MeI was added slowly (0.8 mL, 13 mmol, 2.8 equiv.) with a water bath and the resulting mixture was stirred at room temperature for 5h. Water was poured into the mixture and extracted with Et₂O. The collected organic layer was dried over anhydrous MgSO₄, filtered and evaporated at reduced pressure. The crude was purified over silica gel (hexane/AcOEt) to afford compound 2 as a colorless oil (283 mg, 2.5 mmol, 55%).

¹H NMR (400 MHz, Chloroform-d) δ 4.20 (t, *J* = 2.2 Hz, 2H), 3.40 (s, 3H) 2.08 (tt, *J* = 7.1, 2.2 Hz, 2H), 1.58 – 1.26 (m, 2H), 0.88 (t, *J* = 7.4 Hz, 3H) ppm. **IR** (film)v: 3360, 2940, 2283, 1444, 1020, 1000 cm⁻¹. Data in good agreement with the literature.¹

1-(tert-Butyldimethylsilyloxy)hex-2-yne, 3.



To a solution of hex-2-yn-1-ol (0.5 mL, 4.55 mmol, 1 equiv.) with imidazole (1.55g, 22.7 mmol, 5 equiv.) in anhydrous DCM (0.75 M) was added dropwise a solution of TBSCl (1.03 g, 6.82 mmol, 1.5 equiv.) in DCM (0.76 M) through a canula and stirred 3h. Part of the solvent was removed, portioned with water and extracted with AcOEt. Organic layer was dried over MgSO₄. The crude was filtered, evaporated under vacuum and quickly filtered over alumina (pentane) to afford 3 (947 mg, 4.46 mmol, 98 %).

¹H NMR (400 MHz, Chloroform-d) δ 4.20 (t, *J* = 2.2 Hz, 2H), 2.08 (tt, *J* = 7.1, 2.2 Hz, 2H), 1.58 – 1.26 (m, 2H), 0.88 (t, *J* = 7.4 Hz, 3H), 0.80 (s, 9H), 0.02 (s, 6H) ppm. **IR** (film)v: 2955, 2858, 2322, 1463, 1254, 1081, 837 cm⁻¹. Data in good agreement with the literature.²

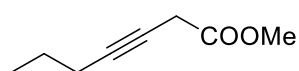
Hex-2-yn-1-yl acetate, 4



To a solution of hex-2-yn-1-ol (0.300 mL, 2.73 mmol, 1 equiv.) in DCM (0.15 M) were added Et₃N (1.5 ml) DMAP (67 mg, 0.55 mmol, 20% mol) acetic anhydride (0.77 mL, 8.19 mmol, 3 equiv.) and stirred for 3 h. Then, the mixture was washed with NaHCO₃ (aq), brine extracted with Et₂O, and dried over MgSO₄. After filtration and quick filtration over alumina (pentane) it afforded 4 (249 mg, 1.77 mmol, 65%).

¹H NMR (400 MHz, Chloroform-d) δ 4.66 (t, *J* = 2.2 Hz, 2H), 2.20 (tt, *J* = 7.1, 2.2 Hz, 2H), 2.09 (s, 3H), 1.59 – 1.45 (m, 2H), 0.97 (t, *J* = 7.4 Hz, 3H) ppm. **IR** (film)v: 2955, 2866, 1719, 1450, 1162, 944 cm⁻¹. Data in good agreement with the literature.³

3-Heptynoic acid methyl ester, 5.



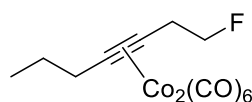
A solution of HNO₃ (aq) (0.038 mL, 0.91 mmol, 20 mol%) with K₂Cr₂O₇ (13 mg, 0.0455 mmol, 1 mol%) was cooled down to 0°C. Then, at maximum stirring speed, NaIO₄ (2.14g, 10 mmol, 2.2 equiv.) was added. A solution of 3-heptyn-1-ol (0.5 mL, 4.55 mmol, 1 equiv.) in ACN (6 mL) was prepared at 0°C and added to the previous solution. The resulting mixture was stirred overnight at room temperature. Then, a solution of NaOH (aq) 1M was poured, extracted with Et₂O and washed with a solution of HCl (aq) 0.1N. The organic layer was dried over anhydrous MgSO₄.

¹H NMR (400 MHz, Chloroform-d) δ: 3.34 (s, 2H), 2.20 (t, J = 7.3 Hz, 2H), 1.54 – 1.50 (m, 2H), 0.97 (t, J = 7.4 Hz, 3H) ppm. **IR** (film) ν: 2964, 2512, 1742, 1443, 1200, 970 cm⁻¹.

The resulting crude of the heptynoic acid was then dissolved in 2 mL of a mixture benzene and methanol (3v:2v) and treated with (trimethylsilyl)diazomethane (3.7 mL, 2.32 mmol, 1.2 equiv). The mixture was left 1h to react. Solvent was evaporated and chromatographed (30% AcOEt in hexanes). It afforded final product 5 (146 mg, 1.04 mmol, 54%).

¹H NMR (400 MHz, Chloroform-d) δ 3.71-3.72 (m, 2H), 3.71 (s, 3H), 2.77 (t, J = 7.3 Hz, 2H), 1.82 – 1.63 (m, 2H), 0.99 (t, J = 7.4 Hz, 3H) ppm. **IR**(film)ν: 2980, 2520, 1719, 1427, 1223 cm⁻¹. Data in good agreement with the literature.⁴

Hexacarbonyl dicobalt complex of 1-fluorohept-3-yne, 44.



To a solution of 3-heptyn-1-ol (110 μL, 1 mmol, 1 equiv.) dissolved in 10 ml of anhydrous DCM at -40°C was added DAST (396 μL, 3 mmol, 3 equiv.). After 4 h, the reaction was left to warm up and dropwise quenched with a solution of 5% Na₂CO₃ (aq). Extraction was performed with DCM and organic layer dried over anhydrous MgSO₄. After filtration, the organic layer (20 mL) was used straight in the next reaction of coordination with octacarbonyl dicobalt (0.342 mg, 1 mmol, 1 equiv.) in 10 ml of hexanes. After 40 min, the crude was chromatographed over silica gel/Et₃N to afford **44** (54 mg 0.13 mmol, 14%).

¹H NMR (400 MHz, Chloroform-d) δ 4.67 (dt, J = 47.0, 5.7 Hz, 2H), 3.21 (dt, J = 24.8, 5.7 Hz, 2H), 2.89 – 2.70 (m, 2H), 1.67 (q, J = 7.7 Hz, 2H), 1.07 (t, J = 7.4 Hz, 3H) ppm. **¹⁹F NMR** (376 MHz, Chloroform-d) δ 14.68 – 14.11 (m, 1F) ppm.

1-Trimethylsilyltetradec-2-yne, 31.

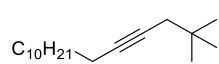


n-Butyl lithium (2.5M, 1.3 mL, 2.66 mmol, 2.4 equiv.) was added dropwise to anhydrous diisopropylamine (0.2 mL, 2.8 mmol, 2.5 equiv.) in freshly distilled Et₂O (3 ml) at -78 °C. The resulting mixture was stirred for 30 min at 0°C and cooled down again to -78°C. A solution of tridecyne (0.2 ml, 1.1 mmol, 1 equiv) in freshly distilled Et₂O (2 mL) was added to the reaction mixture. After 30 min stirring (chloromethyl)trimethylsilane

(0.77 ml, 5.5 mmol, 5 equiv) and hexamethylphosphoramide (1.1 ml, 5.8 mmol, 5.3 equiv) were added. The reaction mixture was stirred at -78°C for 4 h, allowed to warm and stirred overnight at rt. NH_4Cl (aq.) was added to the mixture at 0°C and the aqueous layer was extracted with Et_2O . Organic layer was dried over anhydrous MgSO_4 and concentrated at reduced pressure. Purification over SiO_2 (pentane) afforded the dec-1-yn-1-yltrimethylsilane **31** as an oil (258 mg, 0.97 mmol, 86 %).

^1H NMR (400 MHz, CDCl_3) δ 2.11-2.15 (m, 2H), 1.45-1.50 (m, 2H), 1.42 (t, $J = 2.7$ Hz, 2H), 1.33-1.39 (m, 2H), 1.24-1.30 (m, 14H), 0.88 (t, $J = 6.9$ Hz, 3H), 0.09 (s, 9H) ppm. **^{13}C NMR** (100 MHz, CDCl_3) δ 79.1, 77.4, 32.1, 29.79, 29.76, 29.6, 29.5, 29.4, 29.0, 22.9, 19.1, 14.2, 7.1, -2.0 ppm. **HR-MS** (APCI-LTQ orbitrap) m/z calcd for $[\text{C}_{17}\text{H}_{33}\text{Si}]^+$ 265.2346 found 265.2343. **IR** (film)v: 2937, 2853, 2155, 1707, 1464, 1251, 848.4 cm^{-1} .

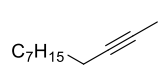
1,1-dimethyl-hexadec-4-yne, **33**.



n -Butyl lithium (2.5M, 0.8 ml, 2.0 mmol, 1.1 equiv) was added dropwise on tridecyne (0.4 ml, 1.75 mmol, 1 equiv) in dry THF (8 ml) at -66°C , followed by hexamethylphosphoramide (4.5 ml, 50 vol%). The resulting mixture was stirred for 30 min and a solution of 1-iodo-2,2-dimethylpropane (0.25 ml, 1.93 mmol, 1.1 equiv) in dry THF (1 ml) was added. Reaction was warmed up to room temperature and heated at 78°C for 2 days. The reaction was quenched with NH_4Cl (aq.), extracted with hexane, dried over MgSO_4 and concentrated at reduced pressure. Purification over SiO_2 (pentane) afforded 1,1-dimethyl-hexadec-4-yne **33** as an oil (306 mg, 1.22 mmol, 70%).

HR-MS (APCI-LTQ orbitrap) m/z calcd for $[\text{C}_{18}\text{H}_{33}]^+$ 249.2577 found 249.2574. **^1H NMR** (400 MHz, CDCl_3) δ 2.14-2.18 (m, 2H), 2.02 (t, $J = 2.4$ Hz, 2H), 1.45-1.51 (m, 2H), 1.35-1.42 (m, 2H), 1.26-1.30 (m, 14H), 0.97 (s, 9H), 0.88 (t, $J = 6.9$ Hz, 3H) ppm. **^{13}C NMR** (100 MHz, CDCl_3) δ 81.8, 78.5, 34.0, 32.1, 31.2, 29.9, 29.8, 29.5, 29.4, 29.3, 29.1, 29.0, 22.9, 18.9, 14.27 ppm. **IR** (film)v: 2930, 1469, 1296, 1200, 982 cm^{-1} .

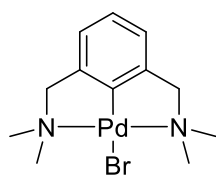
2-Undecyne, **30**.



n -Butyl lithium (1.74M, 1.2 ml, 2.1 mmol, 1.2 equiv) was added dropwise at 0°C on diisopropylamine (0.151 ml, 2.08 mmol, 1.25 equiv) in dry THF (4.5 ml) and the reaction was stirred for 40 min. 1-decyne (0.3 ml, 1.66 mmol, 1 equiv) in dry THF (3 ml) was slowly added, and the mixture was stirred for 2h at 0°C . Iodomethane (0.156 ml, 2.5 mmol, 2.5 equiv) was added and allowed to warm to rt for 4 h. The reaction was quenched with water, extracted with hexane, washed with brine and dried over anhydrous MgSO_4 . After concentration at reduced pressure, purification over SiO_2 (hexanes) afforded undecy-2-yne **30** as a colorless oil (160 mg, 1.05 mmol, 64%).

^1H NMR (400 MHz, CDCl_3) δ 2.14-2.08 (m, 2H), 1.78 (t, $J = 3.0$ Hz, 3H), 1.51-1.43 (m, 2H), 1.39-1.27 (m, 10H), 0.88 (t, $J = 7.0$ Hz, 3H) ppm. **^{13}C NMR** (101 MHz, CDCl_3) δ 79.43, 75.28, 31.85, 29.21, 29.15, 29.1, 28.9, 22.7, 18.7, 14.1, 3.5 ppm. **IR** (film)v: 2952, 1732, 1701, 1437, 1152 cm^{-1} .

Palladium 1,1-(2-bromo-1,3-phenylene)bis(N,N-dimethylmethanamine) complex, **38**.



The 1-bromo-2,6-bis (bromomethyl)benzene (2g, 5,8 mmol, 1 equiv) dissolved in anhydrous DCM was cooled down to 0°C where dimethylamine (10 ml) in anhydrous THF (2M) was added. The cold bath was removed and left under strong stirring at room temperature for 3h30. Water was poured to the mixture, extracted with DCM and washed with brine. The organic layer was dried over anhydrous MgSO₄. Distillation (105°C, 0.2 mmHg) afforded BrC₆H₃(CH₂NMe₂)-2,6 **37** as an oil (832 mg, 53%).

1H NMR (400 MHz, Chloroform-d) δ : 7.34 (d, $J = 7.5$ Hz, 1H), 7.27 (d, $J = 6.0$ Hz, 3H), 3.58 (s, 4H), 2.32 (s, 12H) ppm. Data in good agreement with the literature.⁵

To a solution of Pd₂(dba)₃/CHCl₃ in toluene was added a solution of **37** in toluene under nitrogen and stirred overnight at 60°C. The reaction was then filtered over celite and washed with DCM. After evaporation, the oil was triturated with Et₂O and filtered to afford a white solid **38** (595 mg, 1.6 mmol, 72%). Data in good agreement with the literature.⁶

Trimethyl(oct-2-yn-1-yl)stannane, **35**.



To a solution of 1-chloro-2-octyne (0.559 g, 3.86 mmol, 1 equiv) dissolved in anhydrous THF (6 ml) was added the pincer **38** (0.037 g, 0.097 mmol, 2.5 mol%) and cooled down to 0°C. Then, the hexamethyldithin (0.840 ml, 4.05 mmol, 1.05 equiv.) was added and after 1h, the reaction turned into a dark solution which was stirred for 5 more hours. The solvent was evaporated and the products were purified quickly to afford **35** in 53% yield (flash column chromatography, pentane) to avoid its decomposition. **Warning.** hexamethyldithin and its by products of reaction are toxic such as trimethyltin chloride. Glassware must be cleaned with KOH/EtOH (2g/100 ml) to precipitate the tin.

1H NMR (400 MHz, Chloroform-d) δ : 0.18 (s, 9H, ³J(H-117Sn) = 26.2 Hz, ³J(H-119Sn) = 27.4 Hz), 0.85-0.93 (m, 3H), 1.24-1.38 (m, 4H), 1.40-1.50 (m, 2H), 1.54 (t, 2H, ³J(H-H) = 2.7 Hz), 2.08-2.19 (m, 2H) ppm. **13C NMR**: -9.66 (²J(C-117Sn) = 163.0 Hz, ²J(C-119Sn) = 170.1 Hz), -1.97 (²J(C-117Sn) = 135.8 Hz, ²J(C-119Sn) = 142.6 Hz), 14.03, 19.00, 22.26, 29.29, 31.10, 78.29 (C), 79.53 (C) ppm. Data in good agreement with the literature.⁷

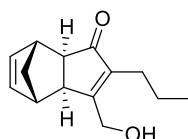
PK reactions procedures

General procedure for alkyne dicobalthexacarbonyl complex formation: To a solution of alkyne 0.5 M in hexane, dicobaltoctacarbonyl (1.1 equiv) was added. The mixture was stirred at room temperature for 2-3 hours under nitrogen depending on alkyne used. The solvent was evaporated at reduced pressure and purified over SiO₂ (hexane/EtOAc gradient if necessary) to afford the complex.

General procedure for PKRs with preformed complex: To a solution of the cobalt complex of alkyne 0.1 M in anhydrous toluene under nitrogen, was added norbornadiene (5 equiv). The mixture was heated at 70 °C overnight. Purification by flash chromatography on SiO₂ (hexane/EtOAc gradient) afforded the Pauson-Khand adducts.

General procedure for PKRs with complex prepared in situ: alkyne 0.1 M is dissolved in toluene and $\text{Co}_2(\text{CO})_8$ (1 equiv) is added. The reaction mixture is stirred under argon over 60 min at rt. Thereafter, norbornadiene (5 equiv) is added and the reaction mixture is heated at 70 °C. After the reaction is completed, the reaction mixture is adsorbed onto a small amount of silica and purified by silica column chromatography (hexane/EtOAc).

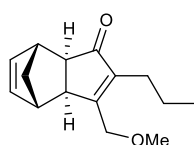
3-(hydroxymethyl)-2-propyl-3a,4,7,7a-tetrahydro-1H-4,7-methanoinden-1-one, **39**.



PKR of hex-2-yn-1-ol **1** was performed according to the general procedure in 0.3 mmol scale with overnight heating affording **39** in 85% combined yield (56 mg, 0.26 mmol) as white amorphous solid. Isomers β -exo-**39** and β -endo-**39** were formed in 10/1 ratio. 3-(hydroxymethyl)-2-propyl-3a,4,7,7a-tetrahydro-1H-4,7-methanoinden-1-one β -exo-**39**.

¹H NMR (500 MHz, CDCl_3) δ 6.30 (dd, $J = 5.5, 3.1$ Hz, 1H), 6.21 (dd, $J = 5.5, 2.9$ Hz, 1H), 4.66 (dd, $J = 14.7, 2.3$ Hz, 1H), 4.51 (dd, $J = 14.7, 4.6$ Hz, 1H), 2.91 (m, 3H), 2.29 (d, $J = 5.1$ Hz, 1H), 2.24 – 2.08 (m, 3H), 1.47 – 1.34 (m, 3H), 1.18 (d, $J = 9.3$ Hz, 1H), 0.88 (t, $J = 7.4$ Hz, 3H). **¹³C NMR** (126 MHz, CDCl_3) δ 209.8, 171.2, 144.7, 138.3, 137.2, 59.6, 52.1, 48.1, 43.6, 42.4, 41.2, 25.1, 21.9, 14.1. **IR** (film) ν : 2970, 1780, 1478, 1254, 1125, 1005 cm^{-1} . **HR-MS (ESI-TOF)** m/z calcd for $[\text{C}_{14}\text{H}_{19}\text{O}_2]^+$ 219.1380, found 219.1381.

3-(methoxymethyl)-2-propyl-3a,4,7,7a-tetrahydro-1H-4,7-methanoinden-1-one, **40**.



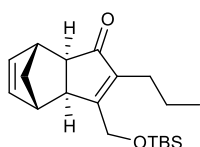
Complexation of **2** was performed according to the general method in 20 mmol scale and 4 h stirring affording **C2** in 95% yield (7.56 g) as an oil. **40** was prepared from previously formed complex according to the general procedure in 0.3 mmol scale with overnight heating affording **40** in 97% combined yield (71 mg, 0.31 mmol) as an oil. Isomers α -exo-**40**, β -exo-**40** and β -endo-**40** were formed in 1/12.5/1.3 ratio. 3-(methoxymethyl)-2-propyl-3a,4,7,7a-tetrahydro-1H-4,7-methanoinden-1-one β -exo-**40**.

¹H NMR (500 MHz, CDCl_3) δ 6.29 (dd, $J = 5.5, 3.1$ Hz, 1H), 6.20 (dd, $J = 5.5, 2.9$ Hz, 1H), 4.34 – 4.25 (m, 2H), 3.41 (s, 3H), 2.91 (br s, 1H), 2.85 (s, 1H), 2.82 (d, $J = 5.1$ Hz, 1H), 2.28 (d, $J = 5.2$ Hz, 1H), 2.25 – 2.08 (m, 2H), 1.47 – 1.35 (m, 3H), 1.17 (d, $J = 9.3$ Hz, 1H), 0.89 (t, $J = 7.4$ Hz, 3H) ppm. **¹³C NMR** (126 MHz, CDCl_3) δ 209.4, 168.9, 145.6, 138.4, 137.1, 69.1, 58.9, 52.1, 48.4, 43.6, 42.4, 41.2, 25.2, 21.8, 14.0 ppm. **HR-MS (ESI-TOF)** m/z calcd for $[\text{C}_{15}\text{H}_{21}\text{O}_2]^+$ 233.1536, found 233.1532. **IR** (film) ν : 2958, 1704, 1455, 1202, 848 cm^{-1} .

2-(methoxymethyl)-3-propyl-3a,4,7,7a-tetrahydro-1H-4,7-methanoinden-1-one α -exo-**40**. **¹H NMR** (500 MHz, CDCl_3) δ 6.27 (dd, $J = 5.4, 3.1$ Hz, 1H), 6.23 (dd, $J = 5.5, 2.9$ Hz, 1H), 4.05 (br s, 2H), 3.33 (s, 3H), 2.95 (br s, 1H), 2.79 (br s, 1H), 2.76 (d, $J = 5.2$ Hz, 1H), 2.70-2.62 (m, 1H), 2.41 – 2.34 (m, 1H), 2.32 (d, $J = 5.2$ Hz, 1H), 1.77 – 1.66 (m, 1H), 1.61 – 1.50 (m, 1H), 1.38 (d, $J = 9.3$ Hz, 1H), 1.22 (d, $J = 9.3$ Hz, 1H), 1.00 (t, $J = 7.4$ Hz, 3H). **¹³C NMR** (126 MHz, CDCl_3) δ 208.5, 180.3, 141.0, 138.0, 137.7, 62.9, 58.5, 52.4, 50.1, 43.5, 42.4, 41.5, 31.9, 21.2, 14.3. **HR-MS (ESI-TOF)** m/z calcd for $[\text{C}_{15}\text{H}_{20}\text{NaO}_2]^+$ 255.1356, found 255.1352.

3-(methoxymethyl)-2-propyl-3a,4,7,7a-tetrahydro-1H-4,7-methanoinden-1-one **β -endo-40**. **^1H NMR** (500 MHz, CDCl_3) δ 5.90 (dd, $J = 5.5, 2.9$ Hz, 1H), 5.74 (dd, $J = 5.5, 2.9$ Hz, 1H), 4.22 (d, $J = 13.8$ Hz, 1H), 4.06 (d, $J = 13.8$ Hz, 1H), 3.41 (s, 3H), 3.36 (t, $J = 4.8$ Hz, 1H), 3.19 (s, 1H), 3.05 (s, 1H), 2.80 (t, $J = 5.2$ Hz, 1H), 2.14 – 2.06 (m, 1H), 2.02 – 1.93 (m, 1H), 1.73 (d, $J = 8.3$ Hz, 1H), 1.60 (d, $J = 8.4$ Hz, 1H), 1.35 – 1.25 (m, 2H), 0.82 (t, $J = 7.4$ Hz, 3H) ppm. **^{13}C NMR** (126 MHz, CDCl_3) δ 209.5, 168.0, 143.9, 132.9, 132.3, 69.7, 59.1, 52.4, 50.0, 46.0, 44.4, 44.0, 24.9, 21.9, 13.9 ppm. **HR-MS** (ESI-TOF) m/z calcd for $[\text{C}_{15}\text{H}_{21}\text{O}_2]^+$ 233.1536, found 233.1546.

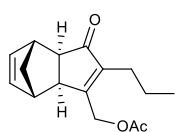
3-((tert-butyldimethylsiloxy)methyl)-2-propyl-3a,4,7,7a-tetrahydro-1H-4,7-methanoinden-1-one, **41**.



Complexation of **3** was performed according to the general method in 3.25 mmol scale and 2 h stirring affording **C3** in quantitative manner (1 g) as a red oil. **41** was prepared from previously formed complex according to the general procedure in 1.01 mmol scale with overnight heating affording **41** in 66% combined yield (220 mg, 0.66 mmol) as an oil. Isomers **α -exo-41**, **β -exo-41** and **β -endo-41** were formed in 1/27/2.5 ratio. 3-((tert-butyldimethylsiloxy)methyl)-2-propyl-3a,4,7,7a-tetrahydro-1H-4,7-methanoinden-1-one **β -exo-41**.

^1H NMR (400 MHz, CDCl_3) δ 6.26 (dd, $J = 3.2$ Hz, $J = 3.2$ Hz, 1H), 6.18 (dd, $J = 2.8$ Hz, $J = 2.8$ Hz, 1H), 4.58 (d, $J = 14.8$ Hz, 1H), 4.48 (d, $J = 15.2$ Hz, 1H), 2.9 (s, 1H), 2.85 (s, 2H), 2.25 (d, $J = 5.2$ Hz, 1H), 2.18 (m, 1H), 2.08 (m, 2H), 1.39 (m, 1H), 1.34 (d, $J = 5.6$ Hz, 1H), 1.17 (d, $J = 9.2$ Hz, 1H), 0.93 (s, 9H), 0.88 (t, $J = 7.6$ Hz, 3H), 0.12 (s, 3H), 0.11 (s, 3H) ppm. **^{13}C NMR** (100 MHz, CDCl_3) δ 209.5, 172, 143.6, 138.3, 137.1, 60.8, 52.6, 48.8, 44.2, 43.2, 41.8, 26.4, 25.8, 22.4, 18.8, 14.7, -4.8, -4.9 ppm. **HR-MS** (ESI-TOF) m/z : Calcd for $[\text{C}_{20}\text{H}_{33}\text{O}_2\text{Si}]^+$ 333.22443, found 333.22463. **HR-MS** (ESI-TOF) m/z calcd for $[\text{C}_{15}\text{H}_{21}\text{O}_2]^+$ 233.1536, found 233.1532. **IR** (film) ν : 2957, 1856, 1670, 1462, 1256, 1091, 839, 715 cm^{-1} .

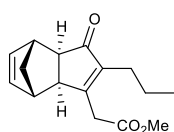
4-propyl-5-acetoxymethyl-tricyclo[5,2,1,0^{2,6}]deca-4,8-dien-3-one, **42**.



Complexation of **4** was performed according to the general method in 2.47 mmol scale and 3 h stirring affording **C4** in quantitative manner (820 mg) as a red oil. Compound **42** was prepared from previously formed complex according to the general procedure in 2.29 mmol scale with overnight heating affording **42** in 60% combined yield (357 mg, 1.37 mmol) as an oil. Isomers **α -exo-42**, **β -exo-42** and **β -endo-42** were formed in 1/30/1.5 ratio. 4-propyl-5-acetoxymethyl-tricyclo[5,2,1,0^{2,6}]deca-4,8-dien-3-one **β -exo-42**.

^1H NMR (400 MHz, CDCl_3) δ 6.25 (dd, $J = 3.1, 3.1$ Hz, 1H), 6.19 (dd, $J = 2.9$ Hz, $J = 2.9$ Hz, 1H), 4.98 (d, $J = 14.3$ Hz, 1H), 4.90 (d, $J = 14.3$ Hz, 1H), 2.91 (s, 1H), 2.78 (s, 1H), 2.72 (d, $J = 5.10$ Hz, 1H), 2.28 (d, $J = 5.10$ Hz, 1H), 2.12 (s, 3H), 2.18 (m, 2H), 1.41 (m, 2H), 1.35 (d, $J = 9.1$ Hz, 1H), 1.14 (d, $J = 9.2$ Hz, 1H), 0.87 (t, $J = 7.6$ Hz, 3H) ppm. **^{13}C NMR** (100 MHz, CDCl_3) δ 209.6, 170.8, 165.8, 147.1, 137.6, 60.9, 52.5, 48.9, 44.0, 42.7, 41.0, 25.5, 22.2, 20.9, 14.4 ppm. **HR-MS** (ESI-TOF) m/z calcd for $[\text{C}_{16}\text{H}_{21}\text{O}_3]^+$ 261.14852, found 261.14845. **IR** (film) ν : 2961, 1746, 1699, 1373, 1223, 1040, 835 cm^{-1} .

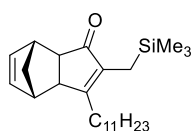
Methyl 2-(1-oxo-2-propyl-3a,4,7,7a-tetrahydro-1H-4,7-methanoinden-3-yl)acetate, 43.



Complexation of **5** was performed according to the general method in 1.79 mmol scale and 2 h stirring affording **C5** in 96% yield (736 mg) as an oil. **43** was prepared from previously formed complex according to the general procedure in 0.76 mmol scale with overnight heating affording **43** in 80% combined yield (159 mg, 0.65 mmol) as an oil. Isomers α -**exo-43**, β -**exo-43** and β -**endo-43** were formed in 1/9/0.5 ratio. Methyl 2-(1-oxo-2-propyl-3a,4,7,7a-tetrahydro-1H-4,7-methanoinden-3-yl)acetate β -**exo-43**.

1H NMR (400 MHz, CDCl₃) δ 6.20 (dd, J = 8.5, 3.0 Hz), 6.25 (dd, J = 5.4, 3.1 Hz, 2H), 3.50 (d, J = 14.8 Hz, 1H), 3.36 (d, J = 15.3 Hz, 1H), 2.92 (s, 1H), 2.77 (d, J = 5.2 Hz, 1H), 2.74 (s, 1H), 2.30 (d, J = 5.2 Hz, 1H), 2.18 – 2.10 (m, 2H), 1.49 – 1.37 (m, 2H), 1.37 (d, J = 11.1 Hz, 1H), 1.17 (d, J = 9.3 Hz, 1H), 0.89 (t, J = 7.4 Hz, 3H). **13C NMR** (100 MHz, CDCl₃) δ 209, 170.3, 165.1, 148.3, 138.6, 138.2, 53.1, 53.0, 51.1, 44.1, 42.7, 42.0, 35.9, 26.2, 22.2, 14.8. **HR-MS** (ESI-TOF) m/z calcd for [C₁₆H₂₁O₃]⁺ 261.1484, found 261.1485. **IR** (film) ν : 2960, 2870, 1741, 1697, 1435, 1325, 1014, 714 cm⁻¹.

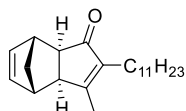
2-((trimethylsilyl)methyl)-3-undecyl-3a,4,7,7a-tetrahydro-1H-4,7-methanoinden-1-one, 51.



Complexation of **31** was performed according to the general method in 0.57 mmol scale, 3 h stirring and quick purification over SiO₂ (pentane), affording **C31** in quantitative yield (297 mg) as a red oil. To a solution of norbornadiene (5.9 mmol, 0.6 ml) in anhydrous toluene (2 ml) at 100°C was added drop-wise a solution of dicobalt complex **C31** in anhydrous toluene (3ml) at a rate of 1.5 ml/hour. The reaction mixture was stirred for 2 h, evaporated and purified over SiO₂ (Hexane/EtOAc) to afford a yellow oil affording **51** in 80% combined yield (182 mg, 0.47 mmol). Isomers α -**exo-51** and α -**endo-51** were formed in 24/1 ratio. 2-((trimethylsilyl)methyl)-3-undecyl-3a,4,7,7a-tetrahydro-1H-4,7-methanoinden-1-one α -**exo-51**.

1H NMR (400 MHz, CDCl₃) δ : 6.25 (dd, J = 5.3, 3.0 Hz, 1H), 6.20 (dd, J = 5.5, 2.9 Hz, 1H), 2.87 (s, 1H), 2.71 (s, 1H), 2.67 (d, J = 5.2 Hz, 1H), 2.46-2.39 (m, 1H), 2.25-2.18 (m, 1H), 2.21 (d, J = 5.0 Hz, 1H), 1.67 (d, J = 13.4 Hz, 1H), 1.57-1.64 (m, 1H), 1.54 (d, J = 13.4 Hz, 1H), 1.50-1.39 (m, 2H), 1.35 (d, J = 9.3 Hz, 1H), 1.17-1.14 (m, 14H), 1.11 (d, J = 9.1 Hz, 1H), 0.88 (t, J = 6.8 Hz, 3H), -0.01 (s, 9H) ppm. **13C NMR** (100 MHz, CDCl₃) δ 209.6, 171.4, 143.4, 138.6, 138.2, 52.5, 49.8, 43.9, 42.77, 42.02, 32.56, 30.60, 30.6, 30.28, 30.26, 30.19, 30.12, 29.99, 28.0, 23.3, 14.8, 14.2, -0.2. **HR-MS** (ESI-TOF) m/z calcd for C₂₅H₄₃OSi(M+H⁺) 387.3078, found 387.3108. **IR** (film) ν : 2917, 1693, 1578, 842 cm⁻¹.

2-((trimethylsilyl)methyl)-3-undecyl-3a,4,7,7a-tetrahydro-1H-4,7-methanoinden-1-one, 52.

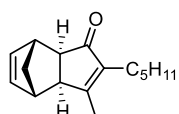


Complexation of **28** was performed according to the general method in 0.57 mmol scale, 3 h stirring and quick purification over SiO₂ (pentane), affording **C28** in quantitative yield (297 mg) as a red oil. To a solution of norbornadiene (5.9 mmol, 0.6 ml) in anhydrous toluene (2 ml) at 100°C was added drop-wise a solution of dicobalt complex **C28** in anhydrous toluene (3ml) at a rate of 1.5 ml/hour. The reaction mixture was stirred for 2 h, evaporated and purified over SiO₂ (Hexane/EtOAc) to afford a yellow oil affording **52** in 80% combined yield (182 mg, 0.47 mmol).

Isomers α -*exo*-**52** and α -*endo*-**52** were formed in 24/1 ratio. 2-((trimethylsilyl)methyl)-3-undecyl-3a,4,7,7a-tetrahydro-1H-4,7-methanoinden-1-one α -*exo*-**52**.

¹H NMR (400 MHz, CDCl₃) δ : 6.25 (dd, J = 5.3, 3.0 Hz, 1H), 6.20 (dd, J = 5.5, 2.9 Hz, 1H), 2.87 (s, 1H), 2.71 (s, 1H), 2.67 (d, J = 5.2 Hz, 1H), 2.46-2.39 (m, 1H), 2.25-2.18 (m, 1H), 2.21 (d, J = 5.0 Hz, 1H), 1.67 (d, J = 13.4 Hz, 1H), 1.57-1.64 (m, 1H), 1.54 (d, J = 13.4 Hz, 1H), 1.50-1.39 (m, 2H), 1.35 (d, J = 9.3 Hz, 1H), 1.17-1.14 (m, 14H), 1.11 (d, J = 9.1 Hz, 1H), 0.88 (t, J = 6.8 Hz, 3H), -0.01 (s, 9H) ppm. **¹³C NMR** (100 MHz, CDCl₃) δ 209.6, 171.4, 143.4, 138.6, 138.2, 52.5, 49.8, 43.9, 42.77, 42.02, 32.56, 30.60, 30.6, 30.28, 30.26, 30.19, 30.12, 29.99, 28.0, 23.3, 14.8, 14.2, -0.2. **HR-MS** (ESI-TOF) m/z calcd for C₂₅H₄₃OSi(M+H⁺) 387.3078, found 387.3108. **IR** (film) ν : 2917, 1693, 1578, 842 cm⁻¹.

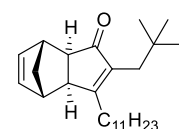
2-ethyl-3-methyl-3a,4,7,7a-tetrahydro-1H-4,7-methanoinden-1-one, **49**.



Complexation of **35** was performed according to the general method in 0.77 mmol scale, 1 equiv of dicobaltoctacarbonyl and 2 h stirring affording **C35** in toluene. After complexation of the reaction, 5 equiv of NBD (3.85 mmol, 400 μ L) were added and heated up to 65°C. **49** was obtained in 90% combined yield (160 mg, 0.69 mmol) as an oil. Isomers α -*exo*-**49** and α -*endo*-**49** and were formed in 25/1 ratio. 2-ethyl-3-methyl-3a,4,7,7a-tetrahydro-1H-4,7-methanoinden-1-one, α -*exo*-**49**.

¹H NMR (400 MHz, Chloroform-*d*) δ 6.25 (dd, J = 5.5, 3.0 Hz, 1H), 6.21 (dd, J = 5.6, 2.9 Hz, 1H), 2.89 (s, 1H), 2.74 (s, 1H), 2.56 (d, J = 4.9 Hz, 1H), 2.24 (d, J = 5.2 Hz, 1H), 2.21 – 2.04 (m, 2H), 2.02 (s, 2H), 1.61 (s, 1H), 1.43 – 1.22 (m, 4H), 1.14 (d, J = 9.2 Hz, 1H), 0.87 (t, J = 7.0 Hz, 2H) ppm. **¹³C NMR** (100 MHz, CDCl₃) δ 209.3, 170.8, 145.2, 138.0, 137.6, 52.3, 52.0, 43.3, 42.1, 41.3, 31.9, 29.7, 23.2, 22.7, 15.5, 13.8 ppm. **IR** (film) ν : 2917, 1693, 1578, 842 cm⁻¹. Data collected are in good agreement with the literature.⁸

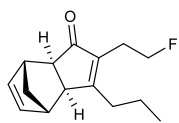
2-neopentyl-3-undecyl-3a,4,7,7a-tetrahydro-1H-4,7-methanoinden-1-one, **56**.



Complexation of **33** was performed according to the general method in 0.69 mmol scale, 2 h stirring and quick purification over SiO₂ (pentane), affording **C14** in quantitative yield (305 mg) as a red oil. **56** was prepared from previously formed complex according to the general procedure in 1.31 mmol scale with overnight heating at 100°C affording **56** in 79% combined yield (388 mg, 1.05 mmol) as a yellow oil. Isomers α -*exo*-**56** and α -*endo*-**56** and were formed in 32/1 ratio. 2-neopentyl-3-undecyl-3a,4,7,7a-tetrahydro-1H-4,7-methanoinden-1-one α -*exo*-**56**.

HRMS (ESI-TOF) m/z calcd for [C₂₆H₄₃O]⁺ 371.08, found 371.3310 (Δ =0.48 ppm). **¹H NMR** (400 MHz, CDCl₃) δ 6.26 (dd, J = 5.6, 3.0 Hz, 1H), 6.21 (dd, J = 5.6, 2.9 Hz, 1H), 2.89 (s, 1H), 2.74 (s, 1H), 2.71 (d, J = 5.3 Hz, 1H), 2.60-2.53 (m, 1H), 2.29-2.22 (m, 1H), 2.26 (d, J = 5.3 Hz, 1H), 2.16 (d, J = 13.1 Hz, 1H), 2.02 (d, J = 13.1 Hz, 1H), 1.45 (m, 1H), 1.45 (m, 1H), 1.33 (d, J = 9.2 Hz, 1H), 1.24 (m, 16H), 1.23 (d, J = 9.2 Hz, 1H), 0.87 (m, 12H). **¹³C NMR** (101 MHz, CDCl₃) δ 209.9, 177.0, 143.2, 138.0, 137.8, 52.0, 49.1, 43.6, 42.4, 41.6, 36.4, 32.0, 30.5, 30.1, 30.0, 29.76, 29.75, 29.67, 29.58, 29.49, 29.47, 27.5, 22.8, 14.3. **IR** (film) ν : 2954, 1620, 1451, 842, 742, 544 cm⁻¹.

2-fluoroethyl-3-propyl-3a,4,7,7a-tetrahydro-1H-4,7-methanoinden-1-one, 45.



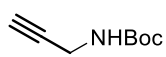
Complexation of **24** was performed according to the general method in 1 mmol scale, 1 equiv of dicobaltoctacarbonyl and 2 h stirring affording **C24** in toluene.

After complexation of the reaction, 5 equiv. of NBD (5 mmol, 260 μ L) were added and heated up to 65°C. **45** was obtained in 10% combined yield (20 mg) as an oil. A mixture of isomers was formed in 25/1 ratio. The determination of which isomer was formed could not be established.

¹H NMR (400 MHz, Chloroform-*d*) δ 6.25 (dd, *J* = 5.5, 3.0 Hz, 1H), 6.21 (dd, *J* = 5.6, 2.9 Hz, 1H), 2.89 (s, 1H), 2.74 (s, 1H), 2.56 (d, *J* = 4.9 Hz, 1H), 2.24 (d, *J* = 5.2 Hz, 1H), 2.21 – 2.04 (m, 2H), 2.02 (s, 2H), 1.61 (s, 1H), 1.43 – 1.22 (m, 4H), 1.14 (d, *J* = 9.2 Hz, 1H), 0.87 (t, *J* = 7.0 Hz, 2H). **¹³C NMR** (100 MHz, CDCl₃) δ 209.3, 170.8, 145.2, 138.0, 137.6, 52.3, 52.0, 43.3, 42.1, 41.3, 31.9, 29.7, 23.2, 22.7, 15.5, 13.8. **¹⁹F NMR** 14.13 (m, 1F). **HRMS** (ESI-TOF) *m/z* calcd for [C₁₅H₂₀O₁F₁]⁺ 235.1493, found 235.1493 (Δ =0.08 ppm).

Chapter III

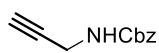
Tert-butyl-prop-2-ynylcarbamate, 58.



Di-*tert*-butyl-dicarbonate (10 g, 47 mmol, 1 equiv.) was dissolved in DCM (0.2 M) and cooled down to 0°C. 3-amino-1-propyne (2.6 g, 47 mmol, 1 equiv.) was added over a period of 30 min, after warmed to room temperature and stirred overnight. The organic layer was extracted successively with HCl (2 N), NaOH (2N) and saturated solution of NaHCO₃ and extracted with DCM. The combined organic layers then were dried over MgSO₄ and the solvent concentrated until an oily residue was observed. *n*-Pentane was added and after standing in the refrigerator for 12 h, the precipitate of **58** was collected by filtration to afford 6 g (82%) as white needles.

¹H NMR (CDCl₃, 400 MHz) δ : 4.69 (br s, 1H, NH), 3.92 (dd, *J*=5.0, 2.3 Hz, 2H, CH₂), 2.21 (t, 1H, *J*=2.3 Hz, CH), 1.45 (s, 9H, 3CH₃). **¹³C NMR** (101 MHz, CDCl₃) δ : 155.2 (CO), 80.12 (CH), 80.06 (Cq), 71.2 (CH₂), 28.3 (3CH₃). Data analysis in good agreement with the literature.⁹

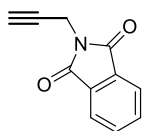
Benzyl prop-2-yn-1-ylcarbamate, 59.



The propargyl amine (0.2 mL, 3.12 mmol, 1 equiv.) was dissolved in THF (0.5M), then Et₃N (0.45 mL, 6.24 mmol, 2 equiv) was added. Benzyl chloroformate (580 μ L, 4.06 mmol, 1.3 equiv.) was then added dropwise at 0°C. After stirring for 1 h at 0 °C and 12 h at room temperature, the mixture was diluted with water and diethyl ether. The phases were separated and the aqueous layer was extracted with diethyl ether (3 x 100 mL). The combined organic phases were dried MgSO₄. The solvent was then removed under reduced pressure and the crude was purified by flash chromatography on silica gel using mixtures of hexane/ethyl acetate, affording **59** in 66% yield as white solid, 390 mg.

¹H NMR (400 MHz, CDCl₃, 60 °C): δ = 7.36-7.29 (m, 5H), 5.14 (s, 2H), 4.85 (s, 1H), 3.99 (dd, J = 5.7, 2.6 Hz, 2H), 2.23 ppm (t, J = 2.6 Hz, 1H). **¹³C NMR** (100 MHz, CDCl₃): δ = 155.8, 136.5, 128.5, 128.2, 128.1, 79.7, 71.6, 67.2, 31.1 ppm. Data analysis in good agreement with the literature.¹⁰

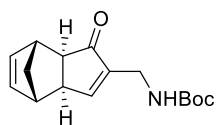
2-(prop-2-yn-1-yl)isoindoline-1,3-dione, 60.



To a solution of phthalimide anhydride (1.2 g, 8.08 mmol, 1 equiv.) dissolved in a mixture of toluene/xylene (0.2M, 1v/1v), was slowly added by a syringe pump over 3h, propargyl amine (0.5 ml, 8.08 mmol, 1 equiv.) dissolved in 2 mL of toluene. Mixture became salty. After complete addition, it was heated up under reflux condition at 110°C overnight and the next day a yellow mixture with black deposits was afforded. Solvent was removed and crude chromatographed to afford 62% of the final product **60** as white solid, 928 mg.

¹H NMR (CDCl₃, 400 MHz) δ = 7.91-7.87 (m, 2H, 2CH), 7.78-7.73 (m, 2H, 2CH), 4.46 (d, J = 2.4 Hz, 2H, CH₂), 2.26 (t, J = 2.4 Hz, 1H, CH). **¹³C NMR** (CDCl₃, 90 MHz) δ = 166.8 (2CO), 134.1 (2Cq+2CH), 131.9(2CH), 123.5 (Cq), 71.4 (CH), 26.9 (CH₂). Data analysis in good agreement with the literature.¹¹

Tert-Butyl(((3aR*,4S*,7R*,7aR*)-1-oxo-3a,4,7,7a-tetrahydro-1*H*-4,7-methanoinden-2-yl)methyl)carbamate, 61.



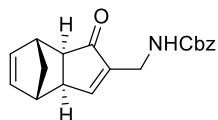
In a round bottom flask equipped with a magnetic stirrer Co₂(CO)₈ (148 mg, 0.58 mmol, 1 equiv.) was put under nitrogen and dissolved in 7 ml of anhydrous toluene. A solution of PPh₃ (153 mg, 0.58 mmol, 1 equiv.) in anhydrous toluene (6 mL) were then added *via* canula. The system was protected from the light and stirred for 45 minutes at room temperature. *N*-Boc-propargylamine **58** (67 mg, 0.58 mmol, 1 eq.) was added to the crude complex and the reaction was heated up to 65 °C. Vacuum cycles were performed in order to displace the CO ligand. The solution was stirred until the complete consumption of the starting material was observed by TLC; the crude complex of the *N*-Boc-propargylamine triphenylphosphine pentacarbonyldicobalt was then directly used in the following reaction without purification.

In Büchi pressure reactor, was dissolved *N*-Boc-propargylamine (0.8 g, 5 mmol, 1 equiv.) in 10 mL of anhydrous toluene. Norbornadiene (2.6 mL, 25 mmol, 5 equiv.) and *N*-Boc-propargylamine triphenylphosphine pentacarbonyldicobalt (100 mg, 0.15 mmol, 0.05 equiv.) dissolved in 10 mL of toluene were added. The reactor was loaded with 2 bar of CO and heated up to 80 °C for 48h. The reactor was then purged and the system was stirred in the open air to oxidize the rests of cobalt, filtered on silica and the solvent was removed. The crude was then purified by flash chromatography using a gradient mixture of AcOEt/Hexanes. The product was obtained as a white solid (1.1 g, 79%).

¹H NMR (400 MHz, CDCl₃) δ = 1.21 (d, J = 9.5 Hz, 1H), 1.39 (d, J = 9.4 Hz, 1H), 1.43 (s, 9H), 2.32 (dt, J = 5.1 and 1.3 Hz, 1H), 2.71 (m, 1H), 2.76 (m, 1H), 2.92 (m, 1H), 3.81-3.96 (m, 2H), 5.02 (br s, 1H), 6.21 (dd, J = 5.6 and 3.0 Hz, 1H), 6.29 (dd, J = 5.6 and 3.1 Hz, 1H), 7.35 (s, 1H) ppm. **¹³C NMR** (100 MHz, CDCl₃) δ = 28.5 (CH₃), 36.3 (CH₂), 41.3 (CH₂), 43.0 (CH), 43.8 (CH), 48.0 (CH), 53.0 (CH), 79.6

(C), 137.2 (CH), 138.6 (CH), 147.1 (C), 155.9 (C), 160.8 (CH), 209.5 (C) ppm. **HRMS** (ESI) calculated for $C_{16}H_{22}NO_3$ 276.1600, found 276.1600 $[M+H]^+$.

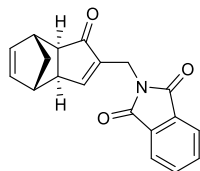
Benzyl (((3aR, 4S, 7R, 7aR)-1-oxo-3a,4,7,7a-tetrahydro-1H-4,7-methanoinden-2-yl)methyl)carbamate, 62.



Complexation of **59** was performed according to the general method in 2.05 mmol scale dissolved in 12 ml of hexane and stirred 1h30 to afford the complex in quantitative yield after quick filtration over SiO_2 (0.97g) as an oil. The freshly formed complex was then reacted with NBD (1.02 mL, 10.08 mmol, 5 equiv.) in 0.2M of toluene and heated up at 80°C overnight. Solvent was removed and purification done to afford 312 mg of a white solid in 50 % yield, ratio *exo/endo* 17:1.

¹H NMR (400 MHz, $CDCl_3$) δ =1.16 (d, J = 9.2 Hz, CH_2 , 1H), 1.34 (d, J = 9.0 Hz, CH_2 , 1H), 2.28 (d, J = 4.9 Hz, CH, 1H), 2.66 (s, CH, 1H), 2.72 (s, CH, 1H), 3.93 (d, J = 5.9 Hz, CH_2 , 2H), 5.02 – 5.11 (m, CH_2 , 1H), 5.44 (bs, NH, 1H), 6.16 – 6.18 (dd, J = 5.5, 2.9 Hz, CH, 1H), 6.25 – 6.27 (dd, J = 5.4, 3.1 Hz, CH, 1H). **¹³C NMR** (101 MHz, $CDCl_3$) δ : 36.69 (CH_2), 41.26 (CH_2), 41.26 (CH), 42.93 (CH), 43.68 (CH), 48.02 (CH), 52.97 (CH), 66.83 (CH_2), 128.10 – 128.23 (CH), 128.55 (CH), 137.10 (CH), 138.54 (CH), 160.84 (CO), 209.24 (CO). **HR-MS** (ESI) calculated for $C_{19}H_{20}NO_3$ 310.1443 found 310.1445 $[M+H]^+$.

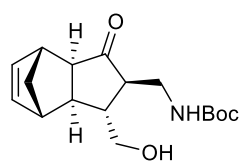
2-(((3aR, 4S, 7R, 7aR)-1-oxo-3a,4,7,7a-tetrahydro-1H-4,7-methanoinden-2-yl)methyl)isoindoline-1,3-dione, 63.



Complexation of **60** was performed according to the general method in 1 mmol scale dissolved in 12 ml of mixture DCM/hexane (5v/1v) and stirred 1h30 to afford red complex in 95% yield (450g) as an oil. The freshly formed complex was then reacted with NBD (0.5 ml, 4.75 mmol, 5 equiv.) in 0.2M of toluene and heated up at 80°C overnight. Solvent was removed and purification done to afford 232 mg of a white solid **63** in 80 % yield, ratio *exo/endo* 25:1.

Mp: 112°C. **¹H NMR** (400 MHz, Chloroform-d) δ = 7.88 (dd, J = 5.5, 3.0 Hz, 2H), 7.74 (dd, J = 5.4, 3.1 Hz, 2H), 7.20 (dt, J = 2.8, 1.5 Hz, 1H), 6.26 (dd, J = 5.6, 3.1 Hz, 1H), 6.20 (dd, J = 5.6, 3.0 Hz, 1H), 4.48 (t, J = 1.7 Hz, 3H), 2.93 (s, 1H), 2.74 (s, 0H), 2.66 (s, 1H), 2.35 (dt, J = 5.0, 1.3 Hz, 1H), 1.39 (dt, J = 9.5, 1.5 Hz, 2H), 1.26 (d, J = 9.4 Hz, 2H). **¹³C NMR** (101 MHz, Chloroform-d) δ = 207.92 (CO), 168.17 (C), 160.64 (CH), 144.99 (2CO), 138.83 (CH), 137.59 (CH), 134.56 (2CH), 132.46 (C), 123.91 (2CH), 53.43 (CH), 48.33 (CH), 44.13 (CH), 43.36 (CH), 41.80 (CH_2), 33.83 (CH_2). **HR-MS** (ESI) calculated for $C_{19}H_{16}NO_3$ 306.1125, found 306.1122 $[M+H]^+$.

Tert-butyl (((1R, 2R, 3aR, 4R, 7S, 7aR)-1-(hydroxymethyl)-3-oxo-2,3,3a,4,7,7a-hexahydro-1H-4,7-methanoinden-2-yl)methyl)carbamate, 64.

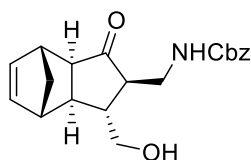


In a quartz flask, starting material **61** (296 mg, 1.08 mmol, 1 equiv.) and benzophenone (196 mg, 1.08 mmol, 1 equiv.) were dissolved in anhydrous methanol (0.03M) then the all mixture was degassed using freeze pump thaw method. The flask was irradiated at 350 nm in a Rayonet[®] photochemical

reactor for 3 hours. After this time, the solvent was removed under reduced pressure and the crude was purified by flash chromatography on silica gel ethyl acetate/hexane solvents affording 150mg of pur product **64**, 45% yield.

¹H NMR (400 MHz, CDCl₃) δ = 1.06 (d, J = 9.2 Hz, 1H), 1.26 (t, J = 7.2 Hz, 1H), 1.41 (m, 11H), 1.70 (m, 1H), 1.99 (t, J = 8.1 Hz, 1H), 2.34 (dt, J = 9.3 and 1.5 Hz, 1H), 2.67 (m, 1H), 2.77 (s, 1H), 3.16 (s, 1H), 3.34-3.48 (m, 2H), 3.73 (dd, J = 7.2 and 10.8 Hz, 1H), 3.96 (dd, J = 4.8 and 10.8 Hz, 1H), 6.15 (dd, J = 3.2 and 5.6 Hz, 1H), 6.20 (dd, J = 2.8 and 5.6 Hz, 1H) ppm. **¹³C NMR** (100 MHz, CDCl₃) δ = 28.5 (CH₃), 38.5 (CH₂), 43.3 (CH), 44.5 (CH), 45.0 (CH₂), 45.1 (CH), 47.6 (CH), 54.3 (CH), 58.6 (CH), 66.3 (CH₂), 80.0 (C), 137.6 (CH), 138.8 (CH), 157.3 (C), 218.1 (C) ppm. **HR-MS** (ESI) calculated for C₁₇H₂₆NO₄ 308.18563, found 308.18555 [M+H]⁺.

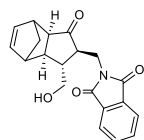
Benzyl (((1R, 2R, 3aR, 4R, 7S, 7aR)-1-(hydroxymethyl)-3-oxo-2,3,3a,4,7,7a-hexahydro-1H-4,7-methanoinden-2-yl)methyl)carbamate **65.**



In a quartz flask, starting material **62** (173 mg, 0.56 mmol, 1 equiv.) and benzophenone (61 mg, 0.56 mmol, 1 equiv.) were dissolved in anhydrous methanol (0.03M) then the all mixture was degassed using freeze pump thaw method. The flask was irradiated at 350 nm in a Rayonet[®] photochemical reactor for 3 hours and solvent removed under reduced pressure. The crude was purified by flash chromatography on silica gel using as eluent a mixture of ethyl acetate/hexane to afford **65** in 40% yield of a colorless oil, 76 mg.

¹H NMR (400 MHz, CDCl₃) : δ 0.97 (d, J = 9.2 Hz, CH₂, 1H), 1.37 (d, J = 9.2 Hz, CH₂, 1H), 1.57 – 1.66 (m, CH, 1H), 1.95 – 2.00 (m, CH exo, 1H), 2.32 (d, J = 9.7 Hz, CH, 1H), 2.68 (d, J = 11.8 Hz, CH, 1H), 2.71 (s, CH, 1H), 3.13 (s, CH, 1H), 3.40 – 3.45 (m, CH₂, 1H), 3.49 – 3.55 (m, CH₂, 1H), 3.71 (dd, J = 10.6 Hz, 7.3 Hz, CH₂, 1H), 3.93 (dd, J = 10.6 Hz, 4.2 Hz, CH₂, 1H), 5.02 (d, J = 12.3 Hz, CH₂, 1H), 5.12 (d, J = 12.2 Hz, CH₂, 1H), 5.43 (bs, NH, 1H), 6.13 (dd, J = 5.7 Hz, 2.9 Hz, CH, 1H), 6.18 (dd, J = 5.7 Hz, 3.0 Hz, CH, 1H), 7.32 (s, CH, 5H). **¹³C NMR** (101 MHz, CDCl₃) : δ 38.89 (CH₂), 43.29 (CH), 44.28 (CH), 45.01 (CH), 45.08 (CH₂), 47.50 (CH), 66.04 (CH₂), 67.08 (CH₂), 128.36 (CH), 137.59 (CH), 138.71 (CH), 157.63 (CO), 217.68 (C). **HRMS** (ESI) calculated for C₂₀H₂₄NO₄ 342.1705, found 342.1711 [M+H]⁺.

2-(((1R, 2R)-1-(hydromethyl)-3-oxo-2, 3, 3a,4,7,7a-hexahydro-1H-4,7-methanoinden-2-yl)isoindoline-1,3-dione, **66.**

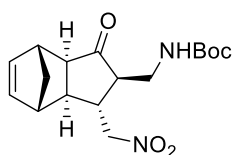


In a quartz flask, starting material **63** (120 mg, 0.39 mmol, 1 equiv.) and benzophenone (143 mg, 0.8 mmol, 2 equiv.) were dissolved in anhydrous methanol (20 mL) then the all mixture was degassed using freeze pump thaw method. The flask was irradiated at 350 nm in a Rayonet[®] photochemical reactor for 4 hours and solvent removed under reduced pressure. The crude was purified by flash chromatography on silica gel using 30% to 40% of ethyl acetate in hexane to afford **66** in 31% yield of a colorless oil, 41 mg, (eluent 40% ethyl acetate in hexane).

¹H NMR (400 MHz, Chloroform-d) δ 7.80-7.82 (m, CH, 2H), 7.68-7.70 (m, CH, 2H), 6.16-6.18 (dd, J = 5.7, 3.0 Hz, CH, 1H), 6.11-6.13 (dd, J = 5.7, 3.0 Hz, CH, 1H), 4.07-4.13 (m, CH₂, 1H), 3.65-3.75 (m, 2CH₂, 3H), 3.15 (s, CH, 1H), 3.04-3.16 (m, CH, 1H), 2.78 (s, CH, 1H), 2.32-2.35 (d, J =9.1 Hz, CH

,1H), 2.01-2.05 (m, CH, 1H), 1.73-1.80 (m, CH, 1H), 1.42-1.46 (m, CH₂, 1H), 1.12-1.14 (m, CH₂, 1H). **¹³C NMR** (101 MHz, cdcl₃) δ 215.91 (CO), 168.65 (2CO), 138.51 (CH), 137.51 (CH), 134.12 (2CH), 132.08 (CO), 123.43 (2CH), 65.68 (CH₂), 54.47(CH), 54.18 (CH), 47.81 (CH), 47.09(CH), 45.58 (CH), 45.15 (CH₂), 43.76 (CH), 37.34 (CH₂). **HRMS** (ESI) calculated for C₂₀H₂₀NO₄ 338.1392, found 338.1396 [M+H]⁺.

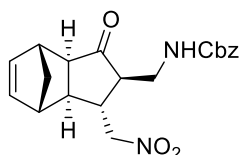
Tert-butyl(((1R*,2R*,3aR*,4R*,7S*,7aR*)-1-(nitromethyl)-3-oxo-2,3,3a,4,7,7a-hexahydro-1H-4,7-methanoinden-2-yl)methyl)carbamate, 67.



Compound **61** (203 mg, 0.74 mmol, 1 eq.) was dissolved in 1 mL of nitromethane in a round bottom flask with a magnetic stirrer. DBU (0.11 mL, 0.02 mmol, 1.1 eq.) was then added and the reaction was irradiated at 50 Watt, 70°C for 40 minutes. The solvent was then removed under reduced pressure and the crude was purified by chromatography on silica gel using mixtures of hexanes/AcOEt of increasing polarities to isolate 150 mg of final product **67** as a yellow oil in 60%.

¹H NMR (400 MHz, CDCl₃) δ = 1.05 (d, *J* = 9.4 Hz, 1H), 1.40-1.48 (m, 10H), 2.25 (m, 2H), 2.43 (m, 1H), 2.61 (m, 1H), 2.80 (s, 1H), 3.19 (br s, 1H), 3.38 (m, 2H), 4.60 (dd, *J* = 12.0 and 8.0 Hz, 1H), 4.84 (dd, *J* = 12.0 and 3.0 Hz, 1H), 4.98 (m, 1H), 6.18 (dq, *J* = 5.7 and 2.9 Hz, 2H) ppm. **¹³C NMR** (100 MHz, CDCl₃) δ = 28.4 (CH₃), 37.0 (CH₂), 40.3 (CH), 44.6 (CH), 44.8 (CH₂), 44.9 (CH), 47.5 (CH), 54.5 (CH), 57.1 (CH), 78.8 (CH₂), 79.9 (C), 137.7 (CH), 138.6 (CH), 156.6 (C), 215.1 (C) ppm. **HR-MS** (ESI) calculated for C₁₇H₂₅N₂O₅ 337.1763, found 337.1765 [M+H]⁺.

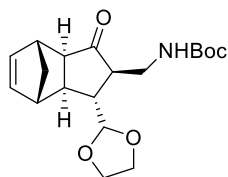
Benzyl (((1R*,2R*,3aR*,4R*,7S*,7aR*)-1-(nitromethyl)-3-oxo-2,3,3a,4,7,7a-hexahydro-1H-4,7-methanoinden-2-yl)methyl)carbamate, 68.



Compound **62** (410 mg, 1.3 mmol, 1 eq.) was dissolved in 2.5 mL of nitromethane in a round bottom flask with a magnetic stirrer. TBAF·3H₂O (418 mg, 1.3 mmol, 1 eq.) were added, and the reaction was allowed to react overnight at 60°C. The solvent was then removed under reduced pressure and the crude was purified by chromatography on silica gel using mixtures of hexanes/AcOEt of increasing polarities to isolate 180 mg of final product **68** as a yellow oil in 40% yield.

¹H NMR (400 MHz, CDCl₃) δ = 1.05 (d, *J* = 9.4 Hz, 1H), 1.40-1.48 (m, 10H), 2.25 (m, 2H), 2.43 (m, 1H), 2.61 (m, 1H), 2.80 (s, 1H), 3.19 (br s, 1H), 3.38 (m, 2H), 4.60 (dd, *J* = 12.0 and 8.0 Hz, 1H), 4.84 (dd, *J* = 12.0 and 3.0 Hz, 1H), 4.98 (m, 1H), 6.18 (dq, *J* = 5.7 and 2.9 Hz, 2H) ppm. **¹³C NMR** (100 MHz, CDCl₃) δ = 28.4 (CH₃), 37.0 (CH₂), 40.3 (CH), 44.6 (CH), 44.8 (CH₂), 44.9 (CH), 47.5 (CH), 54.5 (CH), 57.1 (CH), 78.8 (CH₂), 79.9 (C), 137.7 (CH), 138.6 (CH), 156.6 (C), 215.1 (C) ppm. **HR-MS** (ESI) calculated for C₁₇H₂₃N₂O₅ 371.1607, found 371.1612 [M+H]⁺.

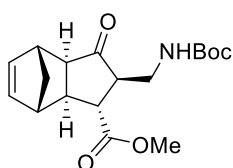
***Tert*-Butyl (((1*R**,2*R**,3*aR**,4*R**,7*S**,7*aR**)-1-(1,3-dioxolan-2-yl)-3-oxo-2,3,3*a*,4,7,7*a*-hexahydro-1*H*-4,7-methanoinden-2-yl)methyl)carbamate, **69**.**



Compound **61** (110 mg, 0.4 mmol, 1 eq.) was dissolved in 12 mL of 1,3-dioxolane, benzophenone (73 mg, 0.4 mmol, 1 equiv.) was then added to the reaction. The system was degassed during 40 minutes and irradiated at 350 nm during 3 hours. The solvent was evaporated and chromatographed to afford compound **69** in 37%.

¹H NMR (400 MHz, CDCl₃) : δ 1.05 (d, *J* = 9.3 Hz, CH₂, 1H), 1.40 (s, CH₃, 9H), 1.40 (m, CH₂, 1H), 1.82 – 1.87 (m, CH, 1H), 2.18 – 2.23 (m, CH, 1H), 2.30 (d, *J* = 9.7 Hz, CH, 1H), 2.71 – 2.76 (dt, *J* = 9.9 Hz, 5.4 Hz, CH, 1H), 2.81 (s, CH, 1H), 3.14 (s, CH, 1H), 2.31 – 2.40 (m, CH₂, 2H), 3.85 – 3.93 (m, CH₂, 2H), 3.98 – 4.03 (m, CH₂, 2H), 5.05 (d, *J* = 3.5 Hz, CH, 1H), 5.28 (bs, NH, 1H), 6.12 – 6.14 (dd, *J* = 5.7 Hz, 3.0 Hz, CH, 1H), 6.19 – 6.21 (dd, *J* = 5.7 Hz, 3.0 Hz, CH, 1H) ppm. **¹³C NMR** (101 MHz, CDCl₃) : δ 28.85 (CH₃), 39.56 (CH₂), 42.22 (CH), 45.13 (CH₂), 45.99 (CH), 46.29 (CH), 48.56 (CH), 54.74 (CH), 55.54 (CH), 65.56 (CH₂), 65.84 (CH₂), 79.47 (C), 105.97 (CH), 137.80 (CH), 139.19 (CH), 156.52 (CO), 218.61 (CO) ppm.

Methyl (1*R*, 2*R*, 3*aR*, 4*R*, 7*S*, 7*aS*)-2-(((*tert*-Butoxycarbonyl)amino)methyl)-3-oxo-2,3,3*a*,4,7,7*a*-hexahydro-1*H*-4,7-methanoindene-1-carboxylate, **82.**



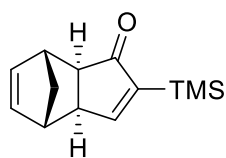
In a round-bottom flask, potassium dichromate (1.6 mg, 0.05 mmol, 2 mol %) was dissolved in a mixture of HNO₃ (2.1 μL, 20 mol %) and H₂O (0.33 mL) at 0°C for 15 minutes. Sodium periodate (124 mg, 0.58 mmol, 2.2 equiv.) was then added and the mixture was stirred at 0°C for 2 hours. In the meantime, a solution of starting material (80 mg, 0.26 mmol, 1 equiv.) dissolved in acetonitrile (0.67 mL) was prepared and kept at 0°C. The resulting cold solution of starting material was added to the first solution and stirred at 0°C for one hour and then let at room temperature for another 3 hours. The reaction was then quenched with 1 mL of a solution of NaOH at 1M and extracted with Et₂O. The organic layer was then washed with a solution of HCl, (1M) and organic layer dried over MgSO₄. The crude of the free acid **82** was directly used in the next reaction of methylation.

In a round-bottom flask, crude of reaction (50 mg, 0.16 mmol, 1 equiv.) was dissolved in a mixture of benzene (0.75 mL) and methanol (0.45 mL). Trimethylsilyldiazometane (317 μL, 0.19 mmol, 1.2 equiv.) was then added dropwise at room temperature. An emission of nitrogen was observed. After 2 hours, the crude was purified by flash chromatography on SiO₂ (eluent AcOEt/hexanes) affording 36 mg of the ester compound **71**, 69% yield over 2 steps.

¹H NMR (400 MHz, CDCl₃) : δ 1.08 (d, *J* = 9.5 Hz, CH₂, 1H), 1.40 (s, 3CH₃, 9H), 1.49 (d, *J* = 9.4 Hz, CH₂, 1H), 2.35 – 2.41 (m, CH, 1H), 2.40 (s, CH, 1H), 2.47 – 2.51 (m, CH, 1H), 2.97 (s, CH, 1H), 3.14 – 3.19 (m, CH, 1H), 3.18 (s, CH, 1H), 3.30 – 3.43 (m, CH₂, 2H), 3.79 (s, CH₃, 3H), 4.93 (bs, NH, 1H), 6.15 – 6.18 (dd, *J* = 5.7, 2.9 Hz, CH, 1H), 6.20 – 6.22 (dd, *J* = 5.7, 3.0 Hz, CH, 1H). **¹³C NMR** (101 MHz, CDCl₃) : δ 28.52 (CH₃), 38.63 (CH₂), 44.69 (CH), 44.91 (CH), 45.50 (CH₂), 47.60 (CH), 48.07 (CH),

52.69 (CH₃), 54.34 (CH), 57.14 (C), 137.91 (CH), 138.51 (CH), 174.93 (CO), 216.02 (CO). HRMS (ESI) calculated for C₃₆H₄₇N₂O₁₀ 667.3231, found 667.3229 [2M+H]⁺.

(3S,4S,7R, 7aR)-2-(trimethylsilyl)-3a-4,7,7a-tetrahydro-1H-4,7-methanoinden-1-one, 73.

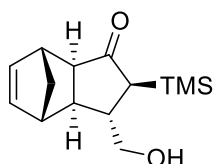


Under nitrogen was weighted Co₂(CO)₈ (0.68 g, 2 mmol, 1.1 eq.) dissolved then in hexane (4 mL). Ethynyltrimethylsilane (0.254 mL, 1.8 mmol, 1 equiv.) was added. The mixture was stirred for 1 h and the crude was filtered over SiO₂ and evaporated at reduced pressure and used in the next step without further purification.

In a pressure reactor purged with nitrogen, the cobalt complex previously form was added (100 mg, 0.164 mmol, 1% mol) with 25 mL of anhydrous toluene. After adding the ethynyltrimethylsilane (0.225 mL, 1.6 mmol, 1 equiv.) and NBD (330 mL 3.2 mmol, 2 eq.) the reactor was purged (without vacuum) with nitrogen and charged with CO at 3 bar. The reaction was heated up at 90 °C overnight. The crude was evaporated at reduced pressure and chromatographed to afford a white solid compound **73** in 90% in a ratio 98:2 exo/endo (315 mg).

Mp: 103 °C. **¹H RMN** (400 MHz, CDCl₃): 0.17 (s, 9H, CH₃), 1.19 (d, J=10 Hz, 1H, CH₂), 1.37 (d, J=10 Hz, 1H, CH₂), 2.28 (ddd, J=5, 2, 1 Hz, 1H, CH), 2.70 (s, 1H, CH), 2.84 (m, 1H, CH), 2.90 (s, 1H, CH), 6.20 (dd, J=6, 3 Hz, 1H, CH), 6.27 (dd, J=6, 3 Hz, 1H, CH), 7.60 (d, J=2 Hz, 1H, CH) ppm. **¹³C RMN** (100 MHz, CDCl₃): -1.7 (CH₃), 41.5 (CH₂), 43.2 (CH), 44.6 (CH), 52.2 (CH), 53.6 (CH), 137.6 (CH), 138.4 (CH), 152.3 (C), 173.2 (CH), 213.4 (CO) ppm.

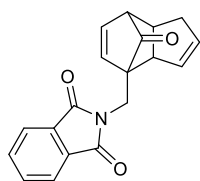
(2S,3S,3aS,4S,7R,7aR)-3-(hydroxymethyl)-2-(trimethylsilyl)-2,3,3a,4,7,7a-hexahydro-1H-4,7-methanoinden-1-one, 74.



The compound **73** (0.150 g, 0.69 mmol, 1 equiv) and benzophenone (0.125 g, 0.69 mmol, 1 equiv.) dissolved in MeOH 0.02M (35 mL). Nitrogen was bubbled through the mixture for 30 minutes and irradiated with 16 UV lamps (350 nm, 8W). After 2h, the crude was evaporated under reduced pressure and purified over SiO₂ in a mixture hexane/AcOEt. It afforded 85% of the compound **74** (173 mg).

¹H RMN (400 MHz, CDCl₃): 0.12 (s, 9H, CH₃), 1.21 (d, J=9 Hz, 1H, CH₂), 1.43 (d, J=9 Hz, 1H, CH₂), 1.89 (sa, 1H, OH), 1.97 (m, 1H, CH), 2.12 (dd, J=10, 2 Hz, 1H, CH), 2.25 (dd, J=9, 5 Hz, 1H, CH), 2.36 (dd, J=9, 1 Hz, 1H, CH), 2.82 (s, 1H, CH), 3.08 (s, 1H, CH), 3.54 (dd, J=10, 7 Hz, 1H, CH₂), 3.76 (dd, J=10, 4 Hz, 1H, CH₂), 6.16 (dd, J=6, 3 Hz, 1H, CH), 6.29 (dd, J=6, 3 Hz, 1H, CH) ppm. **¹³C RMN** (100 MHz, CDCl₃): -1.4 (CH₃), 44.6 (CH₂), 45.0 (CH), 46.7 (CH), 47.8 (CH), 47.9 (CH), 49.2 (CH), 57.6 (CH), 67.3 (CH₂), 138.1 (CH), 138.8 (CH), 220.5 (CO) ppm.

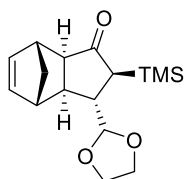
2-((8-oxo-1,3a,7,7a-tetrahydro-4H-4,7-methanoinden-4-yl)methyl)isoindoline-1,3-dione, **77**.



In a quartz flask, starting material **38** (120 mg, 0.39 mmol, 1 equiv.) and benzophenone (143 mg, 0.8 mmol, 2 equiv.) were dissolved in anhydrous methanol (20 mL) then the all mixture was degassed using freeze pump thaw method. The flask was irradiated at 350 nm in a Rayonet reactor (8W) for 4 hours and solvent removed under reduced pressure. The crude was purified by flash chromatography on silica gel (ethyl acetate/hexane) to afford **77** as a colorless oil in 37% yield (44 mg).

¹H NMR (400 MHz, Chloroform-*d*) δ 7.85-7.87 (m, CH, 2H), 7.71-7.74 (m, CH, 2H), 6.54-6.59 (m, CH, 2H), 6.02-6.05 (m, CH, 1H), 5.84-5.87 (m, CH, 1H), 4.03-7.07 (d, *J* = 14.6 Hz, CH₂, 1H), 3.94-3.98 (d, *J* = 14.6 Hz, CH₂, 1H), 2.87-2.92 (m, CH, 1H), 2.68-2.69 (m, CH, 1H), 2.56-2.64 (m, CH₂, 1H), 2.45-2.50 (m, CH, 1H), 2.14-2.21 (m, CH₂, 1H). **¹³C NMR** (101 MHz, Chloroform-*d*) δ 203.89(CO), 169.09 (CO), 136.10 (CH), 135.15 (CH), 134.58 (CH), 134.52 (2CH), 132.44 (CO), 128.31 (CH), 123.80 (2CH), 57.99 (C), 53.64 (CH), 53.57 (CH), 41.62 (CH), 36.58 (CH₂), 34.85 (CH₂). **HR-MS** (ESI) calculated for C₁₉H₁₆NO₃ 306.1130, found 306.1135 [M+H]⁺.

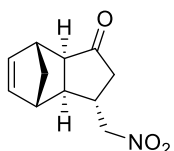
(2*S*,3*S*,3*aS*,4*S*,7*R*,7*aR*)-3-(1,3-dioxolan-2-yl)-2-(trimethylsilyl)-2,3,3*a*,4,7,7*a*-hexahydro-1*H*-4,7-methanoinden-1-one, **76**.



Compound **73** (150 mg, 0.7 mmol, 1 eq.) was dissolved in 1,3-dioxolane, 0.01M, benzophenone (128 mg, 0.7 mmol, 1 equiv.) was then added to the reaction. The system was degassed during 40 minutes and irradiated at 350 nm (8W) during 3 hours with 8 lamps. The solvent was evaporated and chromatographed to afford compound **76** in 80% (207 mg).

¹H NMR (400 MHz, Chloroform-*d*) δ : 6.19 (dd, *J* = 5.6, 3.0 Hz, 1H), 6.14 (dd, *J* = 5.6, 2.9 Hz, 1H), 4.86 (d, *J* = 3.4 Hz, 1H), 4.04 – 3.93 (m, 2H), 3.93 – 3.84 (m, 2H), 3.88 (d, *J* = 3.1 Hz, 1H), 3.05 (s, 1H), 2.79 (s, 1H), 2.38 (d, *J* = 9.4 Hz, 1H), 2.32 (s, 2H), 2.18 (d, *J* = 8.1 Hz, 1H), 1.30 (dd, *J* = 86.5, 9.0 Hz, 1H), 0.11 (s, 9H). **¹³C NMR** (101 MHz CDCl₃) δ 219.93 (CO), 156.53, 138.62, 138.23, 137.72, 105.94, 95.22, 65.21, 65.06, 64.98, 57.25, 56.78, 49.15, 47.05, 46.83, 46.70, 46.61, 45.35, 44.29, 44.25, 44.06, 43.86, 43.66, -0.18, -1.07, -1.33, -1.45, -1.59.

(3*S*, 3*aR*, 4*S*, 7*R*, 7*aR*)-3-(nitromethyl)-2,3,3*a*,4,7,7*a*-hexahydro-1*H*-4,7-methanoinden-1-one, **78**.

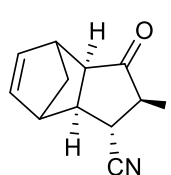


The compound **73** (59 mg, 0.268 mmol, 1 equiv) was dissolved in 1 mL of nitromethane and TBAF (85 mg, 0.0268 mmol, 10 mol%). After an hour, the crude of evaporated and chromatographed to yield to compound **78** in 54% yield.

¹H RMN (400 MHz, CDCl₃): 1.25 (d, *J*=9 Hz, 1H, CH₂), 1.51 (dt, *J*=9 Hz, 1H, CH₂), 2.10-2.17 (m, 1H, CH), 2.38-2.46 (m, 1H, CH), 2.55-2.65 (m, 1H, CH), 2.38-2.46 (m, 1H, CH, 1H, CH₂), 2.55-2.65 (m, 1H, CH), 2.71-2.78 (m, 1H, CH₂), 2.86 (bs, 1H, CH), 3.16 (bs, 1H, CH), 4.50 (*J*=12.7 Hz, 2H, CH₂), 6.18-6.19 (m, 2H, CH₂) ppm. **¹³C RMN** (100 MHz, CDCl₃): 37.2 (CH), 44.6

(CH₂), 45.8 (CH), 46.7 (CH₂), 47.1 (CH), 47.9 (CH), 55.1 (CH), 79.9 (CH₂), 138.1 (C), 138.5 (CH), 220.5 (CO) ppm.

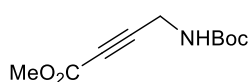
2-methyl-1-oxo-3a,4,7,7a-tetrahydro-1H-4,7methanoindene-3-carbonitrile, 81.



The starting material **63** (90 mg, 0.29 mmol, 1 equiv.) was dissolved in DMF and in a single portion the sodium cyanide (29 mg, 0.59 mmol, 2 equiv.) was added as well as aqueous solution of NH₄Cl (24 mg, 0.44 mmol, 1.5 equiv.) in 46 μ L of distilled water. It was observed a change of color from yellowish starting color to orange followed by a red mixture. After an overnight reaction stirred at room temperature, mixture was neutralized to pH7 and concentrated under high vacuum line. Then, the mixture was re-dissolved in DCM and water. The organic layer extracted and purified over SiO₂ gel to afford **81** in 40% yield as an oil, 21 mg.

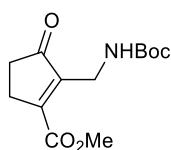
1H NMR (400 MHz, Chloroform-d) δ = 1.09 (s, 9H, CH₃), 1.15 (d, J =10 Hz, 1H, CH₂), 1.35 (d, J =10 Hz, 1H, CH₂), 2.30 (d, J =5 Hz, 1H, CH), 2.68 (bs, 1H, CH), 2.75 (bs, 1H, CH), 2.86 (bs, 1H, CH), 4.41 (s, 2H, CH₂), 6.17 (dd, J =6 i 3 Hz, 1H, CH), 6.27 (dd, J =6 i 3 Hz, 1H, CH), 7.32-7.43 (m, 6H, CH), 7.44-7.46 (m, 1H, CH), 7.63-7.66 (m, 4H, CH) ppm. **13C NMR** (101 MHz, Chloroform-d) 10.6 (CH₃), 41.5 (CH₂), 42.8 (CH), 44.6 (CH), 49.1 (CH), 52.3 (CH), 114.9 (C), 137.5 (CH), 137.9 (CH), 138.2 (C), 156.7 (C), 206.7 (CO) ppm. **HR-MS** (ESI) calculated for C₁₂H₁₂NO, 186.0919 found 186.0922 [M+H]⁺.

Methyl 4-((tert-butoxycarbonyl)amino]but-2-ynoate, 91.



In a schlenk flask, *n*-Butyl lithium, 2.5M (3 mL, 7.52 mmol, 1.1 equiv.) was added dropwise to solution of **58** (1 g, 6.84 mmol, 1equiv) in dry THF (23 mL) at -78 °C. The resulting mixture was stirred for 30 min, then CO₂ balloon dried through concentrated H₂SO₄ bubbler was connected to the mixture with a needle. CO₂ comes from Air liquide bottle of 45 bar, with O₂ \leq 2ppm, CnHm \leq 2ppm, H₂ \leq 0.5 ppm, H₂O \leq 3 ppm, from "the laboratorio general de interacciones moleculares" of the CCiTUB. Reaction was stirred 2-3h and let to warm up. The reaction mixture was poured onto water, acidified and extraction was done with EtOAc. The extracts were dried (MgSO₄) and concentrated. The crude was then without purification dissolved in anhydrous DMF (30 ml) and NaHCO₃ (6.86, 82 mmol, 2.55 equiv.) and MeI (6.50 ml, 106 mmol, 3.3 equiv.) were added. The mixture was stirred overnight at rt and diluted in water; after extraction with Et₂O, it was washed with brine and dried over MgSO₄ and concentrated under reduced pressure. Purification over SiO₂ with increased gradient in hexane/AcOEt afforded 74% yield of a colorless oil. **1H NMR** (400 MHz, Chloroform-d) δ = 1.45 (s, 9H, CH₃), 3.78 (s, 3H, CH₃), 4.07 (br s, 2H, CH₂), 4.74 (br s, 1H, NH) ppm. Good agreement with the literature.¹²

Methyl 2-((tert-butoxycarbonyl)amino)-3-oxocyclopent-1-ene-1-carboxylate, 94.

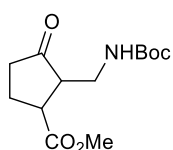


Under nitrogen Co₂(CO)₈ was weighted (5.1 g, 14.6 mmol, 1.1 eq.) and dissolved in a mixture hexane/DCM (0.2M, 2v/1v). Compound **91** (2.6, 13.3 mmol, 1 equiv.) dissolved in a mixture of hexane/DCM (10 mL) was then

added. The mixture was stirred for 2 h and the crude was filtered over SiO₂ and evaporated at reduced pressure and part of it was used in the next step.

In a pressure Büchi reactor purged with nitrogen, the cobalt complex previously form was added (0.588 mg, 1.28 mmol, 1 equiv.) with 53 mL of anhydrous DCM. The reactor was purged and charge with ethylene at 6 bar. NMO (1.5g, 12 mmol, 10 equiv.) was dissolved in 5 mL of anhydrous DCM. Each 20 minutes, 1 mL of NMO solution was added to the reactor. After the last addition, the reaction was left until completion. Directly in the reactor, next step was performed to avoid the instability of the PK adduct.

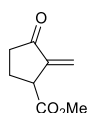
Methyl 2-(((tert-butoxycarbonyl)amino)methyl)-3-oxocyclopentane-1-carboxylate, 95 .



In a pressure reactor already charged with the mixture of **60** was added via a syringe Pd/C (10-25 mol%) dissolved in dry DCM. The system was again purged and charged with 10 bar of H₂. After 2h hour, the reaction was complete. The crude was quickly filtered over celite and chromatographed over SiO₂/Et₃N to afford 45-50% yield of a colorless oil (174 mg).

¹H NMR (400 MHz, Chloroform-d) δ : 4.95 (bs, 1H), 3.76 (s, CH₃), 3.41 (s, 2H), 2.91 (m, 1H, CH), 2.66 (m, 1H, CH), 2.48 (dd, J = 18.7, 8.9 Hz, 1H, CH₂), 2.41 – 2.30 (m, 1H), 2.22 (dd, J = 19.0, 10.5 Hz, 1H, CH₂), 2.10 – 1.94 (m, 1H, CH₂), 1.43 (s, 9H). **¹³C NMR** (101 MHz, cdCl₃) δ 216.73 (CO), 174.22 (CO), 155.98 (CO), 79.40 (Cq), 53.40(CH), 52.56 (CH₃), 52.24 (CH), 44.59 (CH₂), 39.05 (CH₂), 37.48 (CH₃), 28.34 (CH₃), 28.29(CH₃), 24.59 (CH₂). **HR-MS** (ESI) calculated for C₁₃H₂₁NO₅ 272.1498, found 272. 1503 [M+H]⁺.

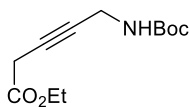
Methyl 2-methylene-3-oxocyclopentane-1-carboxylate, 97.



The compound **95** (174 mg, 0.64 mmol, 1 equiv.) was dissolved in DCM (5 mL). It was then added HCl/MeOH (1.25M, 4 mL, 10 equiv.) and left to react overnight at room temperature. Then, NaHCO₃ was added first to neutralise the reaction and other 10 equivalents were added followed by MeI (0.410 mL, 6.4 mmol, 10 equiv.). The resulting mixture was stirred for 2 days at 40°C and filtered over celite. The crude was evaporated and quickly chromatographed to give **97** as an oil in 46% (45 mg).

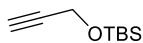
¹H NMR (400 MHz, CDCl₃): δ = 6.16 (d, J = 2.57 Hz, 1H), 5.60 (dd, J = 2.4, 07 Hz, 1H), 3.76–3.68 (m, 1H), 3.75 (s, 3 H), 2.61–2.54 (m, 1H), 2.41–2.27 (m, 1H), 2.24-2.15 (m, 2H). **¹³C NMR** (101 MHz, CDCl₃): δ = 204.7(CO), 173.0(CO), 142.5(C), 120.5(C), 52.5(CH₃), 45.9(CH), 36.8(CH₂), 23.1(CH₂). **ESI-HR-MS** (ESI) calcd for C₈H₁₀O₃Na: 177.0522; found: 177.0529. Data good agreement with the literature.¹³

Ethyl 5-((*tert*-butoxycarbonyl)amino)pent-3-ynoate, **98**.



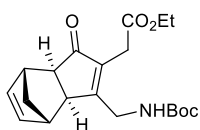
To a solution of compound **58** (200 mg, 1.3 mmol, 1 equiv.) dissolved in anhydrous acetonitrile (2.6 mL) was added CuI (0.37 g, 0.19 mmol, 0.15 equiv.) followed after 5 minutes by ethyl diazoacetate (0.2 mL, 0.29 mmol, 1.5 equiv.). The reaction was left at room temperature for 2 days. The solvent was evaporated under vacuum and the crude was purified by silica chromatography using mixtures pentane/diethyl ether to afford a mixture of the compound **98** and its allenic isomer in a 3:1 ratio, 54 % yield of Colourless oil (170mg). **1H NMR** (CDCl₃, 400 MHz): δ 4.69 (s, 1H), 4.19 (q, 2H); 3.94 (m, 2H), 3.26 (t, 2H), 1.45 (s, 9H), 1.28 (t, 3H). Data in good agreement with the literature.¹⁴

Tert-butyldimethyl(prop-2-yn-1-yloxy)silane, **102**.



In a flask with a magnetic stirrer, 0.5 mL of propargyl alcohol (2-propyn-1-ol) were dissolved in dichloromethane anhydrous (5 mL) under nitrogen. Then, the system was cooled to 0°C and 2 equivalents of imidazole (1.33 g) were added. Finally, 1 equivalent of *tert*-butyldimethylsilyl chloride (1.43 g) was added and the solution was cooled to room temperature. The reaction was left stirring overnight. Next day, reaction had not finished, it was stirred for another night and 0.67 g of TBSCl, 0.45 g of imidazole and 3.7 mL DCM anhydrous were added. Next day, salts were extracted with NH₄Cl and the solvent was dried with MgSO₄. Then, the solvent was evaporate under vacuum and the crude was purified by silica chromatography using mixtures of hexane/AcOEt. This reaction performed in quantitative yield of the compound **102** as a yellowish oil. **1H NMR** (CDCl₃, 400 MHz): δ 3.66 (s, 2H), 2.45 (s, 1H), 0.91 – 0.89 (s, 9H), 0.07 – 0.06 (s, 6H). **13C RMN** (100 MHz, CDCl₃): δ -3.2 (2CH₃), 18.6 (C), 26.1 (3CH₃), 53.2 (CH₂), 74 (CH), 85.0 (C) ppm.

Ethyl 5-((*tert*-butoxycarbonyl)amino)pent-3-ynoate, **99**.



The compound **98** (177 mg, 0.73 mmol, 1 equiv.) was dissolved in hexane (6 mL) under nitrogen. Then dicobalt octacarbonyl (275 mg, 0.8 mmol, 1.1 equiv) was added and left to react 3h. The crude solvent was evaporate under vacuum and purified over silica gel using hexane and AcOEt as eluents. The final product **99** was isolated in 85% yield and engaged in the next reaction.

The cobalt carbonyl complex (343 mg, 0.62 mmol, 1 equiv.) was dissolved in anhydrous toluene (8 mL) followed by the addition NBD (0.315 mL, 3.1 mmol, 5 equiv.) were added. The reaction was heated up to 70°C overnight. Next day, the solvent was evaporated under vacuum and the crude was purified by silica gel using mixtures using mixtures of hexane/AcOEt to afford 72% yield as a yellow oil (161 mg) endo/exo ratio, 10:1.

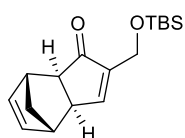
IR(film) ν_{max} : 3363.34, 2958.20, 1705.14, 1508.36, 1369.45, 1247.91, 1166.88, 729.90 cm⁻¹. **1H NMR** (CDCl₃, 400 MHz): δ 6.28 (dd, *J* = 5.6, 3.0 Hz, 1H), 6.22 (dd, *J* = 5.7, 2.9 Hz, 1H), 5.03 (bs, 1H),

4.12 (m, 4H), 3.29 (q, $J = 17.4, 16.8$ Hz, 2H), 2.94 (s, 1H), 2.88 (s, 1H), 2.79 (d, $J = 5.2$ Hz, 1H), 2.35 (d, $J = 5.3$ Hz, 1H), 1.46 (s, 9H), 1.42 – 1.38 (dt, 1H), 1.32 – 1.29 (dt, 1H), 1.25 (t, $J = 7.1$ Hz, 3H).

¹³C NMR (101 MHz, $cdCl_3$) δ 204.52, 172.79, 172.78, 138.22, 137.44, 82.86, 61.24, 52.18, 49.43, 43.75, 42.59, 41.40, 39.62, 28.32, 28.28, 14.10.

HR-MS (ESI) calculated for $C_{20}H_{27}NO_5$ 362.1967, found 362.2002 $[M+H]^+$.

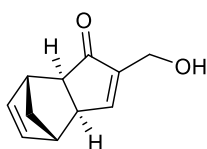
2-(((*tert*-butyldimethylsilyl)oxy)methyl)-3a-4,7,7a-tetrahydro-1-*H*-4,7-methanoinden-1-one, 103.



Compound **102** (0.5 g, 2.9 mmol) was dissolved in hexane (0.2M) followed by dicobalt octacarbonyl (1.05 g, 3.05 mmol, 1.05 equiv.). The reaction was left overnight stirring at room temperature. Solvent was evaporate under vacuum and the crude was filtrated over celite to afford 78% yield of the dicobalt hexacarbonyl complex (617 mg, 2.26 mmol, 1 equiv) which was dissolved in anhydrous toluene (15 mL) and engaged in the next reaction. NBD (0.73 mL, 11.3 mmol, 5 equiv.) was added and the reaction was heated overnight to 70°C. Solvent was evaporated under vacuum and the crude was purified by silica chromatography using mixtures of hexane/AcOEt. Compound **103** was obtained in 55% as a yellowish oil (361 mg).

¹H NMR ($CDCl_3$, 400 MHz): δ 7.38 (q, $J = 1.9$ Hz, 1H), 6.29 (dd, $J = 5.6, 3.0$ Hz, 1H), 6.20 (dd, $J = 5.7, 3.0$ Hz, 1H), 4.35 (t, $J = 2.1$ Hz, 2H), 2.91 (s, 1H), 2.77 (s, 1H), 2.71 (s, 1H), 2.34 (d, $J = 5.0$ Hz, 1H), 1.40 (d, $J = 9.4$ Hz, 1H), 1.26 (d, $J = 9.4$ Hz, 1H), 0.92 (s, 9H), 0.08 (s, 6H).

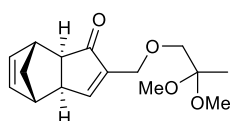
(3aR,4S,7R,7aR)-2-(hydroxymethyl)-3a,4,7,7a-tetrahydro-1-*H*-4,7-methanoinden-1-one, 104.



To a solution of **66** (243 mg, 0.84 mmol, 1 equiv.) dissolved in anhydrous THF (5 mL) at 0°C, was added TBAF (1M, 2.65 mL, 1.8 mmol, 2.2 equiv.). The reaction was stirred overnight at room temperature overnight and afforded after purification over silica gel (hex/AcOEt) the compound **104**, a colourless oil in 80% yield (118 mg).

¹H NMR ($CDCl_3$, 400 MHz): δ 7.37 (dt, $J = 2.6, 1.3$ Hz, 1H), 6.30 (dd, 1H), 6.21 (dd, $J = 5.6, 3.0$ Hz, 1H), 4.36 (s, 2H), 2.93 (s, 1H), 2.80 (s, 1H), 2.72 (s, 1H), 2.36 – 2.34 (m, 1H), 1.42 (dq, $J = 9.5, 1.5$ Hz, 1H), 1.29 – 1.25 (m, 1H). **¹³C NMR** ($CDCl_3$, 101 MHz): δ 209.85, 159.73, 148.87, 138.48, 137.08, 57.76, 53.17, 48.17, 43.60, 42.89, 41.20. **HR-MS** (ESI): calculated for $C_{11}H_{13}O_2$, 177.0915, found 177.0919 $[M+H]^+$.

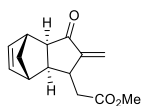
Methyl 2-(((1R,3aR,4R,7S,7aR)-2-methylene-3-oxo-2,3,3a,4,7,7a-hexahydro-1-*H*-4,7-methanoinden-1-yl)acetate, 105.



Compound **104** (21 mg, 0.12 mmol, 1 equiv.) was dissolved in deuterated benzene with an excess of trimethyl orthoacetate (0.10 mL, 0.79 mmol, 6.5 equiv.). The reaction was heated overnight at room temperature, final product **105** was detected in a mixture with the starting material in a 6:1 ratio.

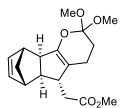
¹H NMR (400 MHz, Chloroform-*d*) δ : 7.37 (s, 1H), 6.31–6.29 (dd, *J* = 5.5, 3.1 Hz, 1H), 6.21 (dd, *J* = 5.6, 2.9 Hz, 1H), 4.36 (s, 9H), 2.93 (s, 1H), 2.80 (s, 1H), 2.72 (s, 1H), 2.35 (d, *J* = 6.0 Hz, 1H), 1.43 (d, *J* = 8.2 Hz, 1H), 1.27 (d, *J* = 9.7 Hz, 1H). **¹³C NMR** (101 MHz, *cdCl*₃) δ 209.88, 159.79, 148.89, 138.48, 137.07, 57.71, 53.18, 50.86, 48.17, 43.60, 42.88, 41.20.

Methyl 2-((1*R*,3*aR*,4*R*,7*S*,7*aR*)-2-methylene-3-oxo-2,3,3*a*,4,7,7*a*-hexahydro-1*H*-4,7-methanoinden-1-yl)acetate, 107.



The compound **104** (150 mg, 0.85 mmol, 1 equiv.) was dissolved in trimethyl orthoacetate (0.9 mL, 7.44 mmol, 9 equiv.). Acetic acid (4 μ L, 0.051 mmol, 0.06 eq) was added to the mixture and the reaction was heated for 2h30 at 120 °C and 150 °C for 3h. After preparative column (*SiO*₂/*Et*₃*N*) eluted with 35% *AcOEt* in hexanes, the second fraction, *R*_f=0.40 was extracted from the plate, dissolved in methanol and filtered with Witman paper. It afforded after evaporation the compound **107** as a colourless oil in 10% (10 mg). **¹H NMR** (400 MHz, Chloroform-*d*) δ 6.21 (s, 1H), 6.03 (d, *J* = 2.2 Hz, 1H), 5.30 (d, *J* = 2.3 Hz, 1H), 3.69 (s, 3H), 3.12 (s, 1H), 2.89 (m, 2H), 2.68 – 2.54 (m, 2H), 2.61 (d, *J* = 54.9 Hz, 1H), 2.45 (d, *J* = 8.1 Hz, 1H), 1.95 (d, *J* = 8.0 Hz, 1H), 1.36 (d, *J* = 9.4 Hz, 0H), 1.24 (m, 3H). **¹³C NMR** (101 MHz, *cdCl*₃) δ : 210, 139.08, 138.37, 119.54, 55.09, 52.14, 51.32, 49.74, 48.37, 47.25, 43.97, 42.28, 41.10.

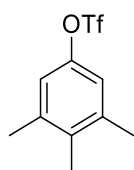
Methyl 2-((5*aS*, 6*S*, 9*R*, 9*aR*)-2,2-dimethoxy-2,3,4,5*a*, 6, 9, 9*a*, 9*b*-octahydro-6,9-methanoindeno[1,2*b*]pyran-5-yl)acetate, 108.



From the same reaction crude to afford **107**, and after preparative chromatography, the major product of reaction was isolated from the preparative plate at *R*_f = 0.6. It afforded compound **108**, in 30% yield. **¹H NMR** (400 MHz, Chloroform-*d*) δ 6.05 (t, *J* = 1.8 Hz, 2H), 3.68 (s, 3H), 3.31 (s, 6H), 2.85 (s, 1H), 2.65 (s, 1H), 2.58 – 2.47 (m, 3H), 2.27 – 2.15 (m, 1H), 2.01 – 1.77 (m, 5H), 1.49 (dt, *J* = 8.6, 1.4 Hz, 1H), 1.36 (dt, *J* = 8.7, 1.6 Hz, 1H). **¹³C NMR** (101 MHz, *cdCl*₃) δ 173.41, 149.52, 137.31, 136.98, 113.46, 112.68, 101.48, 51.43, 49.99, 49.68, 48.90, 47.81, 47.64, 44.16, 43.73, 41.99, 40.01, 26.90, 18.86. **HR-MS** (ESI): calculated for C₁₁H₁₃O₂, 321.1702, found 321.1706 [*M*+*H*]⁺.

Chapter IV

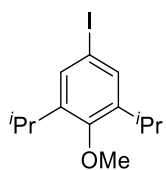
3,4,5-Trimethylphenyl trifluoromethanesulfonate, 114.



Trifluoromethanesulfonic anhydride (0.657 mL, 3.9 mmol, 1.7 equiv.) was added dropwise to a solution of 3,4,5-trimethylphenol (0.151 mg, 2.3 mmol 1 equiv.) and triethylamine (1 mL) in DCM (11.5 mL) at $-15\text{ }^{\circ}\text{C}$ under nitrogen atmosphere. The reaction was left to warm up to room temperature and stirred overnight. Then, the mixture was quenched with H₂O and brine and the aqueous phase extracted with DCM. The combined organic layers were dried with MgSO₄ and concentrated under reduced pressure. Purification by flash chromatography (Combiflash®, hexane) gave **114** (0.540 g, 82%) as a colorless oil.

IR (film): $\nu = 3052, 1420, 1209, 1142, 1014, 956, 842\text{ cm}^{-1}$. **¹H NMR** (400 MHz, CDCl₃): $\delta = 2.15$ (s, 3 H, CH₃), 2.31 (s, 2 H, 2 CH), 6.91 (s, 6 H, 2 CH₃) ppm. **¹³C NMR** (100 MHz, CDCl₃): $\delta = 15.09$ (CH₃), 20.80 (2 CH₃), 117.25 (C), 119.99 (2 CH), 135.58 (C), 138.67 (2 C), 146.77 (C) ppm. **LR-MS** (ESI): $m/z =$ calculated for C₁₀H₁₂F₃O₃S, 269.04 found 269.6 [M + H]⁺.

4-Iodo-2,6-di-iso-propylphenyl methyl ether, 118.

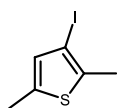


To a solution of 2,6-di-iso-propylphenol (1.91 mL, 10 mmol, 1 equiv.) in anhydrous DMF (15 mL) was successively added cesium carbonate (6.65 g, 20 mmol, 2 equiv.) and iodomethane (1.9 mL, 30 mmol, 3 equiv.) and stirred overnight. Then, Et₂O was added and the organic layer was extracted with NaOH 1M (x2) and water (x2). The combined extracts were dried with MgSO₄ and concentrated at reduced pressure. Purification by flash chromatography on SiO₂ (Combiflash®, hexane) afforded quantitatively the intermediate 1,3-di-iso-propyl-2-methoxybenzene as a colorless oil (1.92 g, quant.). **¹H NMR** (400 MHz, CDCl₃) δ : 1.24 (d, J = 7 Hz, 12H, CH₃), 3.35 (hept, J = 7 Hz, 2H, CH), 3.75 (s, 3H, CH₃), 7.10 (br s, 3H, CH) ppm.

Then the resulting ether (1.5 g, 7.8 mmol, 1 equiv.) was dissolved in glacial acetic acid (10 mL), and then iodine monochloride (1.9 g, 11.7 mmol, 1.5 equiv.) was added. The mixture was heated up to 80 °C. After 1 hour, it was cooled down to room temperature and the solution was poured into a solution of NaHSO₃ (30%) and extracted with DCM. The combined organic layer was dried over anhydrous MgSO₄ and concentrated under reduced pressure. Purification by flash chromatography on SiO₂ (Combiflash®, hexanes/EtOAc gradient) afforded **118** quantitatively as a colorless oil (2.48 g, quant.).

IR (film) ν_{max} : 2963, 1460, 1325, 1199, 1010, 865 cm^{-1} . **¹H NMR** (400 MHz, CDCl₃) δ 1.21 (d, J = 7 Hz, 12H, CH₃), 3.25 (hept, J = 7 Hz, 2H, CH), 3.71 (s, 3H, CH₃), 7.37 (s, 2H, CH) ppm. **¹³C NMR** (100 MHz, CDCl₃) δ 24.0 (4CH₃), 26.7 (2CH), 62.4 (CH₃), 89.4 (C), 133.6 (2CH), 144.7 (2C), 154.7 (C) ppm. **HRMS-ESI** m/z calcd. For C₁₃H₂₀O: 195.1509, found 192.1513 [M-I+H]⁺, calcd. for C₁₃H₂₀IO: 319.0553, found 319.0557 [M+H]⁺.

3-iodo-2,5-dimethylthiophene, 140.



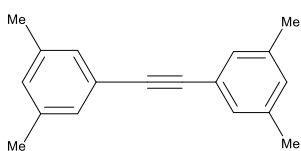
In a 50 mL round bottom flask, was dissolved the 2,5-dimethylthiophene (4.39 mmol, 0.5 mL, 1 equiv.) in a solution of 5 mL of chloroform/acetic acid (1v/1v) then solution of iodic acid (0.96 mmol, 169 mg) in 0.5 mL of distilled water was added followed by iodine (1.53 mmol, 388 mg). A condenser was then added and heated up to reach reflux (100°C) during 2h where the reaction color passed from red to yellow. The mixture was poured into a mixture water/ice. Organic layer was then washed with sodium carbonate, sodium thiosulfate and water and dried over anhydrous magnesium sulfate. Evaporation of the solvent left a yellow oil which was chromatographed on silica column using hexane eluent and afforded 3-iodo-2,5-dimethylthiophene **140** in 76% yield (794mg).

¹H NMR (400 MHz, Chloroform-*d*) δ 6.61 (s, 1H), 2.41 (s, 7H), 2.35 (s, 4H). **DEPCI-MS**: calcd. for C₆H₇IS [M]⁺ 238.09; found 238.0; calcd. for C₆H₈IS [M+H]⁺ 239.09; found 239.0. NMR Experiments are in good agreement with literature.¹⁵

General procedure for the syntheses of acetylenes

In a pressure Schlenk tube fitted with a Teflon screw cap (Kontes HI-VAC) with a magnetic stirring bar was placed under nitrogen atmosphere tetrakis(triphenylphosphine)palladium (6 mol%), CuI (10 mol%) and starting material iodide or triflate (1 equiv.). While stirring, dry toluene (volume necessary to make the starting material 0.20 M) was added. Nitrogen-sparged DBU (6 equiv.) was then added, followed by a purge of the reaction tube with nitrogen. Distilled water (40 mol%) and ice-chilled trimethylsilylacetylene (0.5 equiv.) were added sequentially, and then the sealed tube was capped tightly. The reaction tube, blocked from incidental light, was heated at the corresponding temperature and left stirring at a high rate of speed for the indicated reaction time. Then the reaction mixture was cooled to room temperature and partitioned in ethyl ether and distilled water. The organic layer was washed with 10% HCl (x3), saturated aqueous NaCl, dried over MgSO₄, gravity-filtered and the solvent removed *in vacuo*. The product was purified by flash chromatography on SiO₂ (Combiflash[®], hexanes/AcOEt gradient).

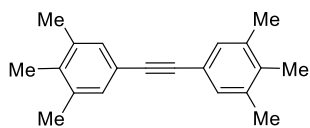
Bis(3,5-dimethylphenyl)acetylene, 110.



Following the general procedure for the Sonogashira reaction, Pd(PPh₃)₄ (223 mg, 0.19 mmol), CuI (62 mg, 0.32 mmol), 3,5-dimethyl-1-iodobenzene **109** (0.47 mL, 3.23 mmol), DBU (2.96 mL, 19.4 mmol), distilled water (24 μ L, 1.29 mmol), ice-chilled trimethylsilylacetylene (234 μ L, 1.6 mmol) and toluene (16 mL) were used. The reaction mixture was heated at 80 °C for 18h. The desired product **110** (451 mg, 75% yield) was isolated by flash chromatography as a white solid.

M.p. 123 °C. **¹H NMR** (400 MHz, CDCl₃): δ = 2.29 (s, 12 H, CH₃), 6.93 (s, 2 H, CH), 7.14 (s, 4 H, CH) ppm. **¹³C NMR** (100 MHz, CDCl₃): δ = 21.08, 88.02, 123.00, 129.22, 130.00, 137.78 ppm. **GC-MS** m/z (%) = 234 (100) [M]⁺. C₂₈H₁₈ (354.45): calcd. C 92.26, H 7.74; found C 92.33, H 7.72.

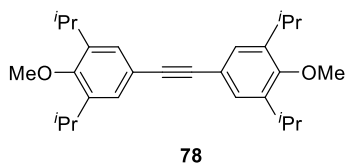
Bis(3,4,5-Trimethylphenyl)acetylene, 115.



Following the general procedure for the Sonogashira reaction, Pd(PPh₃)₄ (141 mg, 0.12 mmol), CuI (38 mg, 0.2 mmol), 3,4,5-trimethylphenyl triflic ether, **113** (540 mg, 2.0 mmol), DBU (1.83 mL, 12 mmol), distilled water (15 μL, 0.81 mmol), ice-chilled trimethylsilylacetylene (145 μL, 1.0 mmol) and toluene (10 mL) were used. The reaction mixture was heated at 65 °C for 18h. Along with non-determined amount of the 5-(trimethylsilylacetylen)-1,2,3-trimethylbenzene and starting material, the desired product **115** was isolated by trituration with methanol as a white solid (110 mg, 42% yield).

IR (film): $\nu = 2923, 1460, 1377, 1211, 1144, 960 \text{ cm}^{-1}$. **¹H NMR** (400 MHz, CDCl₃): $\delta = 2.18$ (s, 6 H, CH₃), 2.27 (s, 12 H, CH₃), 7.18 (s, 4 H, CH) ppm. **¹³C NMR** (100 MHz, CDCl₃): $\delta = 15.38$ (2CH₃), 20.37 (4CH₃), 97.13 (2C), 119.23 (2C), 130.39 (4CH), 136.40 (2C), 137.28 (4C) ppm. **HR-MS ESI:** calcd. for C₂₀H₂₃ [M + H]⁺ 263.1794; found 263.1795; calcd. for C₄₀H₄₅ [2M + H]⁺ 525.3515; found 525.3519.

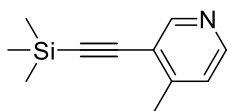
Bis(3,5-di-iso-propyl-4-methoxyphenyl)acetylene, 119.



Following the general procedure, Pd(PPh₃)₄ (523 mg, 0.45 mmol), CuI (143 mg, 0.75 mmol), 4-iodo-2,6-diiso-propylphenyl methyl ether **118** (2.38 g, 7.47 mmol), DBU (6.7 mL, 44.8 mmol), distilled water (54 μL, 2.99 mmol), ice-chilled trimethylsilylacetylene (0.54 mL, 3.74 mmol) and toluene (38 mL) were used. The reaction mixture was heated at 60 °C for 22 hours. Purification afforded **119** (1.00 g, 67%) as a white solid (cryst. methanol).

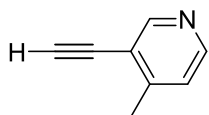
M.p.: 150 °C. **IR (film)** $\nu_{\text{max}}: 2962, 1474, 1307, 1224, 1013, 881 \text{ cm}^{-1}$. **¹H NMR** (400 MHz, CDCl₃) δ 1.25 (d, J = 7 Hz, 24H, CH₃), 3.32 (hept, J = 7 Hz, 4H, CH), 3.74 (s, 6H, CH₃), 7.28 (s, 4H, CH) ppm. **¹³C NMR** (100 MHz, CDCl₃) δ 24.1 (8CH₃), 26.7 (4CH), 62.4 (2CH₃), 88.7 (2C), 119.5 (2C), 122.9 (4CH), 144.1 (4C), 155.0 (2C) ppm; Anal. Calc. for C₂₈H₃₈O₂ + 1/2 H₂O: C, 80.92; H, 9.46; Found: C, 81.28; H, 9.19. **HRMS-ESI** m/z calcd. for C₂₈H₃₉O₂: 407.2945, found 407.2946 [M-I+H]⁺.

((4-methylpyridin-3-yl)ethynyl)trimethylsilane, 128.



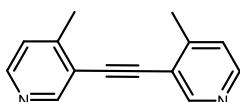
A schlenk flask was charged with 3-Bromo-4-methylpyridine (0.195 mL, 1.74 mmol) Pd(PPh₃)₄ (0.120g, 0.11 mmol) and CuI (0.034 g, 0.17 mmol) blocked from the light. Then, degassed Et₃N (5 mL) was added under a stream of nitrogen followed by trimethylsilylacetylene (0.272 mL, 1.91 mmol, 1.1 equiv). The reaction mixture was sealed and heated up for 16 h at 50 °C. The solvents of the resulting grey mixture were evaporated under vacuum, and was dissolved in DCM (15 mL). The organic phase was washed with saturated sodium bicarbonate solution (5 mL) and extracted with DCM. The combined organic layers dried over MgSO₄. The residue was purified over SiO₂ to yield the corresponding ((4-methylpyridin-3-yl)ethynyl)trimethylsilane in 87% yield (329 mg). **¹H NMR** (400 MHz, Chloroform-d) δ 0.2 (s, 9H, Me), 2.43 (s, 3H, CH₃), 7.13 (d, 1H), 8.3 (d, 1H, CH), 8.67 (d, 1H, CH).

3-Ethynyl-4-methylpyridine, 129.



To a solution of ((4-methylpyridin-3-yl)ethynyl)trimethylsilane, **128** (0.329 g, 1.75 mmol, 1 equiv.) in 3:1 v/v THF/methanol (6mL) was added an excess of anhydrous sodium carbonate (0.850 g, 7 mmol, 4 equiv.). The mixture was stirred overnight, after which the reaction mixture was quenched with water and extracted with diethyl ether. The combined extracts were washed with brine and water, and finally dried over anhydrous MgSO_4 . The crude product was purified by column chromatography on silica gel (hexane as eluent) to afford the product **129** as a colorless oil in 83 % (170 mg). **¹H NMR** (400 MHz, Chloroform-*d*) δ 2.43 (s, 3H, CH₃), 3.72 (s, 1H, CH), 7.25 (d, 1H), 8.56 (d, 1H, CH), 8.95 (d, 1H, CH).

1,2-bis(4-methylpyridin-3-yl)ethyne, 130.



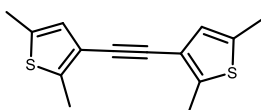
To a solution mixture of 3-ethynyl-4-methylpyridine, **129** (170 mg, 1.45 mmol, 1 equiv.), $\text{Pd}(\text{PPh}_3)_4$ (102 mg, 0.087 mmol, 6 mol %) and CuI (28 mg, 0.145 mmol, 10 mol%), in degassed DBU (1.8 mL, 11.6 mmol, 8 equiv.), was added 3-Bromo-4-methylpyridine (250mg, 1.45 mmol, 1 equiv.). The reaction mixture was maintained at 80°C overnight. After cooling to room temperature, diethyl ether was added and filtered over filter paper. The crude product was purified by column chromatography to afford **130** as a white solid (239 mg, 79%).¹⁶

Mp: 105°C. **¹H NMR** (400 MHz, CDCl_3) 2.39 (s, 6H, CH₃), 7.32-7.38 (m, 2H, CH), 7.44-7.49 (m, 1H, CH), 7.52-7.57 (m, 1H, CH), 7.64-7.69 (m, 2H, CH). **HR-MS** (ESI): calculated for $\text{C}_{14}\text{H}_{13}\text{N}_2$ 209.10732 found $[\text{M}+\text{H}]^+$ 209.1039.

General procedure for the synthesis of the pyridine borane complex.

To a solution of pyridine derivative (1 equiv.) dissolved in toluene was added BH_3/SMe_2 (2 equiv.) at 0°C and left 1h. Petroleum ether was added to the solution and stirred of 30 minutes. After centrifugation, the supernatant was removed and the solid deposit washed again (3×). Filtration gave a white solid

1,2-Bis(2,5-dimethylthiophen-3-yl)ethyne, 141.

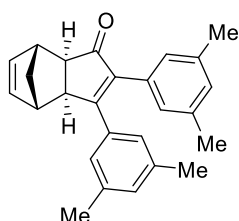


In shlenk sealed tube with teflon-coated, magnetic stir bar was fitted with a rubber septum and flame dried under vacuum. The tube was purged with nitrogen, and charged with $\text{PdCl}_2(\text{PPh}_3)_2$ (59 mg, 0.084 mmol, 2 mol%), CuI (32 mg, 0.168 mmol, 4 mol%) and 2-iodo-3,5-dimethylthiophene **134** (1g, 4.2 mmol, 1 equiv.). While stirring, dry THF (1.96 M), anhydrous NEt_3 (4.2 mL, 7 equiv.) and ice-chilled trimethylsilylethynylene (0.653 mL, 4.62 mmol, 1.1 equiv.) were added. The reaction tube was heated up at 70°C in mineral oil bath, blocked from incidental light, and left stirring at a high rate of speed for 18 h. The following day, reaction mixture was cooled down and 2-iodo-3,5-dimethylthiophene (1g, 4.2 mmol, 1 equiv.), anhydrous NEt_3 (4.2 mL, 7 equiv.) and distilled water (1.68 mmol, 0.030 mL, 40mol%) were added. The mixture was stirred for another 18 h at 70°C. The reaction was partitioned in ethyl ether and distilled water. The organic layer was washed with 10%

HCl, saturated aqueous NaCl and dried over MgSO₄. The solvent was removed under vacuum to afford compound **141** as an oil which was purified over silica gel (481 mg, 55 %).

¹H NMR (400 MHz, CDCl₃, 298 K): δ 2.39 (s, 6H, –CH₃), 2.49 (s, 6H, –CH₃), 6.65 (s, 2H). Positive **ESI-MS**, m/z: 246. HRMS (Positive EI) calcd for C₁₄H₁₄32S₂: m/z = 246.0531; found: 246.0530 [M]⁺.

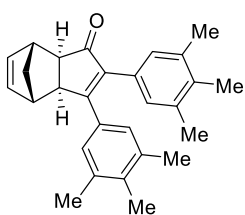
(1S*,2S*,6R*,7R*)-4,5-Bis(3,5-dimethylphenyl)tricyclo[5,2,1,0^{2,6}]-deca-4,8-dien-3-one, 111.



Following the general procedure for the PKR, bis(3,5-dimethylphenyl)acetylene **110** (0.27 mL, 1.14 mmol), dicobalt octacarbonyl (429 mg, 1.25 mmol), and norbornadiene (0.95 mL, 11.39 mmol) were used. The reaction mixture was stirred overnight at 80 °C. Purification by silica gel flash chromatography (hexanes/EtOAc gradient) gave **111** (309 mg, 76%) as a white solid.

M.p. 187 °C. **IR (film)**: 2916, 1694, 1601, 1351, 1243, 685 cm⁻¹. **¹H NMR** (400 MHz, CDCl₃): δ = 1.44 (AB, J = 9 Hz, 1 H, CH₂), 1.48 (AB, J = 9 Hz, 1 H, CH₂), 2.22 (s, 6 H, CH₃), 2.24 (s, 6 H, CH₃), 2.57 (d, J = 5 Hz, 1 H, CH), 2.63 (s, 1 H, CH), 3.10 (s, 1 H, CH), 3.31 (d, J = 5 Hz, 1 H, CH), 6.31 (AB, J = 5, 3 Hz, 1 H, CH), 6.34 (AB, J = 5, 3 Hz, 1 H, CH), 6.79 (s, 2 H, CH), 6.90 (s, 1 H, CH), 6.92 (s, 2 H, CH), 6.96 (s, 1 H, CH) ppm. **¹³C NMR** (100 MHz, CDCl₃): δ = 21.4 (2 CH₃), 21.4 (2 CH₃), 42.0 (CH₂), 43.6 (CH), 44.3 (CH), 50.3 (CH), 52.8 (CH), 126.4 (2 CH), 127.0 (2 CH), 130.0 (CH), 131.4 (CH), 132.3 (C), 135.0 (C), 137.8 (2 C), 137.8 (2 C), 138.0 (CH), 138.5 (CH), 144.1 (C), 169.9 (C), 207.8 (C=O) ppm. C₃₀H₃₄O·0.25H₂O: calcd. C 86.99, H 7.44; found C 86.88, H 7.47. **ESI-HRMS**: calcd. for C₂₆H₂₇O [M+H]⁺ 355.2062; found 355.2064; calcd. for C₅₂H₅₂O₂Na [2M+Na]⁺ 731.3865; found 731.3882 [2M+Na]⁺.

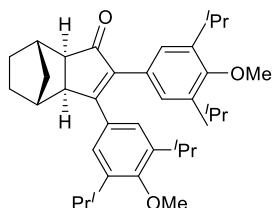
(1S*,2S*,6R*,7R*)-4,5-Bis(3,4,5-Trimethylphenyl)tricyclo[5,2,1,0^{2,6}]-deca-4,8-dien-3-one, 116.



Following the general procedure, bis(3,4,5-trimethylphenyl)acetylene **115** (110 mg, 0.42 mmol), dicobalt octacarbonyl (175 mg, 0.46 mmol), and norbornadiene (0.45 mL, 4.20 mmol) were used. The reaction mixture was stirred for 24 h at 80 °C. Purification by flash chromatography on SiO₂ (hexanes/ EtOAc gradient) gave **3b** (153 mg, 87 %) as a white solid, **116**.

M.p. 188 °C. **IR (film)**: $\tilde{\nu}$ = 2916, 1692, 1502, 1245, 731 cm⁻¹. **¹H NMR** (400 MHz, CDCl₃): δ = 1.42 (AB, J = 9 Hz, 1 H, CH₂), 1.47 (AB, J = 9 Hz, 1 H, CH₂), 2.16 (s, 3 H, CH₃), 2.16 (s, 3 H, CH₃), 2.18 (s, 6 H, CH₃), 2.21 (s, 6 H, CH₃), 2.56 (d, J = 5 Hz, 1 H, CH), 2.65 (s, 1 H, CH), 3.09 (s, 1 H, CH), 3.31 (d, J = 5 Hz, 1 H, CH), 6.30 (AB, J = 5, 3 Hz, 1 H, CH), 6.34 (AB, J = 5, 3 Hz, 1 H, CH), 6.83 (s, 2 H, CH), 7.01 (s, 2 H, CH) ppm. **¹³C NMR** (100 MHz, CDCl₃): δ = 15.4 (CH₃), 15.7 (CH₃), 20.7 (2 CH₃), 20.8 (2 CH₃), 42.1 (CH₂), 43.8 (CH), 44.2 (CH), 50.0 (CH), 52.6 (CH), 127.9 (2 CH), 128.3 (2 CH), 129.6 (C), 131.9 (C), 134.7 (C), 136.4 (4 C), 137.3 (C), 138.0 (CH), 138.5 (CH), 143.5 (C), 169.1 (C), 208.3 (C=O) ppm. C₂₈H₃₀O·0.25H₂O: calcd. C 86.89, H 7.94; found C 86.83, H 8.08. **ESI-HRMS**: calcd. for C₂₈H₃₁O [M + H]⁺ 383.2375; found 383.2372; calcd. for C₅₆H₆₀O₂Na [2M + Na]⁺ 787.4491; found 787.4506.

(1S*, 2S*, 6R*, 7R*)-4,5-Bis(3,5-di-iso-propyl-4-metoxyphenyl)tricyclo[5,2,1,02,6]deca-4-en-3-one, 120.



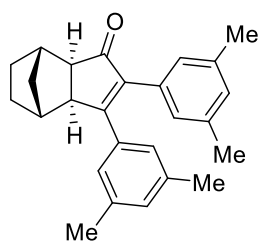
Following the general procedure, bis(3,5-di-iso-propyl-4-metoxyphenyl)acetylene **119** (150 mg, 0.37 mmol), dicobalt octacarbonyl (154 mg, 0.41 mmol) and norbornene (215 mg, 2.21 mmol) were used. The reaction was stirred 5 days at 105 °C. Purification by flash chromatography on SiO₂ (Combiflash®, hexanes/EtOAc gradient) afforded **120** (193 mg, 99%) as a white foam.

IR (film) ν_{max} 2960, 1693, 1468, 1012, 736 cm⁻¹. **¹H NMR** (400 MHz, CDCl₃) δ 1.00(d, J = 7 Hz, 6H, 2CH₃), 1.05 (d, J = 10 Hz, 1H, CH₂), 1.09 (d, J = 7 Hz, 6H, 2CH₃), 1.10 (d, J = 7 Hz, 6H, 2CH₃), 1.14 (d, J = 7 Hz, 6H, 2CH₃), 1.30 (d, J = 10 Hz, 1H, CH₂), 1.39-1.48 (m, 2H, CH₂), 1.64-1.75 (m, 2H, CH₂), 2.25 (s, 1H, CH), 2.48 (d, J = 5 Hz, 1H, CH), 2.62 (s, 1H, CH), 3.16 (s, 1H, CH), 3.20 (hept, J = 7 Hz, 2H, CH), 3.25 (hept, J = 7 Hz, 2H, CH), 3.68 (s, CH₃), 3.69 (s, CH₃), 6.82 (s, 2H, CH), 6.98 (s, 2H, CH) ppm. **¹³C NMR** (100 MHz, CDCl₃) δ 23.8 (2CH₃), 23.8 (2CH₃), 24.1 (2CH₃), 24.4 (2CH₃), 26.5 (CH), 26.6 (CH), 29.0 (CH₂), 29.2 (CH₂), 32.0 (CH₂), 38.8 (CH), 39.4 (CH), 50.6 (2CH), 54.4 (2CH), 62.2 (CH₃), 62.2 (CH₃), 125.0 (2CH), 125.3 (2CH), 129.5 (C), 131.5 (C), 141.6 (2C), 141.8 (2C), 143.4 (C), 154.1 (C), 155.7 (C), 170.5 (C), 208.9 (C=O) ppm. **HRMS-ESI** m/z calcd. for C₃₆H₄₉O₃: 529.3682, found 529.3674 [M+H]⁺; calcd. for C₇₂H₉₇O₆: 1057.7285, found 1057.7257 [2M+H]⁺.

General procedure for hydrogenation

In a flask charged with a solution of the Pauson-Khand adduct (1 equiv.) in EtOH (volume necessary to reach a homogeneous solution), was added under nitrogen Pd/C 10% (5% mol). The flask was flushed with 1 bar hydrogen and the mixture was stirred under hydrogen atmosphere until the total disappearance of the starting material. The solution was filtered on a celite pad, rinsed with methanol and the concentration of the filtrate under reduced pressure afforded the corresponding product which was of high purity (>95%) that any further purification was necessary.

(1S*, 2S*, 6R*, 7R*)-4,5-Bis(3,5-dimethylphenyl)tricyclo[5,2,1,02,6]-deca-4-en-3-one, 112.

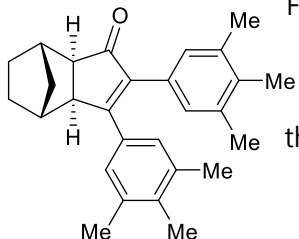


Pd/C (29 mg, 0.03 mmol) was added to a solution of Pauson-Khand adduct **111** (191 mg, 0.54 mmol) in ethanol (5 mL) under nitrogen. The flask was flushed with hydrogen and stirred until the total disappearance of the starting material was observed. The solution was filtered through a celite pad and rinsed with methanol. Concentration of the filtrate under reduced pressure gave **112** (166 mg, 87%) as a white solid. The product was also obtained by PKR of **110** with norbornene following the general procedure (78%).

m.p. 162 °C. **IR** (film): $\tilde{\nu}$ = 2956, 1693, 1601, 1352, 1249, 852 cm⁻¹. **¹H NMR** (400 MHz, CDCl₃): δ = 1.00 (d, J = 10 Hz, 1 H, CH₂), 1.24 (d, J = 10 Hz, 1 H, CH₂), 1.36–1.46 (m, 2 H, CH₂), 1.62–1.70 (m, 2 H, CH₂), 2.13 (s, 1 H, CH), 2.21 (s, 6 H, CH₃), 2.23 (s, 6 H, CH₃), 2.46 (d, J = 5 Hz, 1 H, CH), 2.58 (s, 1 H, CH), 3.17 (d, J = 6 Hz, 1 H, CH), 6.78 (s, 2 H, CH), 6.90 (s, 1 H, CH), 6.91 (s, 2 H, CH), 6.94 (s, 1 H,

CH) ppm. **13C NMR** (100 MHz, CDCl₃): δ = 21.4 (2 CH₃), 21.4 (2 CH₃), 29.1 (CH₂), 29.2 (CH₂), 31.8 (CH₂), 38.6 (CH), 39.7 (CH), 50.8 (CH), 54.1 (CH), 126.5 (2 CH), 127.0 (2 CH), 129.5 (CH), 131.3 (CH), 132.5 (C), 135.2 (C), 137.8 (2 C), 137.8 (2 C), 143.0 (C), 170.0 (C), 209.2 (C=O) ppm.

(1S*, 2S*, 6R*, 7R*)-4,5-Bis(3, 4, 5-trimethylphenyl)tricyclo[5,2,1,0^{2,6}]deca-4-en-3-one, 121.



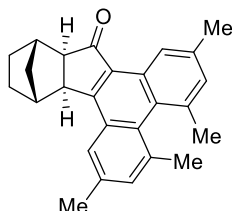
Following the general procedure, Pauson-Khand adduct **116** (153 mg, 0.42 mmol), and Pd/C (22 mg, 0.02 mmol) were used. The reaction was stirred 2 days at room temperature. Filtration through celite and evaporation of the solvent under *vacuum* afforded **121** (149 mg, 97 %) as a white solid.

M.p.: 207 °C. **IR** (film) ν_{\max} , 2955, 1691, 1453, 1352, 1199, 1015 cm⁻¹. **1H NMR** (400 MHz, CDCl₃) δ 0.99 (d, *J* = 10 Hz, 1H, CH₂), 1.23 (d, *J* = 10 Hz, 1H, CH₂), 1.36-1.47 (m, 2H, CH₂), 1.61-1.69 (m, 2H, CH₂), 2.15 (s, 1H, CH), 2.15 (s, 6H, CH₃), 2.17 (s, 6H, CH₃), 2.21 (s, 6H, CH₃), 2.44 (d, *J* = 5 Hz, 1H, CH), 2.57 (s, 1H, CH), 3.17 (d, *J* = 6 Hz, 1H, CH), 6.82 (s, 2H, CH), 6.97 (s, 2H, CH) ppm. **13C NMR** (100 MHz, CDCl₃) δ 15.4 (CH₃), 15.7 (CH₃), 20.7 (2CH₃), 20.8 (2CH₃), 29.1 (CH₂), 29.3 (CH₂), 31.8 (CH₂), 38.9 (CH), 39.6 (CH), 50.4 (CH), 54.0 (CH), 128.1 (2CH), 128.3 (2CH), 129.8 (C), 132.0 (C), 134.6 (C), 136.3 (2C), 136.4 (2C), 137.2, (C) 142.4 (C), 169.2 (C), 209.4 (C=O) ppm.

General Procedure for the Photochemical Reactions

A solution of PK adducts (1 equiv.) and I₂ (1 equiv.) in methanol with the PK adduct at a concentration of 0.018 M was placed into a flask provided with magnetic stirring. The solution was irradiated at 300 nm in a Rayonet reactor equipped with 8 or 16 lamps, in the presence of oxygen at room temperature. The reaction was monitored by TLC. After completion of the reaction, a solution of Na₂S₂O₃ was added, and the aqueous phase was extracted with DCM. The combined organic extracts were dried (MgSO₄), filtered, and concentrated under reduced pressure. The crude reaction product was purified by flash chromatography on SiO₂ (Combiflash®, hexanes/EtOAc gradient).

(8cR*, 9S*, 12R*, 12aS*)-8c,9,10,11,12,12a-Hexahydro-9,12-methano-2,4,5,7-tetramethyl-13H-indeno[1,2-l]phenanthren-13-one 124.



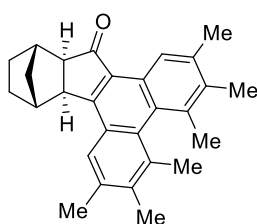
Following the general procedure, compound **116** (50 mg, 0.14 mmol) and I₂ (50 mg, 0.24 mmol) were used. The reaction was irradiated in the presence of oxygen for 36 h. Flash chromatography over silica gel (Combiflash®, hexanes/EtOAc gradient) gave **124** (48 mg, 96%) as a white solid.

M.p. 206 °C. **IR** (film): $\tilde{\nu}$ = 2955, 1686, 1609, 1451, 1247, 731 cm⁻¹. **1H NMR** (400 MHz, CDCl₃) (mixture of atropisomers): δ = 0.98 (br. s, 2 H, CH₂, maj. + min.), 1.44–1.52 (m, 1 H, CH₂, min. + maj.), 1.62–1.69 (m, 1 H, CH₂, min. + maj.), 1.70–1.85 (m, 2 H, CH₂, min. + maj.), 2.51 (s, 3 H, CH₃, min.), 2.53 (s, 3 H, CH₃, maj.), 2.53 (s, 3 H, CH₃, maj.), 2.54 (s, 3 H, CH₃, maj. + min.), 2.55 (s, 3 H, CH₃, min.), 2.58 (s, 3 H, CH₃, maj. + min.), 2.60–2.70 (m, 3 H, CH, maj. + min.), 3.35 (d, *J* = 6 Hz, 1 H, CH, min.), 3.41 (d, *J* = 6 Hz, 1 H, CH, maj.), 7.26 (s, 1 H, CH, maj.), 7.26 (s, 1 H, CH, min.),

7.39 (br. s, 1 H, CH, maj. + min.), 7.74 (s, 1 H, CH, maj.), 7.79 (s, 1 H, CH, min.), 8.90 (s, 1 H, CH, maj.), 8.91 (s, 1 H, CH, min.) ppm. **¹³C NMR (100 MHz, CDCl₃)**: δ = 21.4 (min., CH₃), 21.5 (maj., CH₃), 21.5 (min., CH₃), 21.6 (maj., CH₃), 21.7 (maj., CH₃), 21.8 (maj., CH₃), 21.8 (min., CH₃), 21.8 (min., CH₃), 28.7 (min., CH₂), 29.0 (maj., CH₂), 29.7 (maj., CH₂), 29.8 (min., CH₂), 32.5 (CH₂), 39.2 (min., CH), 39.9 (maj., CH), 40.1 (maj., CH), 41.1 (min., CH), 46.0 (maj., CH), 46.6 (min., CH), 56.6 (maj., CH), 57.1 (min., CH), 121.0 (maj., CH), 121.2 (min., CH), 122.3 (maj., CH), 122.6 (min., CH), 128.4 (C), 128.6 (maj., C), 128.6 (min., C), 130.1 (min., C), 130.6 (maj., C), 130.6 (CH), 132.0 (maj., C), 132.2 (min., C), 132.4 (maj., C), 132.6 (min., C), 133.1 (min., CH), 133.3 (maj., CH), 135.3 (maj., C), 135.3 (min., C), 135.9 (C), 136.4 (min., C), 136.5 (maj., C), 136.9 (maj., C), 136.9 (min., C), 160.2 (min., C), 160.3 (maj., C), 208.8 (min., C=O) 208.9 (maj., C=O) ppm. C₂₆H₂₆O·1/3H₂O: calcd. C 86.63, H 7.46; found C 86.61, H 7.43.

ESI-HRMS: calcd. for C₂₆H₂₇O [M + H]⁺ 355.2062; found 355.2068; calcd. for C₅₂H₅₃O₂ [2M + H]⁺ 709.4046; found 709.4033.

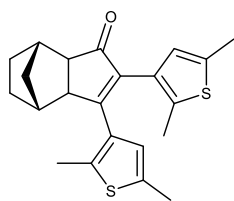
(8cR*,9S*,12R*,12aS*)-8c,9,10,11,12,12a-Hexahydro-9,12-methano-2,3,4,5,6,7-tetramethyl-13H-indeno[1,2-l]phenanthren-13-one, 125.



Following the general procedure, compound 116 (50 mg, 0.13 mmol) was irradiated in the presence of I₂ (33 mg, 0.13 mmol). After 54 h, the crude product was purified by flash chromatography on SiO₂ (Combiflash®, hexanes/EtOAc gradient) to give 125 (45 mg, 93%) as a mixture of atropisomers.

M.p. 219 °C. **IR (film)**: ν = 2915, 1681, 1649, 1443, 1380, 733 cm⁻¹. **¹H NMR (400 MHz, CDCl₃) 6bM**: δ = 0.96 (s, 2 H, CH₂), 1.43–1.50 (m, 1 H, CH₂), 1.72 (dt, J = 12, 4 Hz, 1 H, CH₂), 1.76–1.85 (m, 2 H, CH₂), 2.38 (s, 3 H, CH₃), 2.41 (s, 3 H, CH₃), 2.42 (s, 3 H, CH₃), 2.43 (s, 3 H, CH₃), 2.52 (s, 3 H, CH₃), 2.56 (s, 3 H, CH₃), 2.60 (br. s, 1 H, CH), 2.61 (br. s, 1 H, CH), 2.64 (d, J = 3 Hz, 1 H, CH), 3.39 (d, J = 6 Hz, 1 H, CH), 7.76 (s, 1 H, CH), 8.90 (s, 1 H, CH) ppm. **¹H NMR (400 MHz, CDCl₃) 6bP**: δ = 0.95 (s, 2 H, CH₂), 1.43–1.50 (m, 1 H, CH₂), 1.59–1.66 (m, 1 H, CH₂), 1.67–1.83 (m, 2 H, CH₂), 2.38 (s, 3 H, CH₃), 2.39 (s, 3 H, CH₃), 2.43 (s, 6 H, CH₃), 2.52 (s, 3 H, CH₃), 2.56 (s, 3 H, CH₃), 2.63 (d, J = 6 Hz, 1 H, CH), 2.66 (d, J = 3 Hz, 1 H, CH), 2.69 (d, J = 4 Hz, 1 H, CH), 3.35 (d, J = 6 Hz, 1 H, CH), 7.81 (s, 1 H, CH), 8.92 (s, 1 H, CH) ppm. **¹³C NMR (100 MHz, CDCl₃) mixture 6bM (major)/6bP (minor)**: δ = 16.5 (maj., CH₃), 16.8 (min., CH₃), 16.9 (maj., CH₃), 21.2 (maj., CH₃), 21.2 (maj., CH₃), 21.3 (maj., CH₃), 21.4 (maj., CH₃), 21.5 (min., CH₃), 28.8 (min., CH₂), 29.0 (maj., CH₂), 29.7 (maj., CH₂), 29.8 (min., CH₂), 32.5 (maj., CH₂), 39.1 (min., CH), 39.8 (maj., CH), 40.1 (maj., CH), 41.1 (min., CH), 45.9 (maj., CH), 46.5 (min., CH), 59.8 (maj., CH), 59.2 (min., CH), 121.7 (maj., 2 CH), 121.8 (min., 2 CH), 122.9 (maj., 2 CH), 123.3 (min., 2 CH), 126.2 (maj., C), 127.7 (min., C), 128.3 (maj., C), 129.3 (maj., C), 131.3 (maj., C), 133.1 (maj., C), 133.4 (min., C), 134.0 (maj., C), 134.7 (maj., C), 135.1 (min., C), 135.2 (maj., C), 135.3 (maj., C), 136.1 (maj., C), 137.8 (min., C), 138.0 (maj., C), 159.4 (min., C), 159.6 (maj., C), 208.9 (maj., C=O) ppm. C₂₈H₃₀O·0.2H₂O: calcd. C 87.09, H 7.94; found C 87.31, H 7.97. **ESI-HRMS**: calcd. for C₂₈H₃₁O [M + H]⁺ 383.2375; found 383.2369.

2,3-bis(2,5-dimethylthiophen-3-yl)-3a,4,7,7a-tetrahydro-1H-4,7-methanoinden-1-one, 145.



Under nitrogen atmosphere, the starting material (0.200g, 0.81mmol, 1equiv.) was dissolved in anhydrous toluene (0.081M) followed by the addition of octacarbonyl cobalt complex (0.278 g, 0.81 mmol, 1 equiv.) and NBD (0.413 mL, 4.06 mmol, 5 equiv.). After overnight reaction, the complex mixture was evaporated and preparative chromatographic plate (30% AcOEt

in hexane) was done which afforded 6% yield of the final product **145**. **DEPCI-MS**: calcd. for C₂₂H₂₃OS₂ found [M+H]⁺ 367.5; expected 367.12. Calcd. for C₂₂H₂₅NOS₂ found [M+NH₃]⁺ 383.5, expected 383.14.

Table. The NBO charges for the different substrates according to gas-phase TPSS-D3/def2-TZVPP computations.

Sub	C ₁	C ₂	C ₃	C ₄	(C ₂ -C ₃).100	(C ₁ -C ₄).100	alfa	beta
1	-0.12	-0.08	0.01	-0.45	-9.02	32.77	0	85
2	-0.13	-0.05	0.02	-0.45	-6.90	32.03	7	90
3	-0.11	-0.05	0.02	-0.45	-6.36	33.77	2	63
4	-0.13	-0.07	0.05	-0.45	-11.38	31.86	2	58
9	-0.27	-0.06	-0.01	-0.45	-4.39	17.23	0	49
10	-0.25	-0.17	0.16	-0.47	-32.52	22.37	0	29
11	-0.27	-0.05	0.01	-0.45	-6.26	17.59	9	35
12	-0.28	-0.05	0.01	-0.45	-6.24	16.91	13	33
5	-0.54	-0.03	0.02	-0.45	-4.89	-9.48	8	72
13	-0.88	-0.02	-0.04	-0.44	1.42	-43.77	77	3
14	-0.45	-0.02	-0.02	-0.44	0.21	-0.87	77	2
6	-0.14	-0.03	0.02	-0.14	-4.47	-0.37	16	18

References

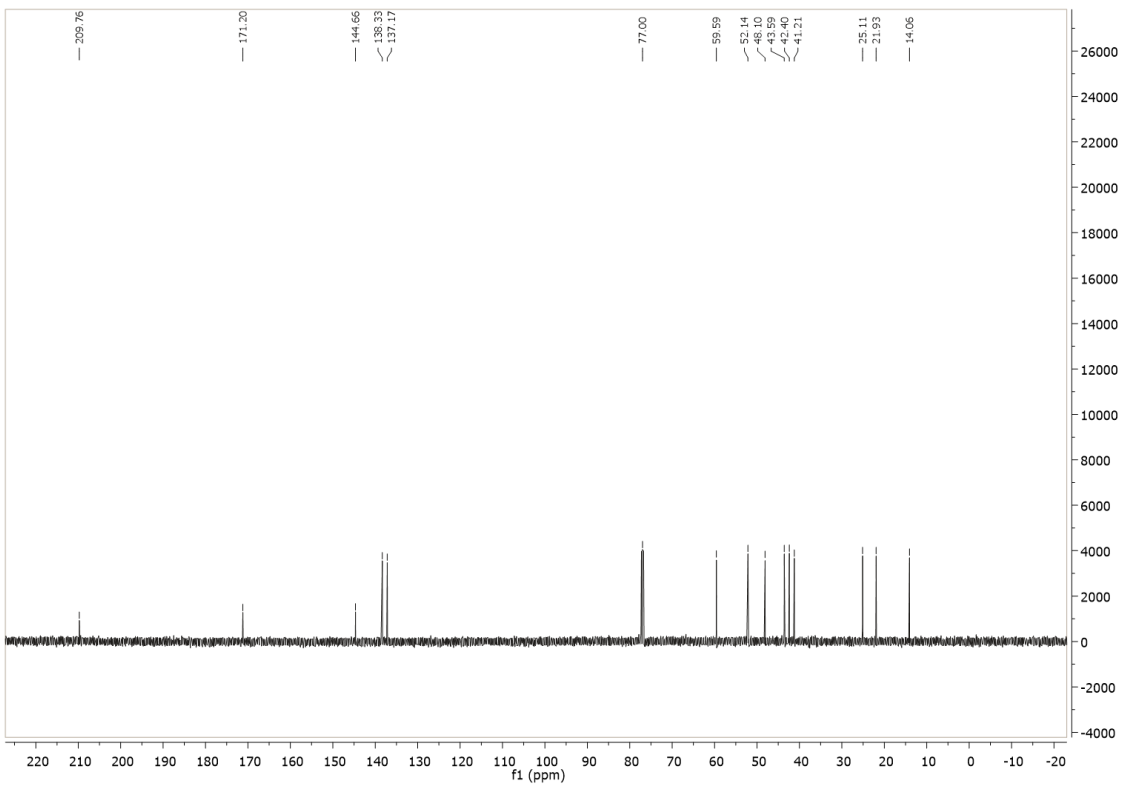
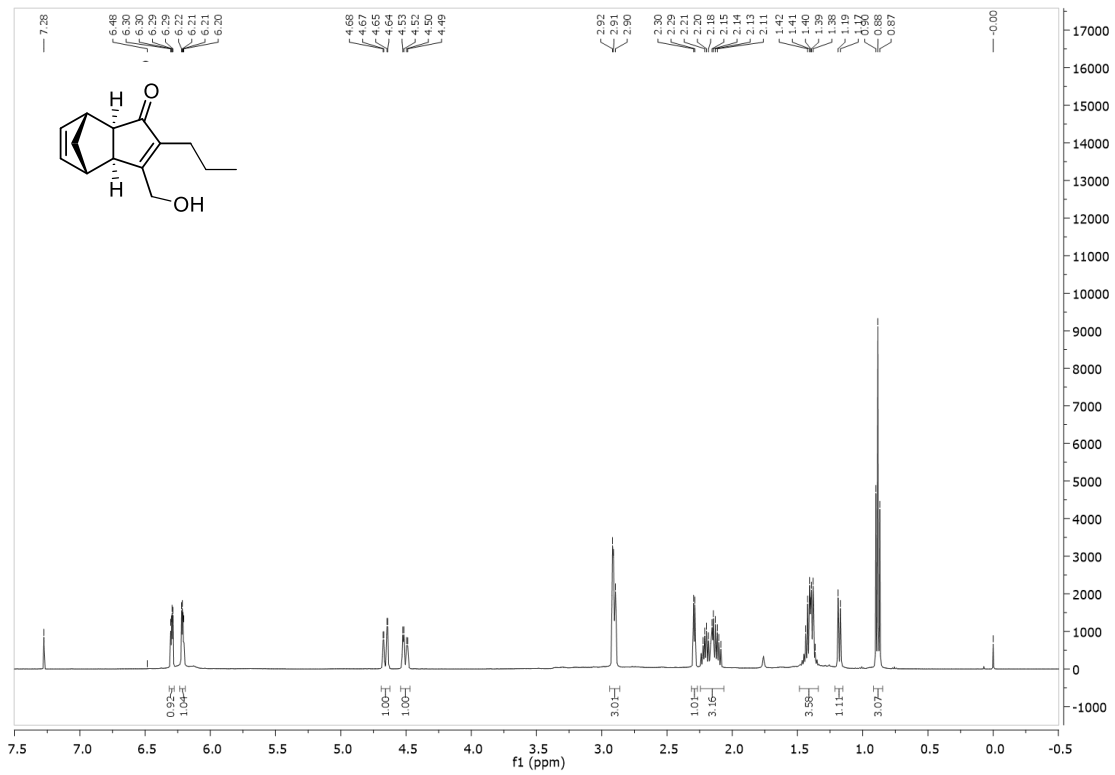
- (1) Couffignal, R. Gaudemar, M. Perriot, P. *Bull. Soc. Chim. Fr.* **1967**, *10*, 3909–3910.
- (2) Adachi, Y.; Kamei, N.; Yokoshima, S.; Fukuyama, T. *Org. Lett.* **2011**, *13*(16), 4446–4449.
- (3) Onishi, Y.; Nishimoto, Y.; Yasuda, M.; Baba, A. *Org. Lett.* **2014**, *16*(4), 1176–1179.
- (4) Colonge, J. Descotes, G. *Bull. Soc. Chim. Fr.* **1959**, 815–816.
- (5) Bonnet, S.; Siegler, M. A.; van Lenthe, J. H.; Lutz, M.; Spek, A. L.; van Koten, G.; Klein Gebbink, R. J. M. *Eur. J. Inorg. Chem.* **2010**, *2010*(29), 4667–4677.
- (6) Alsters, P. L.; Baesjou, P. J.; Janssen, M. D.; Kooijman, H.; Sicherer-Roetman, A.; Spek, A. L.; Van Koten, G. *Organometallics* **1992**, *11*(12), 4124–4135.
- (7) Kjellgren, J.; Sundén, H.; Szabó, K. J. *J. Am. Chem. Soc.* **2004**, *126*(2), 474–475.
- (8) Wang, Y.; Xu, L.; Yu, R.; Chen, J.; Yang, Z. *Chem. Commun. (Camb)*. **2012**, *48*(66), 8183–8185.
- (9) Chachignon, H.; Scalacci, N.; Petricci, E.; Castagnolo, D. *J. Org. Chem.* **2015**, *80*(10), 5287–5295.
- (10) Lin, A.; Zhang, Z.-W.; Yang, J. *Org. Lett.* **2014**, *16*(2), 386–389.
- (11) Al-Qaisi, J. A.; Alhussainy, T. M.; Qinna, N. A.; Matalka, K. Z.; Al-Kaissi, E. N.; Muhi-Eldeen, Z. A. *Arab. J. Chem.* **2014**, *7*(6), 1024–1030.
- (12) Trost, B. M.; Taft, B. R.; Masters, J. T.; Lumb, J.-P. *J. Am. Chem. Soc.* **2011**, *133*(22), 8502–8505.
- (13) Westmeier, J.; Kress, S.; Pfaff, C.; von Zezschwitz, P. *J. Org. Chem.* **2013**, *78*(21), 10718–10723.
- (14) Paul, A.; Einsiedel, J.; Waibel, R.; Heinemann, F. W.; Meyer, K.; Gmeiner, P. *Tetrahedron* **2009**, *65*(31), 6156–6168.

- (15) Sevez, G.; Pozzo, J.-L. *Dye. Pigment.* **2011**, *89*(3), 246–253.
- (16) Moreno-García, P.; Gulcur, M.; Manrique, D. Z.; Pope, T.; Hong, W.; Kaliginedi, V.; Huang, C.; Batsanov, A. S.; Bryce, M. R.; Lambert, C.; Wandlowski, T. *J. Am. Chem. Soc.* **2013**, *135*(33), 12228–12240.
-

CHAPTER VII

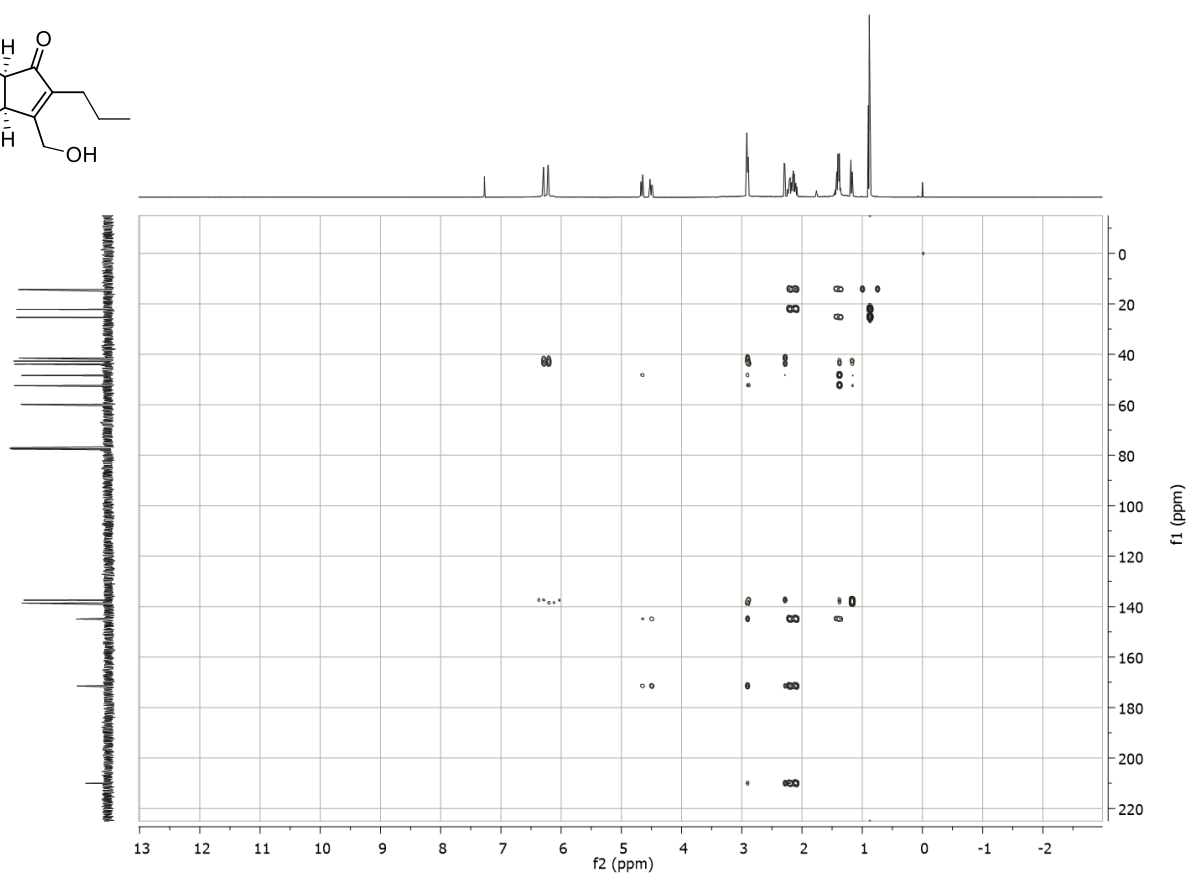
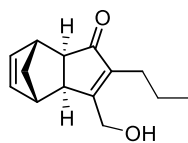
Selected spectra

Selected spectra

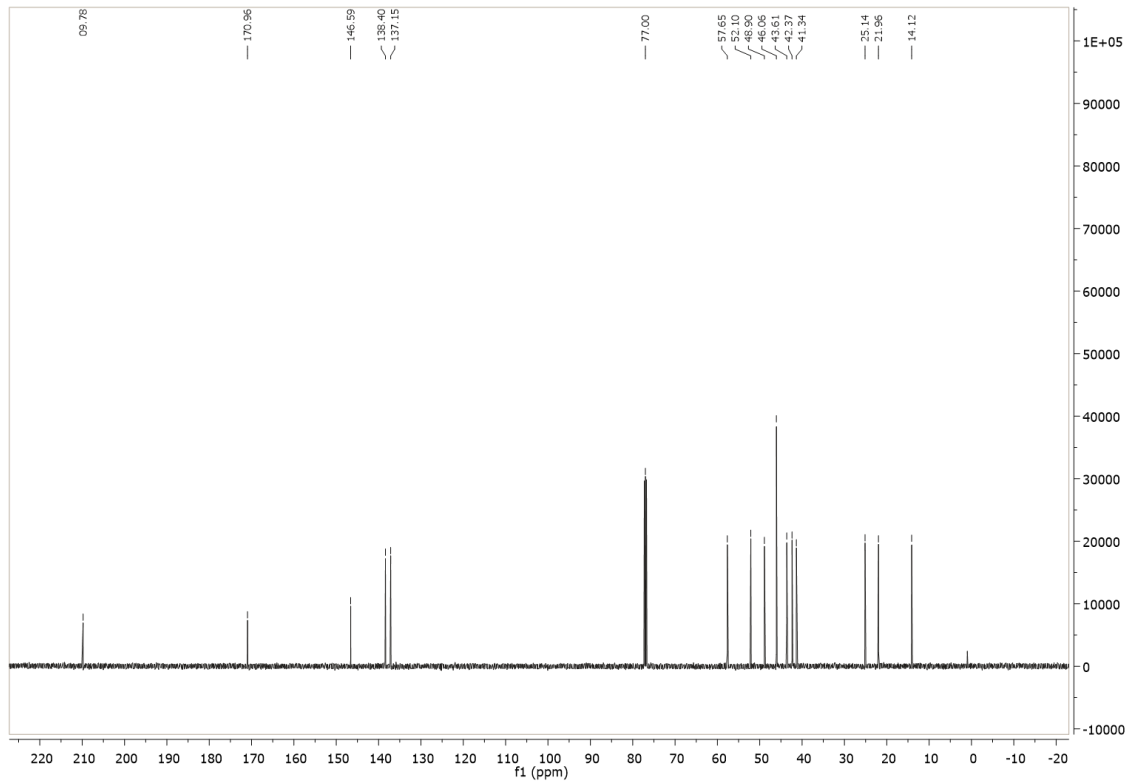
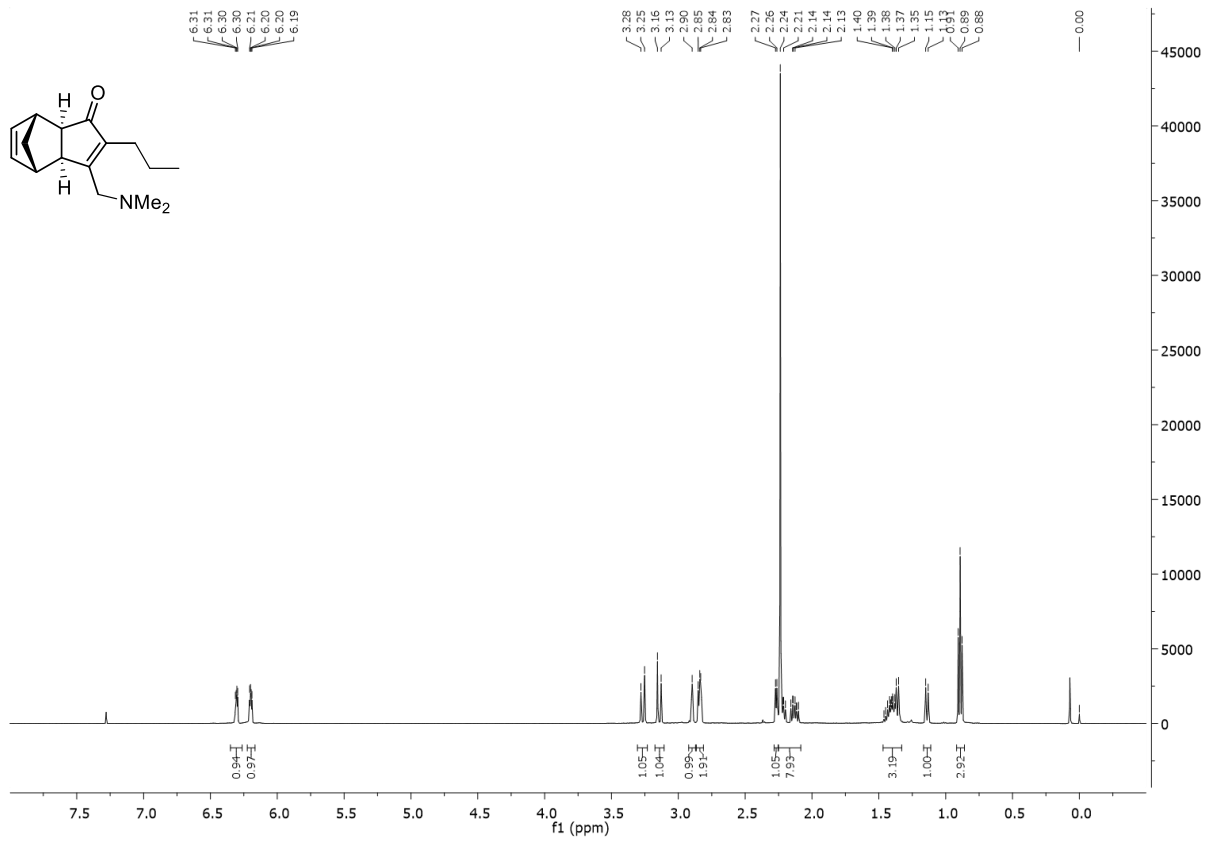


Selected spectra

HMBC

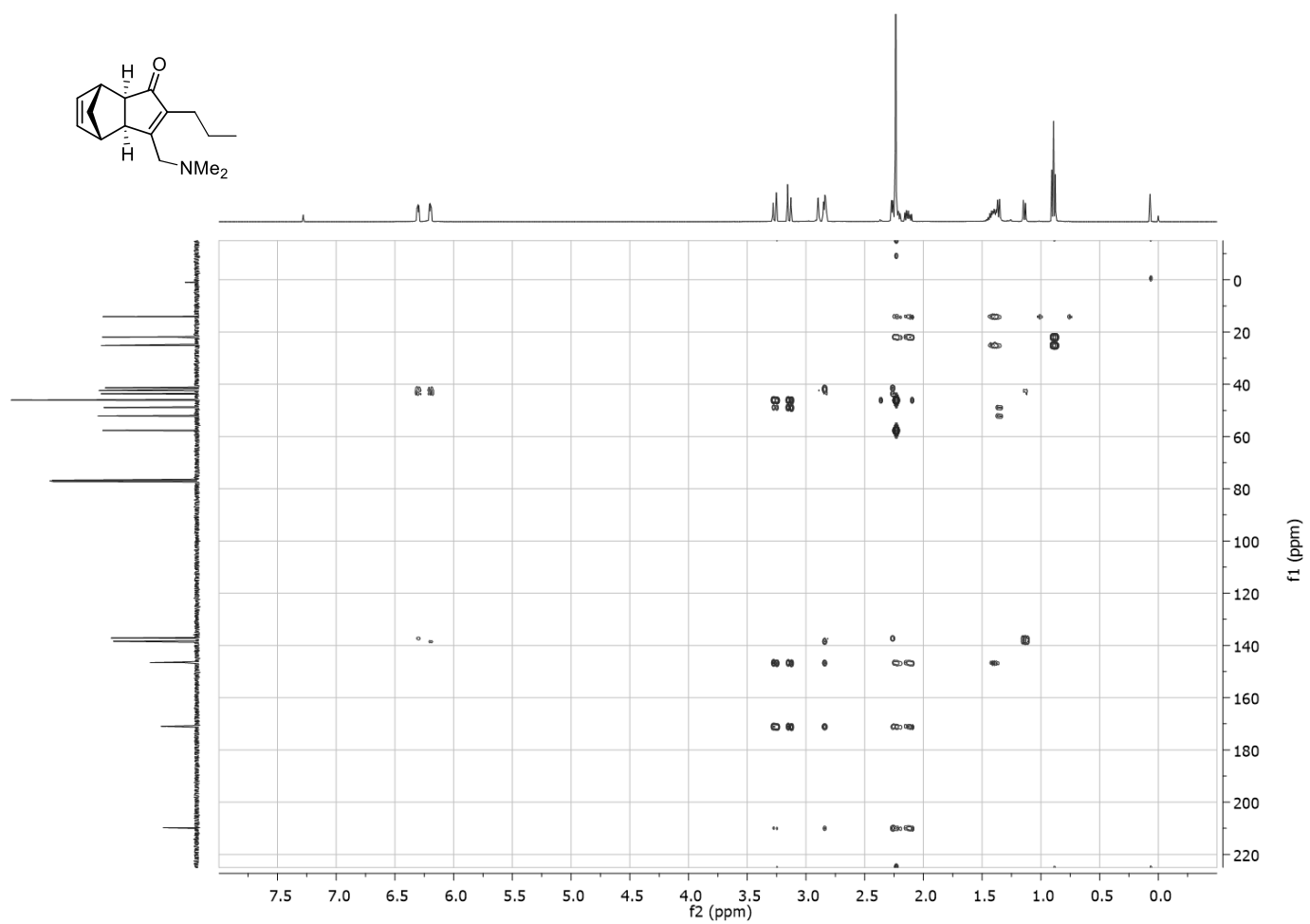
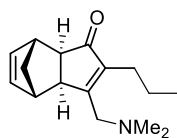


Selected spectra

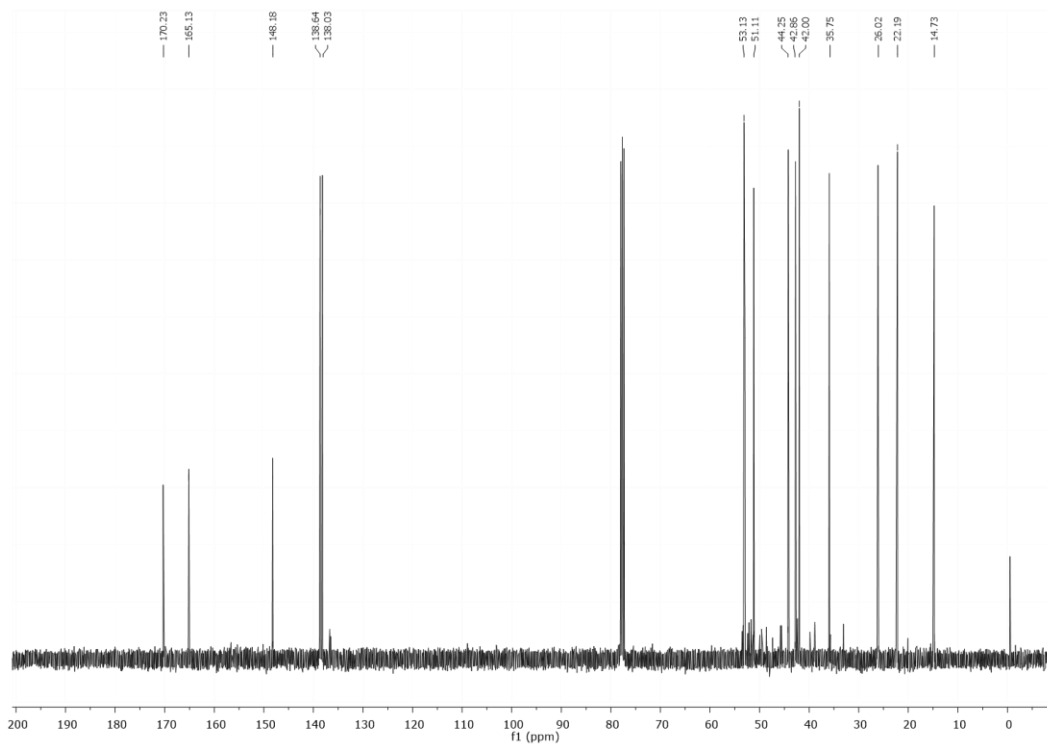
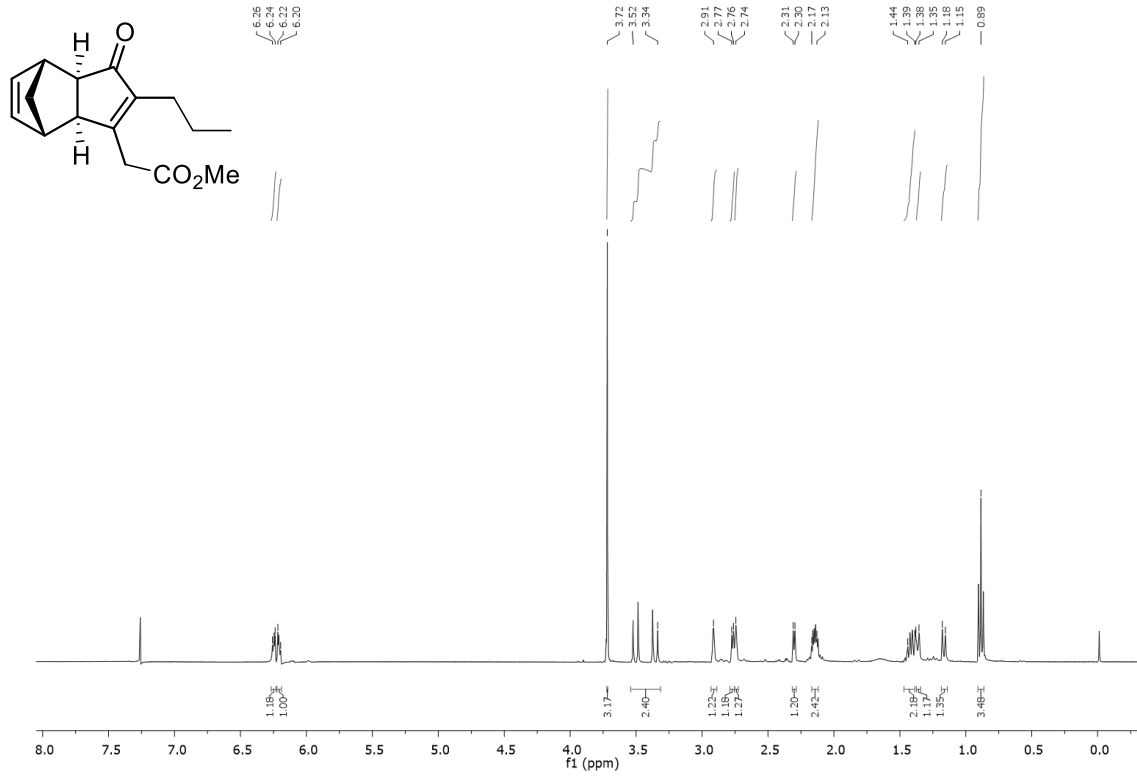


Selected spectra

HMBC

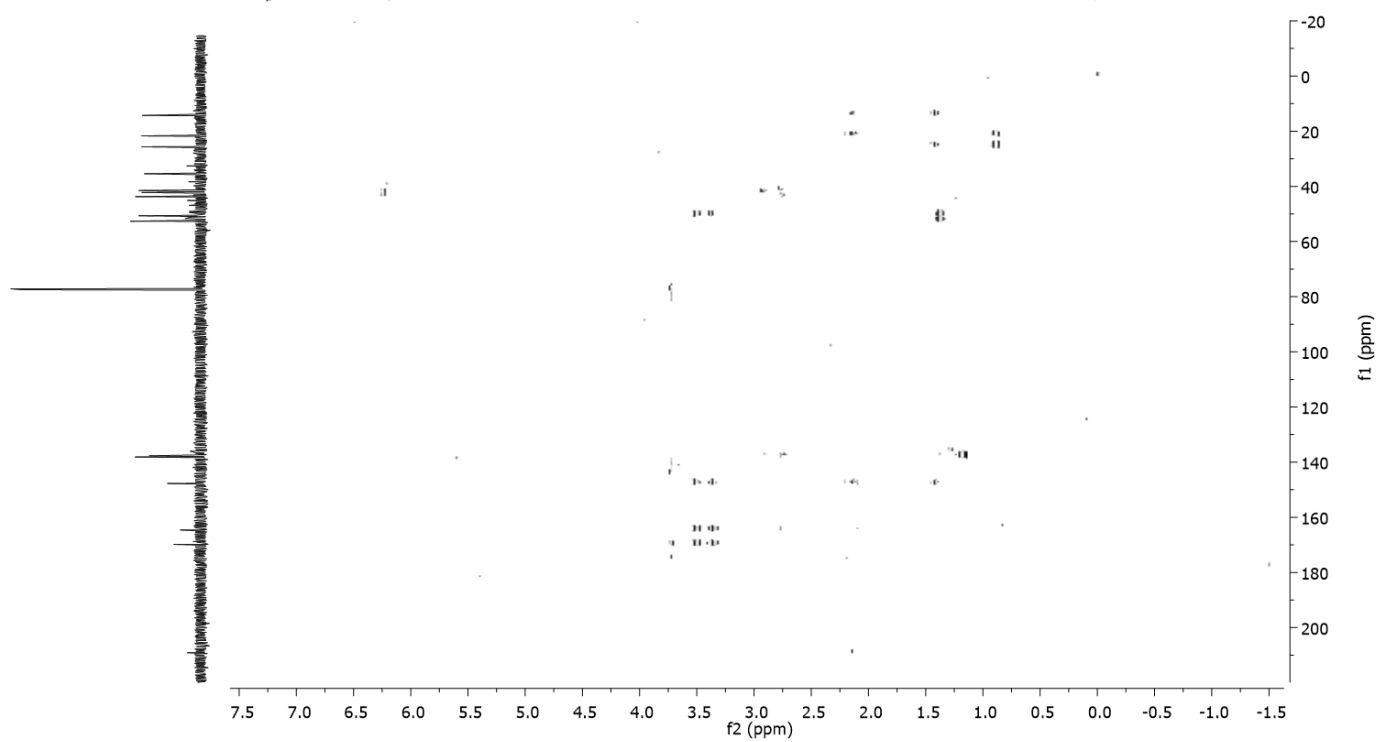
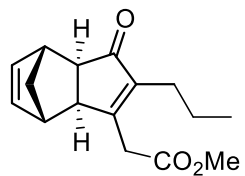


Selected spectra



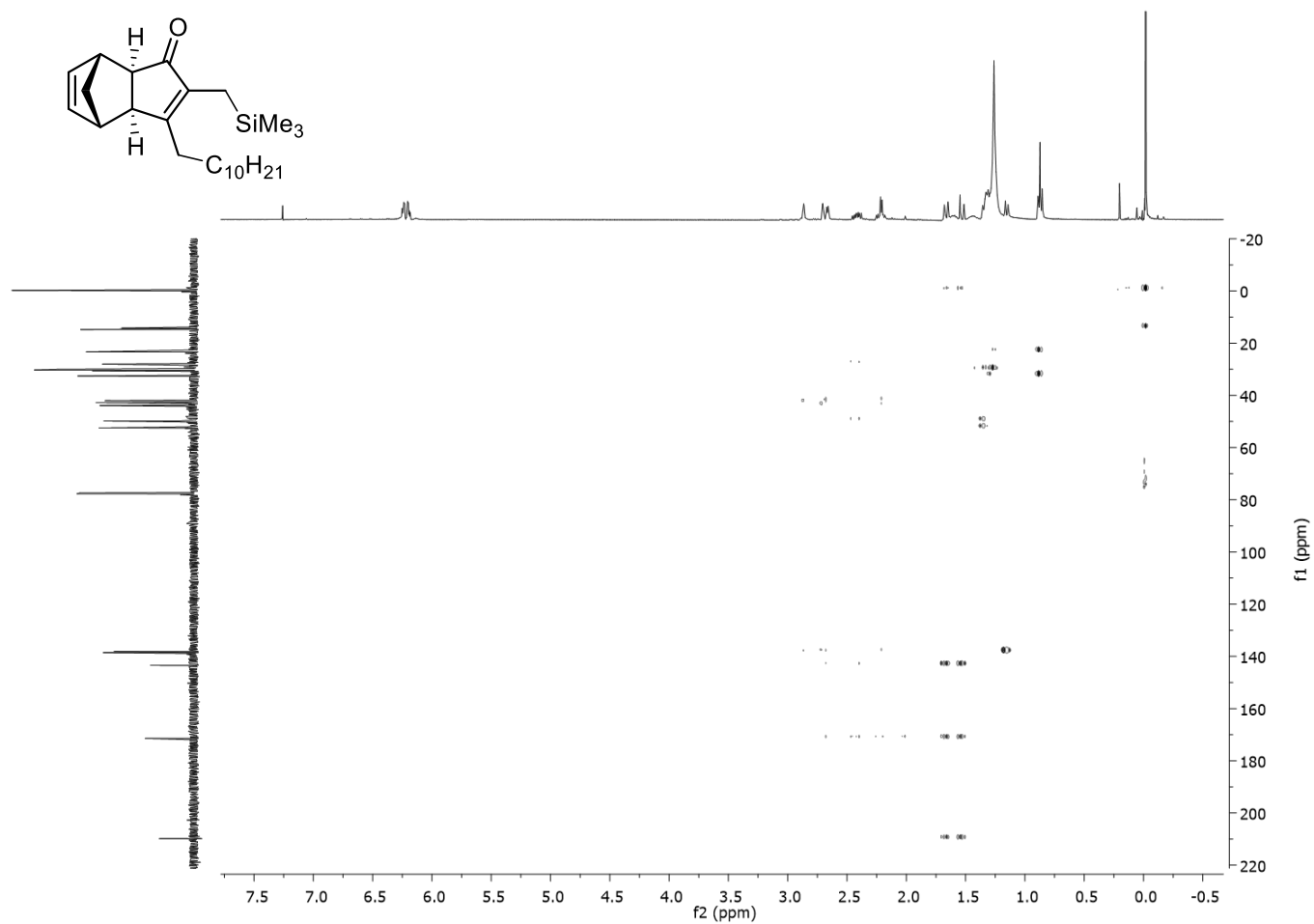
Selected spectra

HMBC

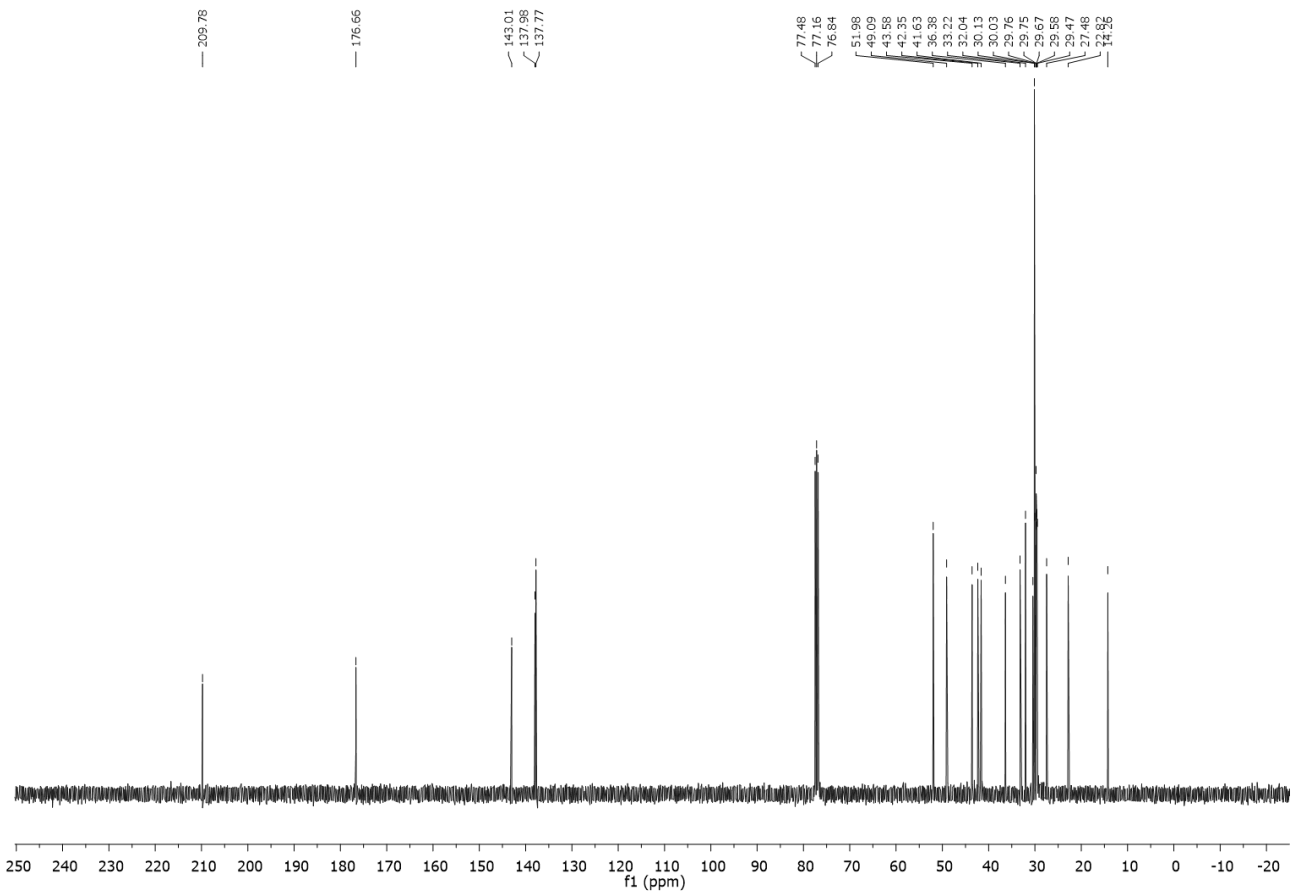
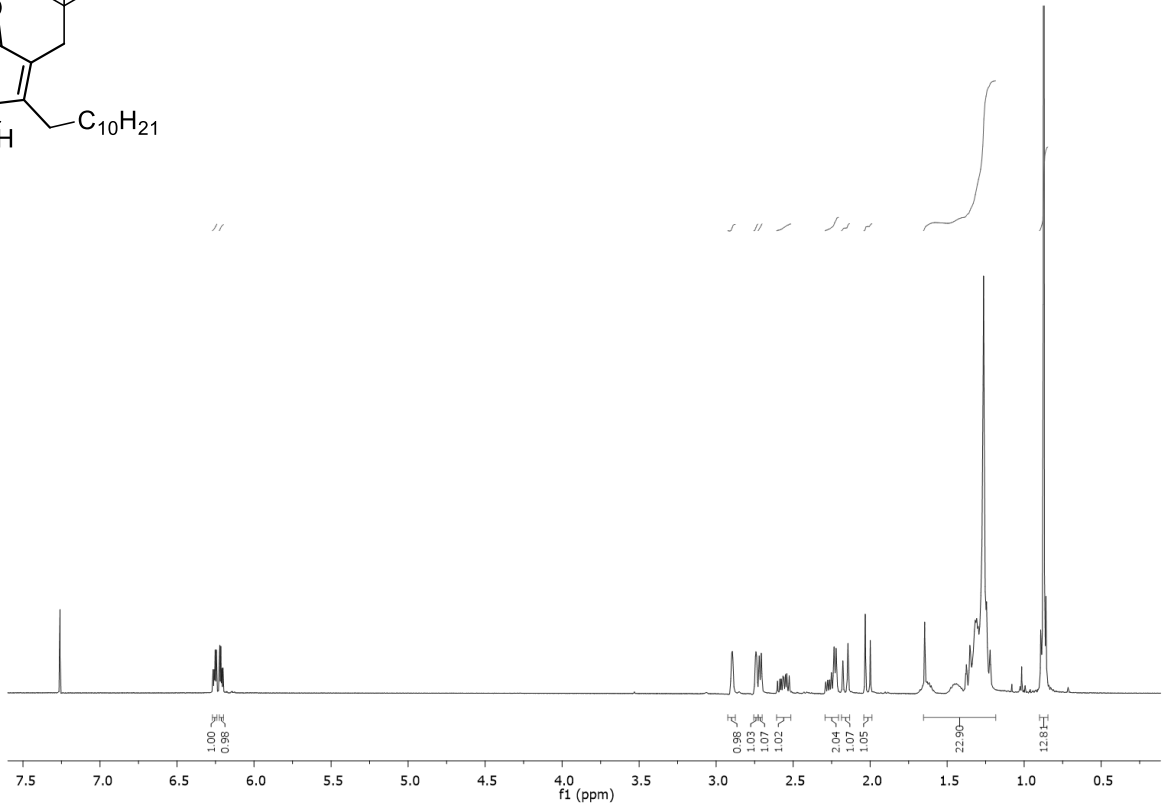
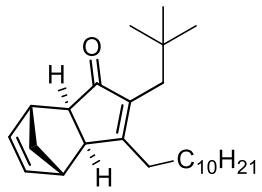


Selected spectra

HMBC

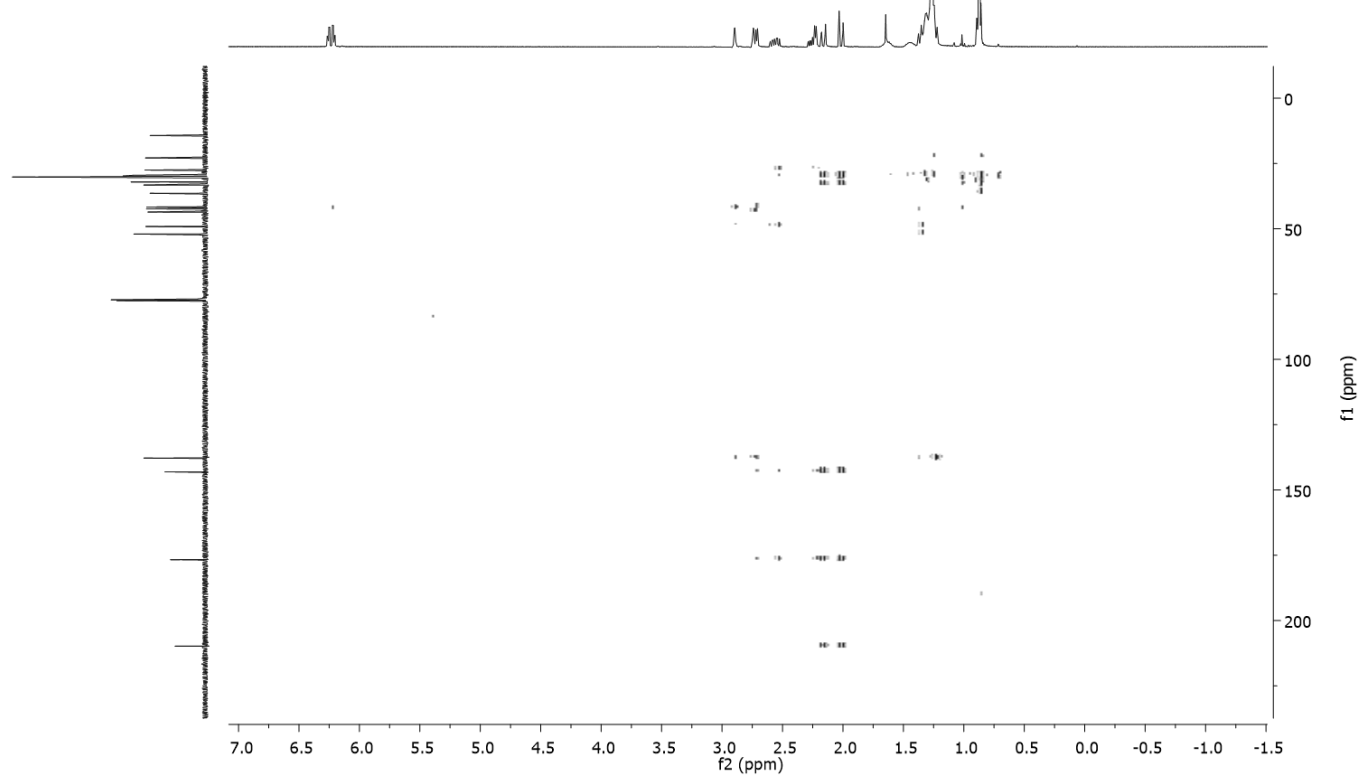
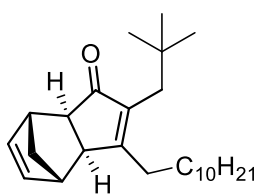


Selected spectra

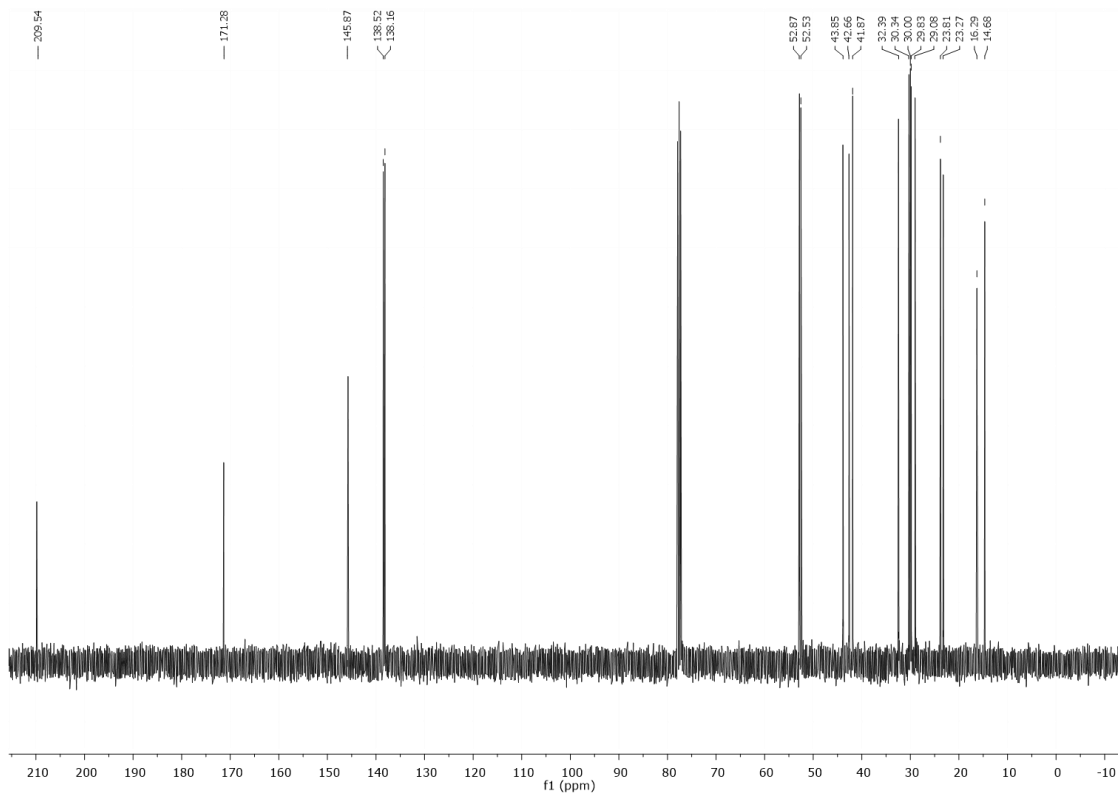
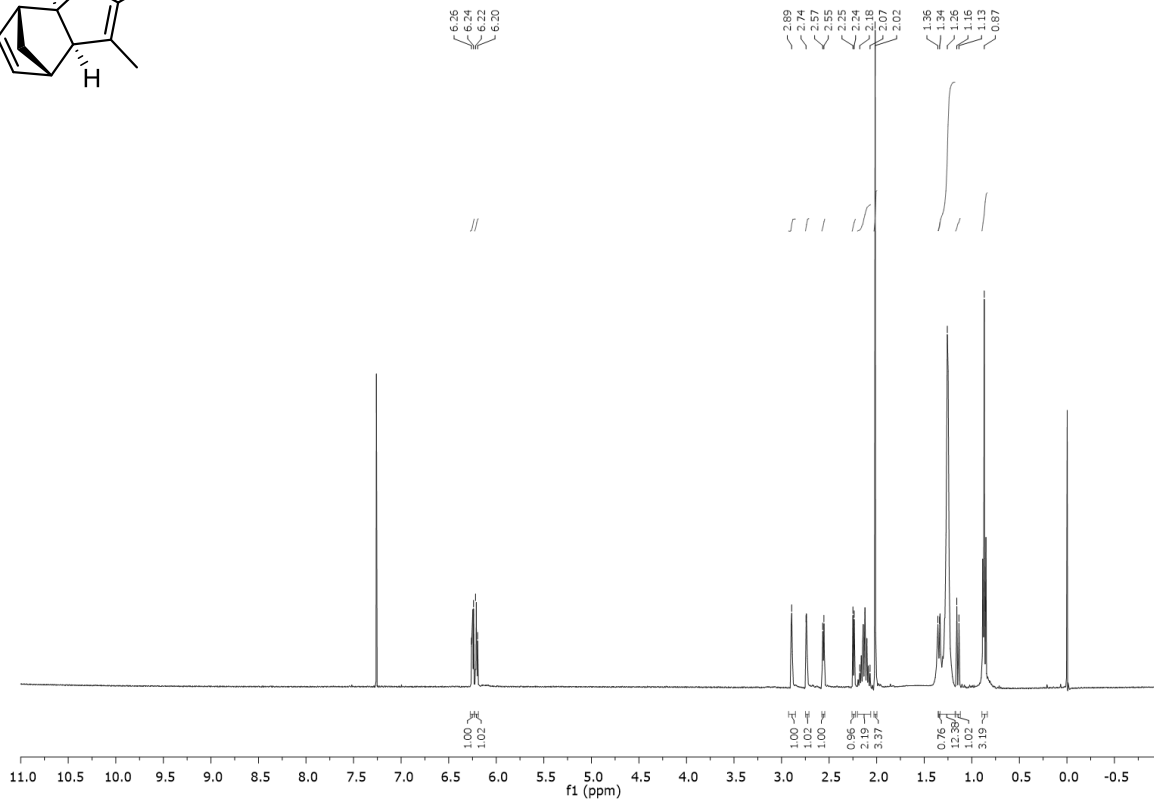
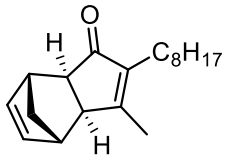


Selected spectra

HMBC

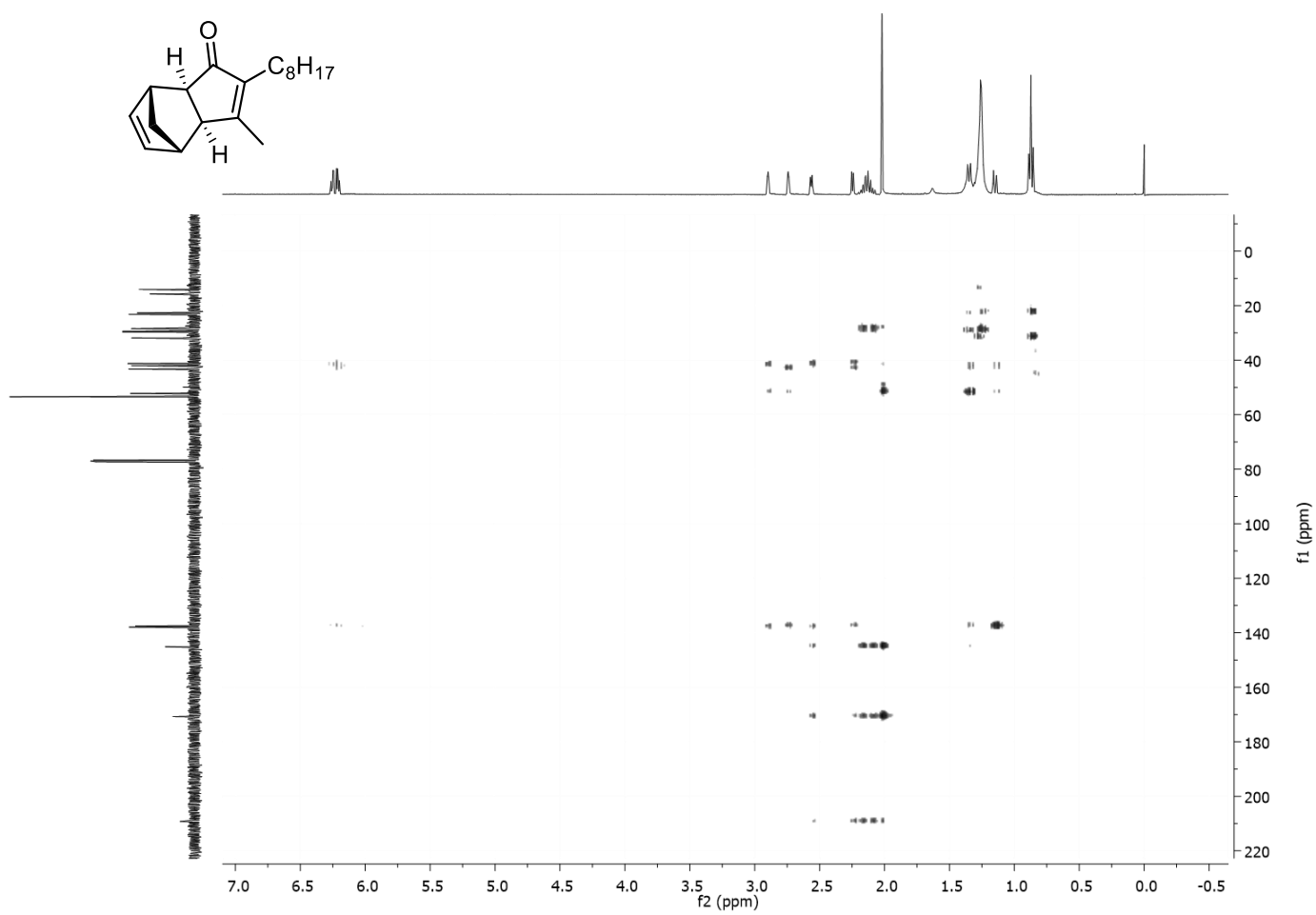


Selected spectra

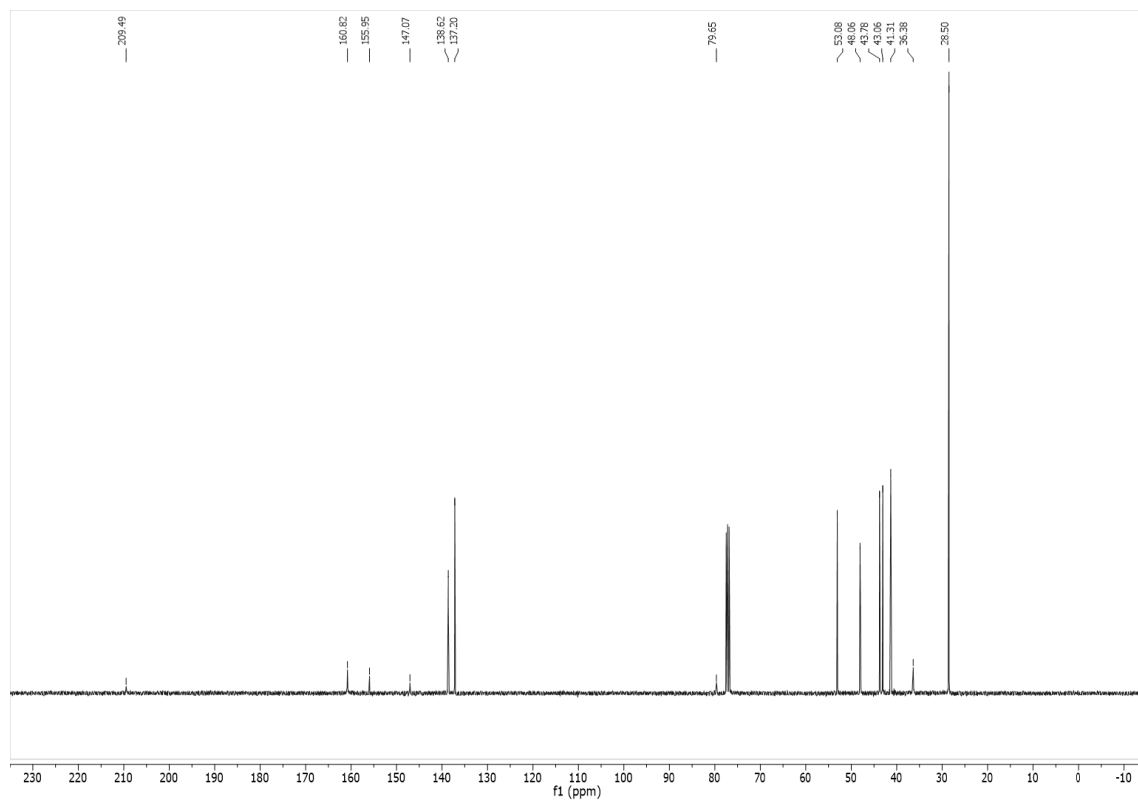
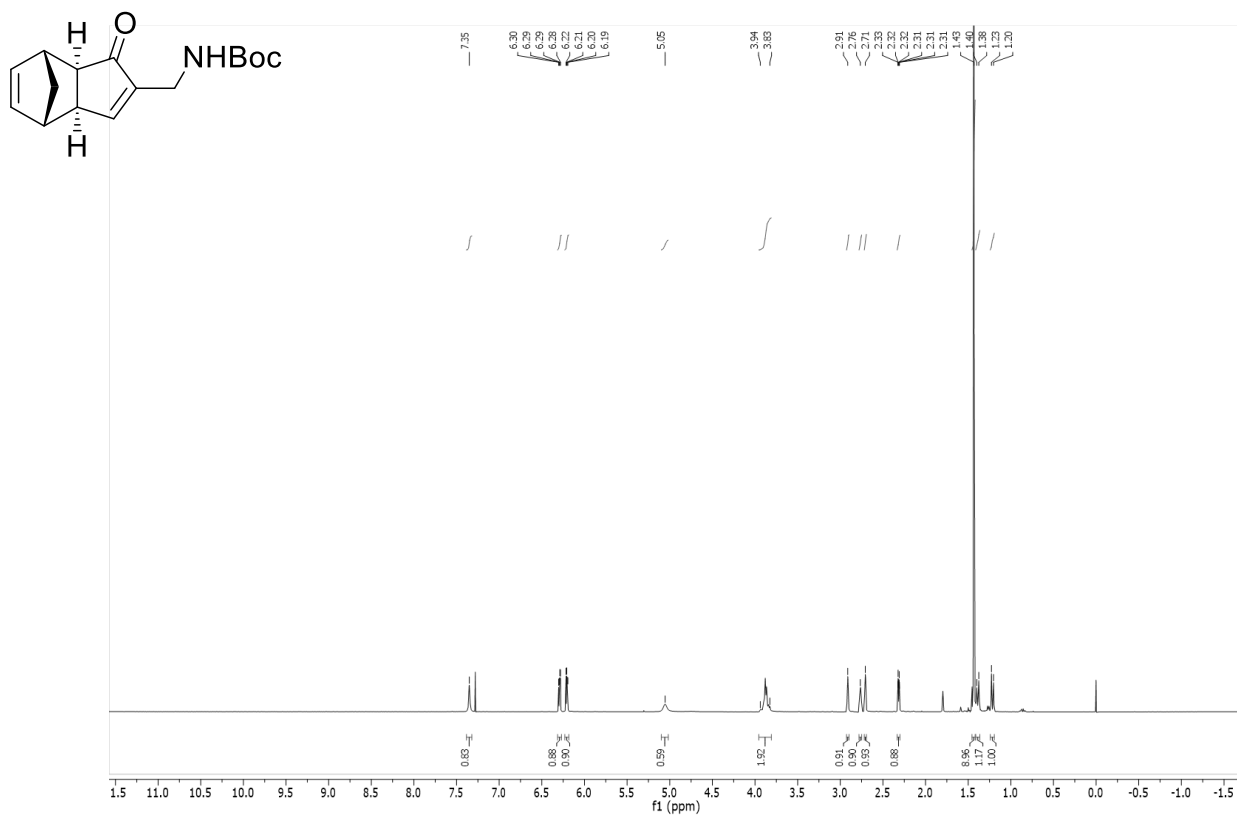


Selected spectra

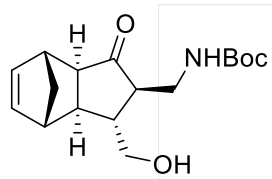
HMBC



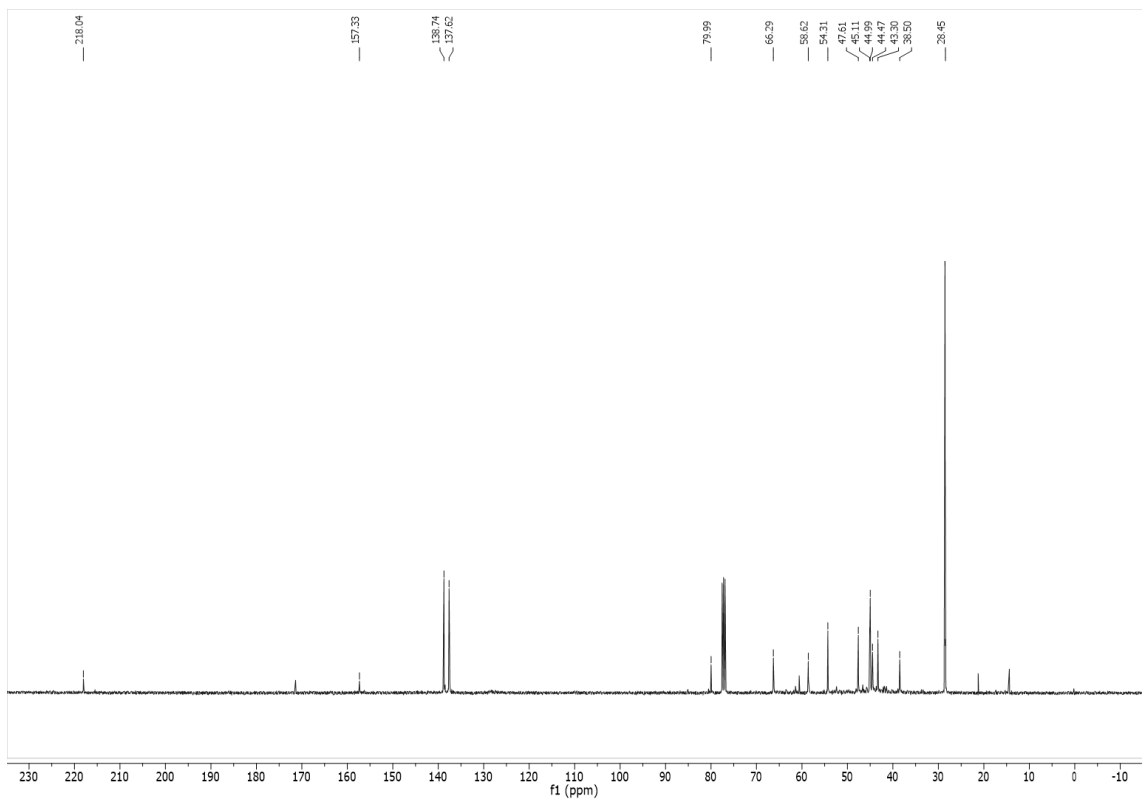
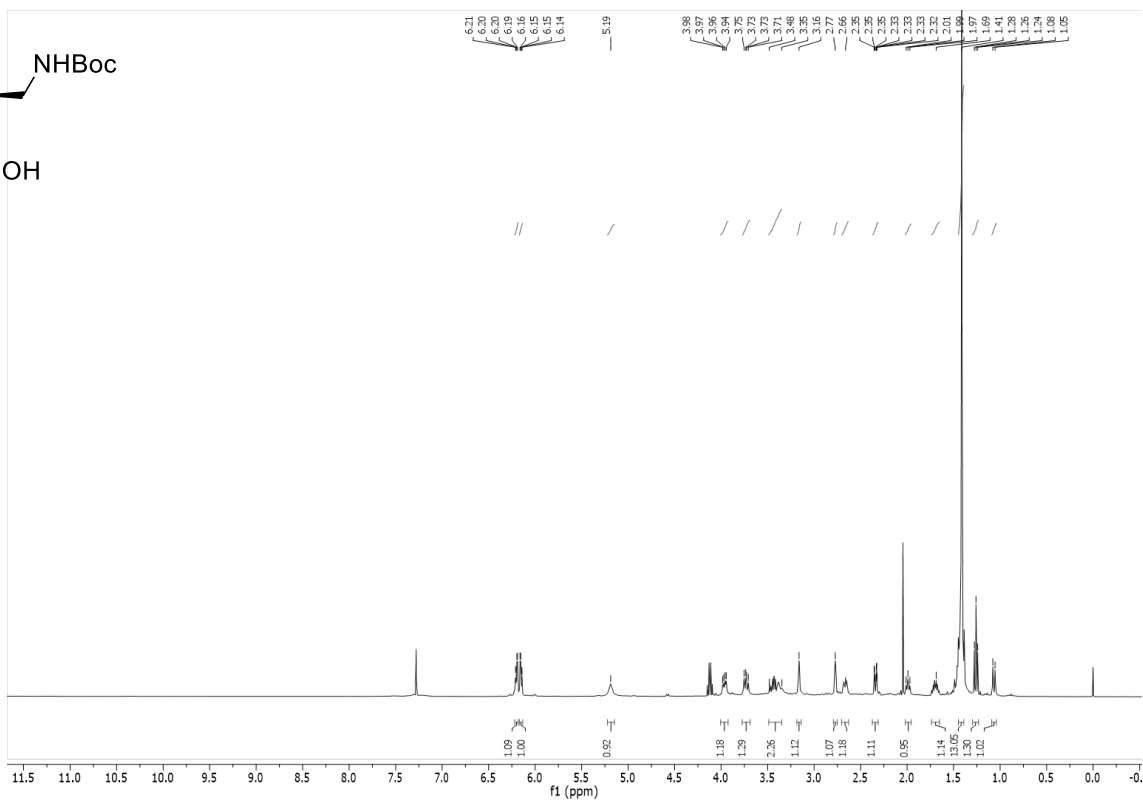
Selected spectra



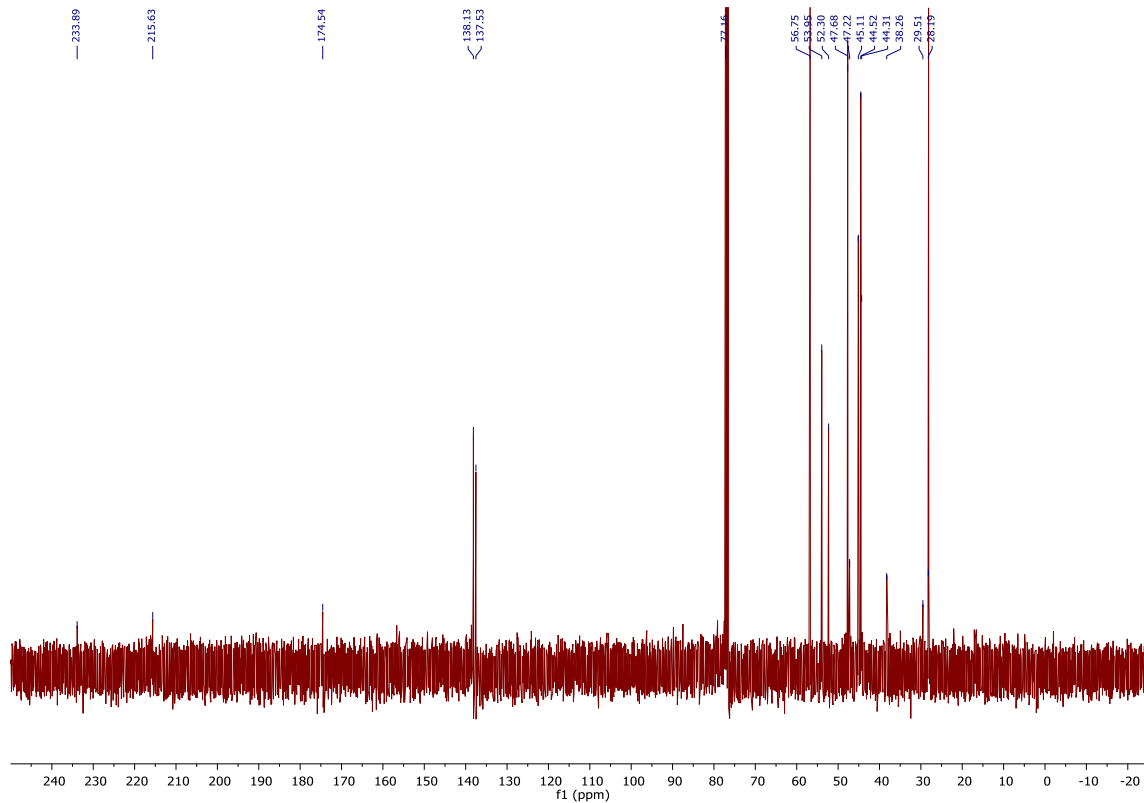
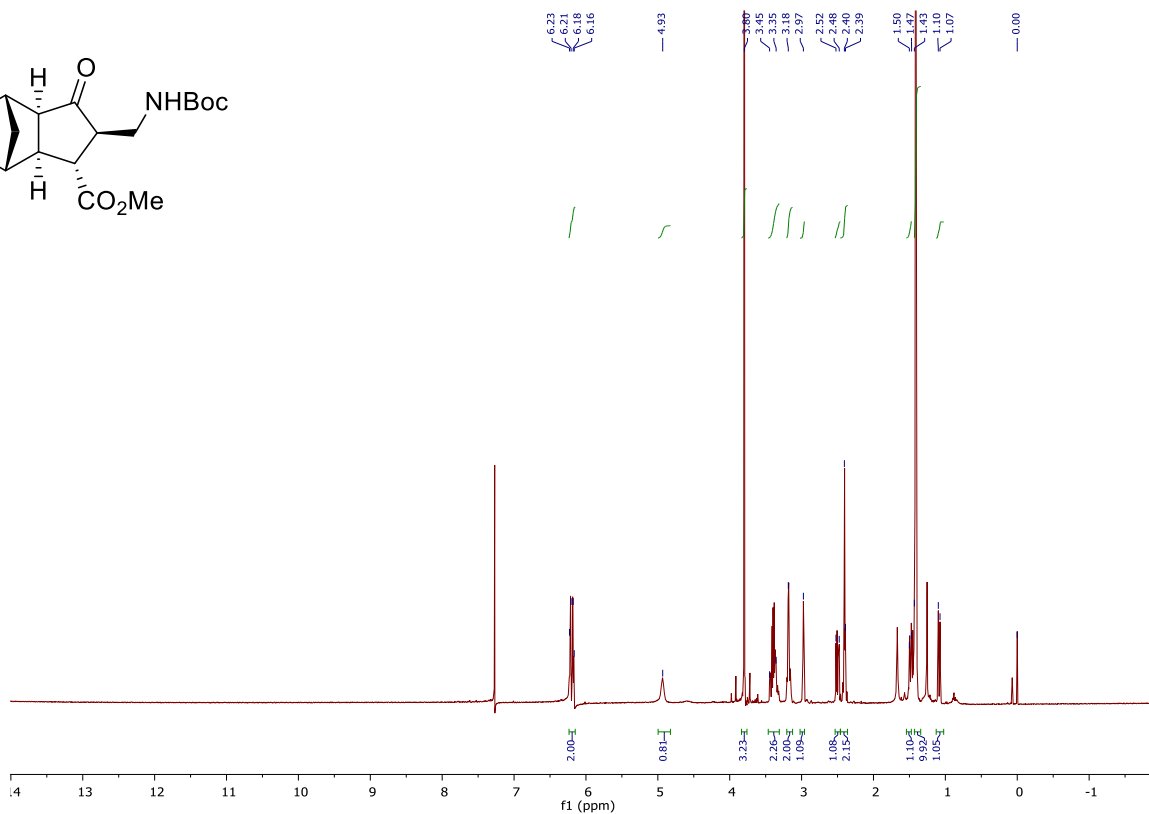
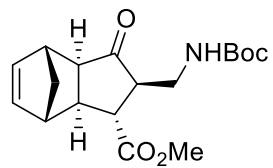
Selected spectra



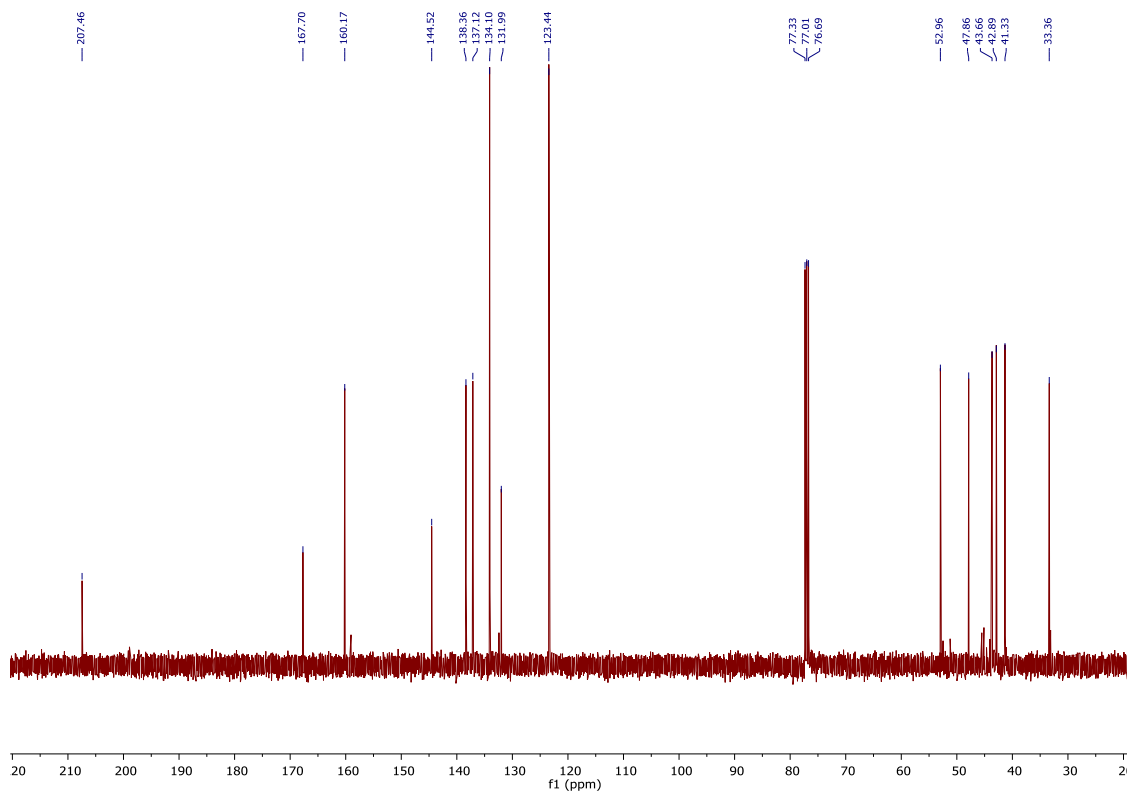
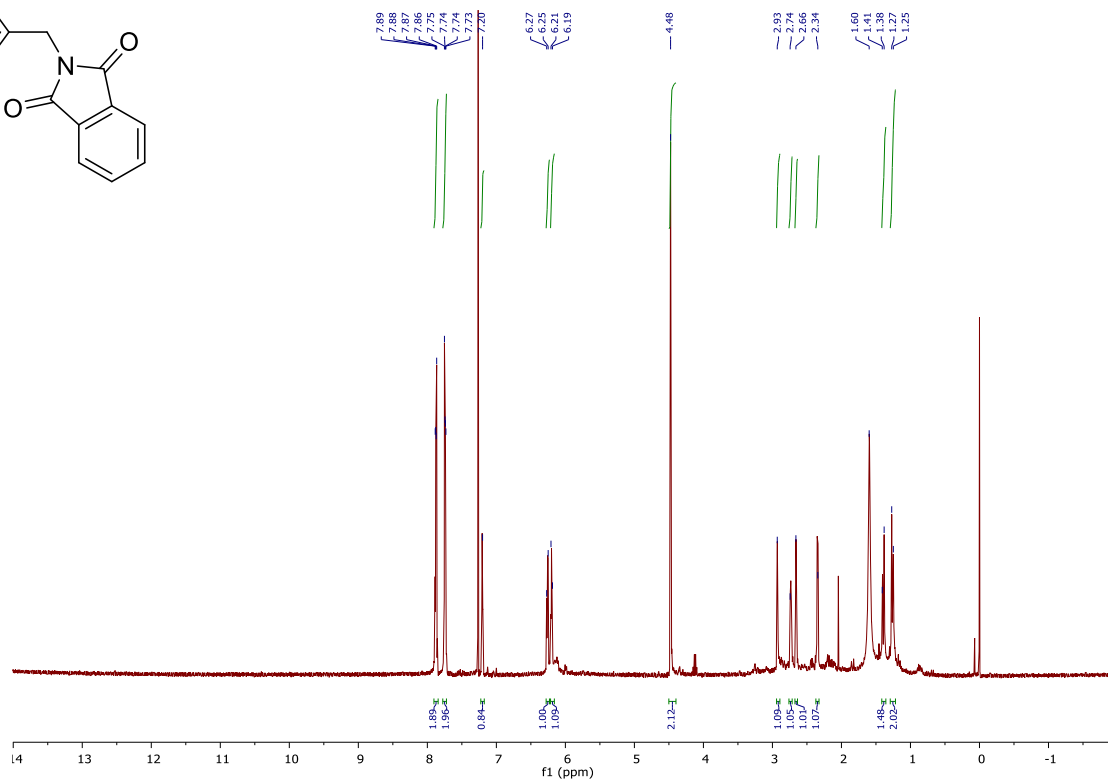
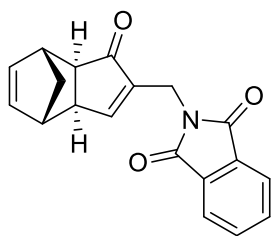
5g



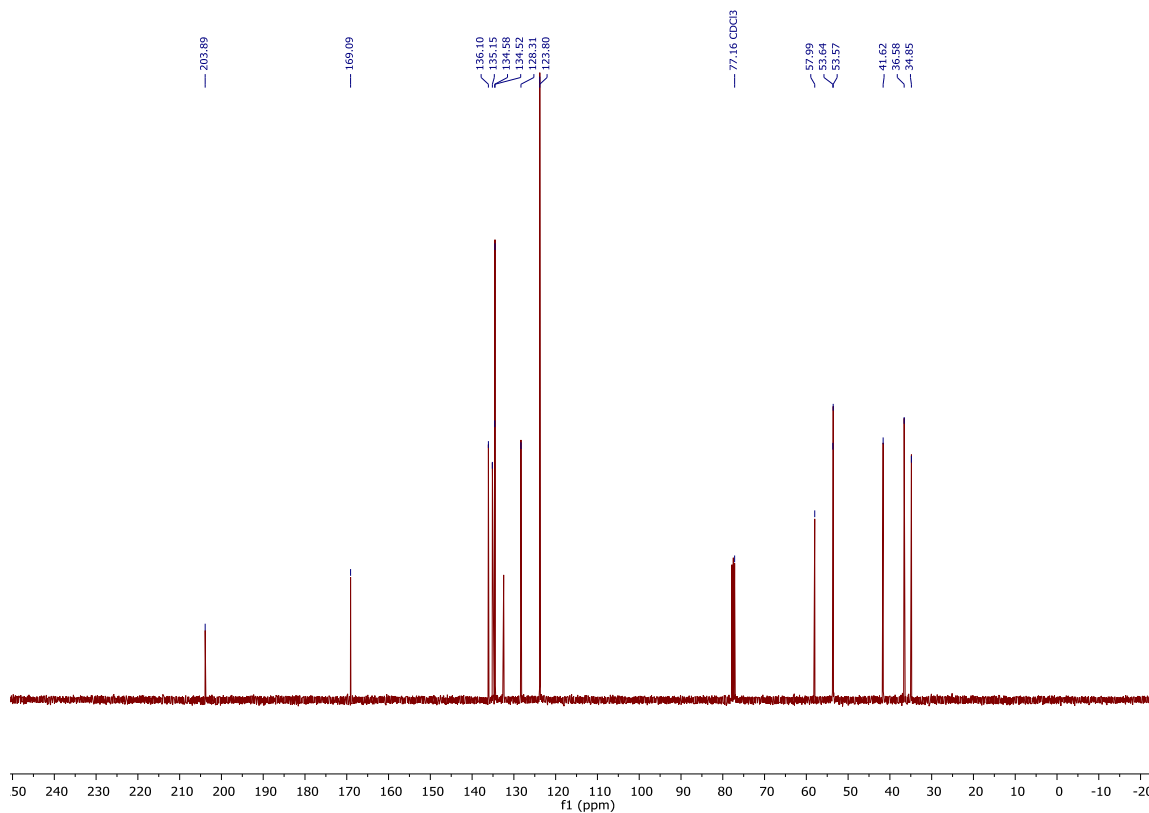
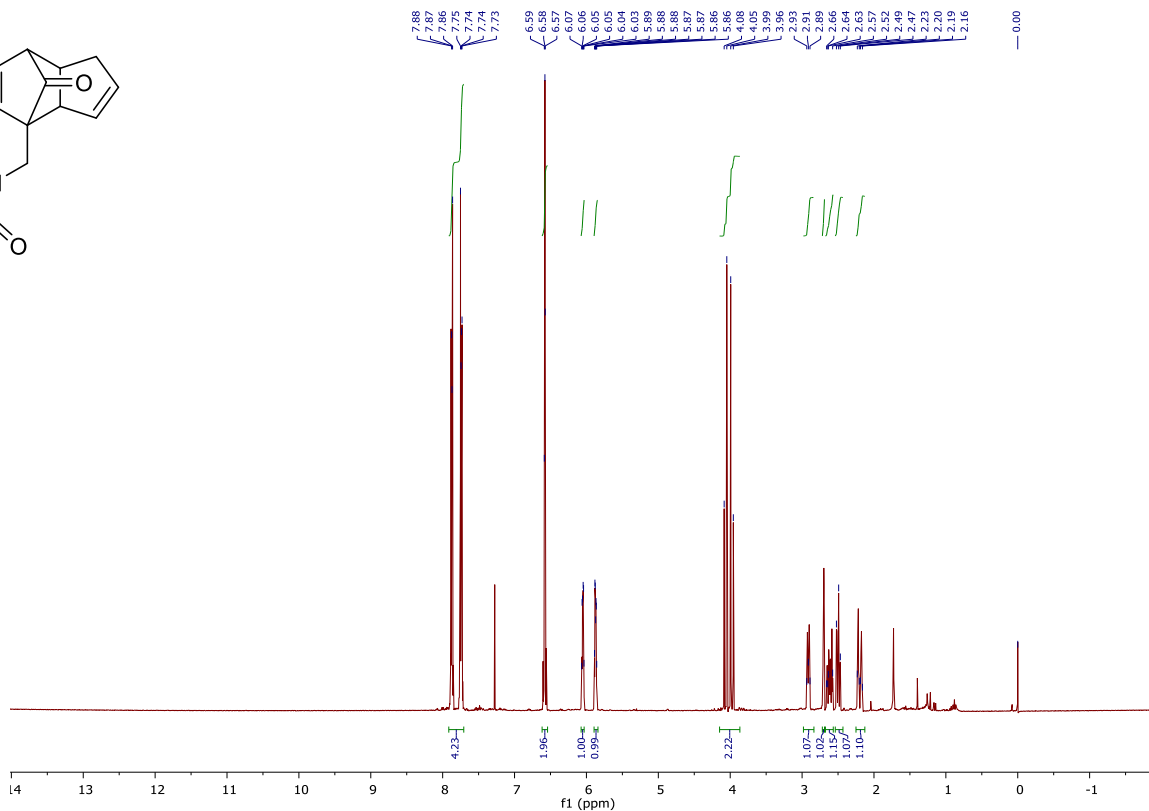
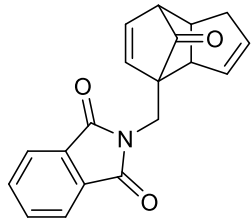
Selected spectra



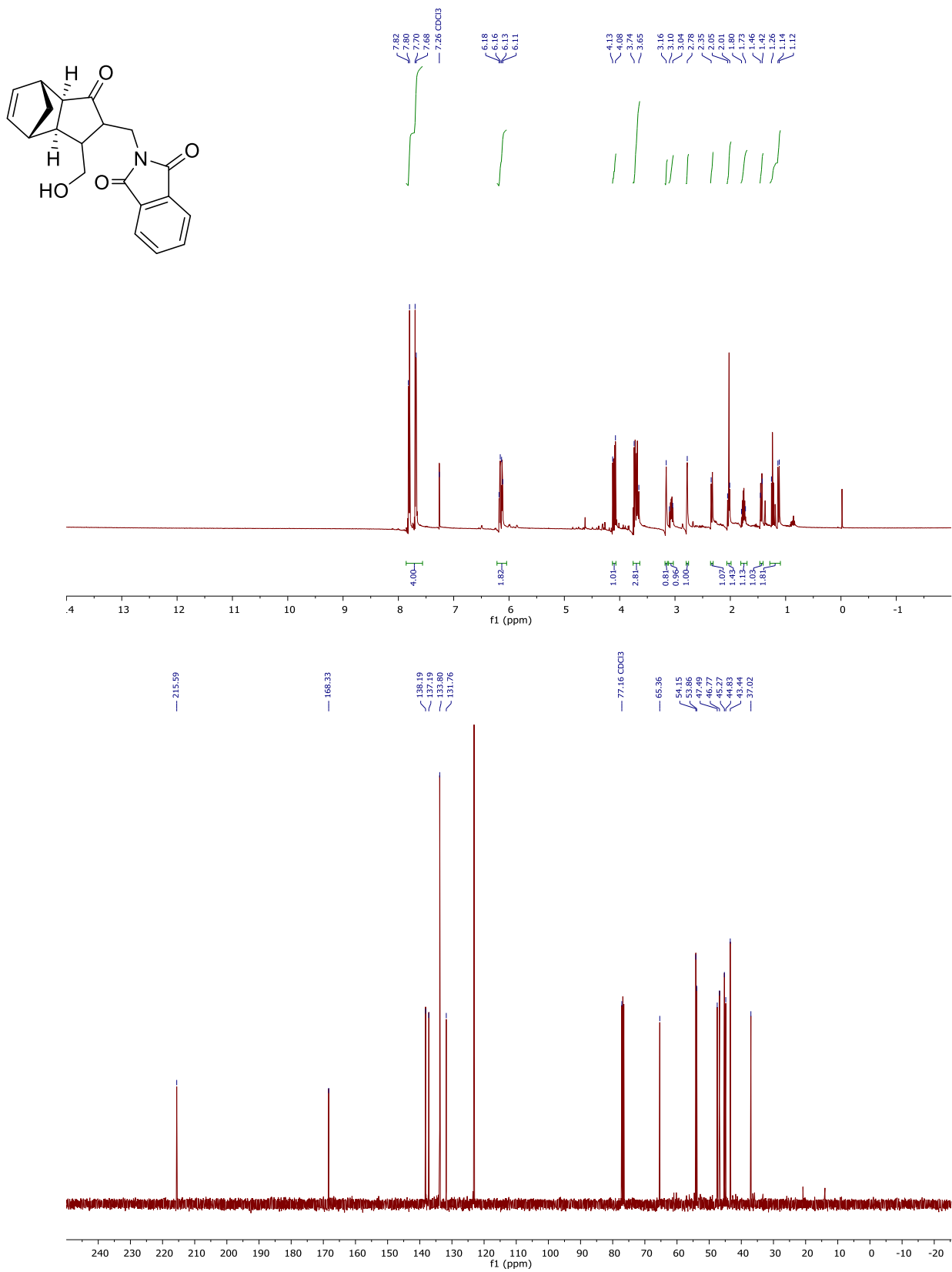
Selected spectra



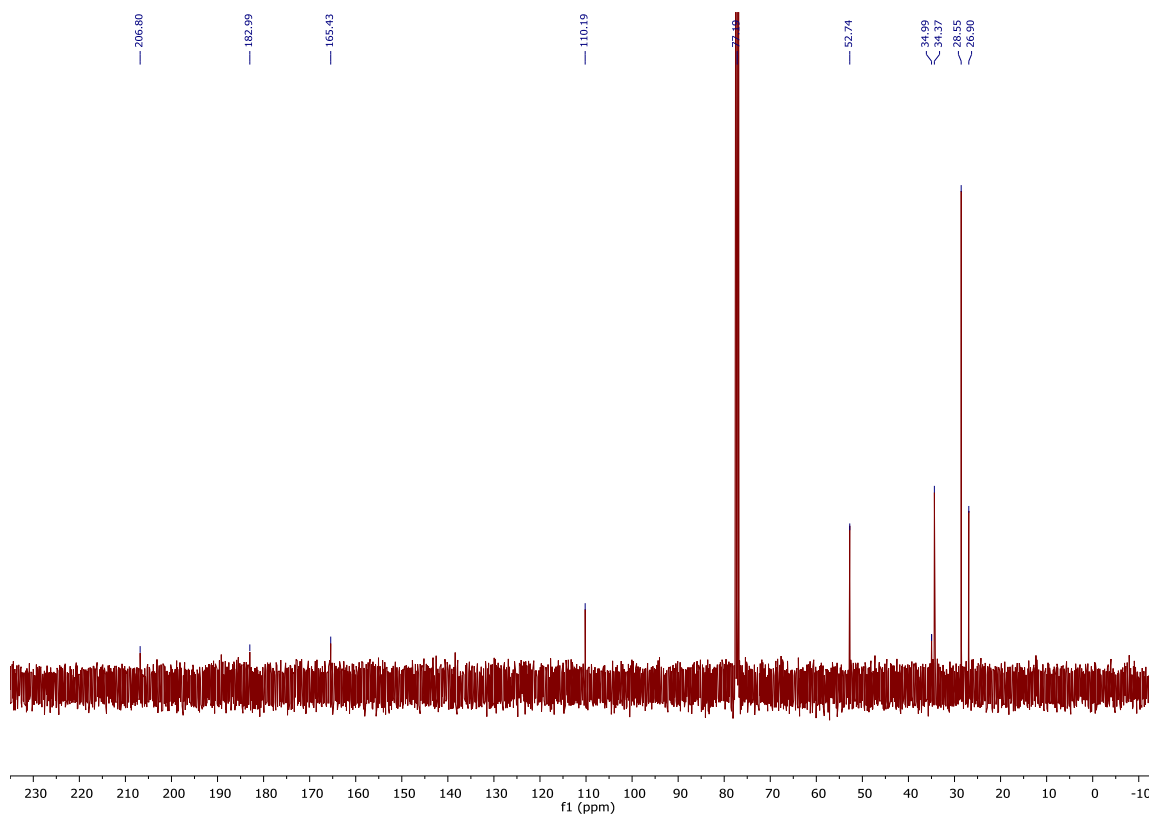
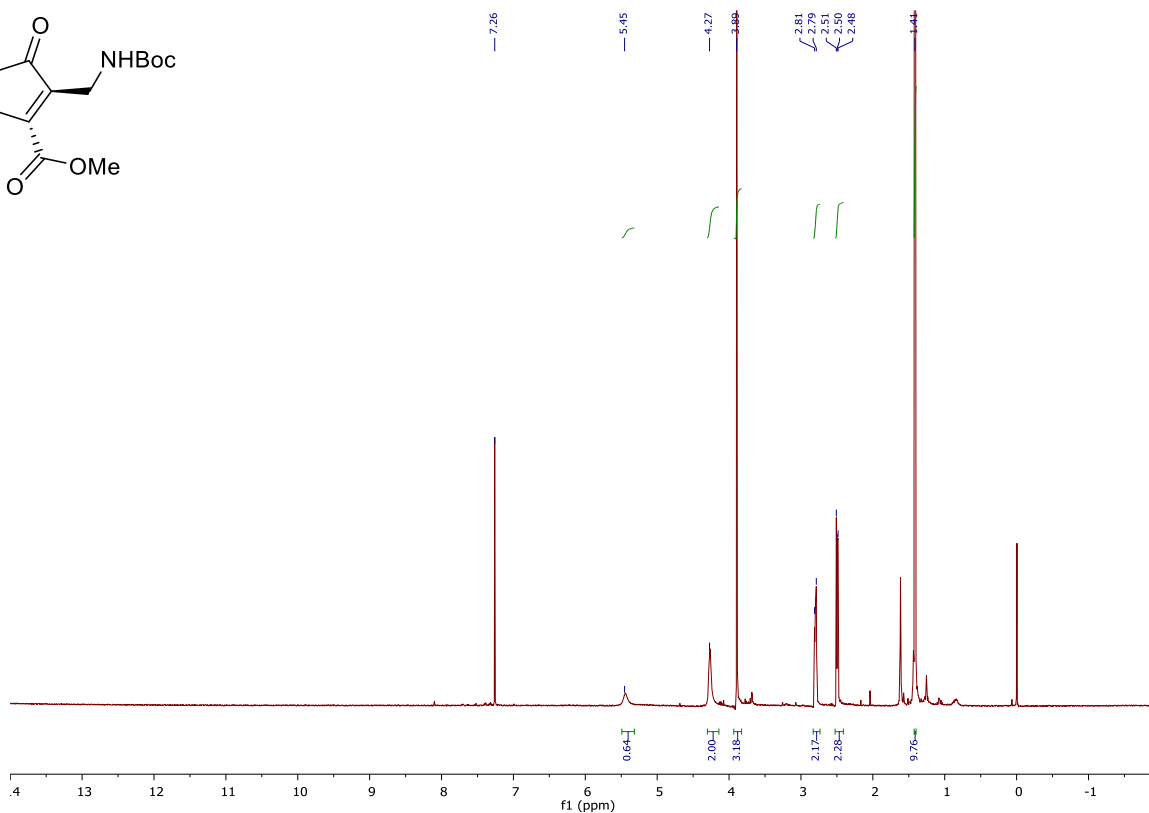
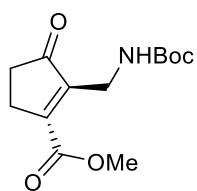
Selected spectra



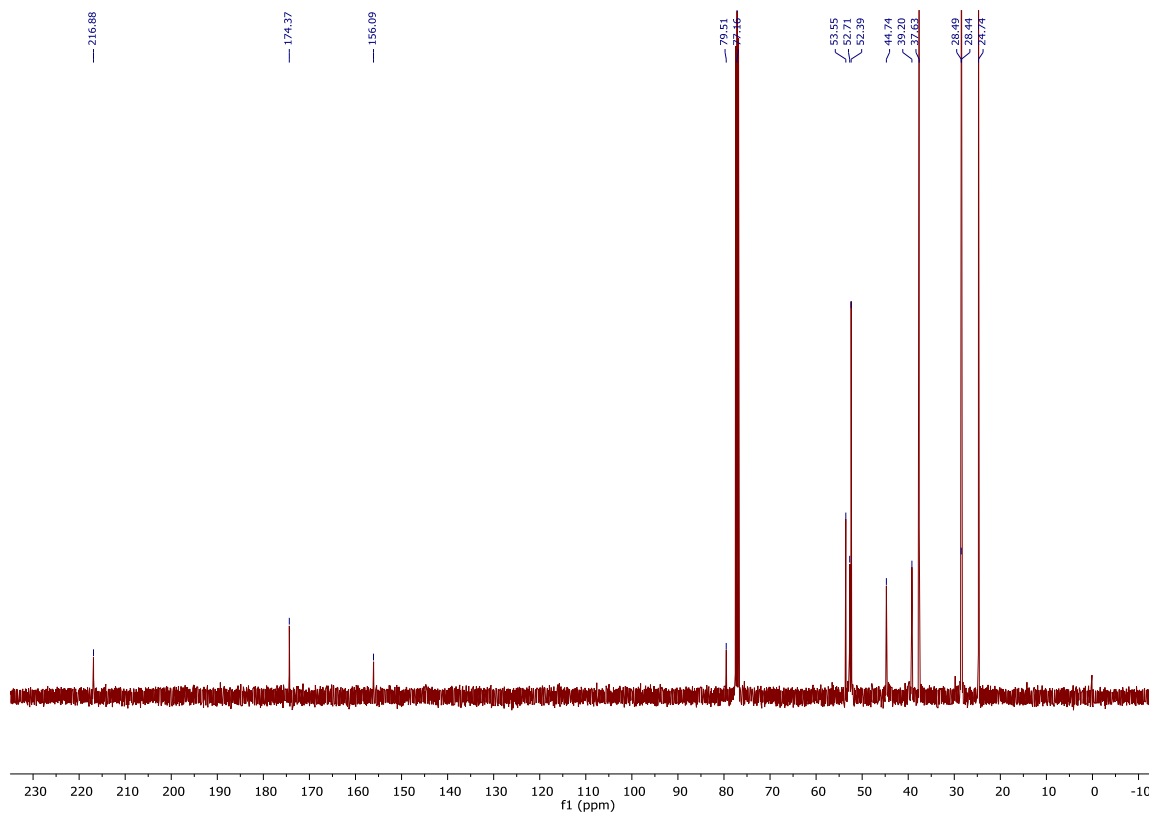
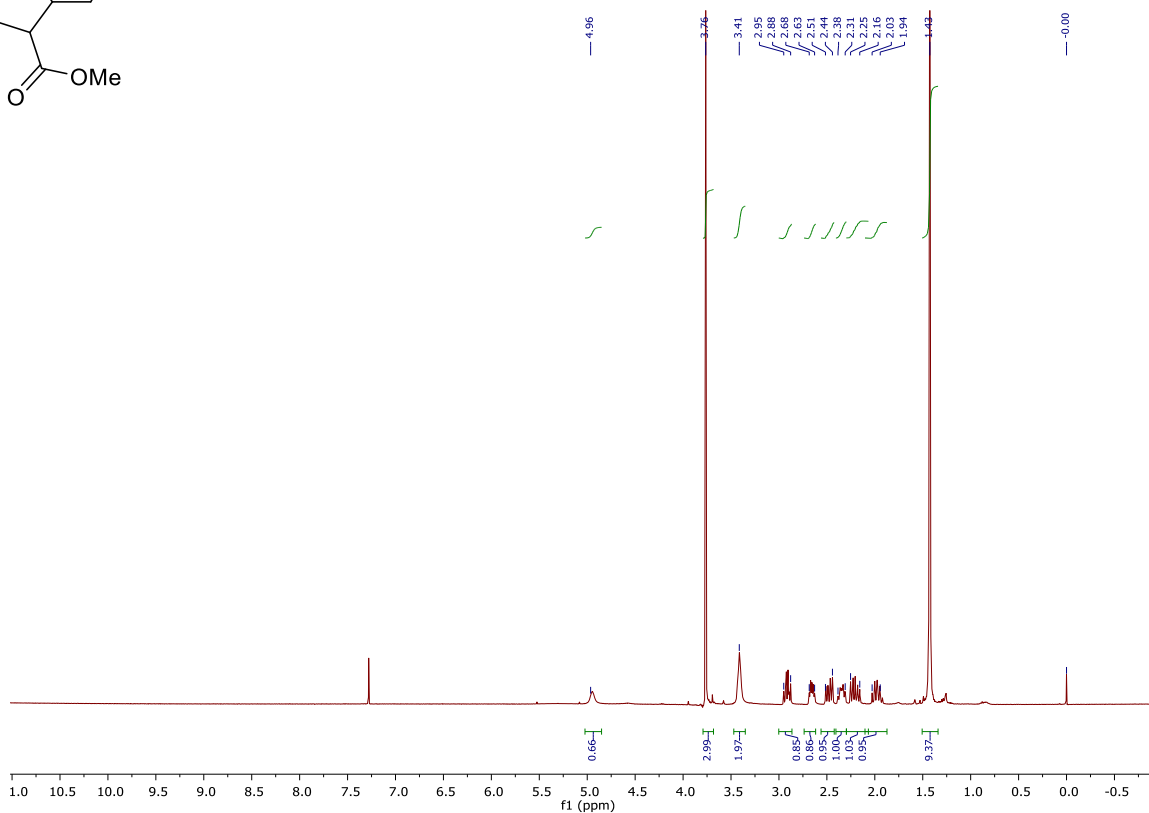
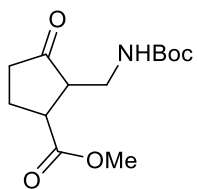
Selected spectra



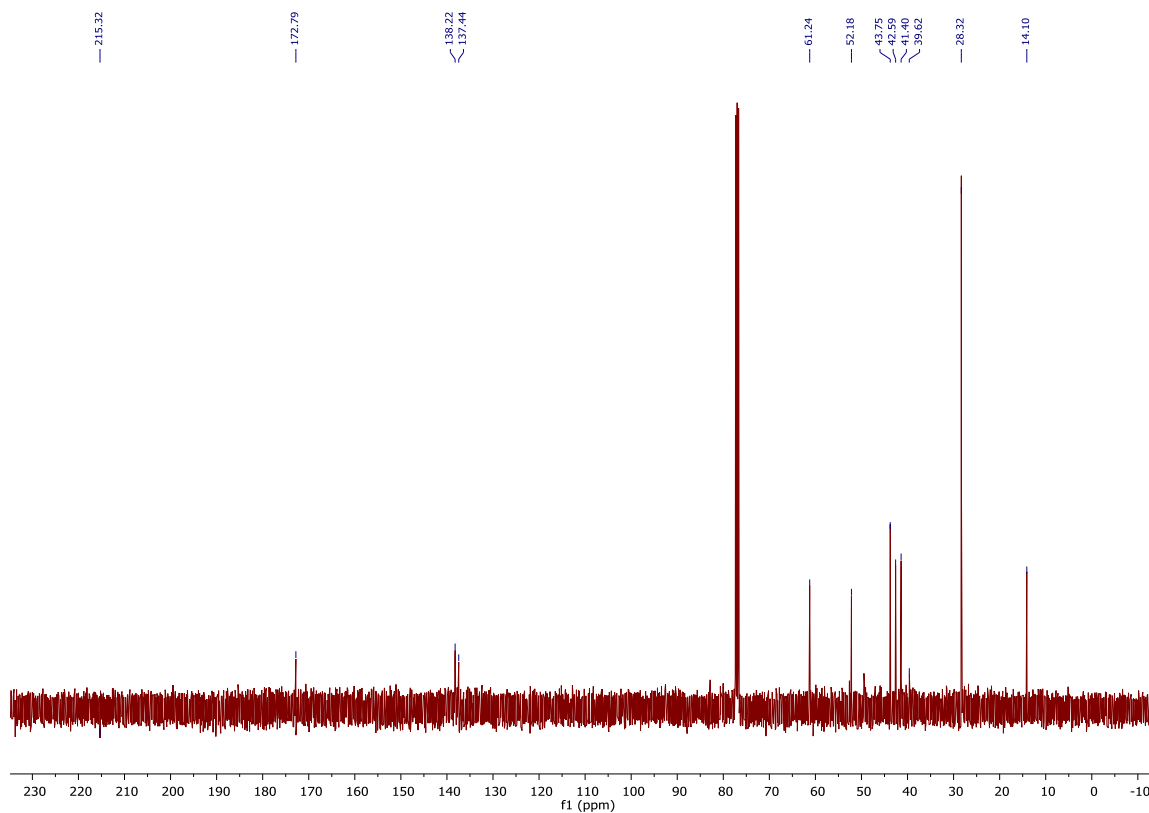
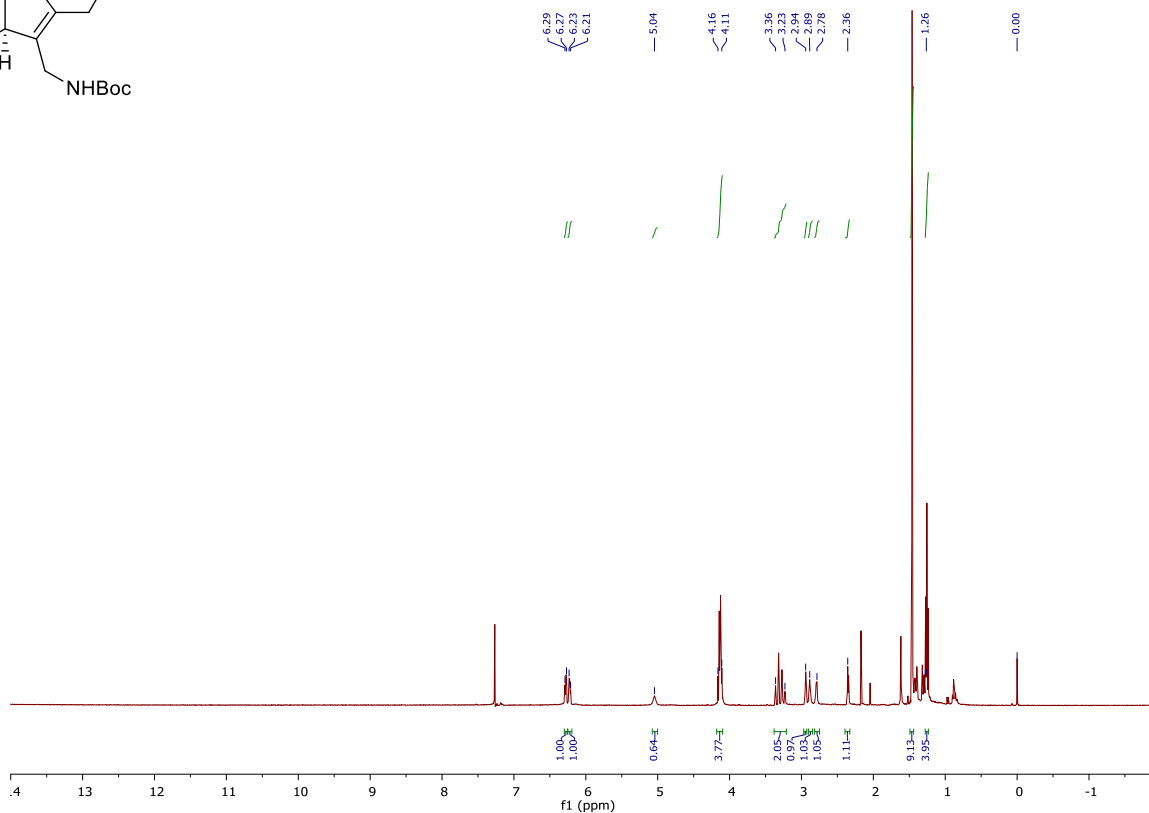
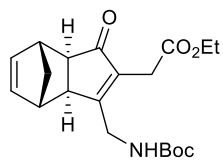
Selected spectra



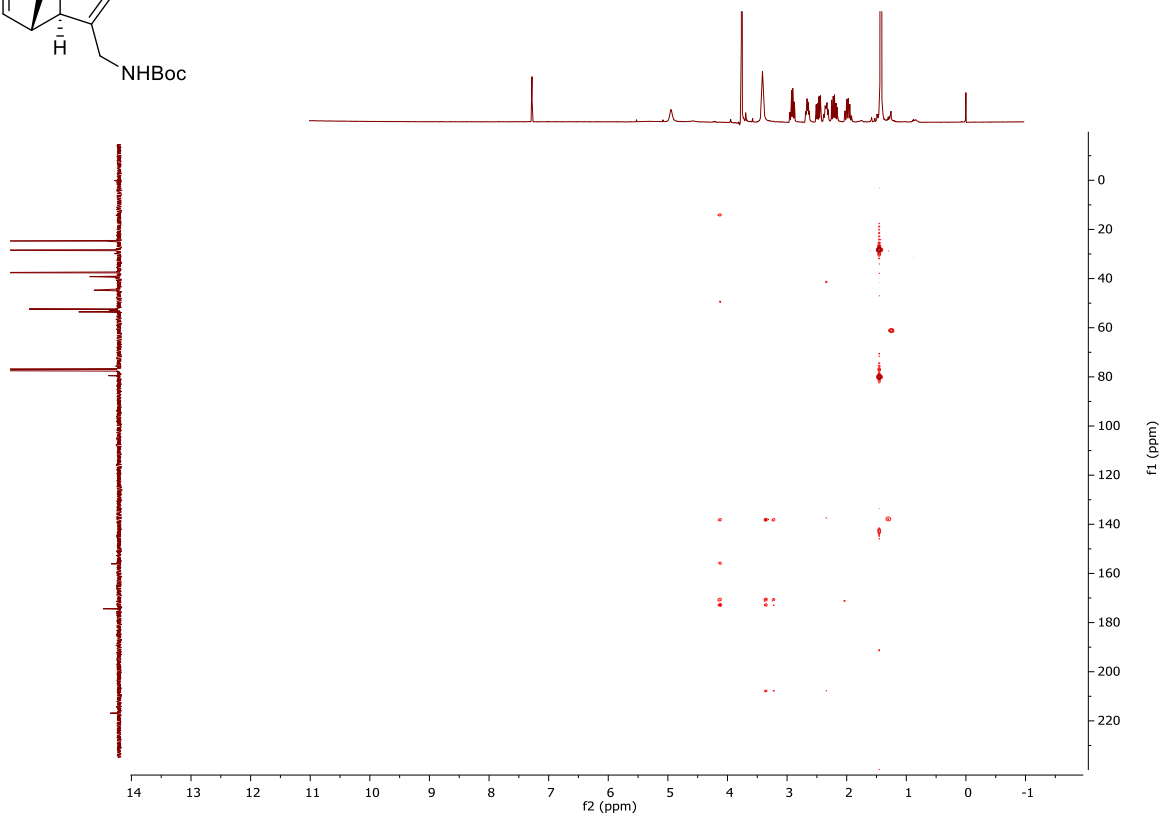
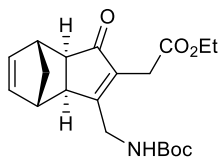
Selected spectra



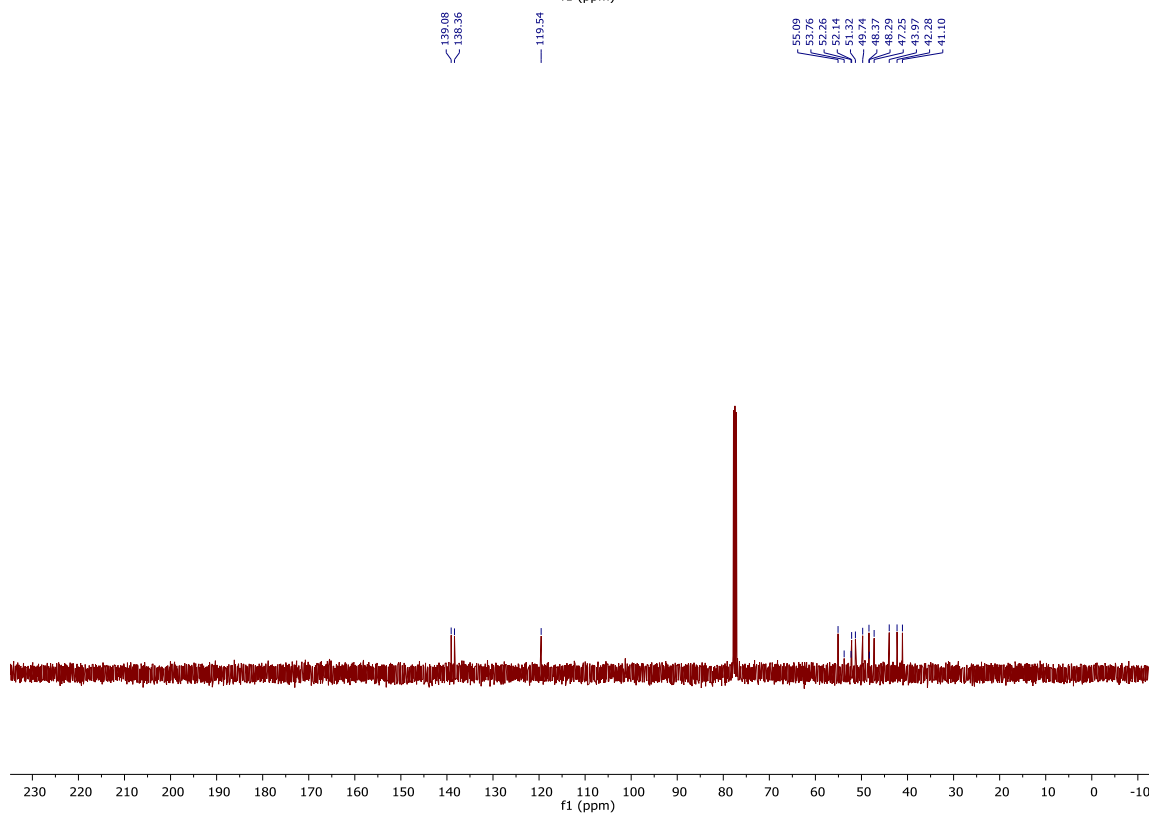
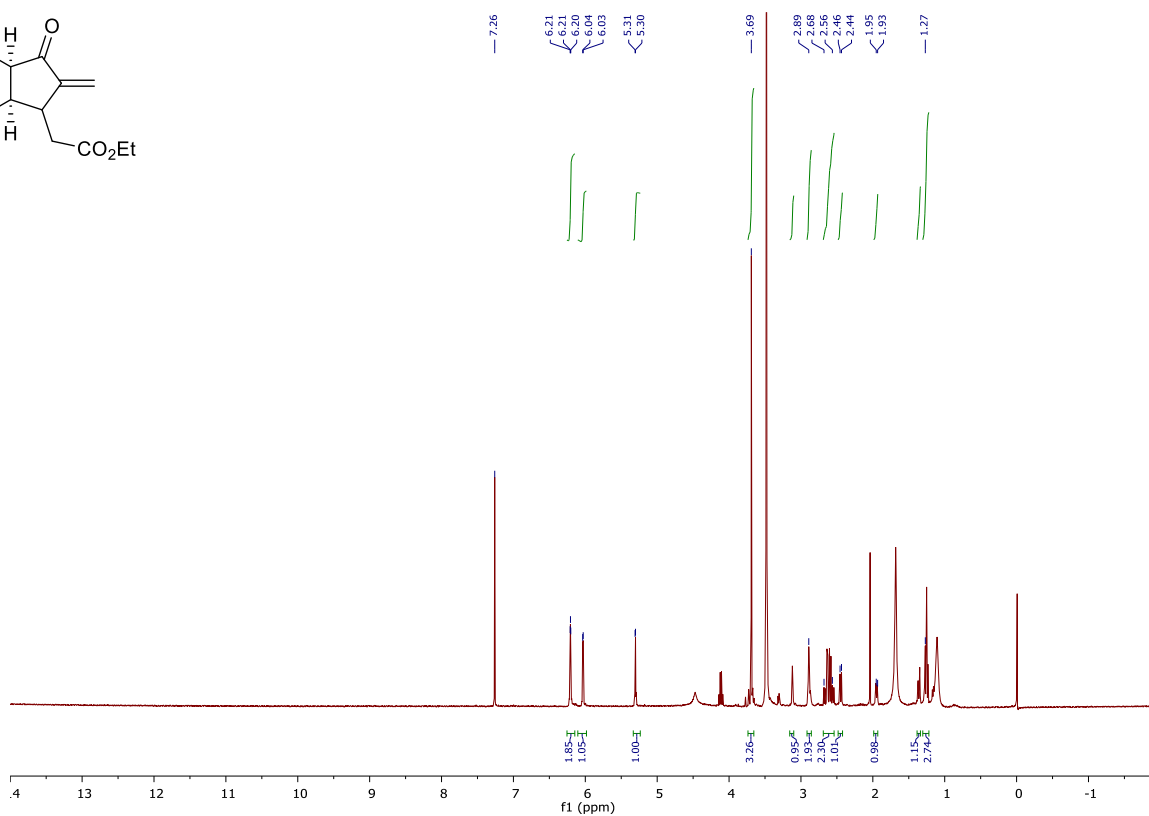
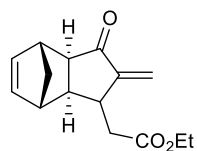
Selected spectra



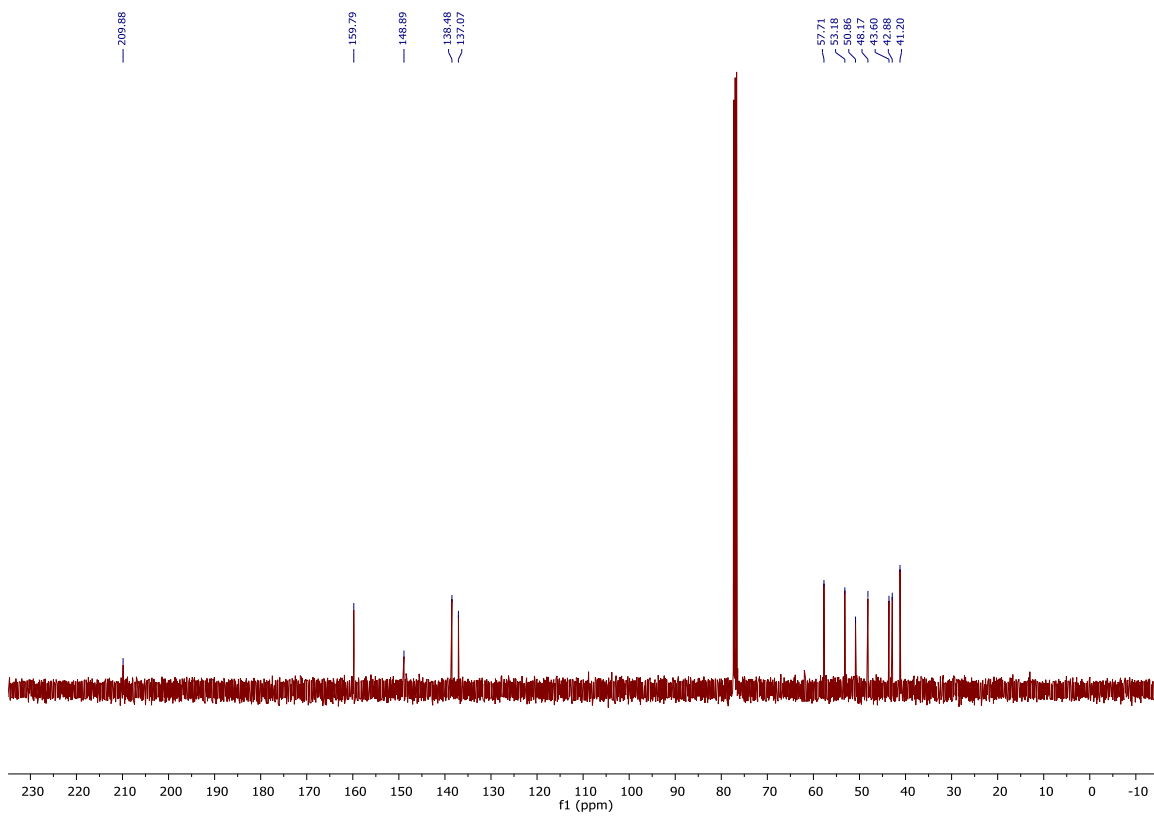
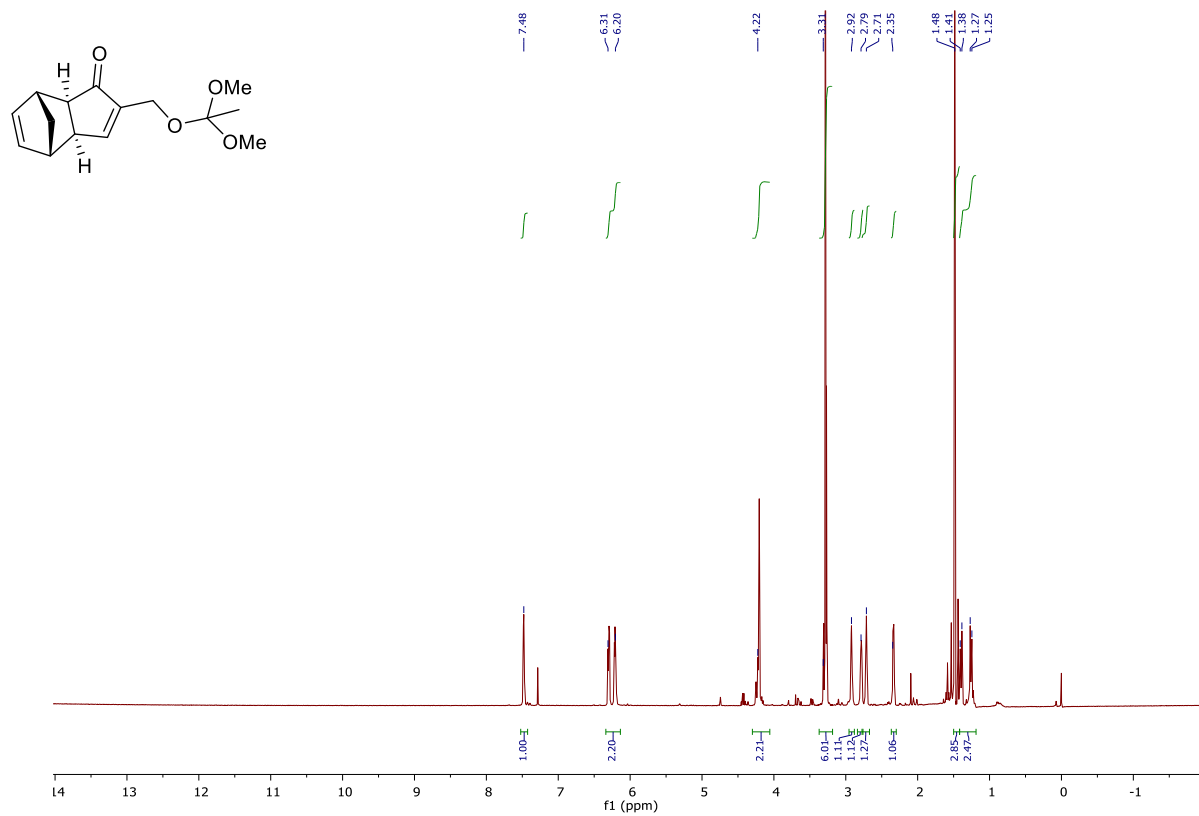
Selected spectra



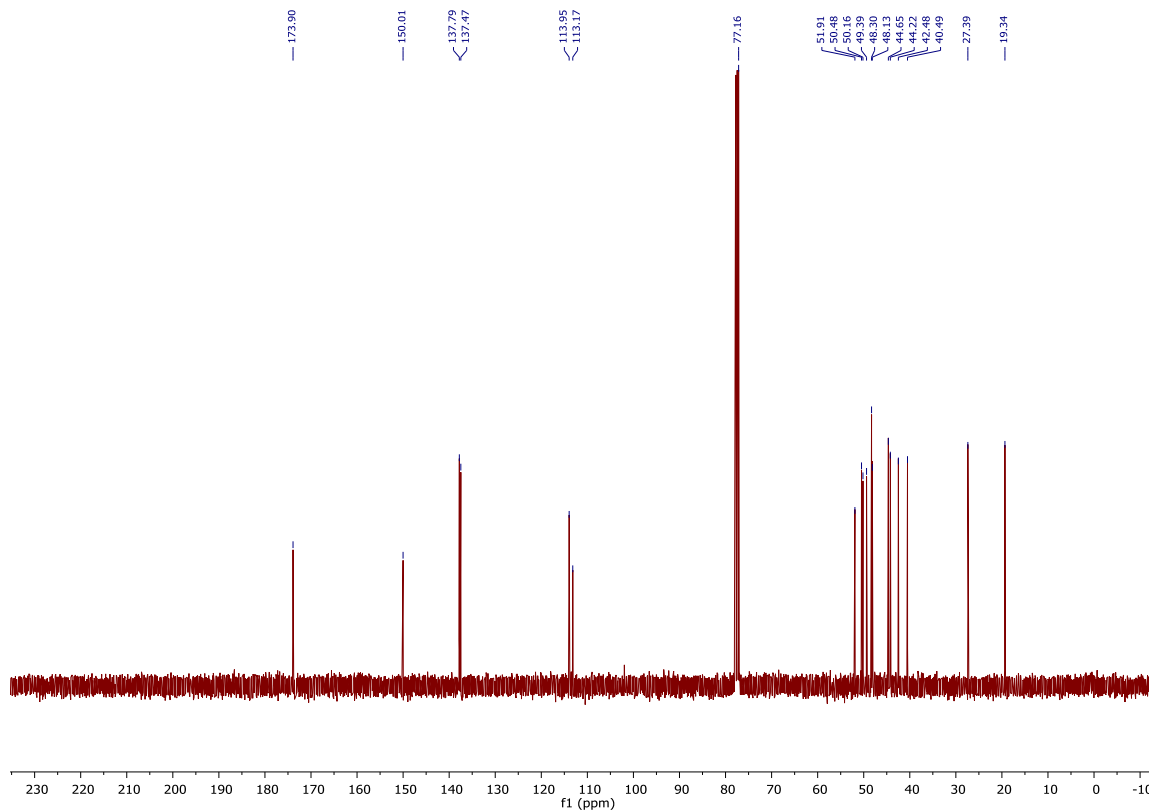
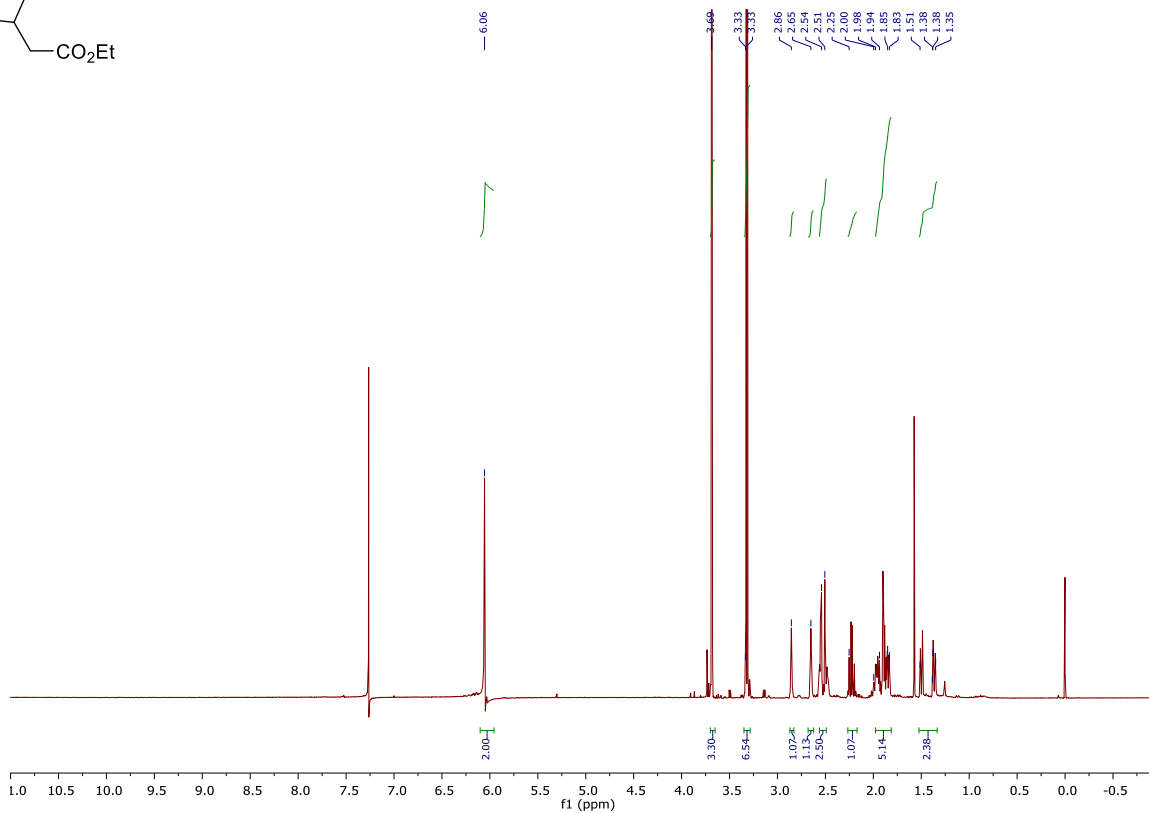
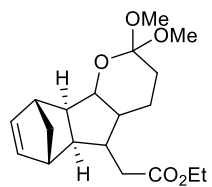
Selected spectra



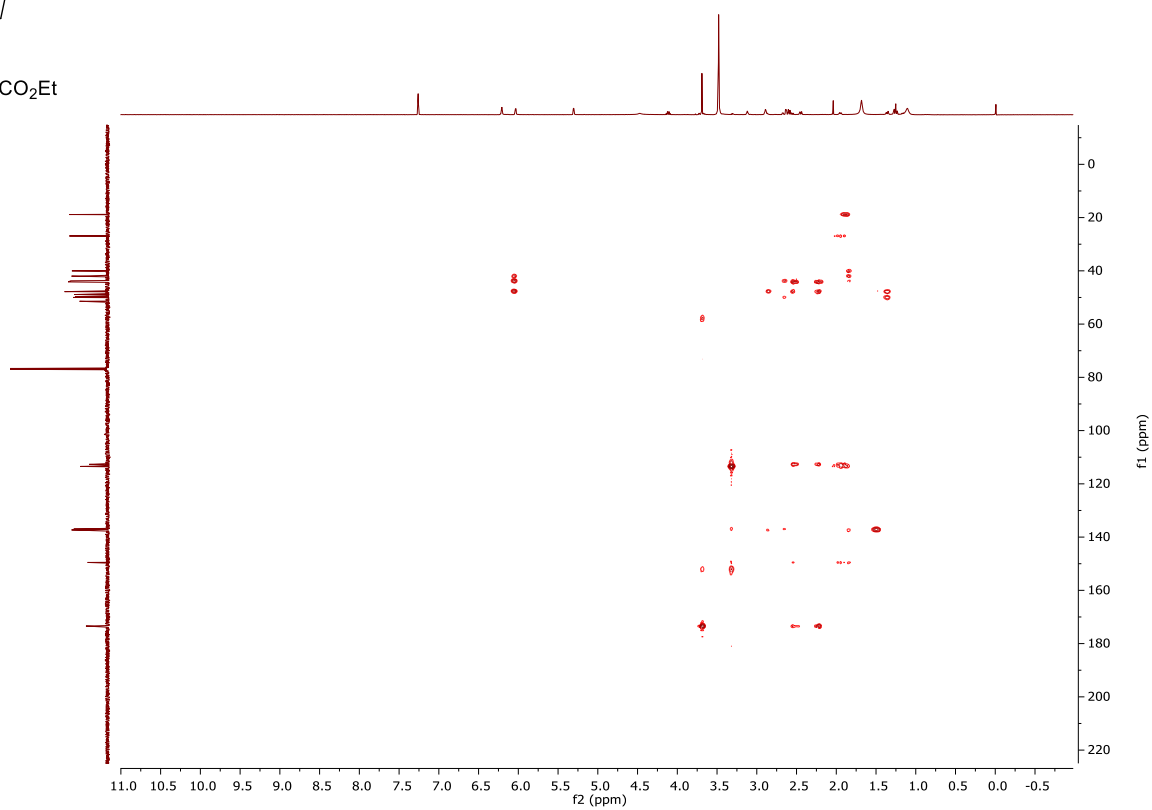
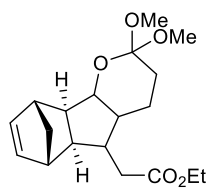
Selected spectra



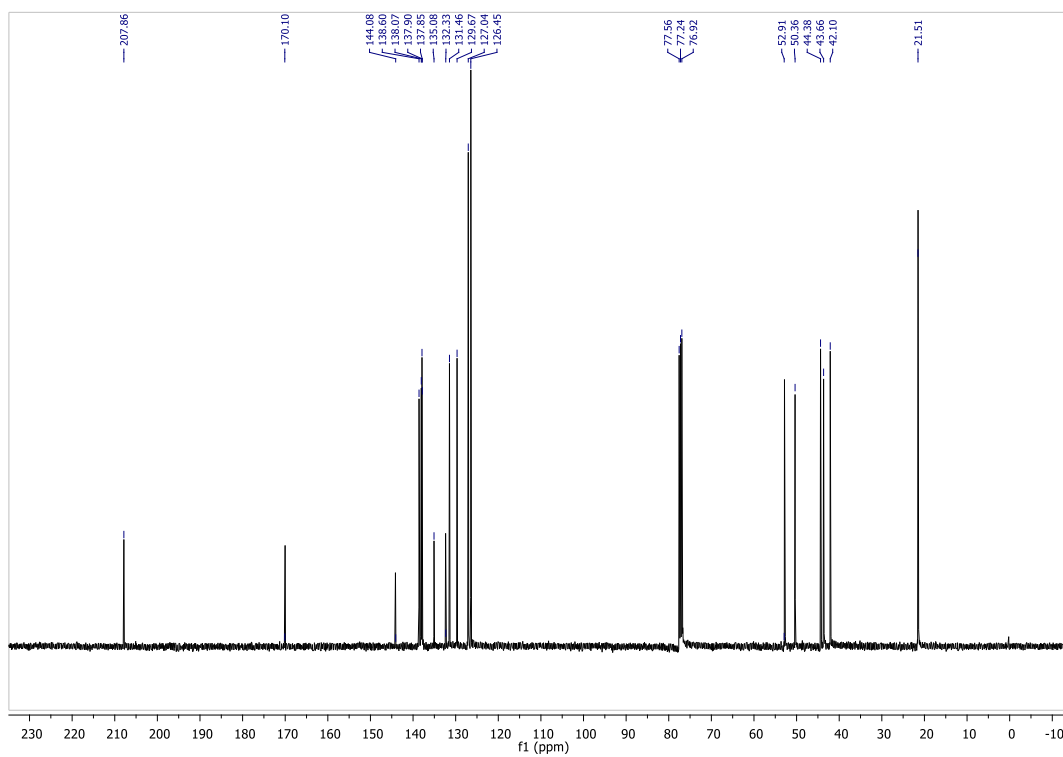
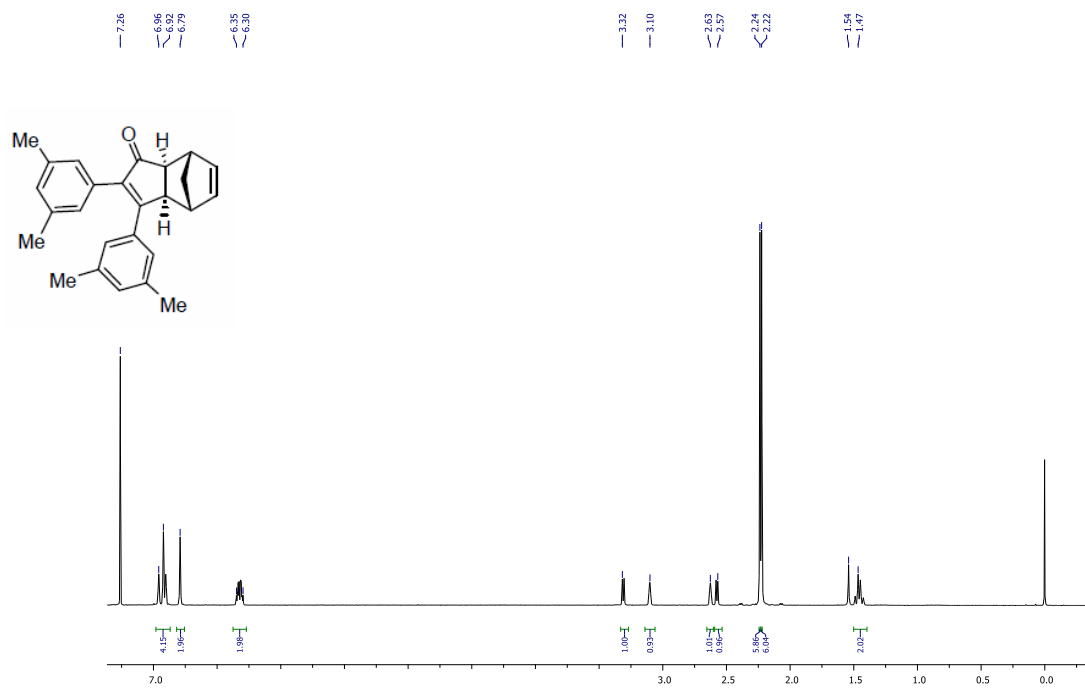
Selected spectra



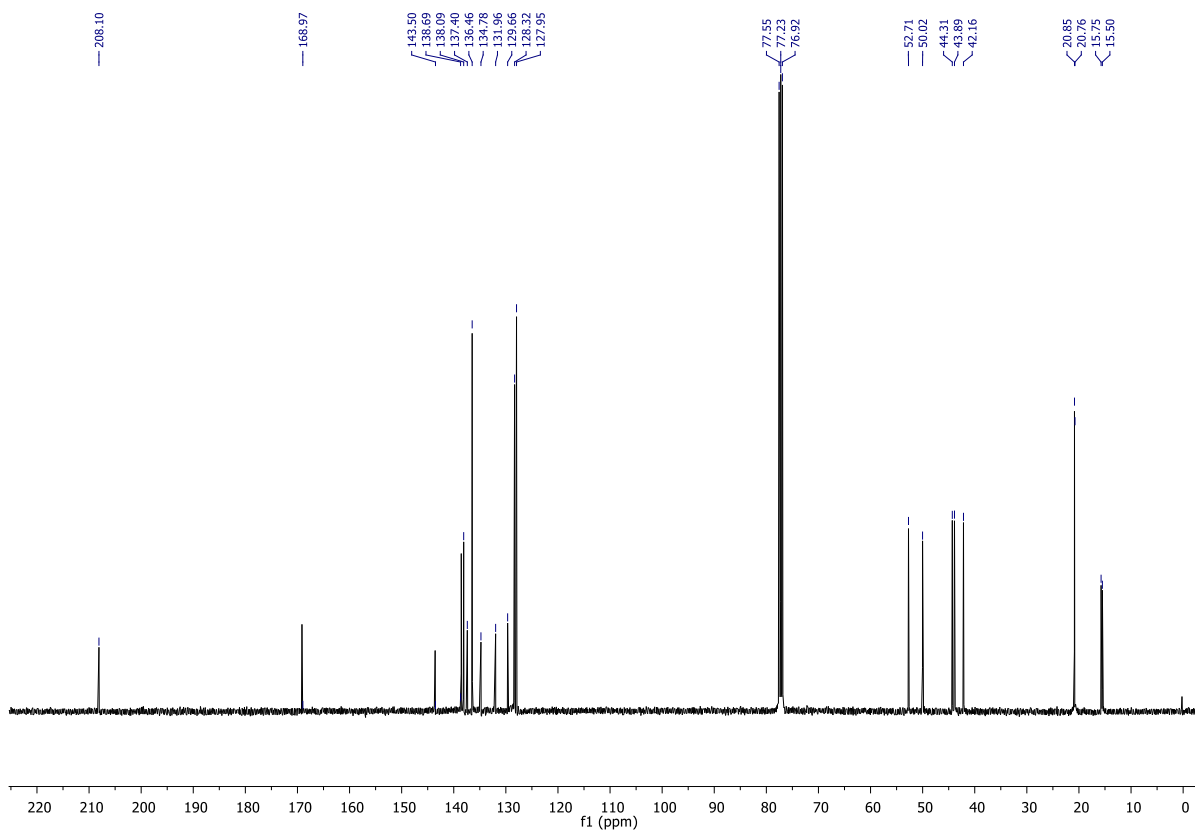
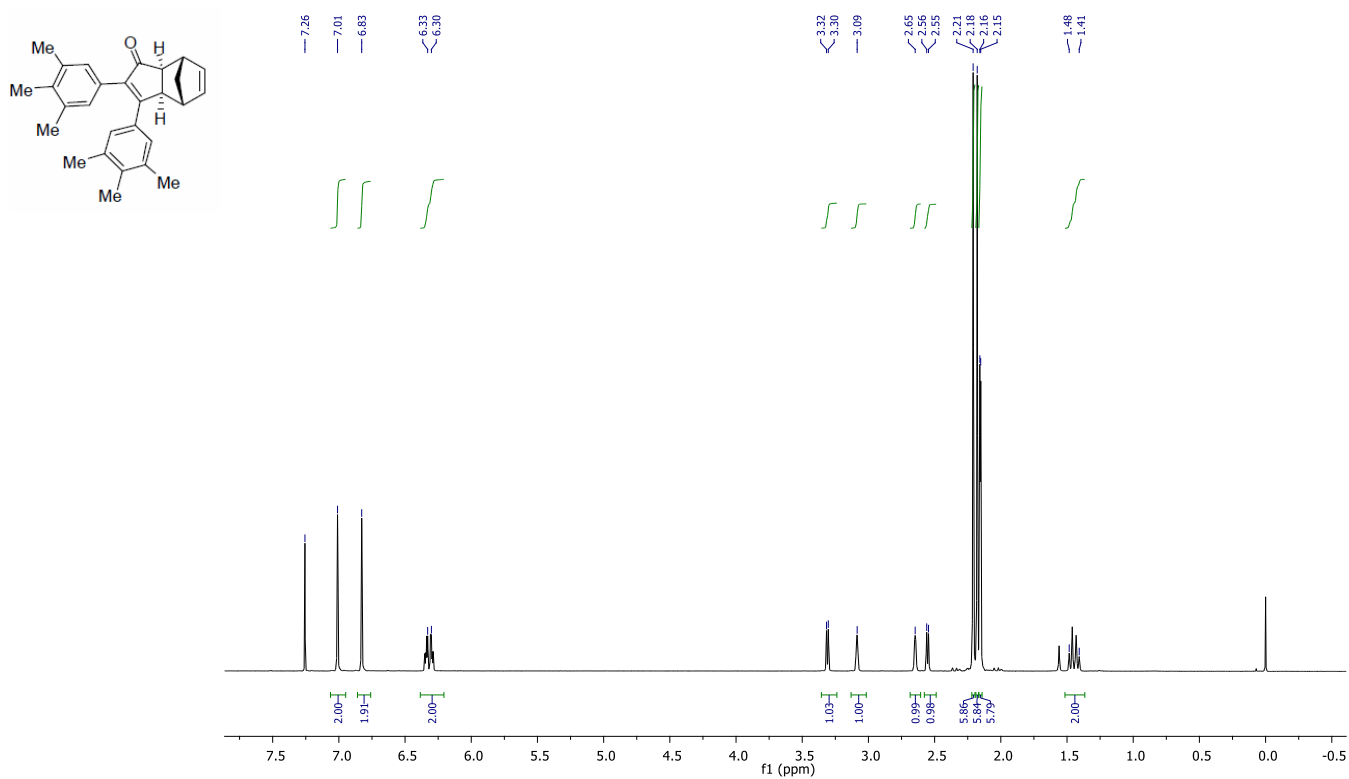
Selected spectra



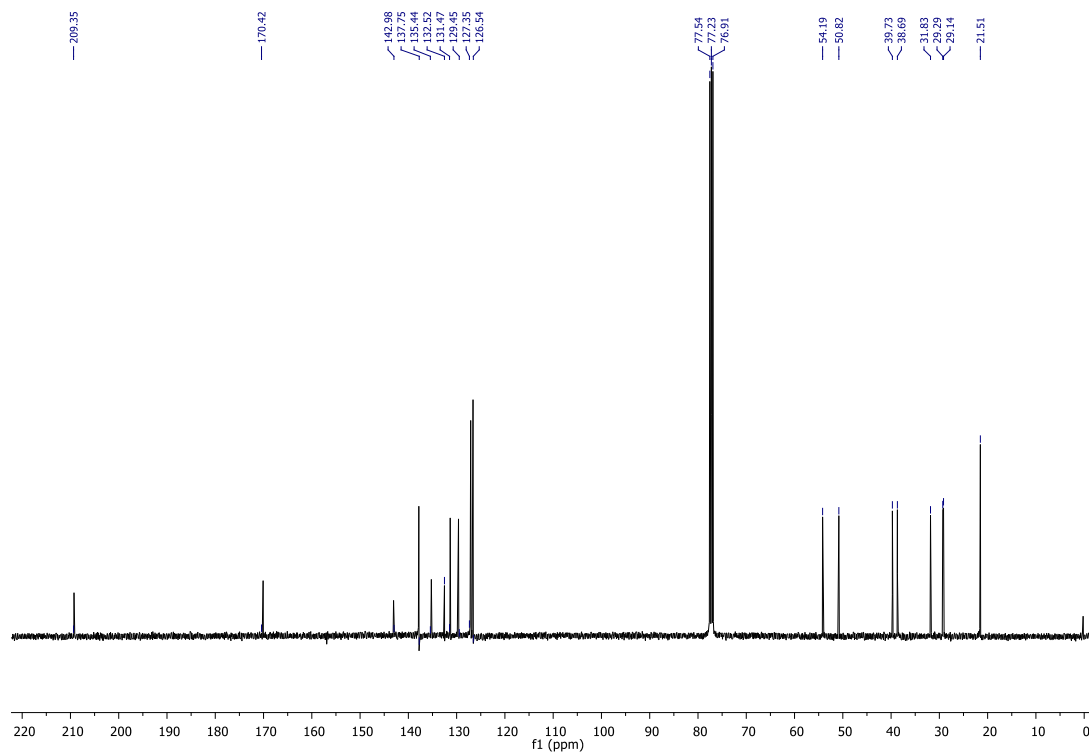
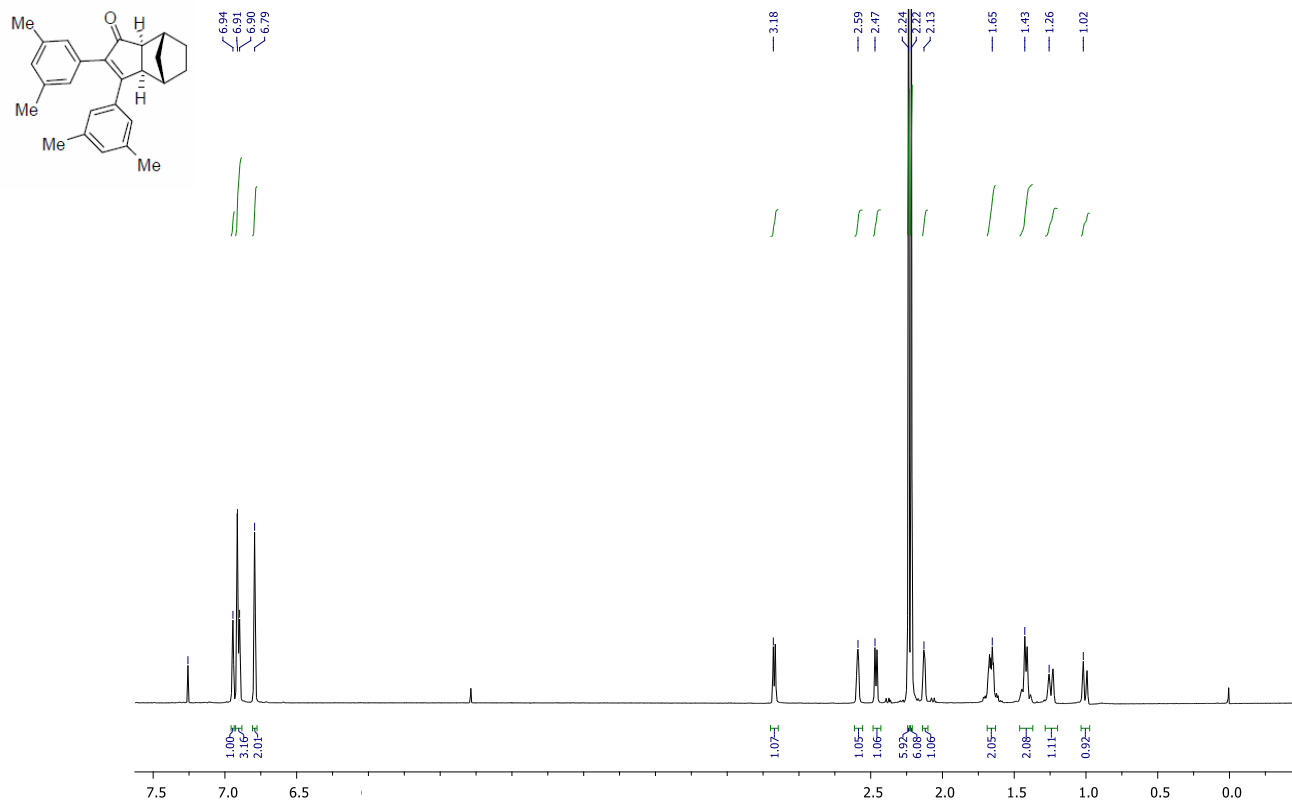
Selected spectra

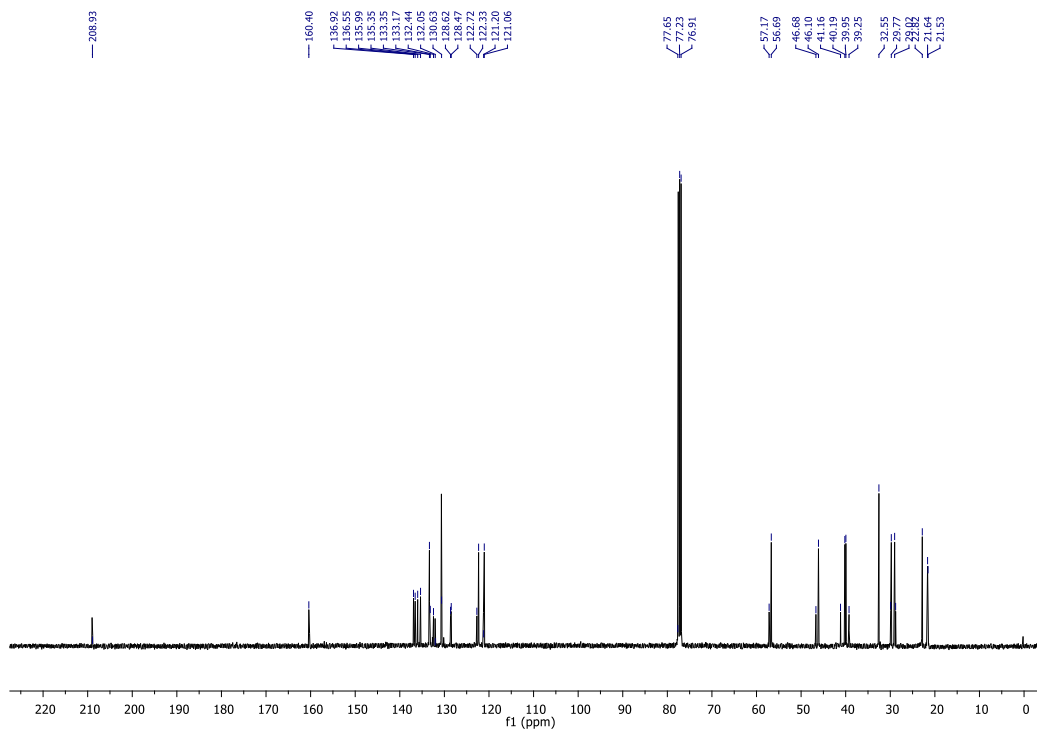
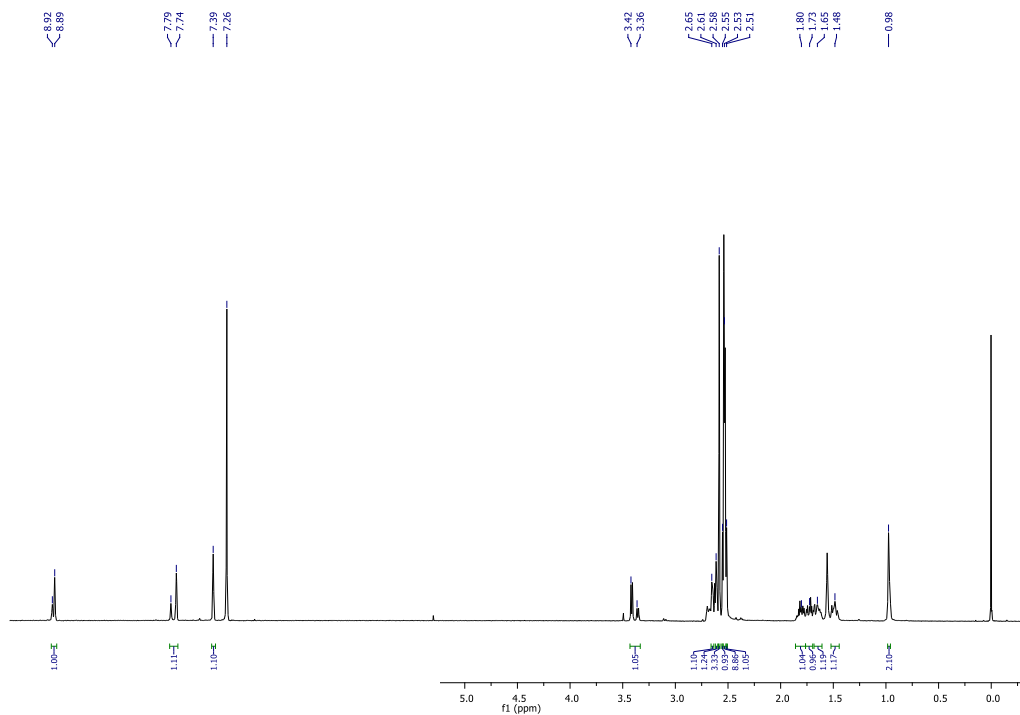
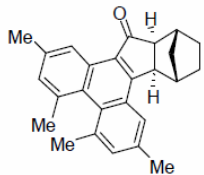


Selected spectra

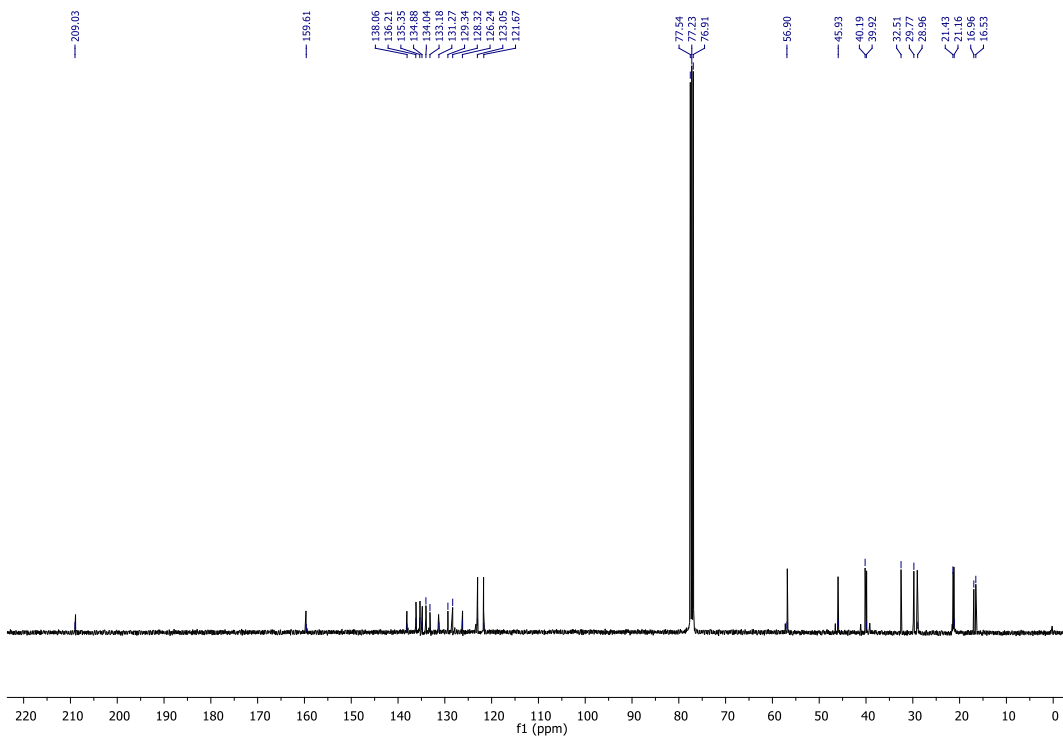
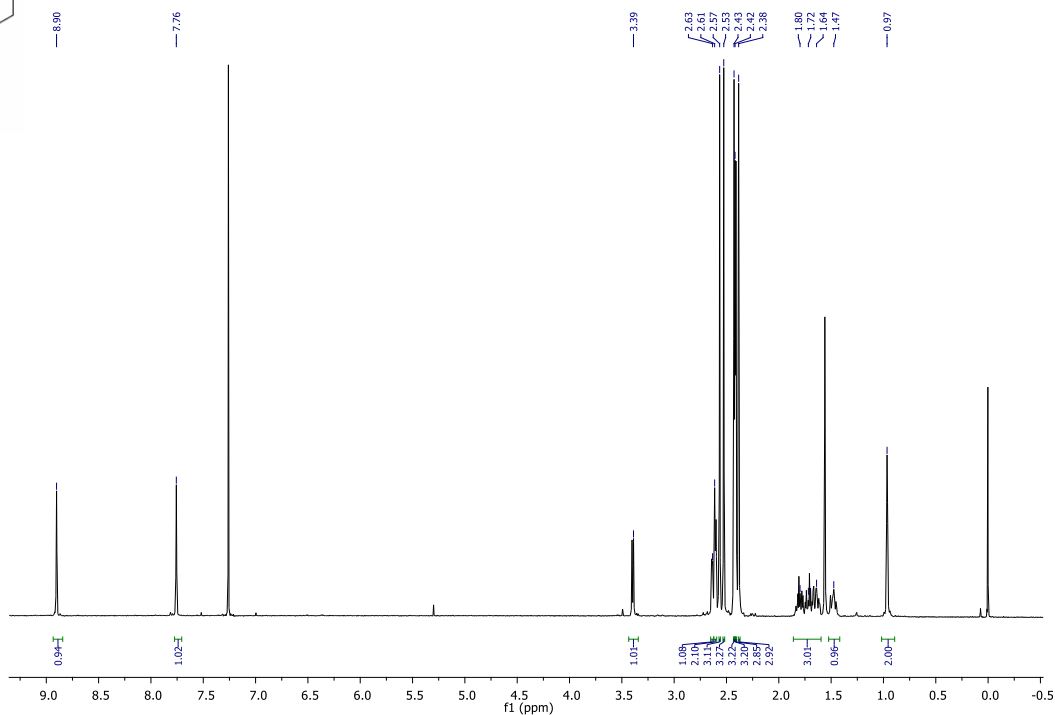
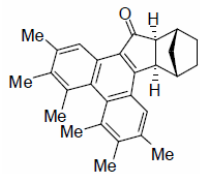


Selected spectra





Selected spectra



Appendix I

Publications

1) *Helical Atropisomers of Strained Phenanthrenes by Photochemistry of Aromatic Pauson–Khand Cycloadducts.*

Yining Ji, Héléa Khaizourane, Alexander N. Wein, Xavier Verdaguer and Antoni Riera.

European Journal of organic chemistry, 2012, 12, 30, 6058-6063.

2) *Regioselectivity of Intermolecular Pauson–Khand Reaction of Aliphatic Alkynes: Experimental and Theoretical Study of the Effect of Alkyne Polarization.*

Erika Fager-Jokela, Mikko Muuronen, Héléa Khaizourane, Ana Vázquez-Romero, Xavier Verdaguer, Antoni Riera, and Juho Helaja.

Journal of organic chemistry, 2014, 79 (22), 10999-11010.

Appendix II

Summary in Catalan

1. Introducció i objectius

La reacció de Pauson-Khand (PKR) descoberta durant l'any 1971 per P. L. Pauson i I. U. Khand, és formalment una cicloadició [2+2+1] entre un alquè, un alquí i una molècula de monòxid de carboni típicament mediada o catalitzada per un complex de cobalt, generalment $\text{Co}_2(\text{CO})_8$.¹ Es formen una ciclopentenona amb tres nous enllaços carboni-carboni i fins a dos nous centres estereogènics, si l'alquè és disubstituit (figura 1).

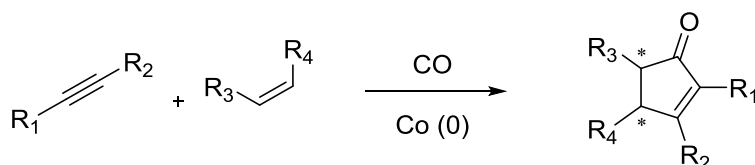


Figura 1.

La PKR és un dels mètodes més utilitzats per a la construcció de compostos amb anells de cinc baules i s'ha fet servir per sintetitzar un bon nombre de productes naturals o d'interès farmacèutic, com entre d'altres, l'ingenol² i la fusarisetin A³ (figura 2).

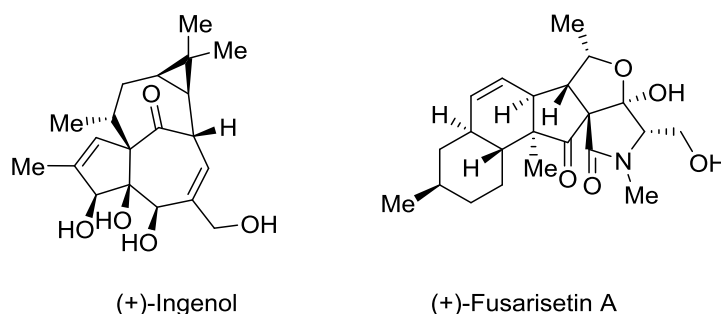


Figura 2.

La PKR pot ser intramolecular o intermolecular. La metodologia més emprada per a la construcció de compostos policíclics complexos amb anells de cinc baules, és la PKR intramolecular. Aquesta versió dona en pocs passos sintètics el adducte final normalment difícilment accessible per vies convencionals, i té poques restriccions pel que fa als grups funcionals dels sistemes emprats.

La PKR intermolecular ha estat menys emprada a causa del rang reduït d'alquens reactius. Només alquens cíclics i tensionats reaccionen d'una manera acceptable, l'etilè essent una excepció a aquesta regla.⁴ Els altres alquens donen lloc a rendiments baixos.

Un altre aspecte a tenir en compte és la regioselectivitat de la reacció. Quan l'alquí és terminal, la seva regioselectivitat es fa fàcil de determinar i només dona un regioisòmer amb el substituent en α de l'adducte (figura 3).

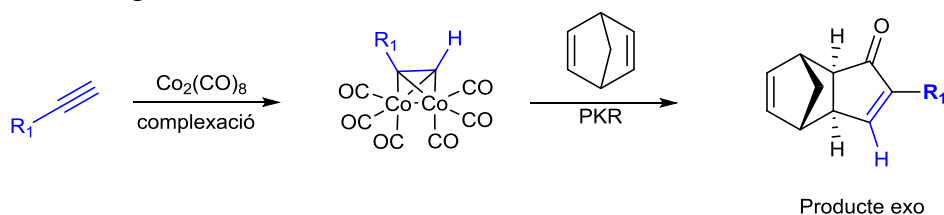


Figura 3.

Els alquins interns poden donar unes mesclades de α i β regioisòmers en proporcions variables. L'ús d'alquins interns ha estat limitat degut a que els resultats de la regioselectivitat són difícilment previsible. Per això, s'ha dedicat molts esforços a l'estudi de la regioselectivitat de la PKR intermolecular d'alquins interns dissimètrics. La primera hipòtesi va ser formulada per Greene i uns col·laboradors l'any 2001⁵. Els autors van proposar que els efectes estèrics i electrònics dels substituents d'alquins interns dissimètrics influeixen en la regioquímica dels productes finals de la PKR⁶ de la següent manera: el substituent més voluminós tendirà a ocupar la posició α al carbonil final, mentre que el substituent més petit preferirà la posició β (figura 4). Si tots dos substituents tinguessin mides similars, el grup més electro-donador aniria en α a la cetona i el més electro-atraent, en β .^{7,8}

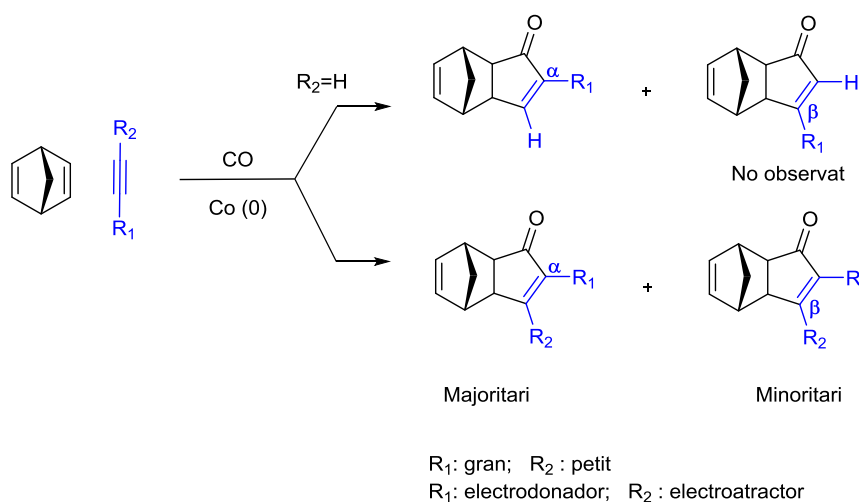


Figura 4.

En el nostre grup de recerca, s'ha observat que els alquins interns dissimètrics com els de la figura 5 donen una regioselectivitat sorprenentment alta o gairebé total.^{7,8,9}

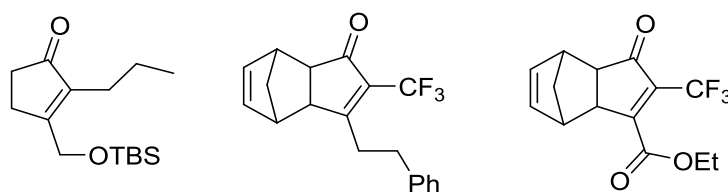


Figura 5.

En el cas de l'adducte amb els substituents CH_2OTBS i propil, de mida similar, les seves propietats electròniques influeixen molt la regioquímica.

També resulta sorprenent el cas del CF_3 i $(\text{CH}_2)_3\text{Ph}$ on el alquí amb substituents amb propietats estèriques i electròniques tan diferents dugués invariablement els adductes α trifluorometilats. Això, suggereix que, o bé l'efecte electro-atraent d'aquest grup és molt menys important de l'esperat, o bé que els efectes estèrics són més importants que els electrònics.

Un altre estudi del grup d'Helaja a Hèlsinki, ha mostrat recentment que l'exemple que Greene i col·laboradors van fer servir per il·lustrar la seva hipòtesi va ser conseqüència d'una anàlisi incompleta dels resultats experimentals. (figura 6).¹⁰ En el cas del difenil acetilè amb els substituents CO₂Et i metil, en para dels anells aromatics Greene i col·laboradors van observar només d'un adducte (amb el CO₂Et en β i metil en α) mentre que Helaja van observar una mescla dels adductes de relació (1:1.3).

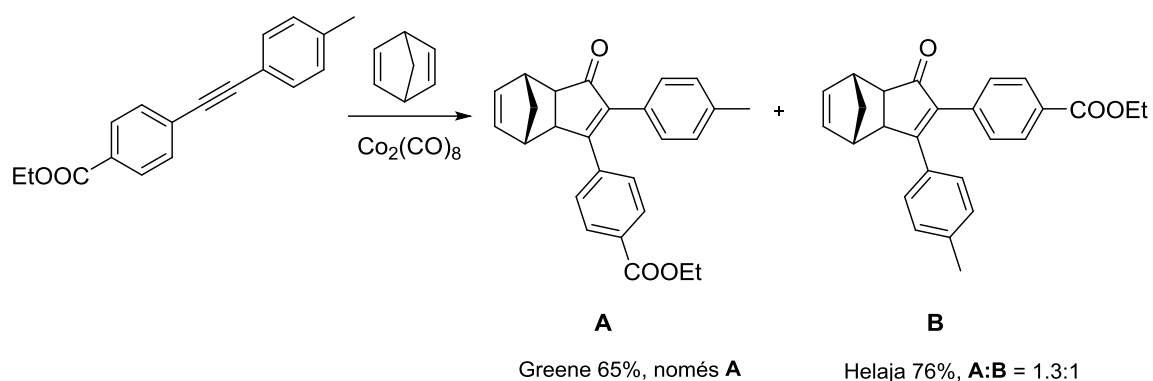


Figura 6.

A més, Helaja i col·laboradors han proposat una aproximació diferent per predir la regioselectivitat de la PKR intermolecular amb alquins amb anells aromàtics de mida semblant, però de propietats electròniques diferents (figura 7). Basat en càlculs DFT de la càrrega dels àtoms emprant orbitals naturals (Natural bonding orbital, NBO), van estudiar l'efecte de les càrregues NBO dels àtoms de carboni en α al carboni de l'alquí, (C1 i C4), a més dels carbonis acetilènics (C2 i C3).

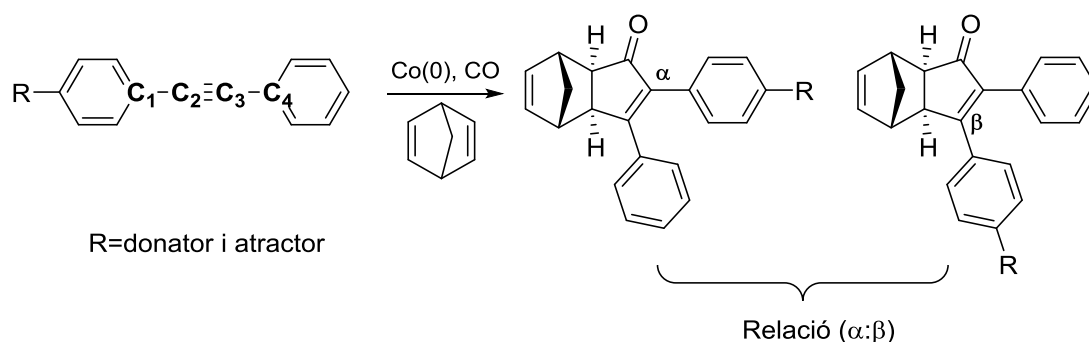


Figura 7.

Encara que les regioselectivitats observades son baixes (1:1.3), els resultats confirmen bé la tendència general proposada per Greene, però amb matisos i una millor correlació entre predicció i resultats (figura 8). A més, la correlació entre la selectivitat de la PKR dels alquins estudiats i els valors de Hammett coincideixen molt bé.

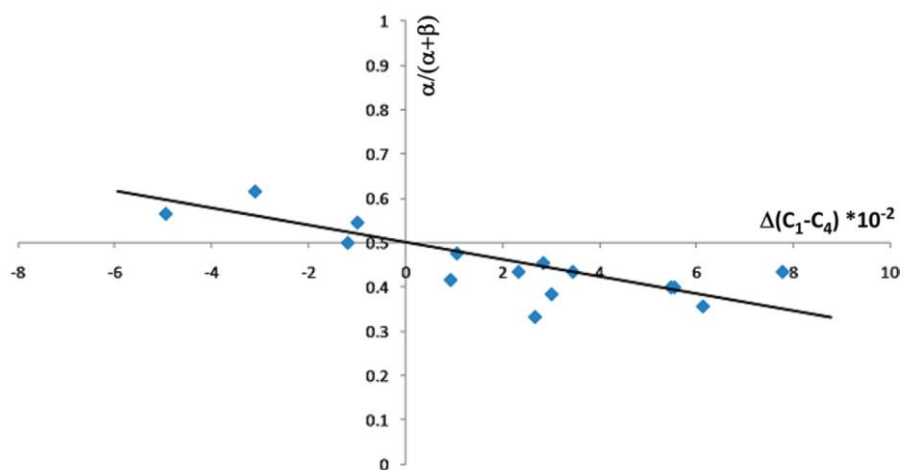


Figura 8.

A la vista d'aquests resultats sobre com pronosticar la regioselectivitat de la PKR intermolecular d'alquins aromàtics dissimètrics interns, hem pensat que aquesta aproximació podria permetre al nostre grup de recerca interpretar els resultats prèviament esmentats en la figura 5 i predir-ne d'altres.

El primer objectiu d'aquesta tesi va ser l'estudi de la regioselectivitat de la PKR intermolecular amb alquins interns, dissimètrics i alifàtics. Per aquest propòsit, es va plantejar una col·laboració amb el grup d'Helaja que va aportar al projecte la seva experiència en l'àrea computacional. Per això, al començament d'aquest treball es varen sintetitzar una varietat d'alquins amb substituents amb diferents propietats electròniques en un extrem i una cadena alifàtica per l'altre. En aquest sentit, l'objectiu va ser estudiar com els substituents afecten la regioselectivitat de la PKR de manera experimental i computacional. Els resultats han sigut descrits en el **capítol 2** (figura 9).

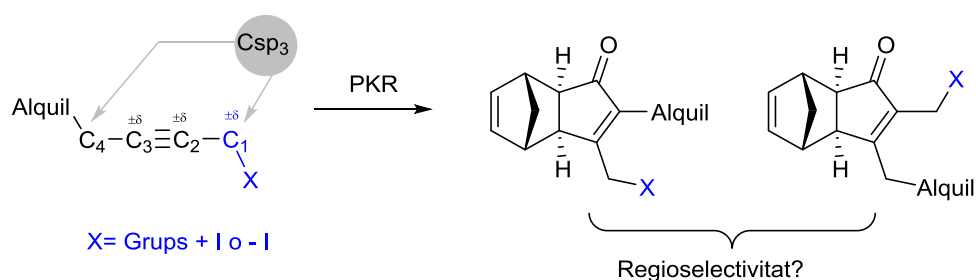


Figura 9.

El nostre grup s'han desenvolupat síntesis de diversos compostos naturals com el Carbovir¹¹, el fitoprostà dPPJ1-I¹² o l'àcid 13-epi-12-oxo fitodienoic¹³ (figura 10) mitjançant reaccions intermoleculars de Pauson-Khand.

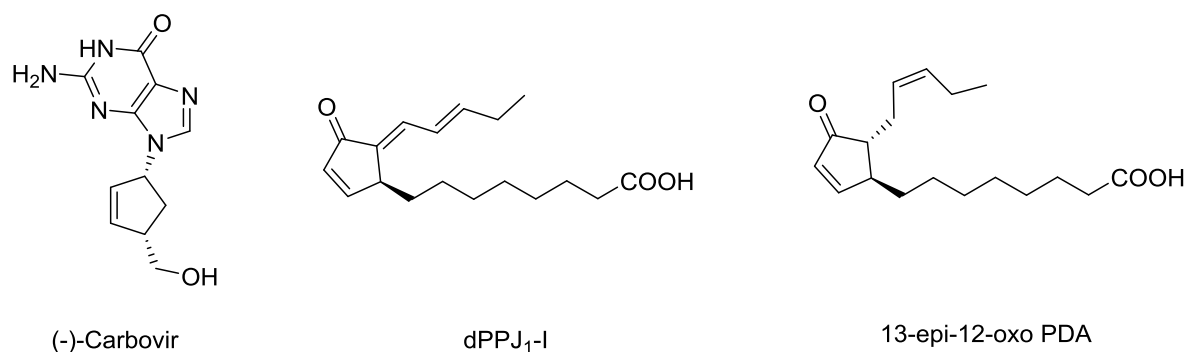


Figura 10.

Tenint en compte els resultats del nostre estudi de la regioselectivitat de la PKR d'alquins interns i per trobar aplicacions de la PKR intermolecular per la síntesi de compostos d'interès biològic, es va plantejar la síntesi de l'èster metílic de la sarcomicina i el jasmonat de metil (figura 11).

Els esforços destinats a la síntesi d'aquests compostos **que constitueixen el segon objectiu de la tesi**, es troben en el **capítol 3**.

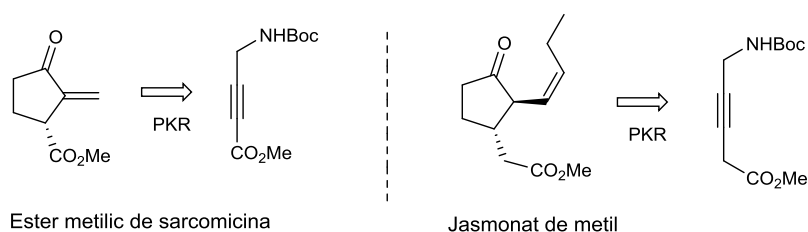


Figura 11.

De manera general, la transformació d'adductes de la PKR segueix habitualment les metodologies tradicionals de química orgànica.¹⁴⁻¹⁶ Entre aquestes possibilitats, podem mencionar la reacció utilitzant la llum que es va desenvolupar en el nostre grup en la tesi d'Agustí Lledó.¹⁷

Es van identificar dues noves reaccions fotoinduïdes: els adductes derivats d'alquins alifàtics experimenten una reacció de transposició per donar el compost **I** mentre que els derivats d'alquins amb substituents aromàtics donen una reacció de ciclació que condueix al compost **II** (figura 12).

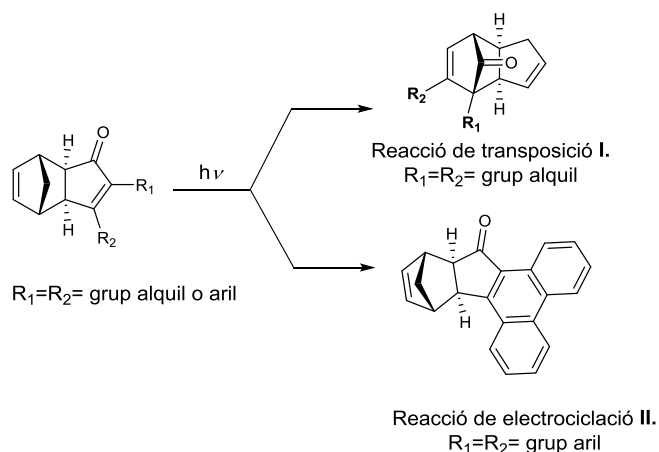


Figura 12.

En la tesi doctoral de Yining Yi, es va identificar que els adductes de PKR amb substituents aromàtics donen lloc a la formació de dos atropoisòmers P i M (figura 13).¹⁸ Aquest fenomen és degut a l'impediment estèric dels substituents metil que imposen la distorsió estructural de la molècula bicíclica de tipus helicènic. Els helicens són una família de molècules policícliques en alguns casos tenen propietats electròniques i tèrmiques que s'han utilitzat per la formació de dispositius electrònics, però s'han estudiat poc en biomedicina.¹⁹

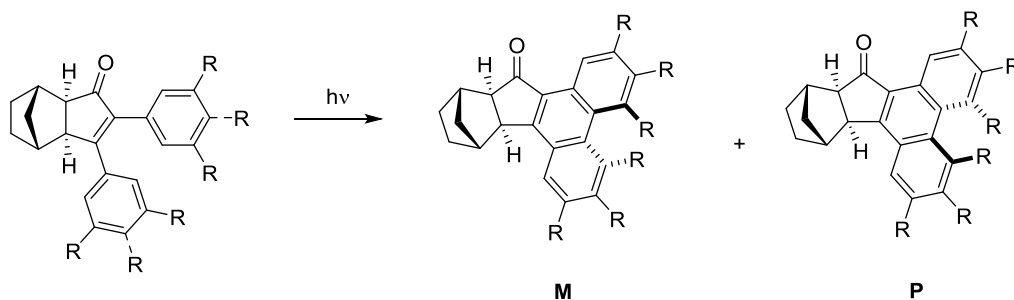


Figura 13.

Seguint el treball desenvolupat per la Dra. Yining Ji, en el capítol 4, es va plantejar completar l'estudi dels adductes de PKR amb alquins aromàtics disubstituïts.

La síntesi de la família de derivats helicènics constitueix la primera part del capítol 4.

En la segona part del capítol 4 es va plantejar l'estudi fotoquímic de PKR d'alquins heterocíclics aromàtics de tipus tiofenil i piridil (figura 14).

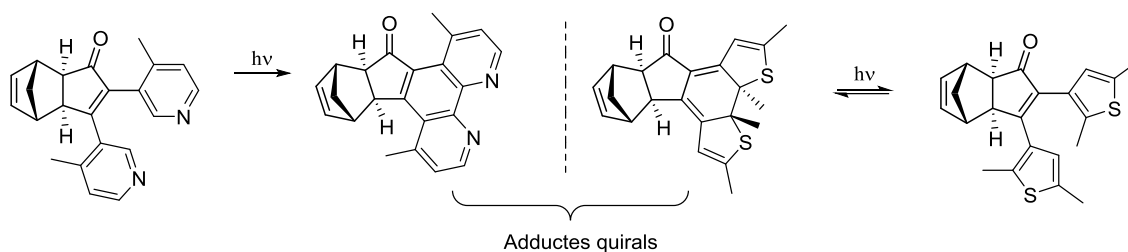


Figura 14.

Els adductes amb anells de fenantrolina podrien constituir potencials candidats per la síntesi de lligands quirals mentre que els tiofenils són coneguts per les seves capacitats per donar reaccions reversibles de fotociclació, per produir compostos anomenats "photoswitch". De fet, aquests compostos podrien ser interessants en l'àrea de dispositius electrònics o en biomedicina.^{20,21}

El tercer objectiu de la tesi doctoral va ser determinar si els grups piridil i el tiofenil serien compatibles amb la PKR i estudiar el comportament d'aquests adductes de Pauson-Khand en la ciclació fotoquímica.

En resum, la present tesi doctoral s'ha centrat exclusivament en la reacció de Pauson-Khand intermolecular amb aquests tres objectius principals:

1. Estudiar la regioselectivitat de la PKR intermolecular d'alquins interns alifàtics.
(capítol 2)
2. Sintetitzar noves molècules bioactives com l'èster metílic de sarcomicina i el jasmonat de metil utilitzant la PKR d'alquins interns.
(capítol 3)
3. Completar l'estudi de la síntesi dels composts helicènics preparats per PKR i reacció fotoinduida i de estendre-ho als precursors heterocíclics.
(capítol 4)

II. Estudi de la regioselectivitat de la PKR intermolecular d'alquins interns dissimètrics

La regioquímica de la PKR intermolecular és un factor difícil de predir; depenent dels substituents de l'alquí, la regioselectivitat dels adductes de PK canvia molt.

Es va acceptar la teoria que el grup més voluminós preferirà la posició α al carbonil i, en absència d'efectes estèrics, aquesta posició serà preferida pel substituent més electrodonador (figura 2.1).

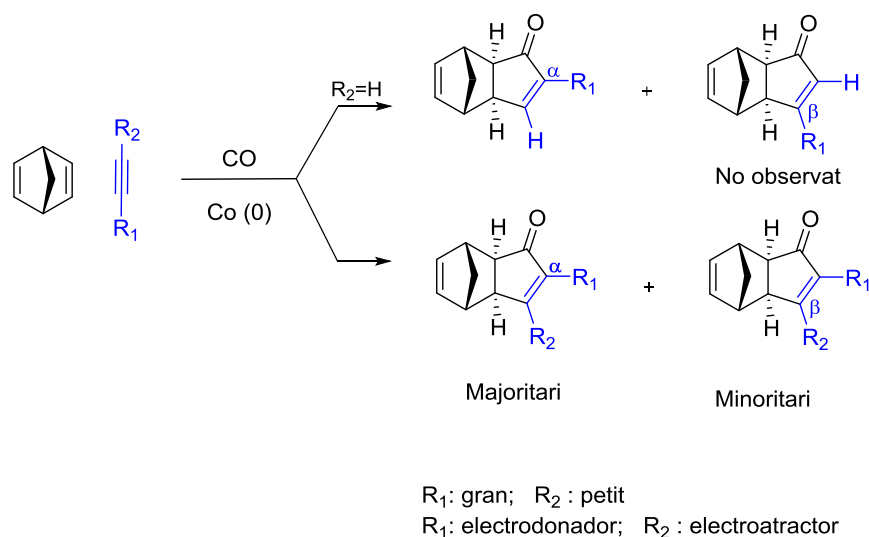


Figura 2.1.

En el cas d'alquins terminals, sempre s'obté l'adducte de PK α -substituït. En canvi, quan treballem amb alquins interns dissimètrics pot donar una mescla de regioisòmers.

Helaja i col·laboradors van centrar la seva atenció en l'efecte electrònic d'alquins diarílics estèricament equivalents. En lloc de calcular la polarització directa del triple enllaç dins el complex de dicobalt (difícil), prèviament proposat per Gimbert, Helaja i col·laboradors van trobar que la regioselectivitat de la PKR es pot correlacionar amb la diferència de càrregues entre els carbonis C1-C4 i C2-C3 del alquí.

Des un punt de vista computacional, d'acord amb els càrregues obtingudes a partir del càlcul dels orbitals naturals (Natural Bonding Orbital, NBO), l'enllaç C-C es forma amb el carboni més ric en electrons de l'alquí (C2 o C3).

Es van mesurar els valors de les càrregues NBO en α a l'alquí (carbonis C1-C4) i en els carbonis acetilènics (carbonis C2-C3). Experimentalment van fer reaccionar diaril alquins funcionalitzats amb norbornadiè per obtenir una barreja de regioisòmers α/β .

Els resultats confirmen bé la tendència general proposada per Greene, però amb matisos i una millor correlació entre predicció i la polarització dels carbonis α (C1-C4) del alquí (figura 2.2).

De fet, els grups electrodonadors (GED) i electroattractors (GEA) indueixen un flux d'electrons per efecte de ressonància al llarg del sistema que portarà a una major diferència electrònica entre dels carbonis (C2-C3) i entre dels carbonis (C1-C4).

Per càlculs DFT, la mesura dels valors relatius NBO al voltant de C2-C3 indica que si la diferència (Δ) de carrega segons NBO (C2-C3) és negativa significa que l'àtom més ric seria C2, el qual implica en la formació d'enllaç C-C que situarà el grup electroattractor en β -posició ciclopentenona.

Llavors, tenint en compte als valors NBO dels (C2-C3) del alquí, seria d'esperar un resultat similar en C1-C4. Per exemple, si la diferència del carrega NBO $\Delta(C1-C4)$ és positiva, això significa que C4 és més ric en electrons que C1, de manera el carboni C2 serà més ric en electrons, proporcionant el grup GED en α de la ciclopentenona final.

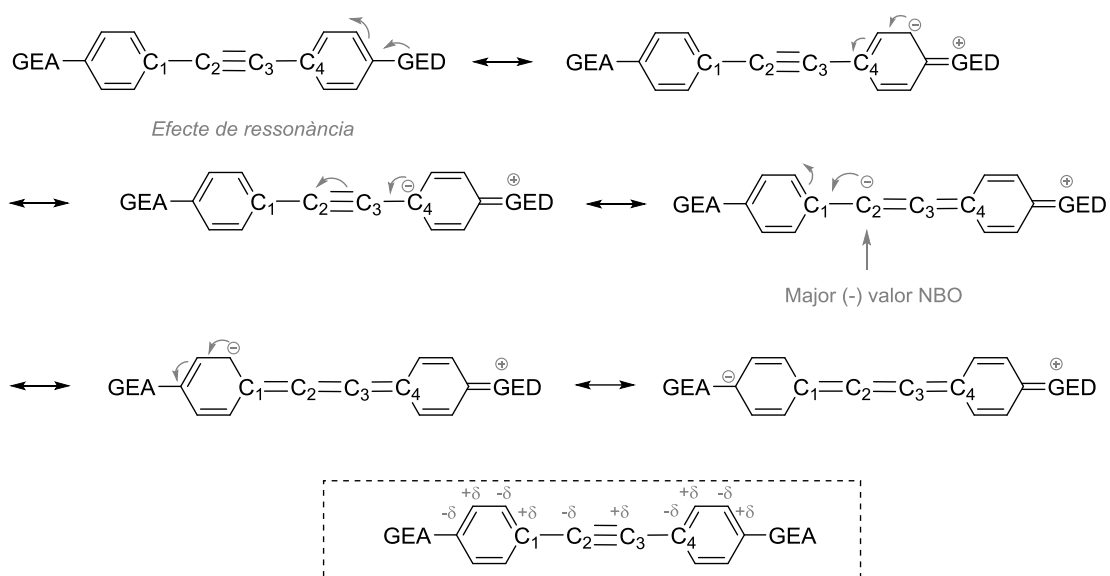


Figura 2.2.

Encara que les relacions de regioisòmers α/β observades van ser menors del que s'esperava (fins a 1:2) els lleugers excessos estaven en d'acord amb la hipòtesi que la polarització de l'alquí en α determina la regioselectivitat α/β de les ciclopentenonas finals a excepció d'alguns casos. Tot i que es sobreestimaren alguns valors, el $\Delta(C1-C4)$ i $\Delta(C2-C3)$ van predir qualitativament els resultats experimentals. Es va observar que $\Delta(C1-C4)$ a partir dels NBO correlaciona amb el resultat regioquímic amb més precisió que $\Delta(C2-C3)$.

A la vista d'aquests resultats sobre com predir la regioselectivitat de la PKR intermolecular d'alquins aromàtics dissimètrics interns, varem pensar que aquesta aproximació podria permetre al nostre grup de recerca interpretar els resultats prèviament esmentats.

L'objectiu d'aquest capítol, va ser estudiar la regioquímica d'alquins interns alifàtics des d'un punt de vista computacional i experimental en col·laboració amb grup de J.Helaja de la Universitat de Hèlsinki.

L'estudi va consistir en establir una relació entre les càrregues en els carbonis acetilènics dels d'alquins dissimètrics i els resultats de la regioselectivitat dels adductes de PKR. Els substituents dels alquins es van dissenyar de tal manera que els resultats observats només seriem causats per efectes inductius sense cap tipus d'influències estèriques.

Per evitar efectes ressonants, cada grup electrònic de l'alquí es va espair deliberadament amb un metilè del triple enllaç. Per un costat, l'alquí presenta una cadena alifàtica de n-propil i a l'altre costat, els grups electrodonadors i electroattractors (figura 2.3).

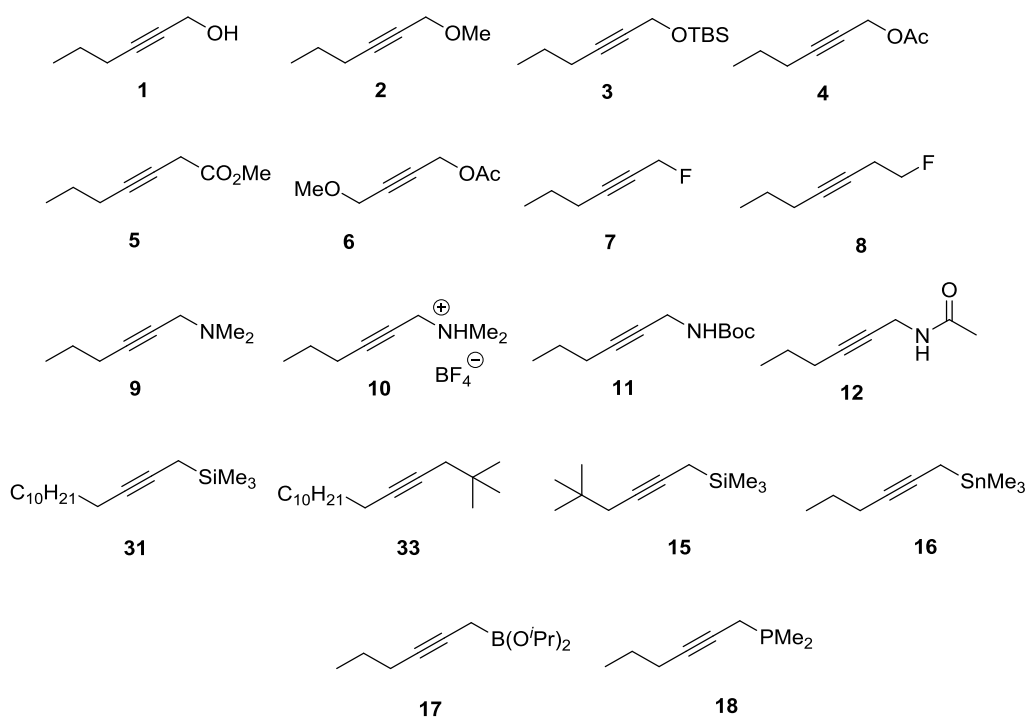


Figura 2.3.

En primer lloc es van sintetitzar els alquins amb substituents oxigenats, nitrogenats i amb fluor. Els derivats oxigenats 2 a 4 es van preparar a partir de 2-hexin-1-ol (1). Per tractament directe amb iodometà i trimetilamina es va obtenir 2 en un 76% de rendiment. El tractament amb cloro *tert*-butil dimetilsilà i trietilamina va conduir a 3 amb un 86% de rendiment (figura 2.4). El compost 4 es va obtenir en un 89% de rendiment per tractament amb anhidrid acètic, trietilamina amb una quantitat catalítica de DMAP.

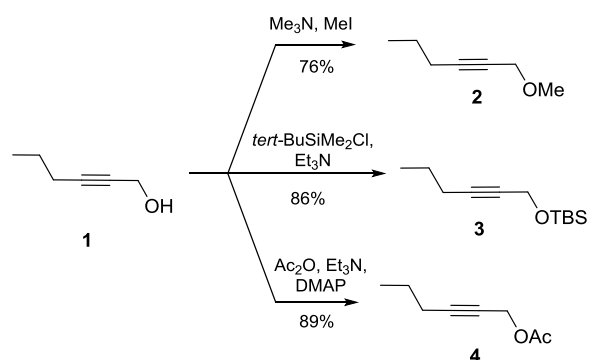


Figura 2.4.

La síntesi de l'alquí 5 amb un èster metílic es va preparar a partir de l'hepta-3-in-1-ol (figura 2.5). Per oxidació de l'alcohol usant periodat de sodi, amb una quantitat catalítica de dicromat de potassi i àcid nítric seguida de metilació usant trimetilsilil diazometà es va obtenir 5 en un 54% de rendiment en dues etapes.

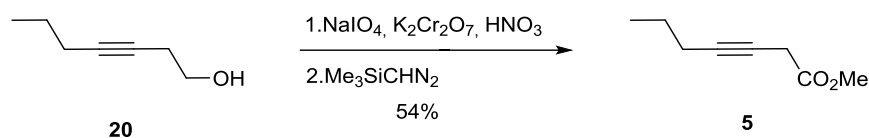


Figura 2.5.

Per provar d'arribar als compostos **7** i **8** es va utilitzar com a agent de fluoració nucleofílica el trifluorosulfur de dietilamina (DAST). Els compostos fluorats van ser difícils de purificar i s'obtenien com una mescla de productes fluorats i altres subproductes (figura 2.6). Solament, es va obtenir el compost **8** però degut a la seva volatilitat i gran caràcter lipofílic, es va preparar el seu complex de cobalt **44** a partir del cru de reacció en 14% de rendiment.

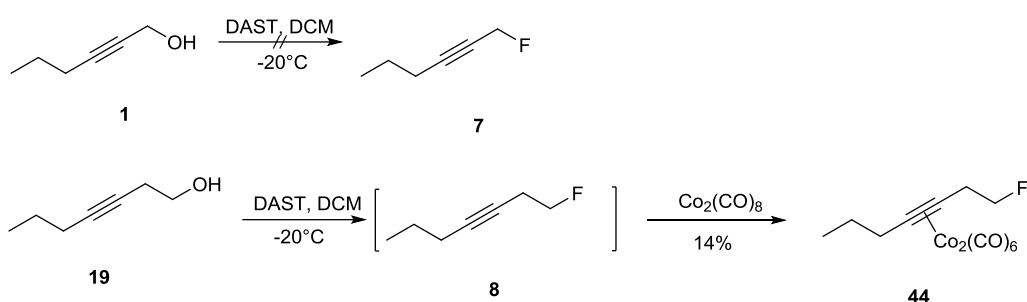


Figura 2.6.

Tant la síntesi de l'alquí **6** com la dels alquins amb una funció nitrogenada en la posició propargílica **9** a **12** es van preparar a Hèlsinki per Erika Fager-Jokela. L'alquí **6** es va preparar a partir del 4-metoxibut-2-in-1-ol (**19**) amb trietilamina i anhídrid acètic dissolts en DCM donant un 89% de rendiment (figura 2.7).

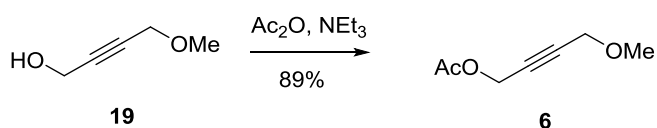


Figura 2.7.

Els alquins **10** a **12** es van fer a partir de la mesilació del compost **1** en 95%, seguida d'una substitució amb dimetilamina per donar el compost **9** en un 43 % que, després d'un tractament amb HBF_4 va conduir al compost **10**. El mateix alquí **1** va permetre obtenir l'amina primària (**21**) per tractament amb l'azida de sodi per donar (**22**) seguit de reducció per obtenir el compost **23** en 55 %.

Finalment, es va funcionalitzar l'amina per donar **11** i **12** en 92% i 88% de rendiment respectivament (figura 2.8).

Summary in Catalan

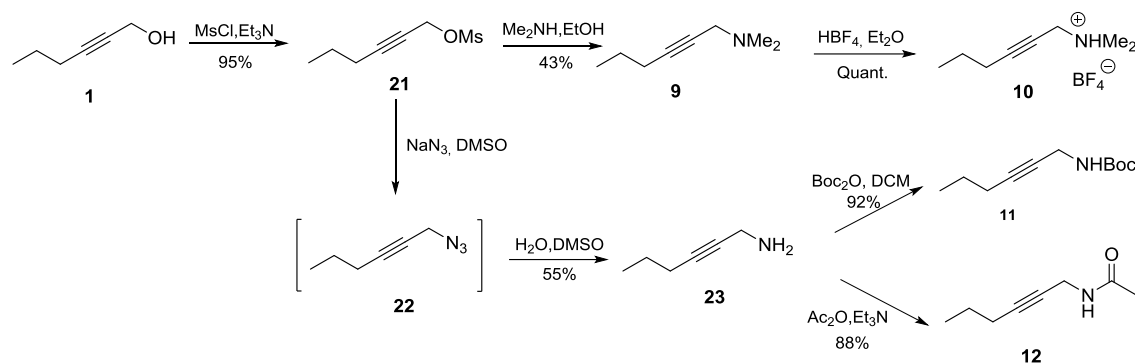


Figura 2.8.

Per tal d'invertir la regioselectivitat de la PKR, es va pensar en posar-hi àtoms menys electronegatius en la posició propargílica de aquí. Segons a la taula d'electronegativitat de Pauling, els elements que tenen un valor d'electronegativitat inferior al de l'àtom de carboni ($\chi 2.55$), es a dir els més electropositius, són els àtoms de bor, fòsfor, silici i estany (figura 2.9). A nivell sintètic, per un tema de estabilitat, només es va considerar la síntesi dels compostos amb silici i estany.

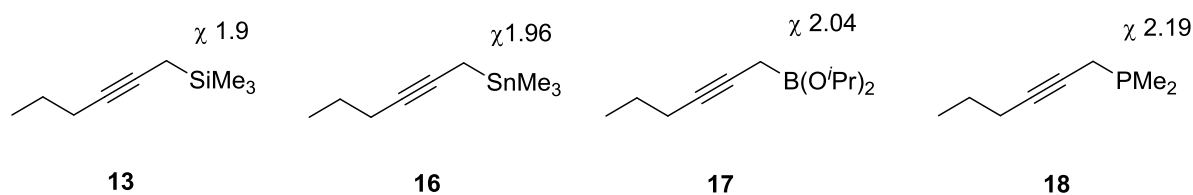


Figura 2.9.

Per la síntesi dels derivats del silici 13, es va a identificar a part de la seva volatilitat que aquesta molècula era inestable causant l'escissió del grup silil. En aquest cas, vàrem decidir canviar el fragment propil per undecil per tal de que fos menys volàtil. Després d'optimització, es va aconseguir formar el producte esperat 31. Es va tractar 28 amb LDA i HMPA a -78°C i es va afegir (clorometil)trimetilsilà (figura 2.10). Es va deixar reaccionar durant 10 hores a -78°C i es va escalfar fins a temperatura ambient i es va agitar durant la nit. Es va detectar predominantment el compost 31 i la formació en petita quantitat dels compostos 31A i B, difícil de purificar en un rendiment del 93% i un relació de (12:1) mesurada per ressonància magnètica nuclear.

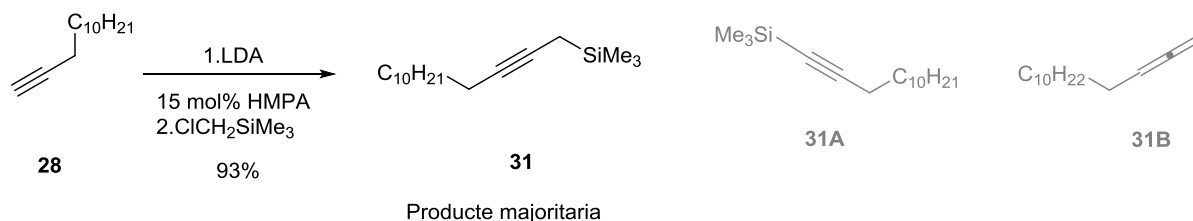


Figura 2.10.

Amb tots els substrats sintetitzats **1 a 16**, **31**, **33** i **35**, el següent pas va consistir en estudiar la reacció de PK en dues etapes de reacció, en primer lloc, es va aïllar els complexos de cobalt i després es van deixar reaccionar amb norbornadiè (NBD).

Els crús de reacció es van cromatografiar i les fraccions purificades riques en regioisòmers minoritaris analitzades per ressonància magnètica nuclear. Els regioisòmers possibles es van detectar mitjançant les integrals dels senyals de protons fàcilment identificades (figura 2.14).

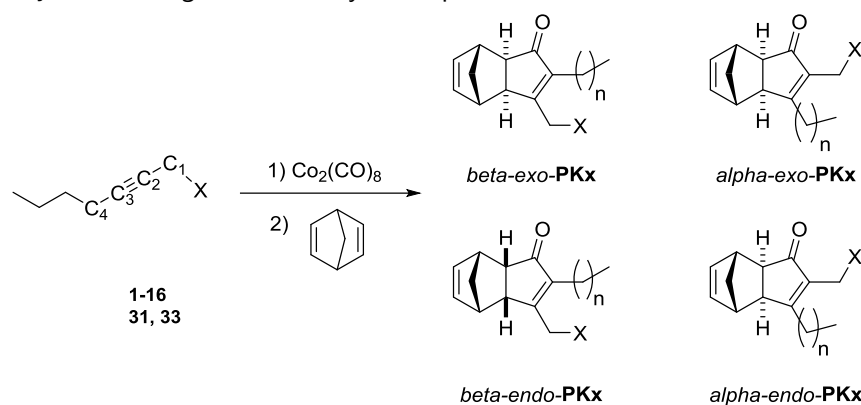
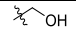
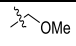
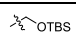
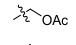
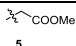
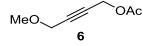


Figura 2.14.

Després, es va comparar la regioselectivitat amb els càlculs teòrics DFT. La predicció computacional de la polarització dels alquins l'han realitzat Mikko Muuronen del grup del Prof. Helaja. Les diferències de càrrega NBO dels carbonis alquínils (C2-C3) i dels α -carbonis (C1-C4) es van calcular per estudiar la influència dels factors electrònics sobre la regioselectivitat (figura 2.18). Els càlculs DFT es van fer en fase gasosa amb TPSS-D3 meta-GGA funcional juntament amb bases de triple ζ d'alta qualitat DEF2-TZVPP. La cadena llarga va ser tractada com propil en tots els càlculs.

Las PKR amb alquins, es va realitzar en diferents condicions (NMO, catalític) i es va comprovar que les condicions estequiomètriques tèrmiques en toluè a 70°C amb cinc equivalents de NBD eren les millors. Els adductes de PK sempre van donar l'isòmer β -*exo* en una alta regioselectivitat. Es va observar una selectivitat total amb alquins **1** i **2** (taula 2.1). L'hex-2-in-1-ol **1** va donar el 72% de rendiment, encara que l'aldehid es va obtenir com a producte secundari a causa de l'oxidació de l'alcohol (taula 2.1, entrada 1). Els derivats OTBS **3** i acetilat **4** van donar regioselectivitat gairebé completa (taula 2.1, entrades 3 i 4). Sorprenentment, l'impediment estèric del grup OTBS no sembla afectar la regioselectivitat. L'alquí disubstituit **6**, que porta el grup metoxi i acetil va donar el adducte de PK amb un rendiment del 34% (taula 2.1, entrada 6). Tot i la més alta regioselectivitat del derivat acetilat **4** en comparació amb el derivat metoxi **2**, el alquí combinat era gairebé no selectiu donant relació regioisomèrica (1:1.1).

Entry	Alkyne used	Ratio $\alpha:\beta$	C1	C2	C3	C4	$\Delta(C1-C4).100$	$\Delta(C2-C3).100$
1		0:1	-0.12	-0.08	0.01	-0.45	32.77	-9.02
2		0:1	-0.13	-0.05	0.02	-0.45	32.03	-6.9
3		~1:27	-0.11	0.05	0.02	-0.45	33.77	-6.36
4		~1:30	-0.13	-0.07	0.05	-0.45	31.86	-11.38
5		~1:22	-0.54	-0.03	0.02	-0.45	-9.48	-4.89
6		1:1.1	-0.14	-0.03	0.02	-0.14	-0.37	-4.47

Taula 2.1.

Des d'un punt de vista computacional, els càlculs de diferències de càrregues NBO dels carbonis alquínils (C2-C3) i els α -carbonis (C1-C4), mostren bé l'efecte de la electronegativitat en la regioselectivitat. Amb els substrats 1 a 4, els valors de las càrregues NBO $\Delta(C1-C4)$ i $\Delta(C2-C3)$ van donar el regioisòmer esperat (taula 2.1, entrades, 1-4). Las càrregues NBO $\Delta(C2-C3)$ va donar valors negatius en bon acord amb la hipòtesi que la formació de l'enllaç C-C té lloc al C2, el carboni acetilènic més ric en electrons (figura 2.15).

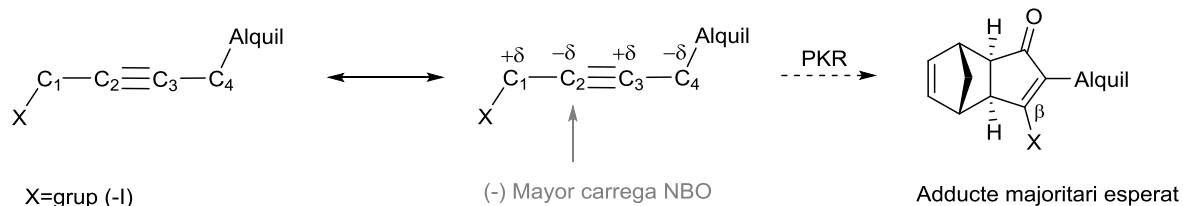


Figura 2.15.

Les diferències de càrrega $\Delta(C1-C4)$ calculades a partir dels alquins 1 a 4 correlacionen una mica millor que els valors $\Delta(C2-C3)$ amb la regioselectivitat. De fet, les diferències de magnituds $\Delta(C1-C4)*100$ eren gairebé idèntics (entre 31 i 32), mentre que els valors $\Delta(C2-C3)*100$ va oscil·lar entre (-6) i (-11) (taula 2.1, entrada, 1-4).

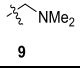

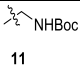
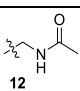
El alquí 5 va donar una alta regioselectivitat tot i tenir una polarització $\Delta(C2-C3)*100$ de -4,89, que prediria un resultat regioquímic menor que alquí 4, (-11,38) (taula 2.1, entrades 4,5). De fet, la posició en α (C1-C4) va ser inversament polaritzada quan el heteroàtom es troba un carboni més lluny de la alquí, en la γ -posició. L'efecte inductor no era més visible en la diferència de càrregues de la α -posició. Així, amb l'alquí 5, la $\Delta(C1-C4)*100$ va donar -9,48, mentre que alquí 4, va donar 31,86.

El alquí substituït 6, que porta el grup metoxi i acetil va donar una barreja de regioisòmers en relació (1:1,1) i 34% de rendiment (taula 2.1, entrada 6). Els dos substituents tenen un efecte electronegatiu similar sobre la polarització de la alquí fent que el resultat de la reacció no sigui

selectiu. Aquest fet es reflecteix millor amb el $\Delta(C1-C4)*100$ de -0.37 que en el $\Delta(C2-C3)*100$ que va donar -4,47.

Las diferències de càrregues dels carbonis alcelilènics $\Delta(C2-C3)$ i els carbonis en α $\Delta(C1-C4)$ calculades poden correlacionar bé amb els experiments. Els càlculs $\Delta(C1-C4)$ prediuen bé el resultat regioquímic qualitativament tot i que la selectivitat va ser clarament sobreestimada. Aquests resultats estaven en bon acord amb el fet que l'enllaç C-C es va formar amb el carboni més ric en electrons de l'acetilè.

La PKR de la sèrie nitrogenada **9** a **12** va donar també una bona selectivitat cap a l'isòmer β -*exo*, però els rendiments i selectivitats van ser generalment més baixos que amb alquins amb oxigen (taula 2.2). La N,N-dimetilhex-2-in-1-amina **9** i la seva sal de tetrafluoroborat **10** van proporcionar exclusivament l'isòmer β -*exo* en 49% i un rendiment del 29% (taula 2.2, entrades 1 i 2). La protonació del grup dimetilamina no inverteix la polarització de l'alquí però l'intensifica. Els N-Boc i N-acetil derivats **11** i **12** van donar 35% i 33% de rendiments amb com a producte principal l'isòmer β -*exo* acompanyat amb quantitats notables d'adductes d' α -*exo* en un (1:3) i (1:1.5) de relació (taula 2.2, entrades 3 i 4).

Entry	Alkyne used	Yield (%)	Ratio $\alpha:\beta$	C1	C2	C3	C4	$\Delta(C1-C4).100$	$\Delta(C2-C3).100$
1	 9	49	0:1	-0.27	-0.06	-0.01	-0.45	17.23	-4.39
2	 10	29	0:1	-0.25	-0.17	0.16	-0.47	22.37	-32.52
3	 11	35	1:3	-0.27	-0.05	0.01	-0.45	17.59	-6.26
4	 12	33	1:1.5	-0.28	-0.05	0.01	-0.45	16.91	-6.24

Taula 2.2.

La diferència d'electronegativitat entre el nitrogen i l'oxigen també era visible en las càrregues obtingudes dels NBO. Això, indica que la polarització de l'alquí induïda per l'alquí nitrogenat és més feble. Els N-Boc i N-acetil derivats **11** i **12** estan polaritzats de manera similar tant en el (C2-C3) com els alquins oxigenats. Quant als valors de (C1-C4), **11** i **12** eren menys polaritzats en la posició α . Això encaixa bé amb els resultats experimentals on la selectivitat és menor en **11** i **12** que en **1-4**.

En el cas dels fluoro alquí **8**, la PKR va ser difícil donant una complexa barreja de productes. Desafortunadament durant l'etapa de complexació, l'alquí va resultar inestable i es va poder aïllar una petita fracció del compost **44** amb un 13% de rendiment (figura 2.16).

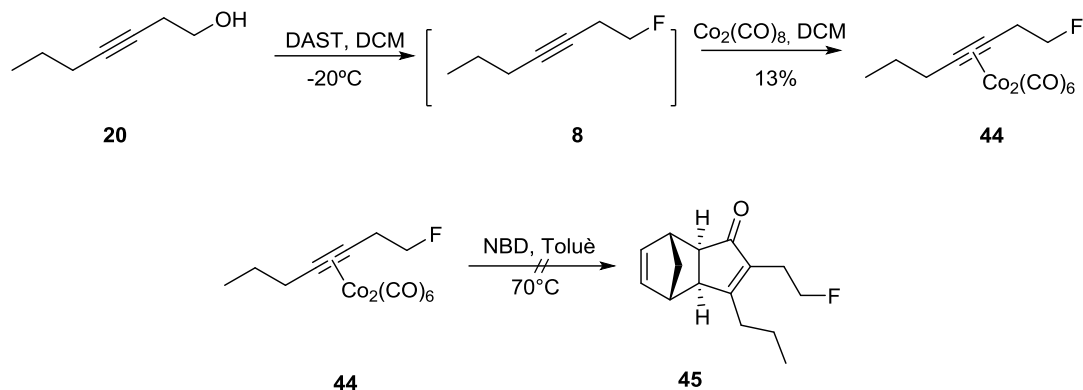


Figura 2.16.

La reacció de PK estequiomètrica amb cinc equivalents de NBD a 70°C, va donar lloc a **45** més una barreja de productes que contenen fluor. Es va confirmar per HR-MS la formació dels adductes PK amb el fluor. La determinació de quin isòmer es va formar no va ser possible de determinar en aquest punt.

Els alquins amb un àtom electropositiu en la posició propargílica es van sotmetre a la PKR. Per primera vegada, la PKR de l'alquí estannil **35** va ser estudiada. Quan la PKR va fer-se, es va observar la formació de un complex de cobalt (**46**) però es va obtenir un adducte de PK (**49**) on el grup estannil s'havia escindit (figura 2.17). El grup pentil es va col·locar en la posició α i el metil en la β -posició de la ciclopentenona. La purificació va proporcionar un rendiment del 90% d'un únic adducte de PK (**49**).

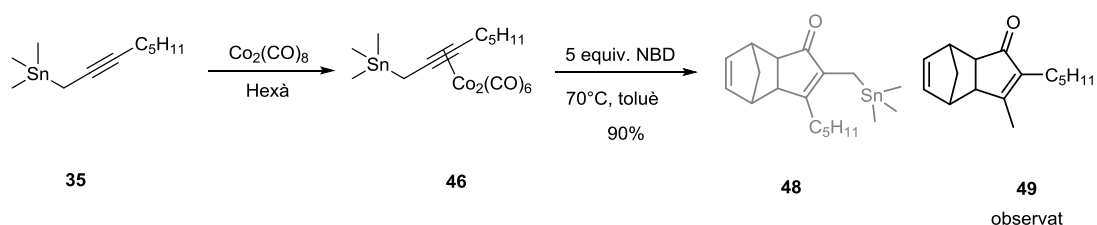


Figura 2.17.

A causa de l'alta inestabilitat del grup estannil, es van utilitzar varietat de condicions (baixes temperatures o afegir lentament el complex de dicobalt hexacarbonil de l'alquí sobre una solució de NBD en toluè a 100°C) i podríem concloure que el complex de dicobalt amb un substituent estannil és inestable. S'obté, per tant, l'adducte de PK del 2-octí en un bon rendiment.

Amb l'alquí **31** es va identificar que el grup silil del complex de cobalt també tenia la tendència de donar en el compost **52** sense el grup silil (figura 2.18).

Summary in Catalan

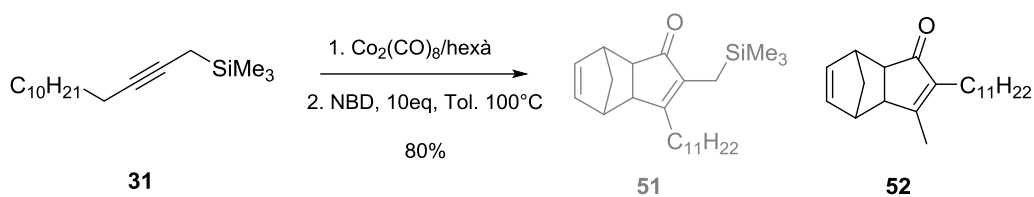


Figura 2.18.

Per aquesta reacció de PK estequiomètrica sí que es va poder millorar el resultat afegint lentament el dicobalt hexacarbonil de l'alquí sobre una dissolució de l'alquè en toluè a $100^\circ C$. Amb una xeringa automàtica durant 3-5 hores es va afegir el complex sobre una solució de 10 equivalents de NBD en toluè (0,04 M respecte de alquí) a $100^\circ C$. Espectacularment, el rendiment va augmentar fins a un 80%. Com podia ser previst, l'alquí amb el trimetilsilil més electropositiu va donar el regioisòmer oposat, l'isòmer α *exo* com l'únic producte i una alta relació *exo/endo* de (24:1).

La reacció de PK de l'alquí **33**, es va fer la PK amb 10 equivalents de NBD a $100^\circ C$ donant un rendiment del 79% d'un únic α -regioisòmer **56** i una extremadament alta relació *endo/exo* 1:32 (figura 2.19).

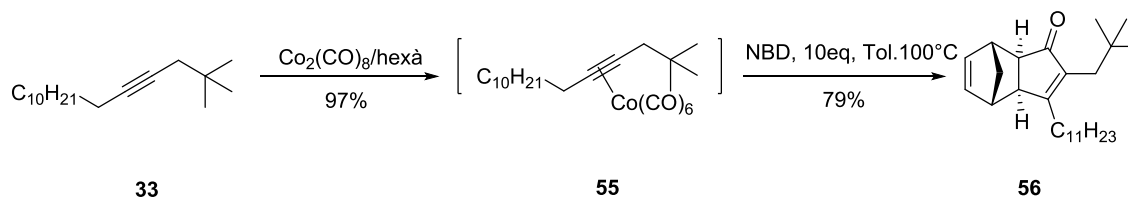
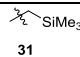
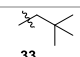


Figura 2.19.

Las càrregues NBO de $\Delta(C1-C4)$ i $\Delta(C2-C3)$ del substrat **31** i **33** indiquen que s'haurien d'obtenir els isòmer α -*exo* (taula 2.3). La regioselectivitat total del alquí **31** correlaciona millor amb els valors $\Delta(C1-C4)$ que les valors $\Delta(C2-C3)$. En el cas del alquí **33**, l'alta regioselectivitat observada no es va correlacionar amb l'efecte de polarització petita en comparació amb els altres alquins estudiats. Però, encara que el seu petit efecte polarització no podria explicar l'alta selectivitat, la $\Delta(C1-C4)$ i $\Delta(C2-C3)$ mostren bé que l'enllaç C-C es formi sobre els rics de carboni més electrons. De fet, la formació exclusiva del α -regioisòmer pot ser deguda a una combinació d'efectes estèrics i electrònics.

Entry	Alkyne used	Yield (%)	Ratio $\alpha:\beta$	C1	C2	C3	C4	$\Delta(C1-C4).100$	$\Delta(C2-C3).100$
1	 31	80	1:0	-0.88	-0.02	-0.04	-0.44	-43.77	1.42
2	 33	79	1:0	-0.45	-0.02	-0.02	-0.44	-0.87	0.21

Taula 2.3.

L'efecte inductor positiu que porta un àtom menys electronegatiu que el carboni α indueix una densitat electrònica major sobre carboni C3 que el C2. Per tant, la diferència de densitat electrònica al voltant de $\Delta(C2-C3)$ seria positiva afavorint el regioisòmer α (figura 2.20).

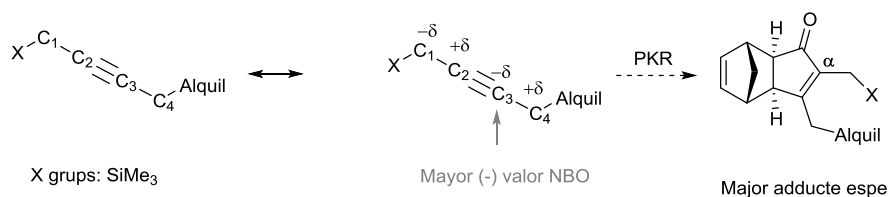


Figura 2.20.

III. Desenvolupament d'una nova metodologia per a la síntesi de productes naturals: l'èster metílic de sarcomicina i jasmonat de metil.

Per començar, es va desenvolupar la síntesi del èster metílic de sarcomicina seguint dos tipus de metodologies involucrant una enantioselectiva i l'altra racèmica (figura 3.1). Es va intentar la síntesi enantioselectiva amb la reacció de PK entre el norbornadiè i la N-Boc-propargilamina o bé amb un alquí disubstituint per la introducció regioselectiva de la dues cadenes en α i β .

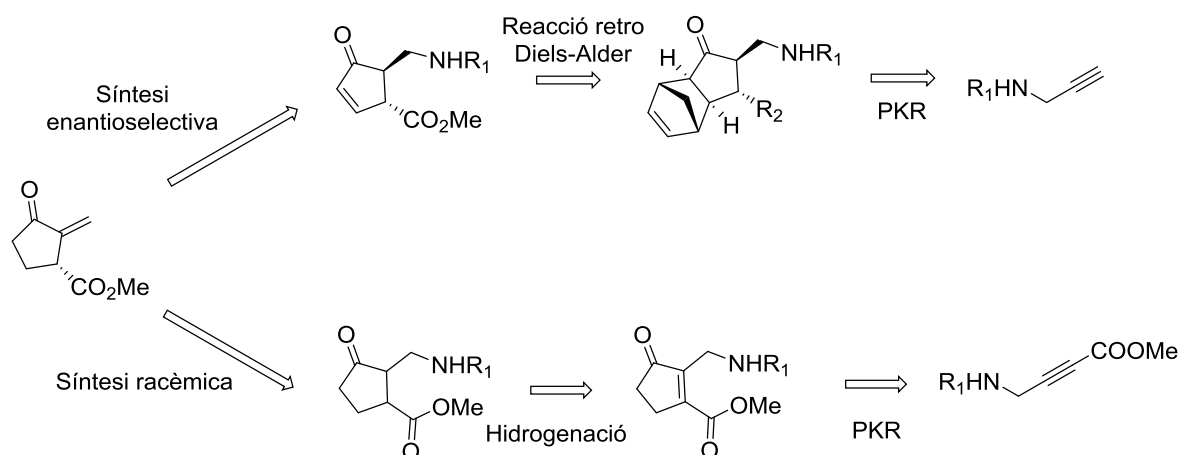


Figura 3.1.

En primer lloc, es va intentar la síntesi enantioselectiva amb la reacció de PK entre el norbornadiè i la N-Boc-propargilamina (figura 3.2). Es va fer la reacció amb 5 equivalents de norbornadiè a 85°C en toluè amb una quantitat catalítica de Co₂(CO)₇PPh₃ obtenint l'adducte **61** en un rendiment del 49% i una elevada selectivitat *exo/endo* de (94:6).

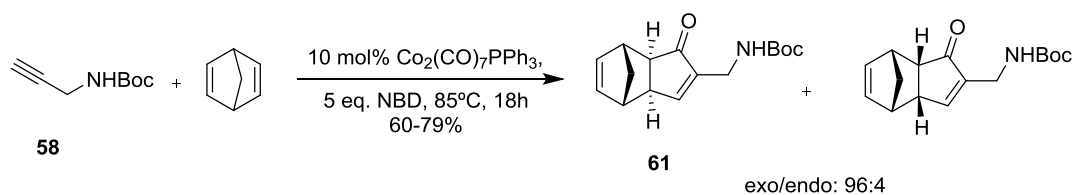


Figura 3.2.

Seguidament, es va realitzar la reacció foto-induïda del compost **61** amb metanol a 350 nm i 1 equivalent de benzofenona. El rendiment de la reacció donant el composte **64** va resultar molt baix i no reproduïble, entre 10 i 54% (figura 3.3).

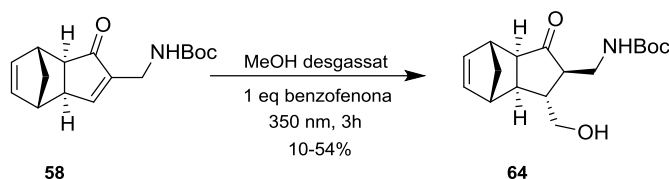


Figura 3.3.

Es va estudiar la influència de la reacció foto-induïda canviant diferents condicions: de temperatura, tipus de vidre, longitud d'ona, concentració de sensibilitzador, escala de la reacció i tipus de grups protectors de l'amina.

Després d'intentar optimitzar els rendiments, van concloure que la reacció és molt difícil de reproduir i a més dóna lloc a molts subproductes de reacció.

Amb una petita quantitat de substrat **64**, hem seguit amb la reacció d'oxidació i metilació. Es va fer la oxidació del alcohol primari en àcid usant una quantitat catalítica de dicromat de potassi en àcid nítric donant el compost **82** que després de la metilació condueix al substrat **71** en un rendiment del 69% (figura 3.4).

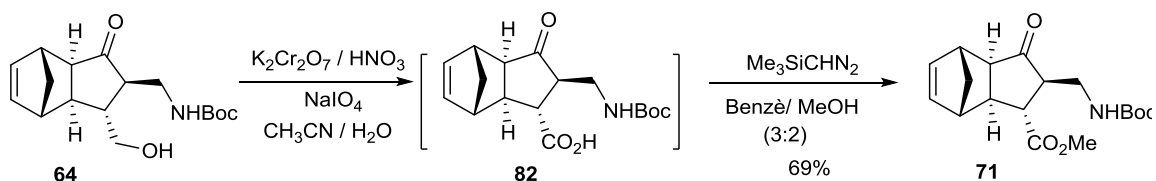


Figura 3.4.

El següent pas consisteix en la reacció de retro Diels-Alder en condicions de microones amb àcid de Lewis (AlCl_3Me). La reacció va tenir lloc en un minut i es va obtenir en el cru molts altres subproductes. Es pot identificar un mica d'adducte de retro Diels-Alder però amb la amina desprotegida que reacciona amb l'anhídrid maleic (**83**) i el adducte de PK desprotegida que reacciona amb l'anhídrid maleic (**84**) (figura 3.5).

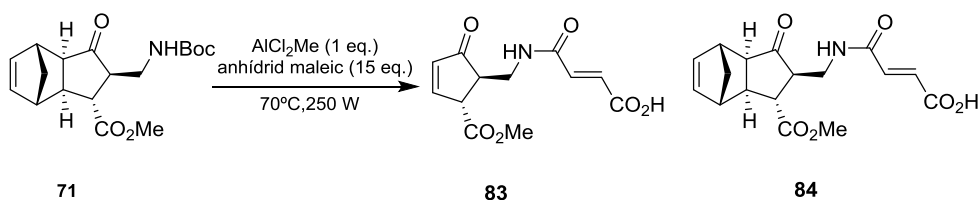


Figura 3.5.

Aquesta primera estratègia, hem mostrat que: 1) el grup protector Boc dels adductes de PK no es adequat. Hem pogut estudiar la reacció foto-induïda en detall com la reacció de retro Diels-Alder de diverses adductes de PK. Es va demostrar que en molts casos hi ha diverses reaccions secundàries. Amb la dificultat d'aconseguir suficient producte per seguir endavant, decidirem

canviar la metodologia i treballar amb una versió mes curta (figura 3.6). Començant amb un alquí disubstituint, la introducció de la dues cadenes en α i β de la ciclopentenona es va aconseguir mitjançant una reacció de PK regioselectiva.

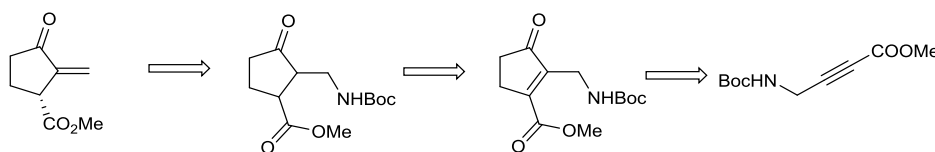


Figura 3.6.

Es va fer PKR amb 3 barg d'etilè, amb NMO a temperatura ambient. Es va identificar que l'adducte de PK **94** no era estable i vam haver de realitzar la següent reacció directament en el mateix reactor de reacció (figura 3.7). Després d'una hidrogenació a 3 barg de pressió de H_2 amb Pd/C, no hi va haver cap problema de purificació i estabilitat. Es va obtenir el compost **95** en 50% de rendiment en 2 passos. A continuació, es va provar el darrer-pas, la hidròlisi àcid del amina (**96**) seguida una β -eliminació. Es va obtenir la sarcomicina **97** en un rendiment total de 15%.

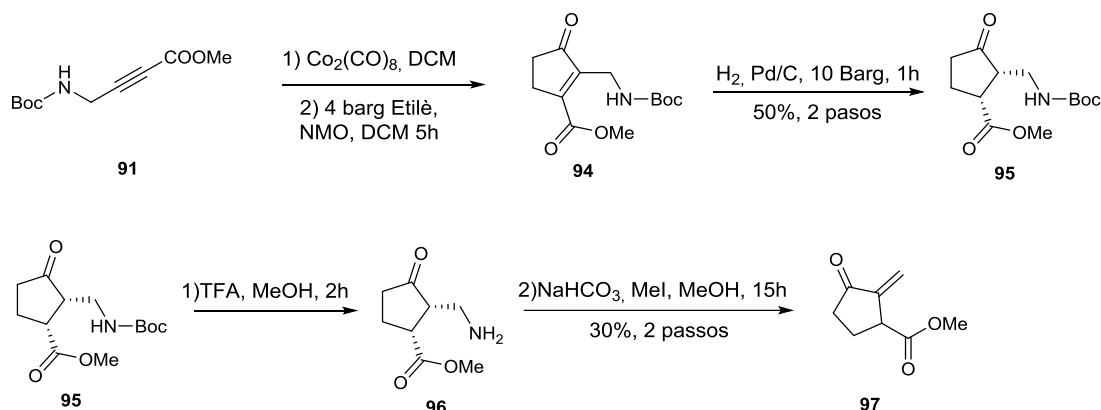


Figura 3.7.

Per tant, s'ha aconseguit per primera vegada la sarcomicina a través d'una reacció de Pauson-Khand intermolecular regioselectiva.

Per la síntesi del jasmonat, es va plantejar como a pas clau, la reacció de Claisen-Johnson permetent obtenir en un pas la introducció de les dues cadenes α i β (figura 3.8). Aprofitant del impediment estèric de l'adducte de PK vam pensar que la reacció de Claisen-Johnson seria estereoespecífica.

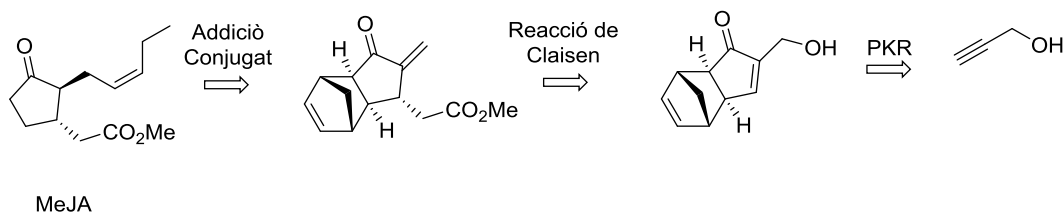


Figura 3.8

La síntesi s'inicia amb la reacció de PK amb l'alcohol propagilic protegit amb un èter silílic. Després d'una desprotecció amb TBAF, es va obtenir el compost **104** en un 67% de rendiment en dos passos (figura 3.9). La següent etapa, constitueix en fer reaccionar l'alcohol amb el ortoacetat de metil i àcid propiònic 120°C.

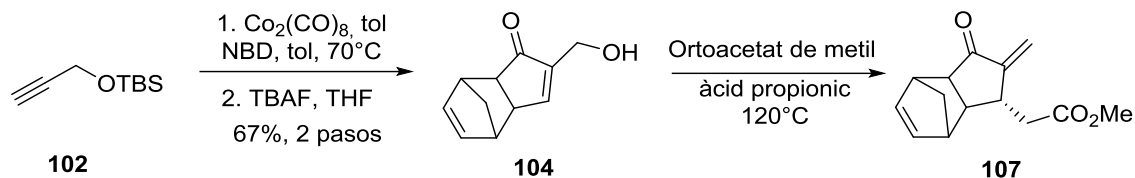


Figura 3.9.

Després d'un primer cop, es va a identificar que l'adducte de Claisen és forma però que dona com a el producte majoritari la reacció entre la enona exocíclica desitjada amb un subproducte del reactiu de partida per donar una reacció de tipus hetero Diels-Alder, (**108**) (figura 3.10).

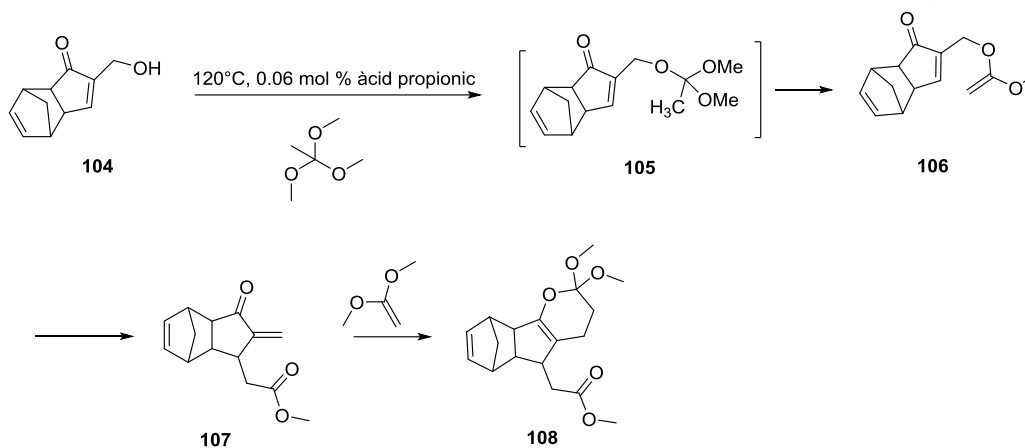


Figura 3.10.

Es va intentar optimitzat la reacció, modificant la concentració, el tipus d'àcid, la temperatura i el dissolvent on es va identificar les millors condicions per formar el compost **105** escalfant a 70°C 17h amb un excés de ortoacetat de metil.

En resum, hem aconseguit, 1) Realitzar per primera vegada, la síntesi de la sarcomicina utilitzant la reacció de Pauson-Khand regioselectiva amb bon rendiment total de 25%. 2) Arribar per primera vegada, a utilitzar la reacció de Claisen amb un substrat derivat de la reacció de Pauson-Khand. 3) Identificar els productes secundaris de la reacció de Claisen (**108**).

IV. Síntesi de nous composts derivats de la reacció de Pauson-Khand mitjançant la electrociclació de derivats de diarilacetilens.

En la tesi d'Agustí Lledó i la tesi de Yining Yi, es van descriure tres reaccions fotoinduïdes dels adductes de PK dependent de les condicions utilitzades i dels substituents del adducte (figura 4.1). Podem mencionar, las reaccions fotoinduïdes de tipus transposició (I), d'addició de metanol (II), i electrocíclica (III).

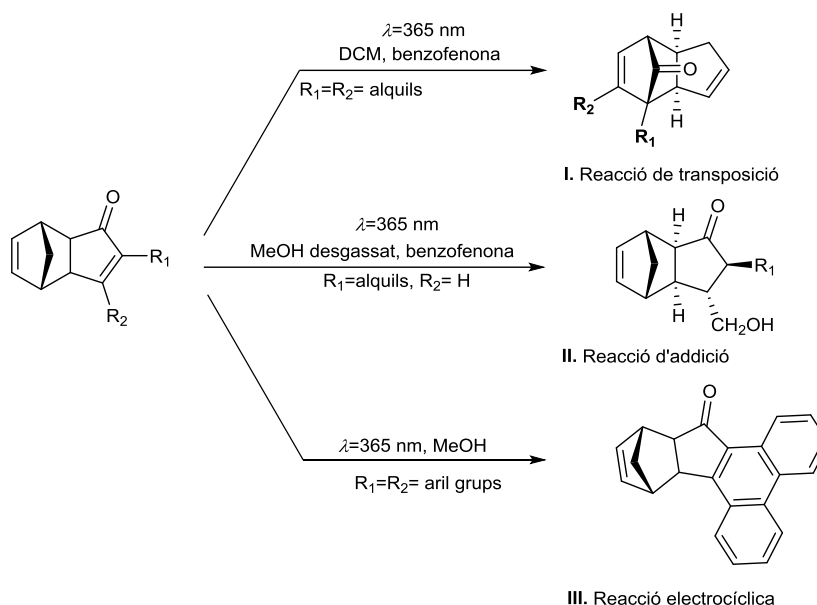


Figura 4.1.

En el treball de la tesi de Yining Yi, es va identificar que els adductes de PKR disubstituïts (112 i 121) i aromàtics donen lloc a la formació de dos atropoisomers P i M (figura 4.2). Aquesta estructura, és deguda a l'impediment estèric dels substituents que imposen la distorsió de la molècula bicíclica (figura 4.2).

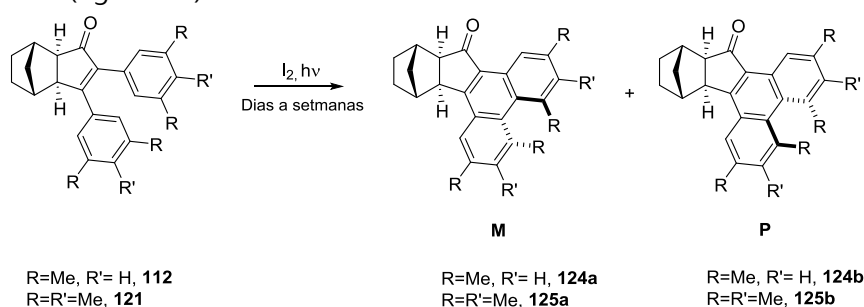


Figura 4.2.

Emprant las condicions prèviament desenvolupades per la Dra. Yining, és va completar l'estudi dels adductes de PKR amb alquins aromàtics disubstituïts per la síntesi d'una família de compostos helicènics.

Es va començar per la síntesi dels alquins 71, 75 i 78 mitjançant reacció de Sonogashira modificada amb bons rendiments (figura 4.3).

Es va descobrir anteriorment que després de la irradiació d'una solució de metanol a 365 nm, la presència d'un grup metil addicional en el compost **121** redueix considerablement la reactivitat cap a la reacció pericíclica en comparació amb el compost **112** (figura 4.6). Per tant, el temps d'irradiació superiors a una setmana són requerits per conduir la reacció cap a la seva terminació per **112**, però, només el 64% de conversió es va aconseguir després de 10 dies d'irradiació en cas de la **121**. Aquesta diferència en la reactivitat concorda amb el fet que la col·locació de grups metil addicionals en les posicions 4 augmenta l'impediment estèric per "juxtaposició" els grups metil situats en les posicions 4 i 5.

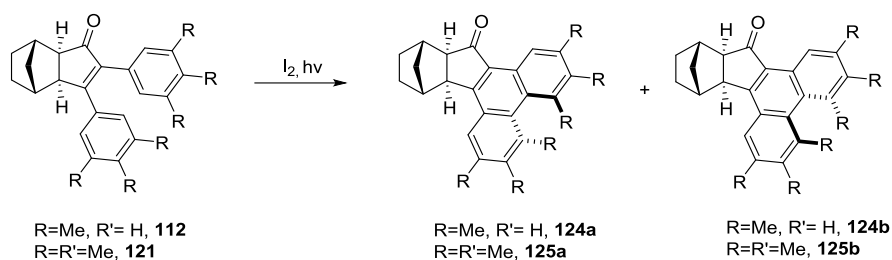


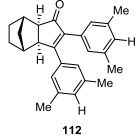
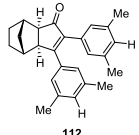
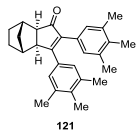
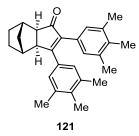
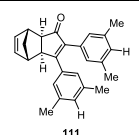
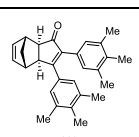
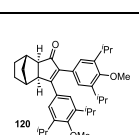
Figura 4.6.

En nostre cas, amb l'aparell Rayonnet de 16 làmpades, la reacció fotoquímica es va realitzar en quantitats estequiomètriques d'agent de deshidrogenació a 300 nm. La reacció va accelerar espectacularment d'una setmana a un màxim de 36 hores en el cas de **112** i de 10 dies a 54 hores en el cas de **121** (taula 4.1, entrades 1,2 i 3,4). A més, les reaccions van tenir lloc amb una conversió total dels materials de partida. El producte fotoquímico va resultar ser una barreja d'atropoisòmers en unes relacions de (3:1) en el cas **112** i (6:1) en el cas del compost **121** (taula 4.1, entrades 1-4).

Els compostos **111** i **116** sense iode van conduir als productes de l'electrociclació/oxidació amb baix rendiment. L'irradiació de **111** en solució de metanol a 300 nm va donar el fenantrè **122**, compost amb un rendiment de només el 33% després de 10 dies mentre que la presència dels grups metil addicionals en el compost **116** donant un rendiment de menys del 13% de **123** després de 6 dies d'irradiació (Taula 4.1, entrades 5,6).

Amb el compost **120**, hem aclarit que el grup isopropílic genera una restricció estructural important que fa que la reacció no es produeixi.

La repulsió entre els dos grups metil en les posicions 3 i 5 dels sistema fenantrènic provoca una distorsió helicoidal del sistema aromàtic pla, donant lloc a la formació d'un producte principal en la barreja dels dues atropoisòmers, confirmat per Rajos X fets per la Dra Yining Ji.

Entradas	Substrate	λ (nm)	Nombre de làmpades	Oxidant	%	Relació M/P	Temps
1	 112	365	8	I ₂	96	3:1	7 dies
2	 112	300	16	I ₂	96	3:1	36 h
3	 121	365	8	I ₂	60	6:1	10 dies
4	 121	300	16	I ₂	94	6:1	53 h
5	 111	300	16	O ₂	33	n.d	10 dies
6	 116	300	16	O ₂	13	n.d	6 dies
7	 120	300	16	I ₂	0	n.d	7 dies

Taula 4.1. *n.d: no determinat.*

La col·locació de grups metil addicionals en les posicions 4 augmenta l'impediment estèric per "juxtaposició" els grups metil situats en 3 i 5 posicions, el que resulta en fenantrens distorsionats més tensos i helicoidals. El cas de l'isopropil mostra limitacions en el disseny de l'adducte de PK que podria ser utilitzat per a formar nous fenantrens. Una millora de l'electrociclació s'ha realitzat amb èxit amb l'aparell Rayonnet. Combinant el treball previ desenvolupat i el present treball, hem pogut per primera vegada preparar composts helicèns obtinguts a partir d'adductes de Pauson-Khand.

En la segona part del capítol 3 es va començar l'estudi de PKR d'alquins que tenen heterocicles aromatics com el tiofenil i piridil.

La síntesi del material de partida de la PKR utilitza la reacció de Sonogashira amb 3-bromo-4-metil piridina (127) on les condicions de reacció anterior. Hem tractat d'optimitzar les condicions

però els rendiments van ser pobres, per sota del 10 % (figura 4.7). Seguidament, la reacció es va fraccionar en tres passos. 1 equivalent de material de partida és fa reaccionar amb l'etniltrimetilsilà i després d'una desprotecció del trimetilsilil amb NaHCO_3 , és va afegir un altre equivalent de 3-bromo-4-metil piridina que va donar un rendiment moderat del 39%.

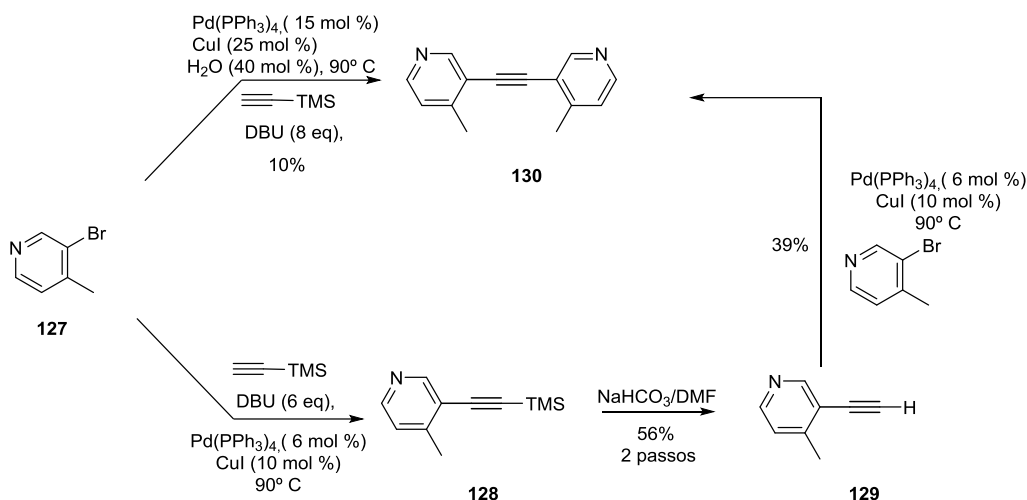


Figura 4.7.

Amb el alquí 130, la formació de complexos de PK és va tractar amb toluè amb 1,05 equivalents de complex dicobalt octacarbonil evitant acuradament la incidència de la llum. Malauradament, es va observar la descomposició directe del complex de dicobalt octacarbonil format-se un dipòsit sòlid negre (figura 4.8).

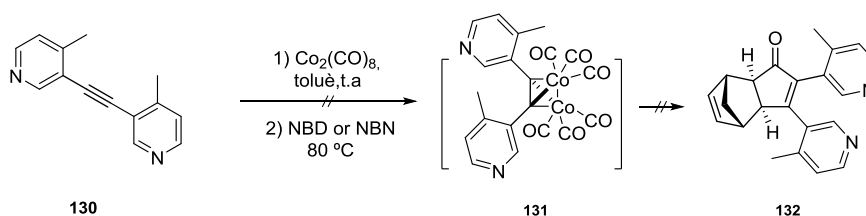


Figura 4.8.

El dicobalt octacarbonil era inestable en presència del fragment de piridina. Es va pensar que els electrons lliures eren potser responsables de la seva descomposició. En conseqüència, es va dissenyar la síntesi del complex de borà 134, per emmascarar els parells d'electrons lliures dels anells de piridina. La reacció es va fer en en toluè sec amb 2 equivalents d'una solució 1 M de BH_3 en THF a 0°C en amb un rendiment 62% (figura 4.9). La posterior reacció de Pauson-Khand amb el compost 134 es va intentar sense èxit potser perquè el compost es insoluble.

Summary in Catalan

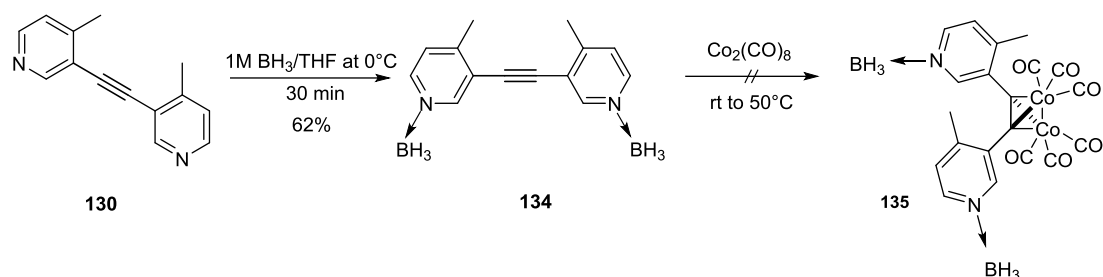


Figura 4.9.

Aquest estudi va permetre provar la reacció de PKR amb bispiridilacetilens. A la vista d'aquests resultats, es va concloure la incompatibilitat del complex dicobalt amb el grup piridil.

El 3-iodo-2,5-dimetiltiofè **140**, material de partida per a la reacció de Sonogashira, es va preparar amb un rendiment del 76% a partir de 2,5-dimetiltiofen **139** per tractament amb una solució de cloroform/àcid acètic, àcid iòdic i iode. El di-(2,5-dimetiltiofenil) alquí, **141** es va obtenir amb un rendiment del 55% mitjançant la reacció de Sonogashira (figura 4.10).

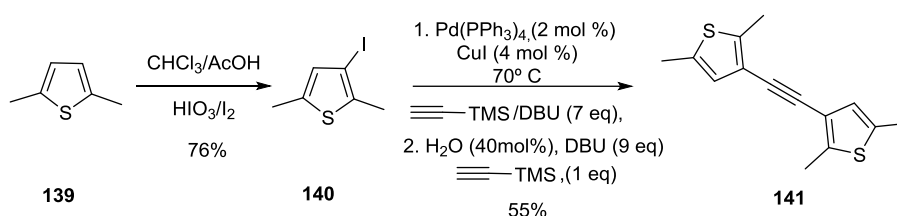


Figura 4.10.

Amb l'alquí **141**, es va realitzar l'estudi de la PKR amb ditiofenilacetilè. Coneixent el comportament d'aquest alquí en condicions PKR, la formació del complex de cobalt hexacarbonil del alquí es va fer sense incidència de la llum i en atmosfera de nitrogen. El alquí es va dissoldre en toluè i es van afegir 1,05 equivalents de complex dicobalt octacarbonil. Després de dues hores de reacció, es podia apreciar per TLC, la formació d'un complex de cobalt verd inusual en un cru de reacció net. In situ, es van afegir posteriorment 5 equivalents de norbornadiè i es van escalfar a 70 o 80°C durant tota la nit (figura 4.11).

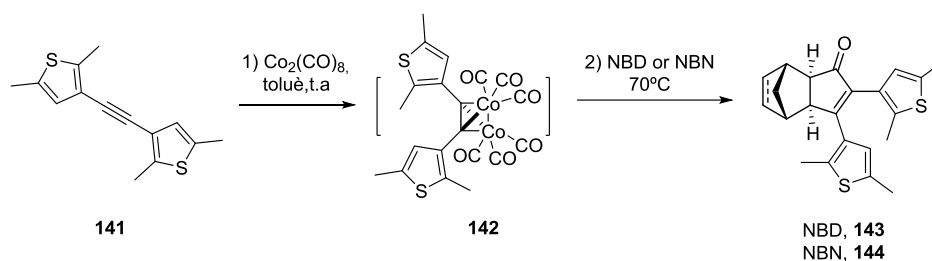


Figura 4.11.

Desafortunadament, es va formar una barreja complexa. La purificació es va realitzar mitjançant cromatografia preparativa obtenint el producte desitjat amb un baix rendiment del 6%. Es van

intentar optimitzar les condicions de reacció canviant la temperatura, el alquè, els equivalents, el dissolvent però sense èxit.

En darrer lloc, es va intentar fer la reacció de electrociclació. L'adducte PK es va dissoldre en DCM (15 mg / ml) i es va irradiar a 350 nm al rayonnet® equipat amb 16 làmpades, durant 1 minut a 296K. L'irradiació UV de l'adducte de PKR derivat del ditiofeniletí del resultar en un canvi de coloració a causa de la formació de l'isòmer cíclic. El material de partida groc va esdevenir una solució de color porpra. El mecanisme per a la transformació fotocromica de la ditiofeniletí inclou electrociclació provocada per la llum UV i la reacció de cicloversió del sistema hexatriè en aproximadament una hora a la llum de sol (figura 4.12).

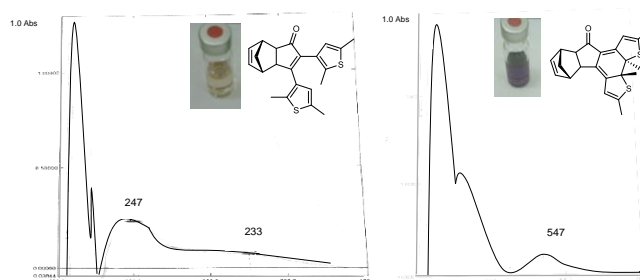


Figura 4.12.

Es va observar el màxim d'absorció en forma d'anell obert a 247 nm ($\epsilon=6.25.103 \text{ L.mol}^{-1}.\text{cm}^{-1}$) i una lleugera corba al voltant de 233 nm ($\epsilon=2.16.103\text{L.mol}^{-1}.\text{cm}^{-1}$). Aquesta solució incolora es converteix en un perfil de color porpra. La forma d'anell tancat té tres estats diferents d'absorció en 251 nm ($\epsilon=7.103 \text{ L.mol}^{-1}.\text{cm}^{-1}$), 328 nm ($\epsilon=6.25.102 \text{ L.mol}^{-1}.\text{cm}^{-1}$) i 547 nm ($\epsilon=6.25.102 \text{ L.mol}^{-1}.\text{cm}^{-1}$).

Després de la irradiació amb llum visible ($\lambda > 400 \text{ nm}$) la forma de color porpra reverteix a l'anell groguenc inicial. Després de sotmetre a la radiació UV, l'isòmer va ser bloquejat per la incidència de la llum, la forma d'anell tancat era perfectament estable després de més d'una setmana, mostrant mateix espectre d'absorció.

Vam tenir el plaer d'observar per primer vegada el "photoswitch" d'adductes de PK que valida la nostra prova de concepte. Desafortunadament, la optimització del rendiment químic de la PKR va ser impossible a causa de la reacció adversa causada pel grup tiofenil que va enverinar la reacció. El complex de dicobalt hexacarbonil es forma i és perfectament estable, però en el moment que el grup tiofenilo està en contacte amb l'alquè, no es produeix la PKR. D'alguna manera, el grup tiofenilo sembla bloquejar la inserció de l'alquè.

Conclusió

En aquest tesi, s'ha centrat la nostra atenció en l'estudi de la reacció de Pauson-Khand intermolecular des d'un punt de vista teòric i sintètic buscant aplicacions a la síntesi de compostos naturals. Es va desenvolupar:

- 1) L'estudi de la regioselectivitat de la PKR intermolecular amb una varietat d'alquins interns, dissimètrics i alifàtics amb substituents amb diferents propietats electròniques per un lloc i una cadena alifàtica per l'altre.

S'ha establert una relació entre els canvis electrònics d'alquins asimètrics i els resultats de la regioselectivitat dels adductes de PKR de manera experimental i computacional. S'ha trobat que els càlculs de diferències de càrrega en els NBO dels α -carbonis correlacionen qualitativament bé amb l'experiment. Per tant, en el cas dels substituents que tenen major electronegativitat que el carboni (-I grups), es va observar que els adductes de PK van donar l'isòmer β -*exo* amb alta regioselectivitat. Mentre que el cas dels substituents que tenen menor electronegativitat que el carboni (+I grups), es va observar que els adductes de PK van donar l'isòmer α -*exo* amb alta regioselectivitat. Els càlculs de diferències de càrrega NBO dels α -carbonis i carbonis dels alquins indiquen que la polarització de l'alquí està induïda per el heteroàtom. Per tant, l'efecte del substituent sobre la polarització de l'alquí en α -posició dels alquins pot predir el resultat de la regioselectivitat de la PKR tot i que només de manera qualitativa.

Els resultats van ser publicats al *Journal of Organic Chemistry*, 2014, 79, 10999-11010.

- 2) **La reacció de PK intermolecular d'alquins interns** va resultar ser la millor metodologia per sintetitzar l'èster metílic de la *rac*-sarcomicina (medicament contra el càncer) en només 2 passos i un rendiment global del 15%.

- 3) Una nova via es va plantejar per obtenir l'èster metílic del jasmonat (fragància) mitjançant una reacció de PK intermolecular d'alquins dissimètrics o terminals.

La primera via utilitza la PKR d'un alquí intern dissimètric. Es va trobar que l'adducte format era l'isòmer oposat al que esperaríem, tot i que la càrrega computacional NBO va correlacionar bé amb el resultat experimental.

La segona via és fer amb la reacció de PK d'alquí terminal on amb els nostres resultats preliminars ens va permetre identificar que la reacció de Claisen-Johnson utilitzada com a pas clau podria aplicar-se en la síntesi de l'èster metílic del jasmonat.

- 4) Aplicacions sintètiques de la reacció de PK intermolecular d'alquins simètrics d'arílics i heterocíclics mitjançant transformacions fotoquímiques.

La reacció d'electrociclació dels adductes de PK d'alquins disubstituïts arílics es va poder optimitzar amb bons rendiments i temps de reacció donant un nou accés a derivats de fenantrens torçats quirals resultant de l'impediment estèric dels adductes de PK imposats pel seus substituents. Els resultats van ser publicats en l'*European Journal of Organic Chemistry*, 2012, 6058-6063.

- 5) La reactivitat d'alquins heterocíclics amb substituents piridil i tiofenil en la reacció de PK va ser estudiada. Mentre que el motiu piridil no va permetre la formació de l'adducte de PK, sí que es va obtenir l'adducte de PK del bis(dimetiltiofenil), tot i que amb baix rendiment. Aquest adducte va mostrar una reacció fotoreversible interessant.

Referencies

- (1) Khand, I. U.; Knox, G. R.; Pauson, P. L.; Watts, W. E.; Foreman, M. I. *J. Chem. Soc. Perkin Trans. 1* **1973**, 977.
- (2) McKerrall, S. J.; Jørgensen, L.; Kuttruff, C. A.; Ungeheuer, F.; Baran, P. S. *J. Am. Chem. Soc.* **2014**, *136*(15), 5799–5810.
- (3) Huang, J.; Fang, L.; Long, R.; Shi, L.-L.; Shen, H.-J.; Li, C.; Yang, Z. *Org. Lett.* **2013**, *15*(15), 4018–4021.
- (4) Rios Torres, R. *Pauson-Khand Reaction: Scope, Variations and Applications*, John Wiley and Sons, 2012.
- (5) Bruin, T. J. M. De; Milet, A.; Gimbert, Y.; Greene, A. E.; Ledss, C. R.; March, R. V. *J. Am. Chem. Soc.* **2001**, No. 10, 7184–7185.
- (6) de Bruin, T. J. M.; Michel, C.; Vekey, K.; Greene, A. E.; Gimbert, Y.; Milet, A. *J. Organomet. Chem.* **2006**, *691*(20), 4281–4288.
- (7) Aiguabella, N.; del Pozo, C.; Verdaguer, X.; Fustero, S.; Riera, A. *Angew. Chem. Int. Ed.* **2013**, *52*(20), 5355–5359.
- (8) Vázquez-Romero, A.; Verdaguer, X.; Riera, A. *Eur. J. Org. Chem.* **2013**, *2013*(9), 1716–1725.
- (9) Vázquez-Romero, A.; Cárdenas, L.; Blasi, E.; Verdaguer, X.; Riera, A. *Org. Lett.* **2009**, *11*(14), 3104–3107.
- (10) Fager-Jokela, E.; Muuronen, M.; Patzschke, M.; Helaja, J. *J. Org. Chem.* **2012**, *77*(20), 9134–9147.
- (11) Vázquez-Romero, A.; Rodríguez, J.; Lledó, A.; Verdaguer, X.; Riera, A. *Org. Lett.* **2008**, *10*

- (20), 4509–4512.
- (12) Iqbal, M.; Evans, P.; Lledó, A.; Verdaguer, X.; Pericàs, M. A.; Riera, A.; Loeffler, C.; Sinha, A. K.; Mueller, M. J. *Chembiochem* **2005**, *6*(2), 276–280.
- (13) Aiguabella, N.; Pesquer, A.; Verdaguer, X.; Riera, A. *Org. Lett.* **2013**, *15*(11), 2696–2699.
- (14) Turro, N. J.; Schuster, G. *Science* **1975**, *187*(4174), 303–312.
- (15) Bach, T.; Hehn, J. P. *Angew. Chem. Int. Ed.* **2011**, *50*(5), 1000–1045.
- (16) Hoffmann, N. *Chem. Rev.* **2008**, *108*(3), 1052–1103.
- (17) Lledó, A.; Benet-Buchholz, J.; Solé, A.; Olivella, S.; Verdaguer, X.; Riera, A. *Angew. Chem. Int. Ed. Engl.* **2007**, *46*(31), 5943–5946.
- (18) Ji, Y.; Verdaguer, X.; Riera, A. *Chem. Eur. J.* **2011**, *17*(14), 3942–3948.
- (19) Gingras, M. *Chem. Soc. Rev.* **2013**, *42*, 968–1006.
- (20) Brieke, C.; Rohrbach, F.; Gottschalk, A.; Mayer, G.; Heckel, A. *Angew. Chemie - Int. Ed.* **2012**, *51*(34), 8446–8476.
- (21) Russew, M. M.; Hecht, S. *Adv. Mater.* **2010**, *22*(31), 3348–3360.

Appendix III

Index molecules

Structures chapter II.



1



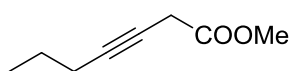
2



3



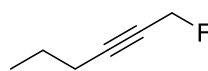
4



5



6



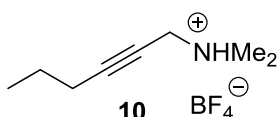
7



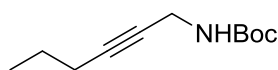
8



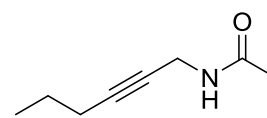
9



10



11



12



13



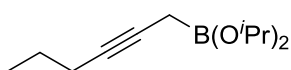
14



15



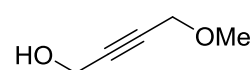
16



17



18



19



20



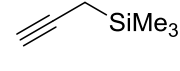
21



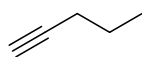
22



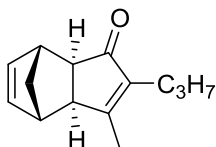
23



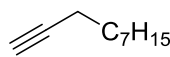
24



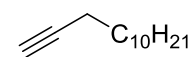
25



26



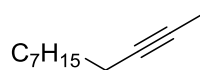
27



28



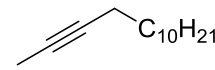
29



30

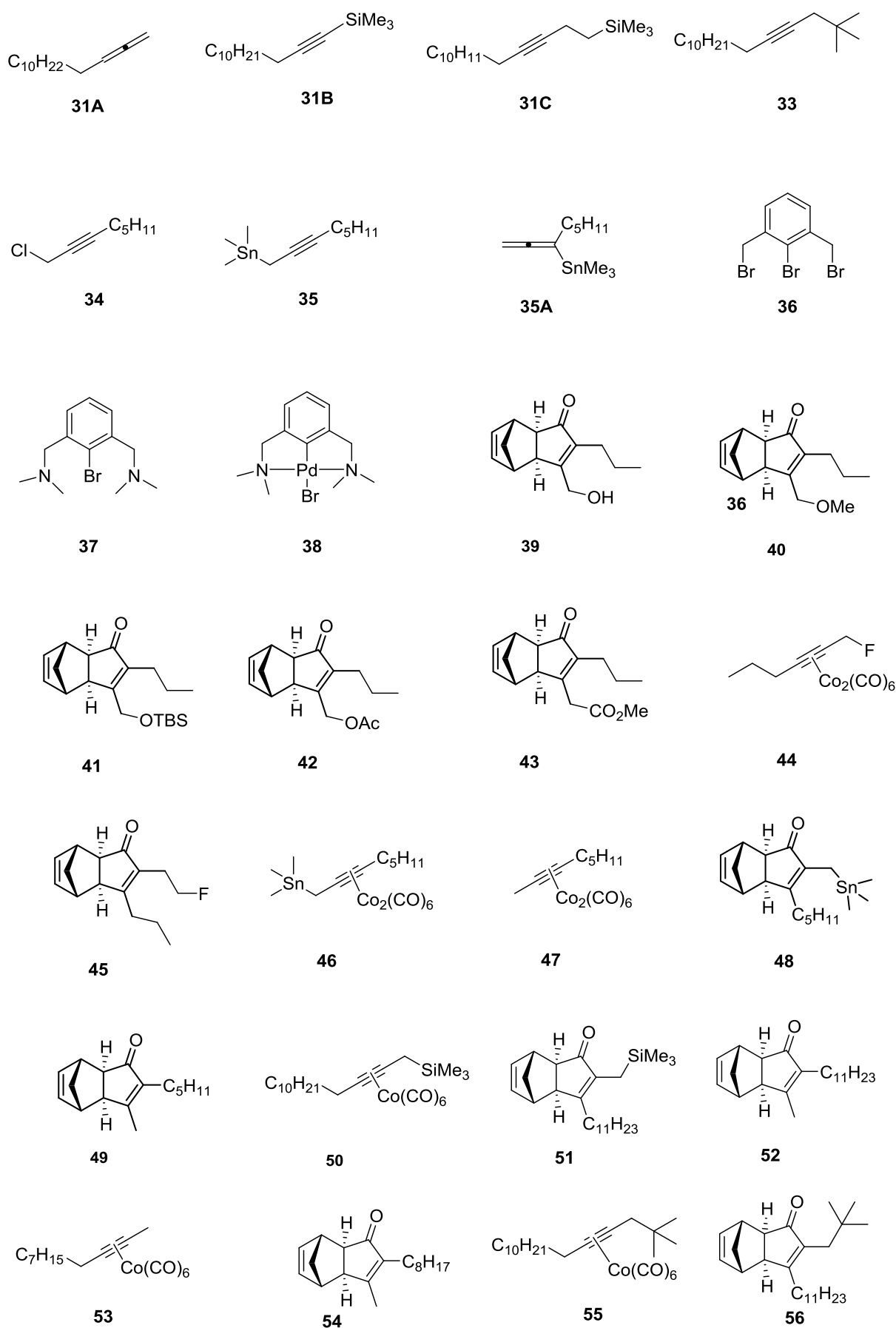


31

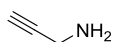


32

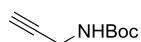
Structures chapter II.



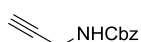
Structures chapter III.



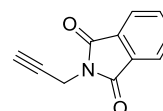
57



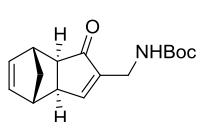
58



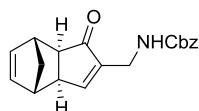
59



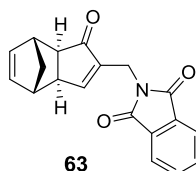
60



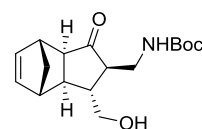
61



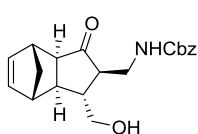
62



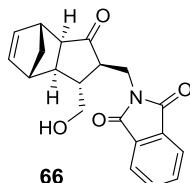
63



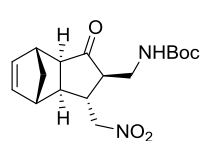
64



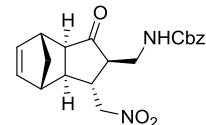
65



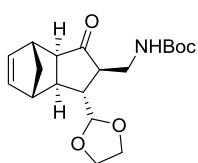
66



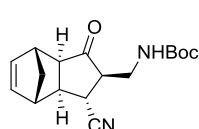
67



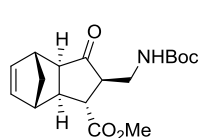
68



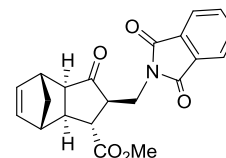
69



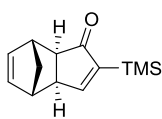
70



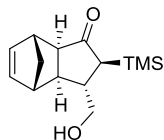
71



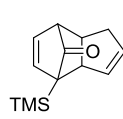
72



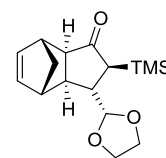
73



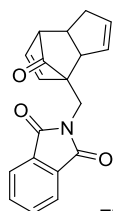
74



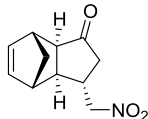
75



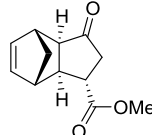
76



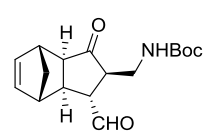
77



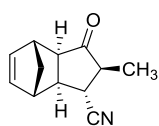
78



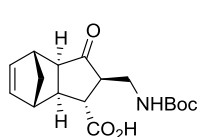
79



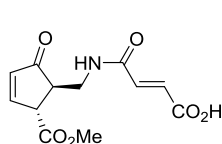
80



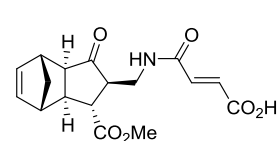
81



82

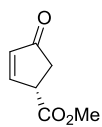


83

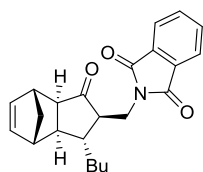


84

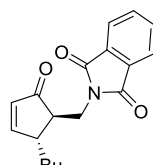
Structures chapter III.



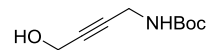
85



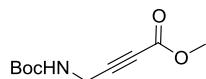
86



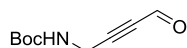
87



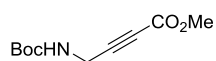
88



89



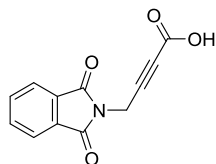
90



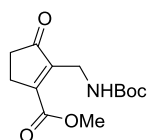
91



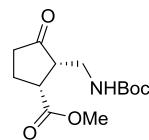
92



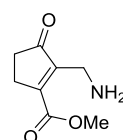
93



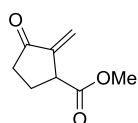
94



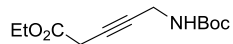
95



96



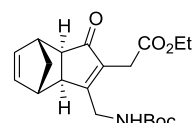
97



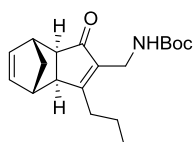
98



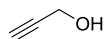
98B



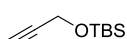
99



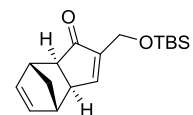
100



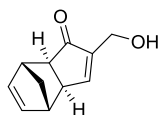
101



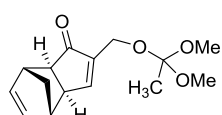
102



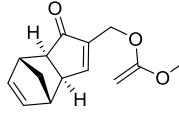
103



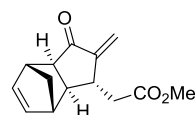
104



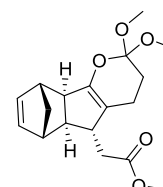
105



106

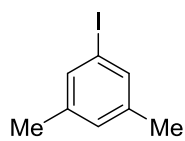


107

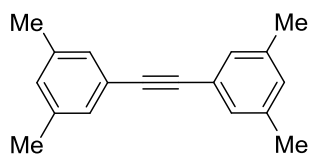


108

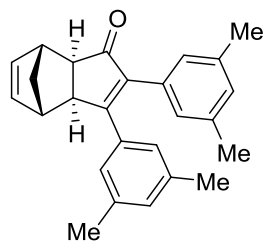
Structures chapter IV.



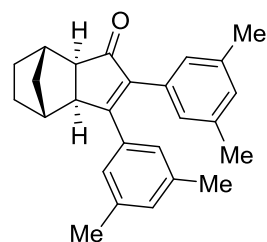
103



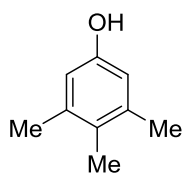
104



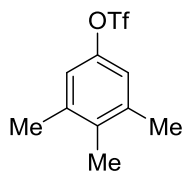
105



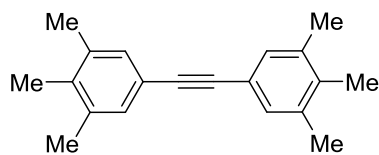
106



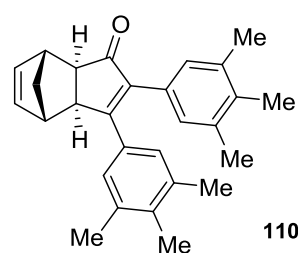
107



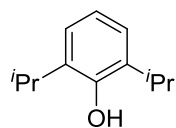
108



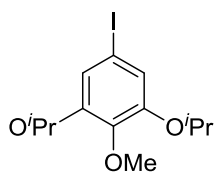
109



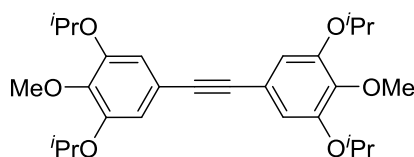
110



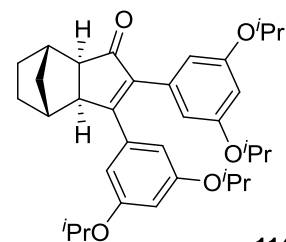
111



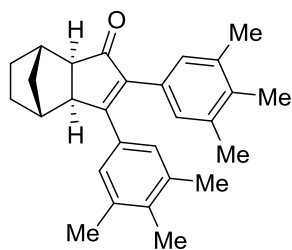
112



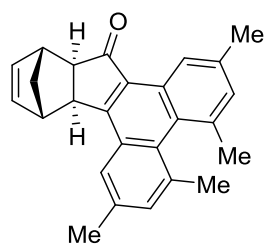
113



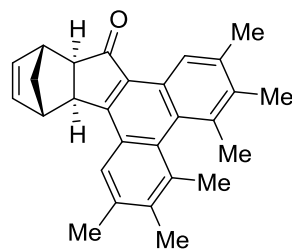
114



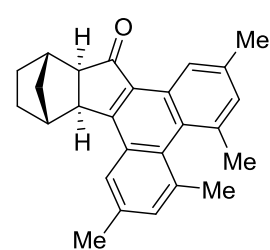
115



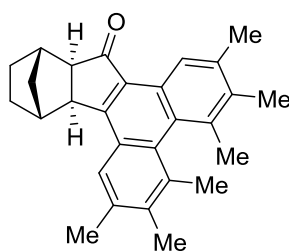
116



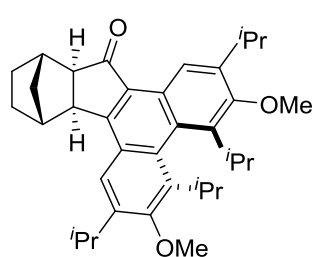
117



118

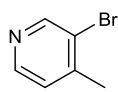


119

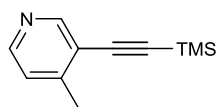


220

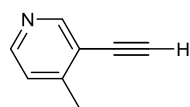
Structures chapter IV.



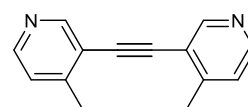
121



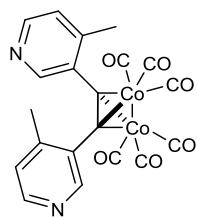
122



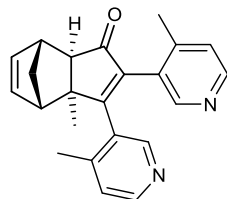
123



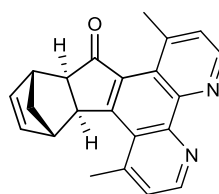
124



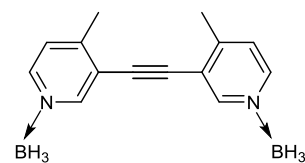
125



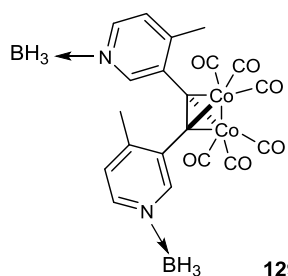
126



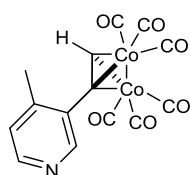
127



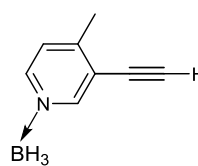
128



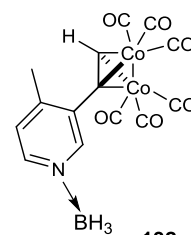
129



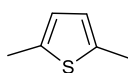
130



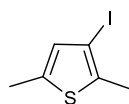
131



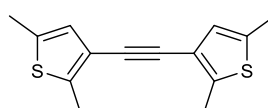
132



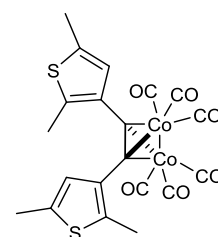
133



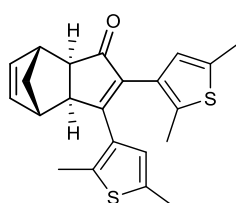
134



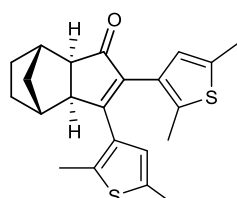
135



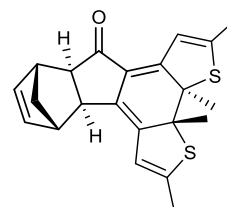
136



138



137



139

